

Unconventional Carbene-Donor Ligands for the Development of New Catalysts

Dissertation

zur Erlangung des mathematisch–naturwissenschaftlichen Doktorgrades

“Doctor rerum naturalium“

der Georg-August-Universität Göttingen

im Promotionsprogramm Chemie

der Georg-August University School of Science (GAUSS)

vorgelegt von
Sven Ole Reichmann
aus Vorwerk

Göttingen, 2016

Betreuungsausschuss

Professor Dr. Dietmar Stalke

Institut für Anorganische Chemie, Georg-August-Universität Göttingen

Privatdozent Dr. Rajendra S. Ghadwal

Anorganische Chemie und Strukturchemie, Universität Bielefeld

Mitglieder der Prüfungskommission

Referent: Professor Dr. Dietmar Stalke
IAC, Georg-August-Universität Göttingen

Korreferent: Privatdozent Dr. Rajendra S. Ghadwal
Anorganische Chemie und Strukturchemie, Universität Bielefeld

Weitere Mitglieder der Prüfungskommission:

Professor Dr. Konrad Koszinowski
IOBC, Georg-August-Universität Göttingen

Dr. Michael John
IAC, Georg-August-Universität Göttingen

Dr. Inke Siewert
IAC, Georg-August-Universität Göttingen

Juniorprofessorin Dr. Selvan Demir
IAC, Georg-August-Universität Göttingen

Tag der mündlichen Prüfung: 13. Oktober 2016

Die vorliegende Arbeit wurde in der Zeit vom April 2013 bis Oktober 2016 unter der Leitung von PD Dr. Rajendra S. Ghadwal im Arbeitskreis von Prof Dr. Dietmar Stalke am Institut für Anorganische Chemie der Georg-August-Universität Göttingen angefertigt.

Ich danke Herrn PD Dr. Rajendra S. Ghadwal

für die interessante Themenstellung und seine Unterstützung sowie für die zahlreichen Diskussionen und weitreichende Anregungen.

Herrn Professor Dr. Dietmar Stalke danke ich

für die Möglichkeit im Umfeld von Herrn PD Dr. Rajendra S. Ghadwal arbeiten zu dürfen, für die hervorragende Möglichkeit die Kristallographie kennenzulernen und ein Teil seines Arbeitskreises zu sein.

To my family

Success is the ability to go from one failure to another with no loss of enthusiasm.

Winston Churchill.

Table of Contents

Abbreviation Index.....	VIII
Compound Index.....	X
1. Introduction.....	1
1.1. Carbenes	1
1.2. <i>N</i> -Heterocyclic Carbenes.....	4
1.3. Mesoionic Carbenes	11
1.4. C2-Arylation Strategies and Synthesis of Mesoionic Carbenes.....	14
1.5. Methods to Quantify the Steric and Electronic Properties of NHCs	15
1.6. Scope	20
2. Results and Discussion	23
2.1. The Synthesis of the <i>N</i> -Heterocyclic Carbene IPr.....	23
2.2. Functionalised bis-NHCs.....	25
2.3. Palladium-Catalysed C2-Arylation of a nNHC	28
2.3.1. Coordinating and Non-Coordinating Anions	30
2.3.2. Crystal Structures of IPrPhX Salts	33
2.3.3. Substrate Scope	35
2.3.4. Crystal Structures of (IPrPh-R)I salts.....	36
2.3.5. Proposed Catalytic Cycle	39
2.4. Nickel-Catalysed C2-Arylation of an nNHC.....	41
2.4.1. Substrate Scope	43
2.4.2. Crystal Structures of (IPrPhR)Br	44
2.4.3. Proposed Catalytic Cycle	45
2.5. Electronic and Steric Properties of MICs and their precursors	46
2.5.1. Calculation of Tolman Electronic Parameter (TEP)	46
2.5.2. NMR Measurements	48
2.5.3. Percent Buried Volume Calculation.....	48
2.6. Coin Metal Complexes of (IPrPh)I (7a)	50

2.7.	Application of Copper Catalysts (26–28) in Click Chemistry	55
2.8.	Threefold Click Chemistry: Improved Procedure.....	58
3.	Conclusion and Outlook	61
4.	Experimental Section	63
4.1.	General Procedures	63
4.2.	Analytical Methods.....	63
4.2.1.	Mass Spectrometry	63
4.2.2.	NMR Spectroscopy.....	63
4.2.3.	Elemental Analysis	63
4.2.4.	Computational studies	64
4.3.	Synthesis and Characterisation	65
4.3.1.	Synthesis of bis(2,6-diisopropylphenyl)diazabutadiene	65
4.3.2.	Synthesis of 1,3-bis(2,6-diisopropylphenyl)imidazolium chloride (IPr ^H Cl)....	66
4.3.3.	Synthesis of 1,3-bis(2,6-diisopropylphenyl)imidazole-2-ylidene (IPr) (1)	67
4.3.4.	Synthesis of bis(1,3-bis(2,6-diisopropylphenyl)-4-diphenylsilane- 5-hydro-1 <i>H</i> -imidazol)-copper chloride Ph ₂ Si[(IPr ^H)CuCl] ₂ (4)	68
4.3.5.	Synthesis of [4-(chlorodiphenylsilyl)-1,3-bis(2,6-diisopropyl-phenyl)-imidazole-2-ylidene] copper(I) chloride [Ph ₂ (Cl)Si(IPr)Cu]Cl (6).....	69
4.3.6.	Synthesis of 1,3-bis(2,6-diisopropylphenyl)-2-phenyl-imidazolium iodide (IPrPh)I (7)	70
4.3.7.	Large Scale Synthesis of (7)	71
4.3.8.	Synthesis of 1,3-bis(2,6-diisopropylphenyl)-2-phenyl-imidazolium tetrafluoroborate (IPrPh)BF ₄ (8).....	72
4.3.9.	Synthesis of 1,3-bis(2,6-diisopropylphenyl)-2-phenyl-imidazolium hexafluorophosphate (IPrPh)PF ₆ (9)	73
4.3.10.	Synthesis of 1,3-bis(2,6-diisopropylphenyl)-2-phenyl-imidazolium triflate (IPrPh)CF ₃ SO ₃ (10)	74
4.3.11.	Synthesis of 1,3-bis(2,6-diisopropylphenyl)-2-(<i>p</i> -tolyl)-imidazolium iodide (IPrPh-4-Me)I (12).....	75

4.3.12.	Synthesis of 1,3-bis(2,6-diisopropylphenyl)-2-(<i>o</i> -tolyl)-imidazolium iodide (IPrPh-2-Me)I (13).....	77
4.3.13.	Synthesis of 1,3-bis(2,6-diisopropylphenyl)-2-(4-methoxyphenyl)-imidazolium iodide (IPrPh-4-OMe)I (14).....	78
4.3.14.	Synthesis of 1,3-bis(2,6-diisopropylphenyl)-2-(4-(methoxycarbonyl) phenyl)-imidazolium iodide (IPrPh-4-CO ₂ Me)I (15).....	79
4.3.15.	Reaction Optimisation.....	80
4.3.16.	Recycling of the Catalyst	81
4.3.17.	Modified Method for the Synthesis of (IPr) ₂ Pd (19)	82
4.3.18.	Reaction of IPr and PhI with 1 mol% of (IPr) ₂ Pd.....	83
4.3.19.	Synthesis of 1,3-bis(2,6-diisopropylphenyl)-2-phenyl-imidazolium bromide (IPrPh)Br (20)	84
4.3.20.	Synthesis of 1,3-bis(2,6-diisopropylphenyl)-2-(<i>p</i> -tolyl)-imidazolium bromide (IPrPh-4-Me)Br (21)	85
4.3.21.	Synthesis of 1,3-bis(2,6-diisopropylphenyl)-2-(4-methoxyphenyl)-imidazolium bromide (IPrPh-4-OMe)Br (22)	86
4.3.22.	Reaction Optimisation.....	87
4.3.23.	Coincidental synthesis of 1,4-bis(2,6-diisopropylphenyl)-2-phenyl-1 <i>H</i> -imidazole.....	88
4.3.24.	Synthesis of [1,3-bis(2,6-diisopropylphenyl)-2-phenyl-imidazol-4-ylidene] copper(I) iodide (IPrPh)CuI (26) from CuI.....	89
4.3.25.	Synthesis of [1,3-bis(2,6-diisopropylphenyl)-2-phenyl-imidazol-4-ylidene] copper(I) iodide (IPrPh)CuI (26b) from CuCl	90
4.3.26.	Synthesis of [(1,3-bis(2,6-diisopropylphenyl)-2-phenyl-imidazol-4-ylidene)-(1,3-bis(2,6-diisopropylphenyl)-imidazol-2-ylidene)] copper(I) iodide [(IPrPh)Cu(IPr)]I (27)	91
4.3.27.	Synthesis of [(1,3-bis(2,6-diisopropylphenyl)-2-phenyl-imidazol-4-ylidene)-(1,3-bis(2,6-diisopropylphenyl)-imidazol-2-ylidene)] copper(I) tetrafluoroborate [(IPrPh)Cu(IPr)]BF ₄ (27a).....	92
4.3.28.	Synthesis of Bis[1,3-bis(2,6-diisopropylphenyl)-2-phenyl-imidazol-4-ylidene] copper(I) iodide [(IPrPh) ₂ Cu]I (28)	93

4.3.29.	Synthesis of Bis[1,3-bis(2,6-diisopropylphenyl)-2-phenyl-imidazol-4-ylidene] silver (I) tetrafluoroborate ($[(\text{IPrPh})_2\text{Ag}(\text{I})\text{BF}_4]$ (29).....	94
4.3.30.	Synthesis of 1-benzyl-4-phenyl-1 <i>H</i> -1,2,3-triazol (30)	95
4.3.31.	Synthesis of 2-(1-benzyl-1 <i>H</i> -1,2,3-triazol-4-yl)ethanol (31).....	96
4.3.32.	Synthesis of 1-benzyl-4-butyl-1 <i>H</i> -1,2,3-triazol (32)	97
4.3.33.	Synthesis of 2-(1-benzyl-1 <i>H</i> -1,2,3-triazol-4-yl)propan-2-ol (33)	98
4.3.34.	Synthesis of 2-(1-benzyl-1 <i>H</i> -1,2,3-triazol-4-yn)pyridine (34)	99
4.3.35.	Synthesis of 1,1'-(2-methyl-2-((4-phenyl-1 <i>H</i> -1,2,3-triazol-1-yl)methyl)propane-1,3-diyl)bis(4-phenyl-1 <i>H</i> -1,2,3-triazole) $\text{C}_2\text{H}_3(\text{C}_3\text{H}_3\text{N}_3(\text{Ph}))_3$ (35).....	100
4.3.36.	Synthesis of 1,1'-(2-methyl-2-((4-phenyl-1 <i>H</i> -1,2,3-triazol-1-yl)methyl)propane-1,3-diyl)bis(4-phenyl-1 <i>H</i> -1,2,3-triazole) (36)	101
4.3.37.	Synthesis of 2,2'-(1,1'-(2-((4-(2-hydroxyethyl)-1 <i>H</i> -1,2,3-triazol-1-yl)methyl)-2-methylpropane-1,3-diyl)bis(1 <i>H</i> -1,2,3-triazole-4,1-diyl))diethanol (37).....	102
4.3.38.	Synthesis of 1,1'-(2-methyl-2-((4-neopentyl-1 <i>H</i> -1,2,3-triazol-1-yl)methyl)propane-1,3-diyl)bis(4-(tert-butyl)-1 <i>H</i> -1,2,3-triazole) (38).....	103
4.3.39.	Synthesis of 1,1'-(2-methyl-2-((4-propyl-1 <i>H</i> -1,2,3-triazol-1-yl)methyl)propane-1,3-diyl)bis(4-propyl-1 <i>H</i> -1,2,3-triazole) (39)	104

5. Crystallographic Section 106

5.1.	Crystal Selection and Manipulation.....	106
5.2.	Data Collection and Processing	106
5.3.	Structure Solution and Refinement	106
5.4.	Treatment of Disorder.....	107
5.5.	Determined Structures.....	109
5.5.1.	1,3-bis(2,6-diisopropylphenyl)imidazole-2-yliden (IPr) (1).....	109
5.5.2.	1,3-bis(2,6-diisopropylphenyl)imidazoliumiodide (IPr·HI)	110
5.5.3.	1,3-bis(2,6-diisopropylphenyl)imidazoliumiodide (IPr·HI*1,4-dioxane)	111
5.5.4.	4-(chlorodiphenylsilyl)-1,3-bis(2,6-diisopropyl-phenyl)-2,3-dihydro-1 <i>H</i> -imidazole copper chloride $\text{CuCl}(\text{IPr})\text{SiPh}_2\text{Cl}\cdot\text{toluene}$ (6).....	112
5.5.5.	Bis(1,3-bis(2,6-diisopropylphenyl)-2,3-dihydro-1 <i>H</i> -imidazol-4-yl)diphenylsilane-copper chloride $\text{Ph}_2\text{Si}[(\text{IPr})\text{CuCl}]_2$ (4)	113

5.5.6.	1,3-bis(2,6-diisopropylphenyl)-2-phenyl-imidazolium palladium triiodide (IPrPh)PdI ₃ (7b)	115
5.5.7.	1,3-bis(2,6-diisopropylphenyl)-2-phenyl-imidazolium iodide (IPrPh)I (7a) ...	116
5.5.8.	1,3-bis(2,6-diisopropylphenyl)-2-phenyl-imidazolium tetrafluoroborate (IPrPh)BF ₄ (8)	117
5.5.9.	1,3-bis(2,6-diisopropylphenyl)-2-phenyl-imidazolium hexafluorophosphate (IPrPh)PF ₆ (9)	118
5.5.10.	1,3-bis(2,6-diisopropylphenyl)-2-phenyl-imidazolium triflate (IPrPh)CF ₃ SO ₃ (10).....	119
5.5.11.	1,3-bis(2,6-diisopropylphenyl)-2-(<i>p</i> -tolyl)-imidazolium iodide (IPrPh-4-Me)I (12).....	120
5.5.12.	1,3-bis(2,6-diisopropylphenyl)-2-(<i>p</i> -tolyl)-imidazolium iodide (IPrPh-2-Me)I (13).....	121
5.5.13.	1,3-bis(2,6-diisopropylphenyl)-2-(4-methoxyphenyl)-imidazolium iodide (IPrPh-4-OMe)I (14)	122
5.5.14.	1,3-bis(2,6-diisopropylphenyl)-2-(4-(methoxycarbonyl) phenyl)-imidazolium iodide (IPrPh-4-CO ₂ Me)I (15).....	123
5.5.15.	1,3-bis(2,6-diisopropylphenyl)-2-(<i>p</i> -tolyl)-imidazolium bromide (IPrPh-4-Me)Br (21)	124
5.5.16.	1,3-bis(2,6-diisopropylphenyl)-2-(4-methoxyphenyl)-imidazolium bromide (IPrPh-4-OMe)Br (22)	125
5.5.17.	1-(2,6-diisopropylphenyl)-1 <i>H</i> -imidazole	126
5.5.18.	[1,3-bis(2,6-diisopropylphenyl)-2-phenyl-imidazol-4-ylidene] copper(I) iodide (IPrPh)CuI (26)	127
5.5.19.	[(1,3-bis(2,6-diisopropylphenyl)-2-phenyl-imidazol-4-ylidene)-(1,3-bis(2,6-diisopropylphenyl)-imidazol-2-ylidene)] copper(I) iodide [(IPrPh)CuIPr]I (27)	129
5.5.20.	[(1,3-bis(2,6-diisopropylphenyl)-2-phenyl-imidazol-4-ylidene)-(1,3-bis(2,6-diisopropylphenyl)-imidazol-2-ylidene)] copper(I) tetrafluoroborate [(IPrPh)Cu(IPr)]BF ₄ (27a)	130
5.5.21.	Bis[1,3-bis(2,6-diisopropylphenyl)-2-phenyl-imidazol-4-ylidene] copper(I) iodide [(IPrPh) ₂ Cu]I (28)	131

5.5.22.	Bis[1,3-bis(2,6-diisopropylphenyl)-2-phenyl-imidazol-4-ylidene] silver (I) tetrafluoroborate [(IPrPh) ₂ Ag]BF ₄ (29)	133
5.5.23.	Bis(1,3-Bis(2,6-diisopropylphenyl)imidazole-2-yliden palladium iodide)	135
5.5.24.	2-(1-benzyl-1-1,2,3-triazol-4-yl)propan-2-ol.....	136
5.5.25.	1-benzyl-4-butyl-1 <i>H</i> -1,2,3-triazole.....	137
5.5.26.	2-(1-benzyl-1 <i>H</i> -1,2,3-triazol-4-yl)ethanol.....	138
6. Crystal Structure Determination in Collaborations		139
6.1.	Structures determined for Svenja Düfert	139
6.1.1.	7-methoxy-1-methyl-10a,11-dihydro-5 <i>H</i> -benzo[<i>e</i>]furo[3',4':6,7]naphtho[1,8- <i>bc</i>]oxepin-13(10 <i>H</i>)-one	139
6.2.	Structures determined for Jonas Ammermann.....	140
6.2.1.	1-(5-Methyl-3-(9 <i>H</i> -xanthen-9-yl)-1 <i>H</i> -indole-1-yl)ethan-1-one	140
6.3.	Structures determined for Bernd Waldecker.....	141
6.3.1.	4,9-Bis(9 <i>H</i> -xanthene-9-ylidene)-1,3,4,6,8,9-hexahydropyrano[3,4- <i>g</i>]-isochromene 141	
6.3.2.	4,6-Bis(9 <i>H</i> -xanthene-9-ylidene)-4,6,7,9-tetrahydro-1 <i>H</i> ,3 <i>H</i> -pyrano[3,4- <i>g</i>]- isochromene	142
6.4.	Structures determined for Simon Biller	143
6.4.1.	(+)-(R)-Linorexpin.....	143
6.4.2.	2-((2-(4-bromo-3-methylphenyl)-2-oxoethyl)thio)-6-oxo-4-(thiophen-2-yl)-1,6- dihydropyrimidine-5-carbonitrile	144
6.5.	Structure determined for Yan Li	145
6.5.1.	SOR_LY_023	145
6.6.	Structures determined for Alexander Paesch.....	146
6.6.1.	2-Phenyl-4-diphenylphospan-1,3-bis(2,6-diisopropylphenyl)-imidazolium- Kupfer(I)iodid ([(<i>Ph</i> ₂ P-IPrPh)-Cu(I)-I]).....	146
6.6.2.	Bis[2-phenyl-1,3-bis(2,6-diisopropylphenyl)-imidazolium]- palladium(II)dichloride ([IPrPh) ₂ -Pd(II)-Cl ₂])	147
7. References		148

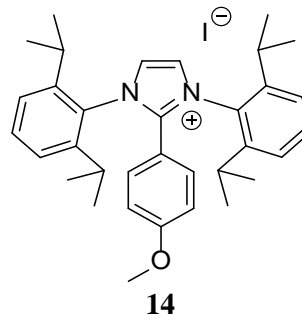
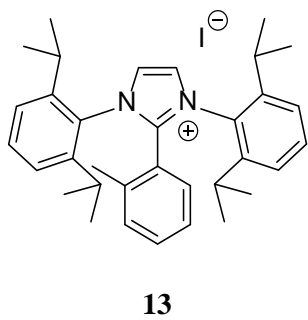
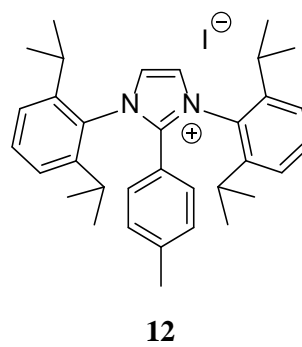
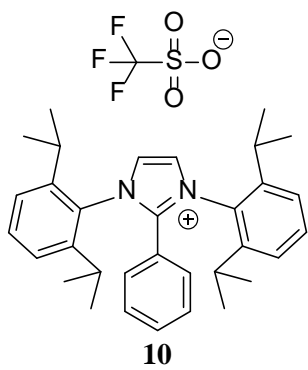
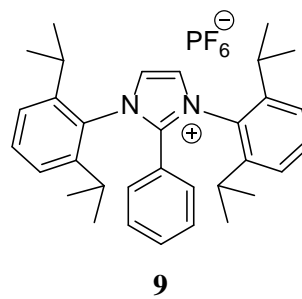
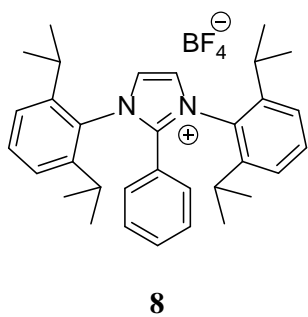
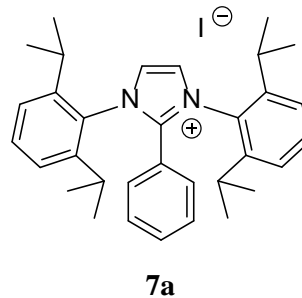
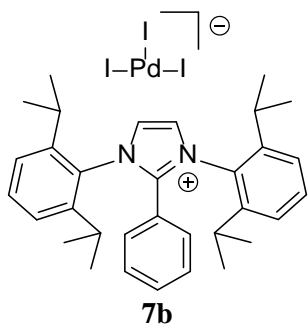
Appendix	156
Curriculum Vitae	157

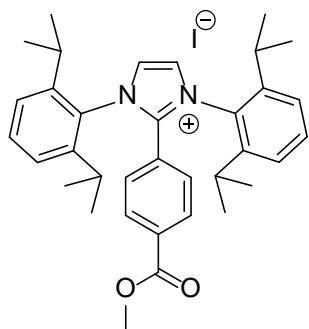
Abbreviation Index

Å	Ångstrom	HMBC	Heteronuclear Multiple Bond Correlation
Ad	Adamantyl	HSAB	Hard and Soft Acids and Bases
aNHC	abnormal <i>N</i> -heterocyclic carbene	HSQC	Heteronuclear Single Quantum Correlation
amu	atomic mass unit	Im	Imidazole
BASF	Batch Scale Factor	IMes	1,3-Bis(2,4,6-trimethylphenyl)imidazol-2-yliden
CS	Compact Spheres	IPr	1,3-Bis(2,6-diisopropylphenyl)imidazol-2-yliden
CSD	Cambridge Structural Database	<i>i</i> Pr	<i>iso</i> -Propyl
CCDC	Cambridge Crystallographic Data Base	IR	Infrared Spectroscopy
d	distance / doublet	<i>t</i> Bu	1,3-Bis(<i>tert</i> -butyl)imidazol-2-yliden
dba	dibenzylideneacetone	LUMO	Lowest Unoccupied Molecular Orbital
DCM	Dichloromethane	M	Molar
DFT	Density Functional Theory	mCPBA	<i>meta</i> -Chloroperbenzoic acid
Dipp	2,6-diisopropylphenyl	Me	Methyl
DMSO	Dimethyl sulfoxid	Mes	Mesityl (2,4,6-trimethylphenyl)
DOSY	Diffusion-Ordered Spectroscopy	MHz	Megahertz
DSE	Dissipated Spheres and Ellipsoids	MIC	Mesoionic Carbene
ECC	External Calibration Curve	MS	Mass Spectrometry
ED	Expanded Discs	<i>n</i> BuLi	<i>n</i> -Butyllithium
EI	Electron Ionisation	NHC	<i>N</i> -heterocyclic carbene
ESI	Electrospray Ionisation	NHBC	<i>N</i> -heterocyclic biscarbene
eq.	equivalents	NMR	Nuclear Magnetic Resonance
esd	estimated standard deviation	nNHC	normal <i>N</i> -heterocyclic carbene
<i>et al.</i>	<i>et alii</i> , and others	OA	Oxidative Addition
Et ₂ O	Diethylether		
h	hour		
HOESY	Heteronuclear Overhauser Effect Spectroscopy		
HOMO	Highest Occupied Molecular Orbital		

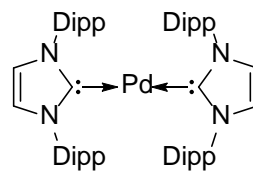
Ph	Phenyl
pK _a	Acid Dissociation Constant
ppm	parts per million
ppmw	parts per million by weight
R	any residue
RE	Reductive Elimination
rNHC	remote <i>N</i> -heterocyclic carbene
rt	room temperature
s	singlet
SambVca	S alerno m olecular b uried v o lume c alculation
<i>t</i> Bu	<i>tertiary</i> Butyl
TEP Parameter	Tolman Electronic
TfOH Acid	Trifluoromethanesulfonic
THF	Tetrahydrofuran
TMEDA	<i>N,N,N',N'</i> - Tetramethylethylenediamine
tol	toluene
UV-Vis	Ultraviolet-visible spectroscopy
z	charge

Compound Index

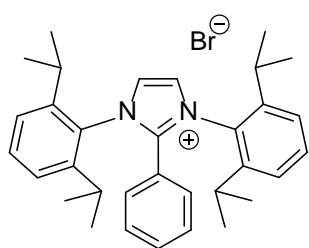




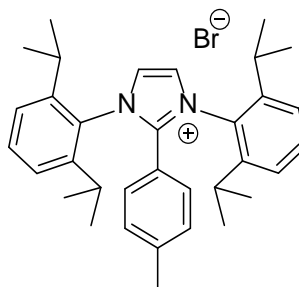
15



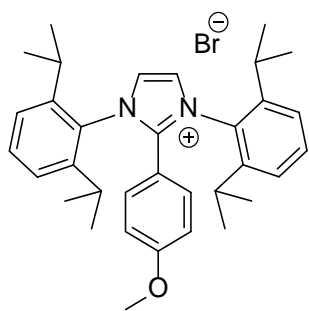
19



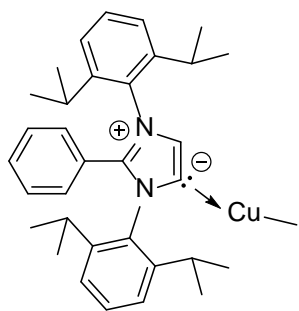
20



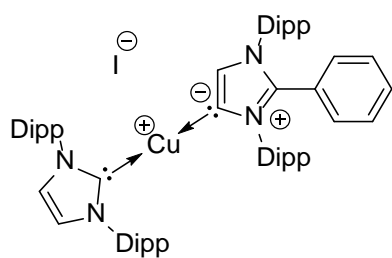
21



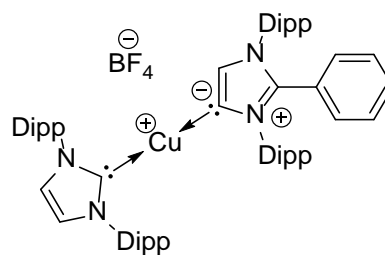
22



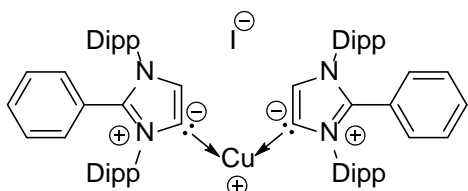
26



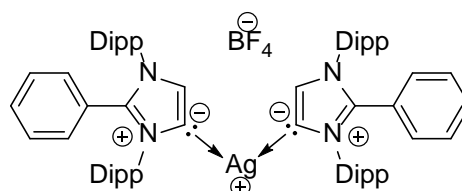
27



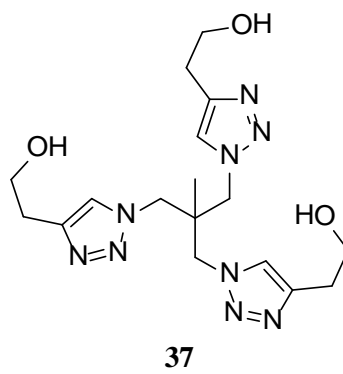
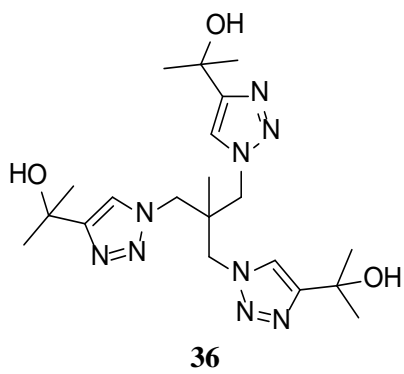
27a



28



29



1. Introduction

1.1. Carbenes

In general, carbenes are neutral compounds featuring a divalent carbon atom. The valence shell of the carbene carbon atom contains only six electrons, which classifies it as an electron deficient compound. Carbene compounds tend to be highly reactive and therefore usually exist as intermediates in organic transformations.

In the early 19th century *Dumas et al.* assumed methylene as the smallest thinkable carbene. Using a hygroscopic compound like concentrated sulphuric acid they tried to experimentally dehydrate methanol.^[1] Nowadays it is known that their reaction conditions just lead to dimethylether.^[2] Some names of scientists have to be mentioned who worked on the fundamental understanding of carbenes in the early days of this research field. *Nef* presented his general understanding and the chemistry of the methylene in an remarkable essay in 1897 (*Nef*).^[3] During the following century many scientists worked on dihalocarbenes (*Geuther*)^[4], highly-reactive transition states of carbenes (*Buchner*)^[5] and transition metal carbene complexes (*Tschugajeff*).^[6]



Figure 1.1: Lewis diagram of methylene.

The electronic structure of the methylene is directly influencing its geometry. The geometry of the ligand around the carbene carbon atom could either be linear or bent. To distinguish between the bent and the linear geometry of the carbene carbon atom sp^2 and sp -hybridisations were discussed for the methylene. The linear structure of the carbene could be referred back to a sp hybrid orbital of the carbene carbon atom and two pure p -orbitals. This configuration characterises the triplet carbene which could also be described as a diradical due to its electron distribution (Figure 1.2, right). The bent structure could be ascribed to the sp^2 -hybridisation of the carbene carbon atom. In this hybridisation mode carbene compounds tend to be more stable due to three sp^2 -orbitals which exhibit partial s character and is thereby energetically stabilised. The electrons can be distributed in two different ways. The two electrons could be paired in the sp -orbital, which leads to the singlet carbene ground state $\sigma^2 p_\pi^0$ (Figure 1.2). A triplet ground state ($\sigma^1 p_\pi^1$) could be reached if one electron occupies the sp -orbital and one electron occupies the p -orbital with parallel spin (Figure 1.2). There are two further, less stable singlet states known ($\sigma^0 p_\pi^2$, $\sigma^1 p_\pi^1$) which energetically lie too high in energy for significant occupations and will not be discussed any further.^[7]

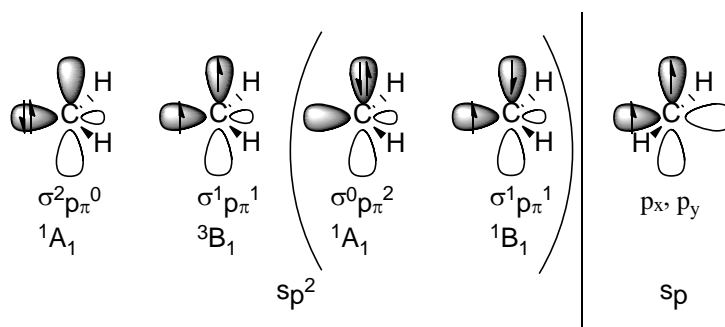


Figure 1.2: Orbital occupation of the electronic ground states of methylene.

A milestone in carbene chemistry was set in 1958 by *Breslow*, who increased the stability of carbenes through aminosubstituents.^[8] In 1960 *Wanzlick et al.* published the first stable *N*-heterocyclic carbenes (NHC) (Figure 1.3) characterised only by its chemical behaviour.^[9] Molecular weight measurements did not support their discovery at that time. Later on they could describe the so called “*Wanzlick equilibrium*” between a monomeric and a dimeric structure, which fits properly to their earlier molecular weight measurements.^[10] Since these discoveries it was actually possible to synthesise a crystalline, dimeric carbene precursor for further research.

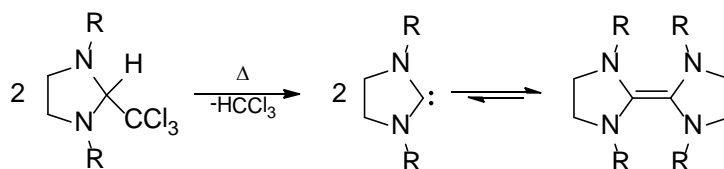


Figure 1.3: The synthesis of a NHC and the following dimerization called the “*Wanzlick equilibrium*”.

In 1964 *Fischer* and *Maasböl* discovered the first transition metal carbene complex which is nowadays known as the *Fischer carbene complex* (Figure 1.4).^[11] A nucleophilic attack of methyllithium (MeLi) at a carbonyl ligand of the tungsten hexacarbonyl complex ($\text{W}(\text{CO})_6$) yields $(\text{CO})_5\text{W}(\text{C}(\text{Me})\text{OLi})$. After a protonation followed by a methylation with diazomethane the *Fischer carbene complex* $(\text{CO})_5\text{W}=\text{C}(\text{Me})\text{OMe}$ could be obtained.

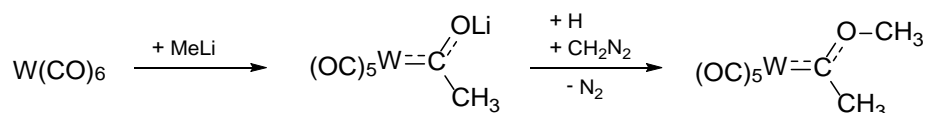


Figure 1.4: Synthesis of the first metal carbene complex by *Fischer*.

The *Fischer* carbenes are characterised by a metal centre in a low oxidation state. Furthermore, a heteroatom (e.g. oxygen or nitrogen) is connected to the carbene carbon atom which possesses p-donor strength to stabilise the carbene. *Fischer* carbenes are based on the σ -donation of the lone pair electrons of the carbene to an empty d-orbital of the metal, and π -backbonding from a filled metal d-orbital to the unoccupied p-orbital of the carbon atom.

In 1968 *Öfele* published the synthesis of chromium *N*-heterocyclic carbene complex (Figure 1.5).^[12]

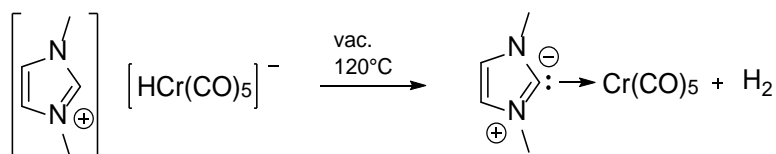


Figure 1.5: Transition metal carbonyl carbene complex by Öfele.

The decomposition of 1,3-dimethylimidazolium-hydrogen-pentacarbonylchromate(-II) under high vacuum at 120°C yields 80% of the transition metal-carbonyl-carbene complex which was further characterised using NMR spectroscopy, mass spectrometry and infrared spectroscopy.

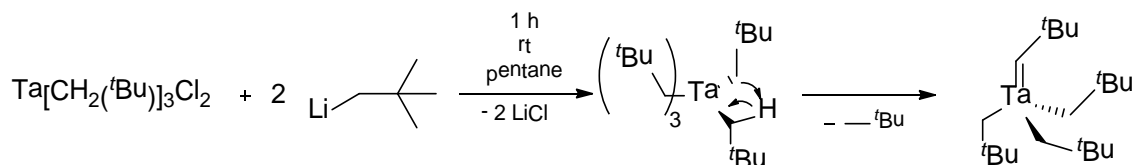


Figure 1.6: Synthesis of the first Schrock carbene.

Six years later Schrock presented another type of carbene complexes. The reaction of two equivalents neopentyl lithium with trineopentyltantal dichloride yields an orange solution, which could be characterized as $(\text{Me}_3\text{CCH}_2)_3\text{Ta}=\text{C}(\text{H})\text{CMe}_3$. From the transition state one equivalent of neopentane will be eliminated after the α -hydrogen abstraction.^[13] Schrock carbene complexes contain metal centres in high oxidation states and a hydrogen or carbon substituent at the carbene atom. Therefore, the carbene is not stabilized through these substituents.

The metal carbenes discovered by Fischer and Schrock differentiate through their bonding characteristics and as a result in their reactivity. Both classes of complexes underlie different types of carbenes. Fischer carbenes are singlet carbenes, Schrock carbenes are triplet carbenes. The singlet carbene in the Fischer complex shows two paired electrons occupying the sp^2 -hybrid orbital. The hybrid orbital can form a σ -donor bond with the unoccupied orbital of the metal. The p-backbonding occurred from the occupied d-orbital of the metal into the unoccupied p-orbital of the carbene carbon atom. Because of the dominant σ -donor bond the carbene carbon atom carries a positive charge and reacts thereby as electrophile. In Schrock carbenes each electron occupies the sp^2 -hybrid orbital and the p-orbital. These orbital could interact with the occupied orbital of the metal. Two covalent bonds were formed which were polarized towards the carbene carbon atom, which gives the carbene carbon atom a negative charge and a nucleophilic reactivity.

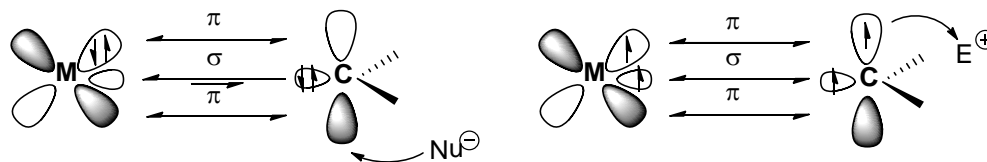


Figure 1.7: Bonding situation and reactivity of metal carbene complexes.

In 1989 Bertrand *et al.* presented the synthesis of the first stable, acyclic carbene (Figure 1.8).^[14] They could prove the carbene character of this compound performing and analysing different following reactions e.g. cyclopropanation reactions, oxirane formation or [1+1]-addition to isocyanides.

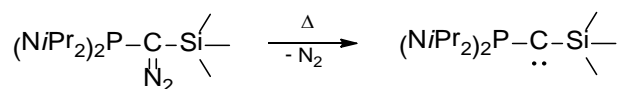


Figure 1.8: Thermolysis of [bis(diisopropylamino)phosphine](trimethylsilyl)diazomethane by *Bertrand et al.*

Hereafter, *Arduengo et al.* proved stable carbenes when they synthesised imidazole-2-thiones via a carbene intermediate that turned out to be stable under aqueous conditions (Figure 1.9).^[15] This patent was the beginning of their effort towards stable NHCs which *Arduengo et al.* finally presented several years later based on this accidental, but ground-breaking discovery.

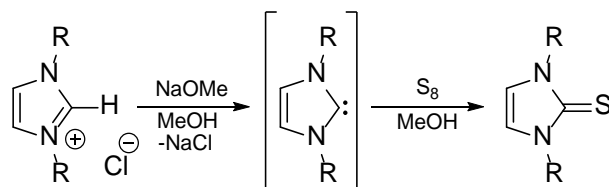


Figure 1.9: Industrial synthesis of imidazolin-2-thiones including the carbene as a plausible transition state.

It was again *Arduengo et al.* who published the synthesis of the first stable NHC in 1991.^[16] They used sterically demanding adamantyl (Ad) ligands as residues and prepared the NHC from the imidazolium chloride by using sodium hydride (NaH) and a catalytic amount of dimethyl sulfoxide (DMSO) in tetrahydrofuran (THF) (Figure 1.10, C).

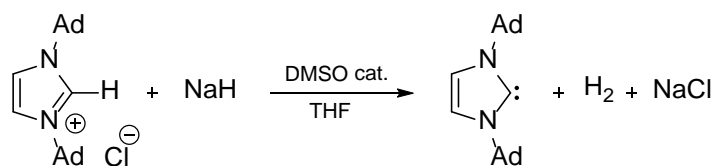


Figure 1.10: The first stable *N*-heterocyclic carbene by *Arduengo et al.*

This stable nucleophilic carbenes should allow convenient investigations of NHCs.

In 1995 *Grubbs et al.* developed a series of ruthenium based *Schrock* carbenes which are nowadays widely used as efficient metathesis catalysts. Four years later they published about a more stable and active second generation *Grubbs'* catalyst, in which one phosphine ligand was replaced by a NHC ligand (chapter 0, Figure 1.22). For the development of these catalyst and their metathesis reactions the Noble Prize in chemistry 2005 was awarded to *Yves Chauvin*, *Robert H. Grubbs* and *Richard R. Schrock*, underlining the importance of catalysis and catalyst manipulation.

1.2. *N*-Heterocyclic Carbenes

Synthesis

Coming back to the discovery of *Arduengo et al.* the known carbenes from the “*Wanzlick* equilibrium” could be stabilised and isolated. NHCs extended the field of carbenes, representing also a divalent carbene carbon atom like methylene.^[17]

Different routes are available to alkylate 1*H*-imidazole. One possibility is the nucleophilic substitution at the nitrogen atom of the 1*H*-imidazole. It is then possible to symmetrically or

asymmetrically N, N' -alkylate the 1*H*-imidazole depending if the reaction is done in one step or two.^[18]

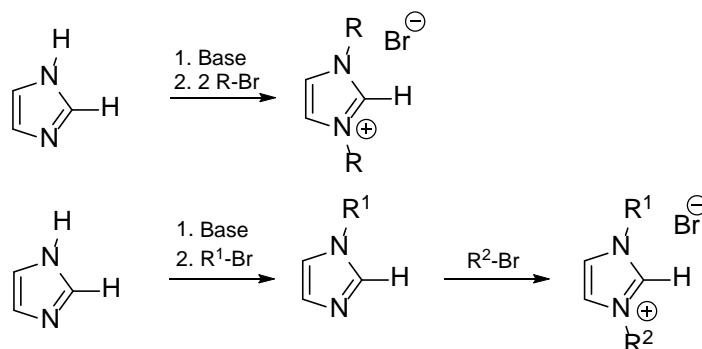


Figure 1.11: Symmetric and asymmetric N, N' -alkylation of 1*H*-imidazole.

Kuhn et al. developed a method for the synthesis of imidazol-2-thione. It is a condensation reaction of a α -hydroxyketone with a N, N' -substituted thiourea. The imidazole-2-thione could then reductively desulfonated with potassium to yield the free carbene.^[19]

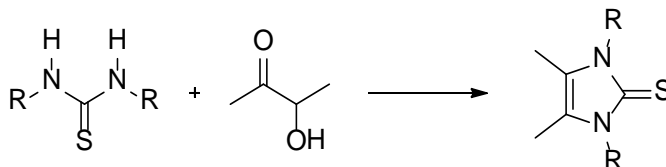


Figure 1.12: Synthesis of imidazolium-2-thione.

Another way to synthesize a free NHC is the reaction of the imidazolium chloride salt in a solvent mixture of ammonia and THF with a stoichiometric amount of sodium hydride. The reaction has to be performed at minus 30°C for just a few minutes and delivers pure product after evaporation of the ammonia.^[20] The preferred and therefore used synthesis is a two-step reaction leading to the imidazolium chloride salt which is further deprotonated to obtain the free NHC.

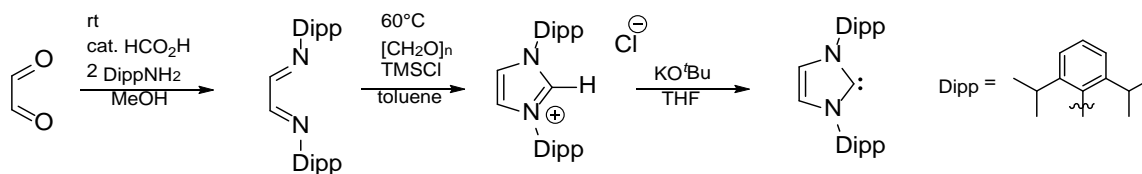


Figure 1.13: Three step synthesis of a NHC.

Stability

NHCs are thermally stable and mostly feature a singlet ground state. The environment of the carbene carbon atom in a NHC affects its steric and electronic effect and controls the multiplicity of the carbene ground state. It is well established that the singlet ground state is promoted by σ -electron withdrawing and electronegative substituents. σ -electron donating substitutions promote the triplet ground state. Furthermore, the mesomeric effect plays an important role for the stability of the ground state. The substituents at the carbene carbon atom could be classified in three categories. The first category provides π -electrons for the carbene carbon atom, while the second withdraw π -electrons from the carbene carbon atom. The third category are carbon atoms which are part of a conjugated system.^[21]

Nevertheless, most of the linear π -acceptor substituted carbene centres are in the singlet ground state. The mixed case of a π -acceptor and a σ -donor substituent at the carbene carbon atom shows almost linear geometry like the phosphanyl(silyl)carbene $(R_2N)_2P-C-SiR_3$ (Figure 1.14) or (phosphanyl)(phosphonio) carbenes reported by *Bertrand et al.*^[22] Moreover, conjugated systems can stabilise triplet carbenes from μs to at least several minutes.^[23] However, more essential for this discovery was the steric factor which minimises the risk of dimerization to olefins and suppresses the reaction with oxygen.^[23-24]

In the case of two π -donors as substituents at the carbene carbon atom the singlet carbene is bent at the carbene centre and therefore stabilised. The four-electron-three-centre π -system in this motif suggests a partial multiple bond character and is represented for example in diaminocarbenes, dimethoxycarbenes and dihalocarbenes. The electronic structure of heterocyclic five membered carbenes and especially the NHCs are well characterised by theoretical and experimental means.^[25] *Bertrand et al.* discussed the impact of different heteroatoms as direct neighbour of carbene carbon atoms and their influence on the stability of these compounds.^[26] Three different ways have been presented maintaining the electro neutrality of the carbene centre and therefore stabilising the singlet carbene.^[27] The π -donor, σ -acceptor ligands lead to a bent structure like in most NHCs. The electron density of the lone pair at the donor atom (i.e. nitrogen) is donated into the unoccupied p-orbital of the carbene carbon atom (Figure 1.14, I). Likewise, the electron density of the carbene carbon atom will be reduced by the σ -acceptor influence of the heteroatom. The stabilisation of the linear carbene (Figure 1.14, II) arises from the π -accepting properties of the heteroatoms (i.e. boron). The electron density of the carbene carbon atom could be transferred to the p-orbitals of the heteroatom while at the same time the heteroatom has a σ -donating effect.

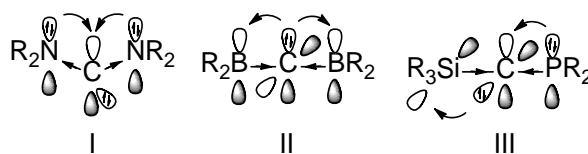


Figure 1.14: Stabilisation of the carbene atom.

A combination of a π -donating, σ -accepting heteroatom and a π -accepting, σ -donating heteroatom will also stabilise the linear carbene carbon atom (Figure 1.14, III).

The most popular NHCs are the diaminocarbenes which consist of a five membered ring in which two nitrogen atoms enclose the carbene carbon atom. If one nitrogen atom is replaced by another heteroatom, such as sulphur or oxygen the heterocyclic structure is still named as NHC. The basic motifs for NHCs are therefore imidazole, thiazole and oxazole (Figure 1.15, A-C). But also triazole and pyrazole basic frameworks are used to generate carbene ligands (Figure 1.15, D-F).



Figure 1.15: N-heterocyclic base frames (A-C). Basic structures: Triazole-, pyrazole- and imidazole-carbenes (D-F).

Nevertheless ring sizes from four to seven membered rings have been synthesised and characterised (Figure 1.15, G-I).^[28]

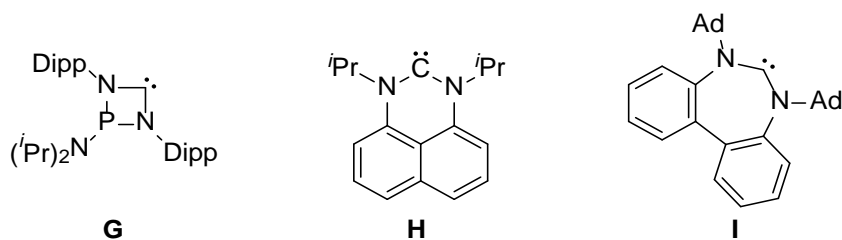


Figure 1.16: Examples of four-membered NHCs by *Grubbs et al.* (G), six-membered NHCs by *Richeson et al.* (H), and seven-membered NHCs by *Stahl et al.* (I).^[29]

In all these cases the steric demand of the residues at the nitrogen atoms (iPr, Dipp, Ad) is relatively high. In the instance of the six- and seven-membered ring systems an increased steric demand at the carbene backbone is mandatory. Apart from these NHCs different cyclic and acyclic carbenes are known, too. Till the beginning of the 21st century all known stable carbenes which were not diaminocarbenes comprise a heteroatom substituted carbene centre. During the last fifteen years cyclic and acyclic mono- and di-heteroatom substituted carbenes were synthesised as shown in Figure 1.15 (J-N).^[30] The most extensively studied NHCs are among the three groups of triazols-, pyrazole- and imidazole-carbenes (Figure 1.15, D-F).

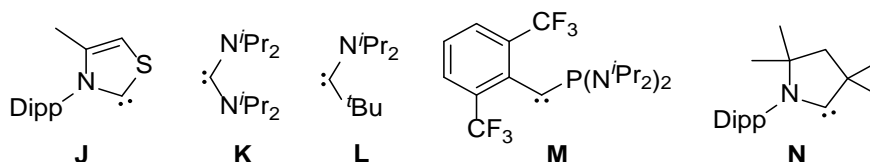


Figure 1.17: Selected carbenes reported before 2004 (J-N).

The main reasons why these diaminocarbenes are so well understood is the facile access, the impressive stability of the free carbene and the remarkable coordination behaviour towards metal centres. Due to the steric and electronic properties of the NHC, the σ -donor strength is much higher compared to the electron-richest phosphine ligands.^[31] Although the electronic structure of phosphines and NHCs are quite similar, they have a major difference in their topology. The geometry of the metal coordinated phosphine is trigonal pyramidal and the metal is therefore not sterically shielded. The phosphine ligands have a direct influence on the donor atom. In contrast, the ligands at the NHCs nitrogen atoms are typically bent towards the carbene centre (chapter 1.2) and therefore towards the coordinated metal, which increases the impact of the substituents on the metal.^[32] An advantage of both classes of compounds is the steric and electronic tuning ability. The basic imidazole structure allows a tuning at the nitrogen atoms and the possibility to functionalise the backbone carbon atoms (C4/C5). The former determines the steric bulk of the ligand and has only less effect on the electronic density at the carbene carbon atom. The latter has a greater influence on the heterocyclic moiety and therefore on the electronic properties. In Figure 1.18 the simplified representation of the frontier orbitals of an NHC as well as their interaction with the metals d-orbitals is shown.

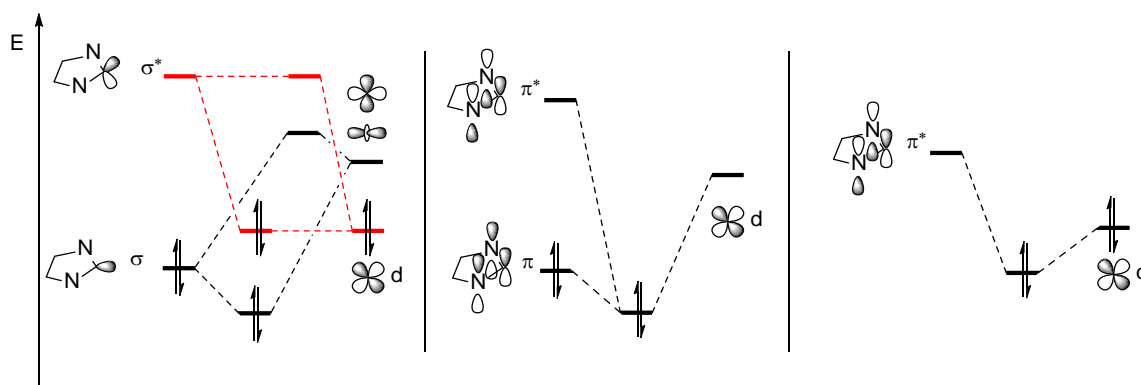


Figure 1.18: Simplified representation of the frontier orbitals and interaction with the d orbitals of a transition metal atom for NHCs. Adapted from Refs.^[33]

NHCs firstly were considered to be almost pure σ -donor ligands with the σ orbital (Figure 1.18, left) donating electrons to the molecular orbital of the complex. However, it was further suggested that the π - and π^* -orbital of the NHC can also contribute to the NHC-metal bond. Electron rich metal atoms are meant to donate electron from their d-orbital into the π^* -orbital of the NHC which is called π -backdonation (Figure 1.18, right). NHC also could stabilise electron deficient metals as shown in Figure 1.18 in the middle. Tertiary phosphines and NHCs have a similar electronic structure. The orbital interaction, donation from the σ -orbital into the d-orbital of the metal and backdonation from the metal to the phosphine, is absolutely comparable with the interaction of the NHC. Only the π -, π^* -interaction could not be observed for the phosphine which maybe the reason for the weaker donor ability of the phosphines. The NHC can therefore flexibly react to the constitution of the metal orbitals. Furthermore thermochemical investigations and calculations on different NHC-complexes have also shown that the NHC-metal bond is much stronger than the phosphine metal bond what makes the NHCs to very attractive ligands.^[34]

Until now, there is an ever increasing interest in the development of new stable *N*-heterocyclic carbenes and transition metal complexes especially for their application in catalysis, as easily shown by a SciFinder hit search of the keywords “carbene” and “*N*-heterocyclic carbene”.

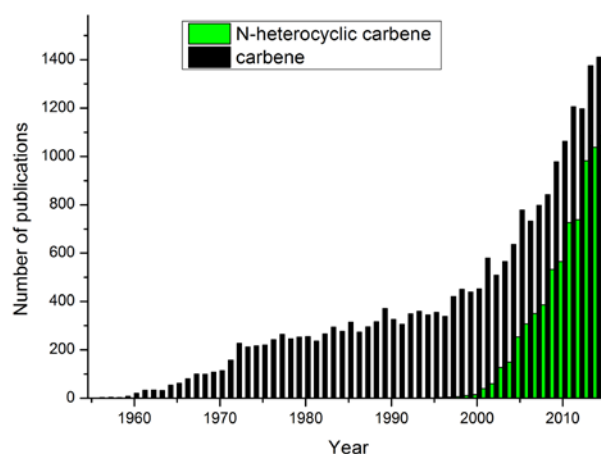


Figure 1.19: SciFinder search as obtained on 13.09.2016. Search results were taken as entered for the topic ‘carbene’ and ‘*N*-heterocyclic carbene’. Document type was refined to Journal, Letter, Report and Review. Duplicates were removed. Results were analysed by the publication year and exported.

Reports of carbene chemistry increased slowly from the 1950ies until 1990. With the first synthesis of a stable NHC the number of publications increased rapidly from about 450 per year to 1400 publications per year. This number is still increasing what indicates the actuality and advantages of this kind of chemistry in coordination chemistry and catalysis.

N-heterocyclic carbenes (NHCs) are extensively used as ligands in organometallic and transition metal chemistry. They are also found to be very efficient organocatalysts in synthesis.

In addition to homogeneous catalysis diverse class of main-group compounds, which were otherwise either detected under extreme experimental conditions or only studied *in silico*, have been stabilised by employing NHCs. Main group compounds-(Figure 1.20) and transition metal (Figure 1.21) complexes featuring an NHC ligand are remarkably stable and often exhibit high catalytic activity. NHCs continue to attract attention in the chemical society.

1												18
	2	13	14	15	16	17						
Li [35]	Be [36]	B [37]	C [38]	N [39]		F [40]						
Na [35f]	Mg [35d, 38c, 41]	Al [38c, 41b, 42]	Si [43]	P [37a, 44]	S [44b, 45]	Cl [46]						
K [35f, 47]	Ca [35d, 41a, 48]	Ga [42c, 42e, 49]	Ge [50]	As [37a, 44b, 51]	Se [44b, 45, 52]	Br [46b, 53]						
	Sr [35d, 41a, 48]	In [42c, 42e, 49b, 54]	Sn [43a, 50b, 50e, 50f]	Sb [37a, 55]	Te [44b, 56]	I [57]						
	Ba [41a, 48]	Tl [42e, 58]	Pb [50b, 50f, 59]	Bi [60]								

Figure 1.20: s- and p-block elements in the periodic table of elements of which NHC complexes exist. Complexes which show catalytic activity are marked in green.

3	4	5	6	7	8	9	10	11	12				
Sc [61]	Ti [35c, 62]	V [62a, 62b]	Cr [12, 62a, 63]	Mn [64]	Fe [64a, 65]	Co [64a, 66]	Ni [64a, 67]	Cu [68]	Zn [38c, 41a, 69]				
Y [35c, 61b, 62a, 70]	Zr [35c, 62a, 62b, 62d]	Nb [71]	Mo [63, 72]	Tc [64c, 73]	Ru [64a, 74]	Rh [75]	Pd [67, 75e]	Ag [75b, 76]	Cd [69]				
La [77]	Hf [62b, 62d]	Ta [78]	W [63, 72]	Re [64c]	Os [79]	Ir [80]	Pt [81]	Au [82]	Hg [69]				
Ce [83]		Nd [77b, 83]		Sm [70a, 77]	Eu [70]			Dy [77b]	Ho [84]	Er [70b, 77a]		Yb [70, 77a]	Lu [61b]
		U [85]											

Figure 1.21: f- and d-block elements in the periodic table of elements of which NHC complexes exist. Complexes which show catalytic activity are marked in green.

Grubbs' second generation olefin metathesis catalyst is the most prominent example of these types of compounds (Figure 1.22, right). The catalyst contains a transition metal and a carbene ligand, which has strong donor properties and therefore increases the stability of the complex. This makes the second generation catalyst more favourable compared to the first generation *Grubbs'* catalyst containing more labile phosphine ligands (Figure 1.22, left).^[86]

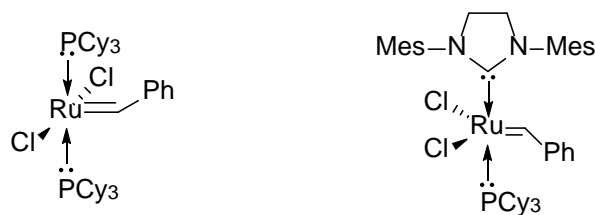


Figure 1.22: First generation *Grubbs'* catalyst (left) and second generation *Grubbs'* catalyst (right).

Numerous late transition metal complexes as well as main group complexes are known to be catalytically active (see Figure 1.20). C-C bond forming reactions, polymerisation, hydrosilylation and cross-coupling reactions are just a selection of what could be done with nNHC metal complexes (Figure 1.23).

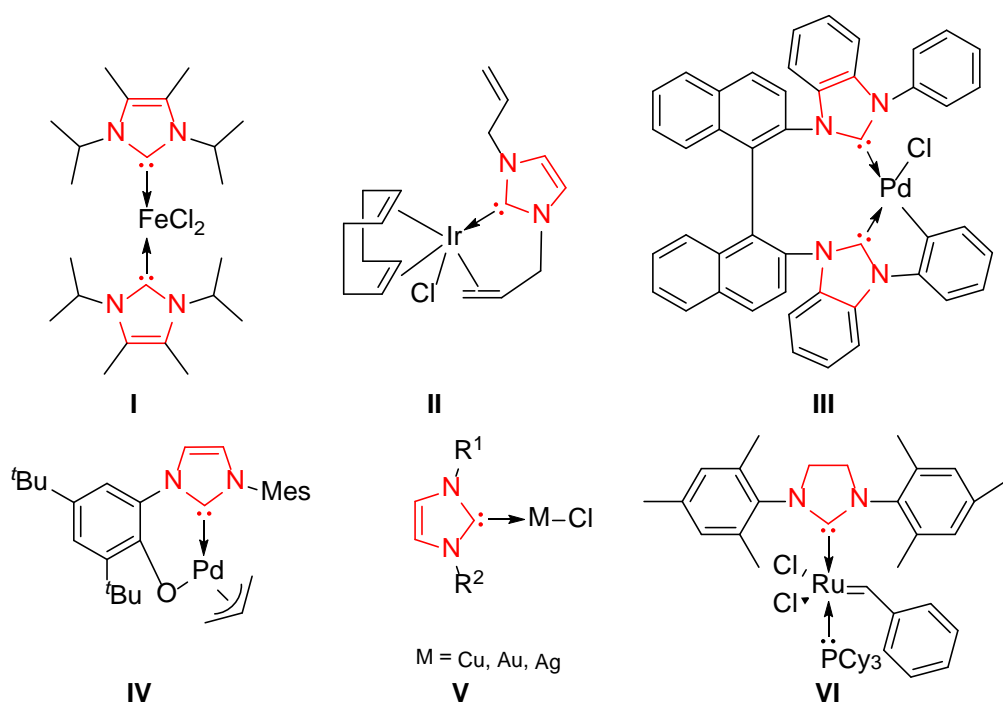


Figure 1.23: Different nNHC catalysts. **I:** Atom transfer radical polymerisation catalyst;^[87] **II:** Alkyne hydrosilylation catalyst;^[88] **III:** Friedel-Crafts reaction catalyst;^[89] **IV:** Suzuki-Miyaura cross-coupling catalyst;^[90] **V:** Catalyst for the carbonylation of boronic esters ($R^1 = iPr$, $R^2 = Mes$, $M = Cu$)^[91], Catalyst for [4 + 3] cycloaddition of allenedienes ($R^{1,2} = Mes$, $M = Au$)^[82c], Catalyst for the carbomagnesiation of enynes ($R^{1,2} = IMes$, $M = Ag$)^[76]; **VI:** Olefin metathesis catalyst.^[92]

Furthermore, chiral nNHCs could be a useful tool as catalysts in the total synthesis of pure enantiomers. Two selected examples are shown in Figure 1.24. Compound **A**, allows the enantio- and diastereoselective desymmetrisation of 1,3-diketones to generate the indane base frame for the natural product bakkenolide **S**.^[93] Compound **B** is a chiral *Grubbs* catalyst which is used for the desymmetrisation of trialkenes by an asymmetric ring closing reaction.^[94]

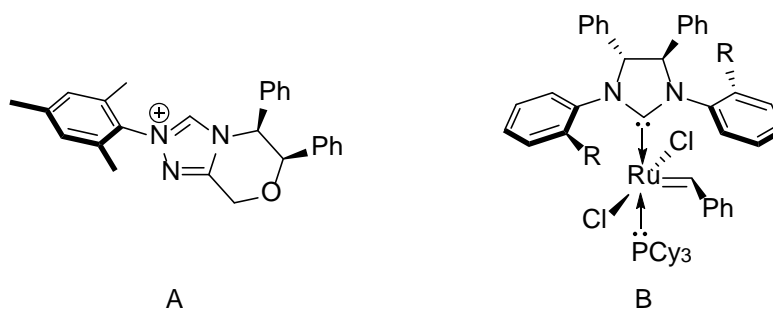


Figure 1.24: **A:** Chiral triazolium salt used in the synthesis of bakkenolide **S**. **B:** Catalyst for desymmetrization of triolefins ($R = \text{Me}$ or ^iPr).

Based on the manifold possibilities of tuning the electronic and steric properties, NHCs arouse a great interest among scientists. Especially their stabilising behaviour towards low-valent main group elements^[43b, 43d, 43j, 44e, 95] or complexes with metals in a high oxidation state^[96], convince scientists of the properties as capable ligands. Further research resulted in such diverse developments like imidazolium-based lipids (Figure 1.25, right)^[97], NHC-based pincer ligands as photosensitiser^[98], NHC-stabilised nanoparticles^[99], water soluble NHCs^[100] and plenty catalysts.^[68d, 94, 101]

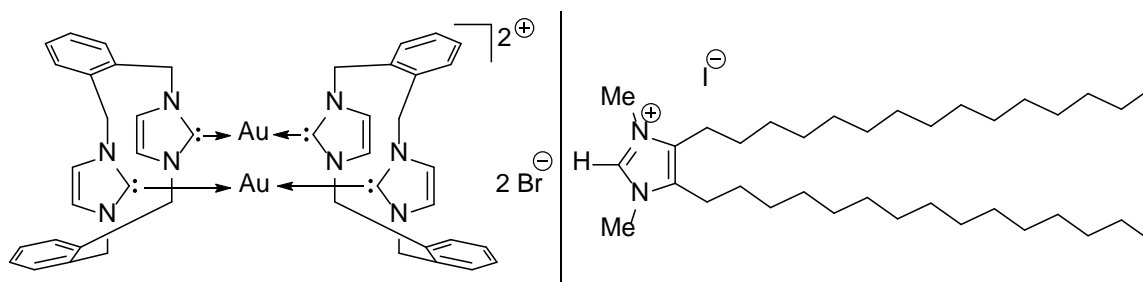


Figure 1.25: Dinuclear gold(I) carbene complex pairing antitumor activity with luminescence^[102] (left) and 4,5- C_{15} -1,3-dimethyl-1*H*-imidazolium iodide a imidazolium-based lipid with cytotoxic activity^[97] (right).

Furthermore NHCs are recognized as materials in different research fields like organic light-emitting diodes^[103], in medicine as drug or as theranostic (Figure 1.25, left)^[104], for polymerization^[105] or as ionic liquids.^[82a, 106]

1.3. Mesoionic Carbenes

Besides diaminocarbenes that are considered as normal NHCs (nNHCs), the classes of mesoionic carbenes (MIC)^[107] and remote *N*-heterocyclic carbenes (rNHC) extend the list of potential NHCs (Figure 1.26). rNHCs are defined through the position of the heteroatom. The heteroatom must not be next to the carbene carbon atom. rNHCs could also be MICs and nNHCs. Another term for MICs, which can be found in literature, is abnormal *N*-heterocyclic carbenes (aNHCs) but would not be used in this work. The feature of having just six valence electrons is on the contrary not an essential condition. Methylene (Figure 1.26, **A**) and a normal NHC (nNHC) (Figure 1.26, **B**) show an electron sextet. If the π -donation of an adjacent nitrogen atom is considered, the formal negatively charged carbene carbon atom fulfils an electron octet (Figure 1.26, **C**). This is also true for MICs like compound **D** (Figure 1.26) where no resonance structure could be written without formal charges.

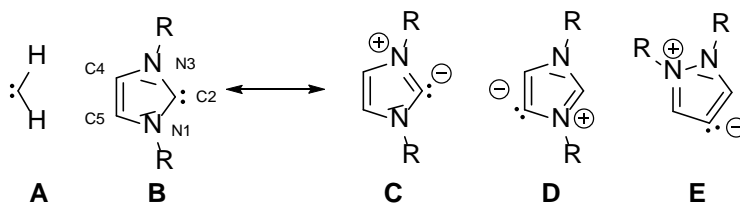


Figure 1.26: Methylene (A), nNHC (B), resonance structure of nNHC (C), MIC (D) and rNHC (E).

MICs show quite different electronic properties compared to nNHCs. Only one nitrogen moiety is stabilising the carbene atom so that the impact of the second nitrogen moiety is reduced. MICs are significantly more electron-donating owing to the lowered σ -withdrawal from the carbene carbon atom as indicated by the *Tolman* electronic parameter (TEP).^[108] Additionally to the stronger σ -donor properties MICs are described as weaker π -acceptors compared to their normal isomers.^[109] The TEP is an indirect measure of the donor strength of a donor ligand (phosphines or NHCs) measured by the CO stretching frequency of the ligand-NiCO₃ complex. Further details of the method are described at the end of the introduction.

For MICs the “*Wanzlick equilibrium*”, and therefore a dimerization of this compound is not possible, because two carbanions had to be combined. A closer look at the carbene bound to a metal makes clear that the nNHC and the MIC behave the same way. Both abandon their divalency and six valence electrons count to reach the stable tetravalent, octet character in the NHC-metal complex.

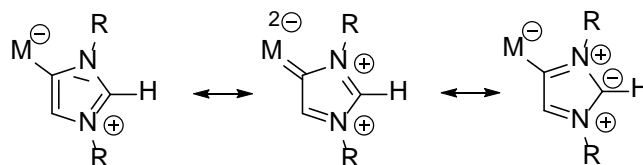


Figure 1.27: Metal coordination to a MIC and mesomeric structures.

Crabtree et al. published the first MIC iridium complex which was found by accident, as they investigated the reaction of a pyridine substituted imidazolium salt and an iridium hydride complex to give the chelate (Figure 1.28).^[110]

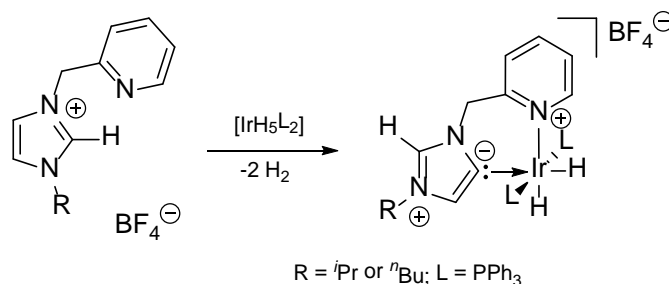


Figure 1.28: The first transition metal NHC complex with an abnormal binding mode.^[110]

The first free MIC was presented by *Bertrand et al.*^[111] In 2009 they synthesised *N,N'*-Bis(2,6-diisopropylphenyl)-*N*-(2-oxo-2-phenylethyl) benz-imidamide as a precursor in a condensation reaction with either tetrafluoroboric acid, hydrobromic acid or hydrochloric acid in acetic anhydride (Figure 1.29). After deprotonation of 1,3-bis(2,6-diisopropylphenyl)-2,4-diphenyl imidazole tetrafluoroborat with potassium hexamethyldisilazide they could isolate the free MIC

and characterise it by NMR spectroscopy and X-ray diffraction experiments.

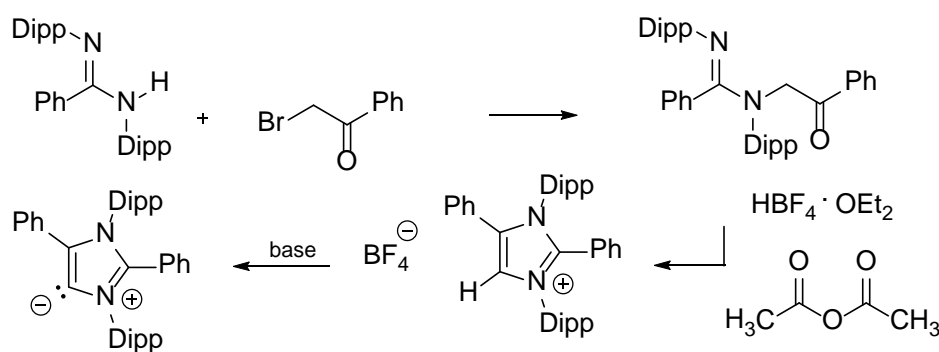


Figure 1.29: Synthesis of *Bertrand et al.* leading to the first free MIC in 2009.^[111]

Furthermore, *Frenking* calculated the $\text{p}K_{\text{a}}$ value of the parent imidazolium salt to be $\text{p}K_{\text{a}} \sim 33$ which is 9 $\text{p}K_{\text{a}}$ units higher than that for the loss of the C2 bound proton of IPr HCl.^[111-112]

MICs and its metal complexes are also used in organometallic chemistry and catalysis. Furthermore, MICs could be used for the same applications then their normal isomers. MICs containing light absorbing dyes for *Grätzel* solar cells or as photosensitizer are already known. Also medical applications are known from MICs complexes.

But as for nNHCs the main application is still catalysis. MICs are used in ring opening polymerisation reactions,^[113] in click chemistry,^[114] different coupling reactions,^[115] hydrosilylations,^[114b] hydrohydrazinations,^[116] hydrogen transfer reactions^[117] and furan-yne reactions (Figure 1.30).^[118]

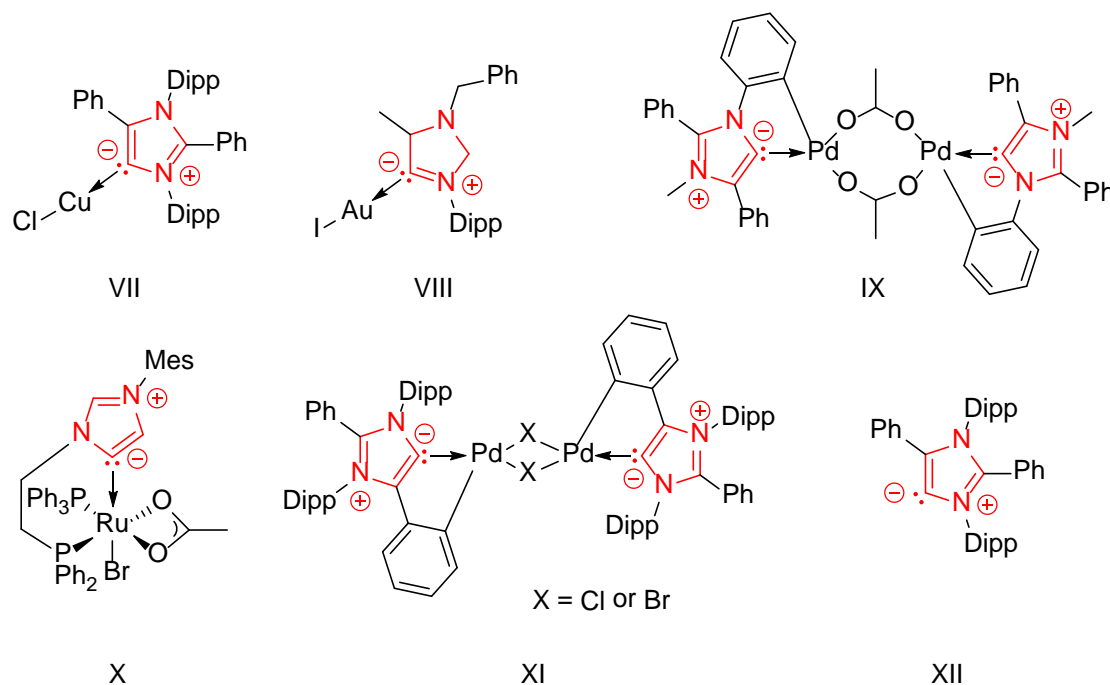


Figure 1.30: Selected MIC catalysts. **VII:** Click Chemistry catalyst;^[114c] **VIII:** Catalyst for the hydrohy-drazination of terminal alkynes;^[116] **IX:** Oxidative *Heck* coupling catalyst;^[115e] **X:** Ruthenium catalyst for hydrogen transfer reactions;^[117c] **XI:** Catalyst for the activation of aryl halides in *Suzuki-Miyaura* cross couplings;^[115c] **XII:** Catalyst for the ring opening polymerization of cyclic esters.^[113]

1.4. C2-Arylation Strategies and Synthesis of Mesoionic Carbenes

In order to isolate an MIC, different synthetic approaches can be made. The first proven option is the blocking of the C2-position of the NHC with an aryl group. Blocked C2-positions with alkyl groups mostly lead to migration of the alkyl group to the C4/C5-position upon deprotonation.^[119] *Bertrand et al.* showed this behaviour for the reaction of IPr with benzoyl chloride. The migration of the benzoyl group takes place upon deprotonation of the C4 position (Figure 1.31).

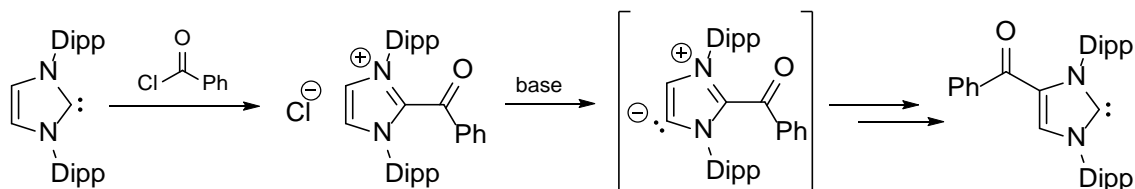


Figure 1.31: Migration of the substituent at the C2 position upon deprotonation of the C4 position.

They could show that the migration process involves the formation of a short living MIC that reacts as a nucleophile with the protonated form generating a bis-adduct and free IPr. The nucleophilic IPr itself reacts again with the bis-adduct to yield the C4 functionalised product of Figure 1.31 and regenerate the C2 blocked precursor salt.

Another method uses the variation of the side arms leading to an asymmetric imidazolium salt. Because of the different steric demand of the side arms the metal phosphine complex gives a selective C-H oxidative addition reaction to yield an MIC (Figure 1.32).^[120]

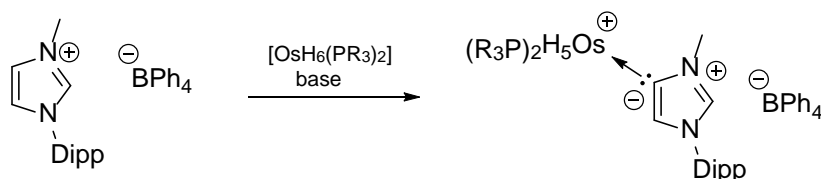


Figure 1.32: CH oxidative addition of a metal phosphine complex to an asymmetric substituted imidazolium salt.

A third possibility is the linking of two C2 blocked NHCs through a methylene bridge between the imidazole nitrogen atoms. The forced chelating effect of the imidazolium salt ensures the deprotonation at the backbone protons in the applied direct metallation procedure (Figure 1.33).^[121]



Figure 1.33: Chelating bis-MIC ligand complexing a Pd(II) atom.

In 2010, *Robinson et al.* synthesised the first anionic *N*-heterocyclic bis-carbene (NHBC) polymer.^[35e] This compound contains a normal and a deprotonated C4-position in the same imidazolium ring. They prepared the NHBC by lithiation of IPr in hexane and generated the polymeric structure by adding THF or *N,N,N',N'*-tetramethylethylenediamine (TMEDA) as donorbase (Figure 1.34).

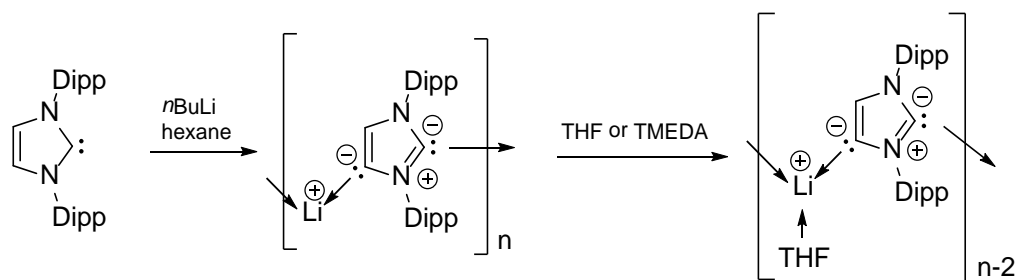


Figure 1.34: Synthesis of the anionic NHBC and its polymer by *Robinson et al.*

The NHBC could be used for further manipulations as a valuable precursor for MICs.

1.5. Methods to Quantify the Steric and Electronic Properties of NHCs

In this chapter a short description of typical methods which were employed to characterise NHCs should be given. Powerful and state of the art methods to determine the donor ability of NHCs utilise infrared spectroscopy (IR) and nuclear magnetic resonance spectroscopy (NMR). Furthermore, computational chemistry is used to estimate steric parameters of NHCs and ultraviolet-visible spectroscopy (UV/Vis) is applied to determine their pK_a values.

Tolman Electronic Parameter

The most commonly used method to determine the electronic properties of NHCs is the *Tolman* electronic parameter (TEP)^[122], which was originally developed to determine the electronic properties of tertiary phosphines^[123]. Metal carbonyl complexes like $[\text{Ni}(\text{CO})_3(\text{L})]$ (**A**), $[\text{IrCl}(\text{CO})_2(\text{L})]$ (**B**) and $[\text{RhCl}(\text{CO})_2(\text{L})]$ (**C**) are used to determine the σ -donor strength of a ligand by measuring the IR stretching frequencies of the carbonyl ligands (Figure 1.35). **A** was the first complex which was used for determination the TEP followed by **B** and **C**.

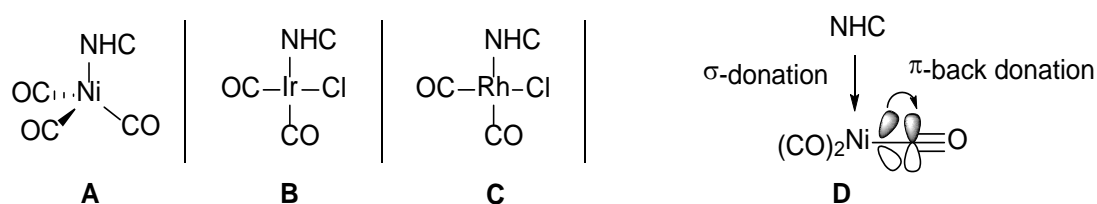


Figure 1.35: Metal carbonyl complexes which are used for IR measurements (**A-C**). Graphical description of the TEP method (**D**).^[124]

Depending on the electron density at the metal centre the IR stretching frequencies of the carbonyl ligand changes. If more electron density is concentrated at the metal, the metal–carbon bond is strengthened due to π -backbonding into the π^* -CO anti-bonding orbital (Figure 1.35, **D**). However, this weakens the carbon-oxygen triple bond resulting in a reduced bond-stretching vibrational frequency. If the metal is on contrast less electron-rich, fewer π -backbonding will occur, and therefore the carbon-oxygen triple bond is stronger with an increased $\nu(\text{CO})$. One can then compare the electronic properties (σ -donating abilities) of different carbene ligands by evaluating the IR stretching frequencies of the chosen metal-complexes. The TEP is the vibrational stretching frequency of the normal mode with A_1 symmetry (approx. 2050-2100 cm^{-1}).

The IR measurements are subject to restrictions. They are strongly solvent-dependent so that for a meaningful comparison the same solvents should be used. A general drawback of this method is that, the measurement of the CO stretching frequency on the NHC metal carbonyl compounds is an indirect measurement of the π -donating ability of the metal atom in the complex. For a better reliable determination of the NHC-metal bond-nature, the absolute electron density at the metal should be measured directly. For that reason, TEP values should be compared carefully also with respect to the saturation and substitution of the NHC. Nevertheless, the TEP is hence a good approximation for the π -donating ability of the metal centre and will therefore be used as a measure for the electronic properties of the NHC. As mentioned above, not only the nickel tricarbonyl ligand complexes are made to determine the TEP. Moreover, due to the high toxicity of nickel tetracarbonyl other transition metal carbonyl complexes had to be found to measure the TEP. Iridiumchloride dicarbonyl ligand $[\text{IrCl}(\text{CO})_2\text{L}]$ and the rhodiumchloride dicarbonyl ligand complexes $[\text{RhCl}(\text{CO})_2\text{L}]$ were therefore prepared as alternative complexes. In both cases two carbonyl stretching frequencies are quoted due to the *cis* arrangement of the carbonyl ligand. As a lot of examples were measured for the iridium complex, NHC ligands can be compared to their nickel analogues with the help of a linear correlation between the nickel and iridium systems, which was first proposed by *Chianese et al.*^[125] and re-evaluated in 2008 by *Kelly et al.* (equation 1).^[31]

$$\text{TEP} = 0.847 \nu_{\text{av}}(\text{CO})[\text{Ir}] + 336 \text{ cm}^{-1} \quad (\text{equation 1})$$

Wolf and Plenio suggested the use of the rhodiumchloride dicarbonyl ligand complex to measure the TEP.^[126] Some more NHC complexes were synthesised from the rhodium species which allowed a correlation to the iridium complexes. The linear correlation between the iridium and the rhodium systems was repeatedly re-evaluated to give the final equation:

$$\nu_{\text{av}}(\text{CO})[\text{Ir}] = 0.923 \nu_{\text{av}}(\text{CO})[\text{Rh}] + 141.2 \text{ cm}^{-1} \quad (\text{equation 2})$$

With these two equations data from all three systems can be compared properly with minor uncertainties. In Figure 1.36 some selected examples are presented.

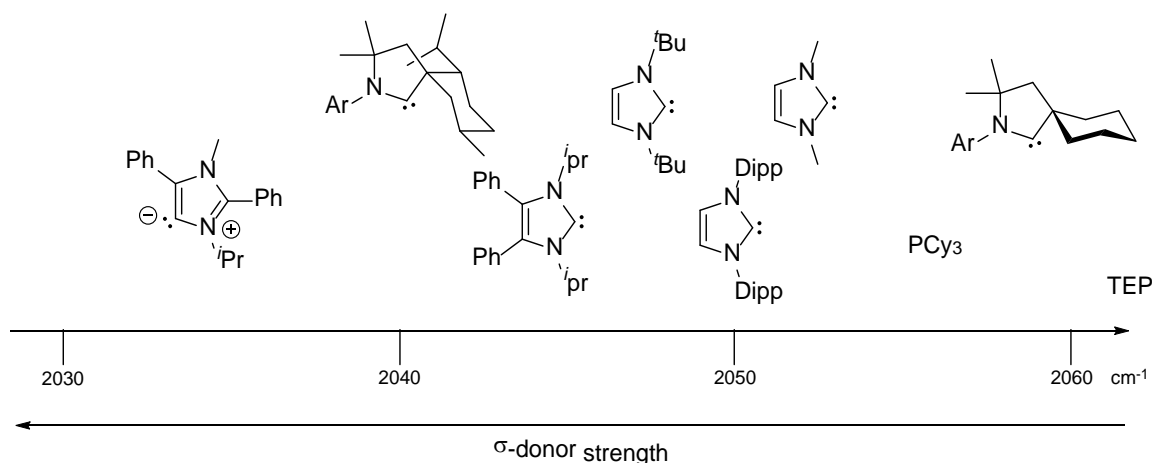


Figure 1.36: Classification of NHCs due to their estimated TEP values, from IR spectroscopy of $[\text{IrCl}(\text{CO})_2(\text{NHC})]$.^[124]

The Steric Parameter by Tolman

An early method to define a steric parameter for ligands like phosphines and NHCs was proposed by *Tolman*. He suggested measuring a cone angle θ in order to quantify the size of the ligand. For a phosphine compound the cone is defined with the metal atom at the vertex and the residues at the perimeter of the cone. This angle is named the *Tolman* cone angle θ and can be applied to any ligand (Figure 1.37, left).

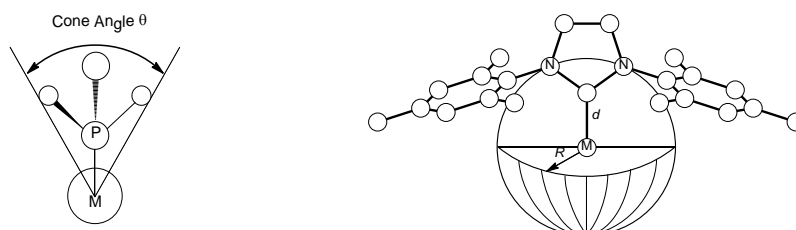


Figure 1.37: The Tolman cone angle (left). Graphical representation of the buried volume (%Vbur) of a NHC metal complex (right).

In order to measure the dimension of a large steric environment as in NHCs *Nolan et al.* proposed a method based on crystallographic data. *Nolan* defined a length (A_L) and a height (A_H) parameter along the M-NHC bond.^[127] But this early model supplies only rough data. Therefore *Nolan* and *Cavallo* developed the buried volume parameter (%V_{bur}), as an alternative model (Figure 1.37, right).^[34a] The steric demand is defined by the percentage of the space of a theoretical sphere around the metal centre which is occupied by a ligand in the first coordination sphere. This occupation value is calculated by the SambVca (**S**alerno **m**olecular **b**uried **v**olume **c**alculation) software developed by *Cavallo et al.*^[32]

For the calculation original crystallographic data has to be used. If just the ligand is available a fictive metal atom must be defined, which is coordinated to the ligand. The metal centre is then located perpendicular to the mass centre of the nitrogen atoms (X_N) (first coordination sphere of the carbene carbon atom) through the carbene carbon atom (Figure 1.38, left). Analogously one can approach phosphines with a mass centre of the three carbon atoms (X_C) and the perpendicular axis to the metal through the phosphorous atom (Figure 1.38, right).

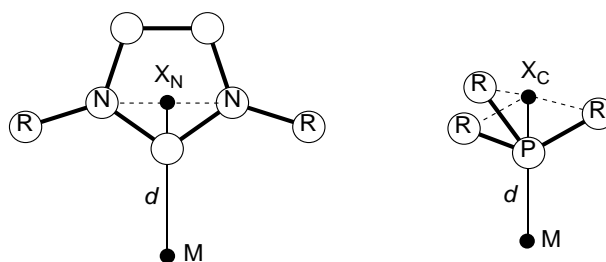
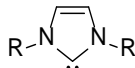
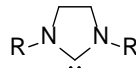


Figure 1.38: Positioning of the fictive metal atom in NHC (left) and PR_3 ligands (right).

Further values needed for the calculation, like sphere radius, M-(NHC) bond distance, mesh spacing and sets of atoms radii are available and pre-set. The bond distance and sphere radius is suggested by *Cavallo et al.* owing to DFT calculation results of a series of NHC complexes.

Table 1-1: Some selected % V_{bur} values for NHC ligands. Bond radii scaled by 1.17 for the atoms, radius of the sphere $R = 3.5 \text{ \AA}$.^[132]
 Mes = mesityl, Dipp = 2,6-diisopropylphenyl, Ad = Adamantyl.

Residues		
Me-	24.9	25.4
Et-	26	25.9
Ph-	30.5	31.6
Tol-	30.5	32.4
Mes-	31.6	35.7
Dipp-	33.6	35.7
^t Bu-	35.5	36.2
Ad-	36.1	36.6

The selection in Table 1-1 shows increasing % V_{bur} for various ligand residues of unsaturated and saturated NHC ligands. The values for the saturated NHCs are larger due to the slightly wider N–C–N angle due to the backbone saturation.

¹³C-NMR Measurements

The chemical shift is a proper tool to determine the electronic properties of ligands as the electronic environment of the nucleus is closely related to its shift.^[128] Moreover, the NMR measurement is much more precise than infrared experiments. In this method, $[\text{PdBr}_2(\text{}^i\text{Pr-bimy})(\text{L})]$ is used to measure the electronic properties. The dimer $[\text{PdBr}_2(\text{}^i\text{Pr}_2\text{-bimy})_2]$ is broken by two equivalents of the ligand to be tested (Figure 1.39).^[129]

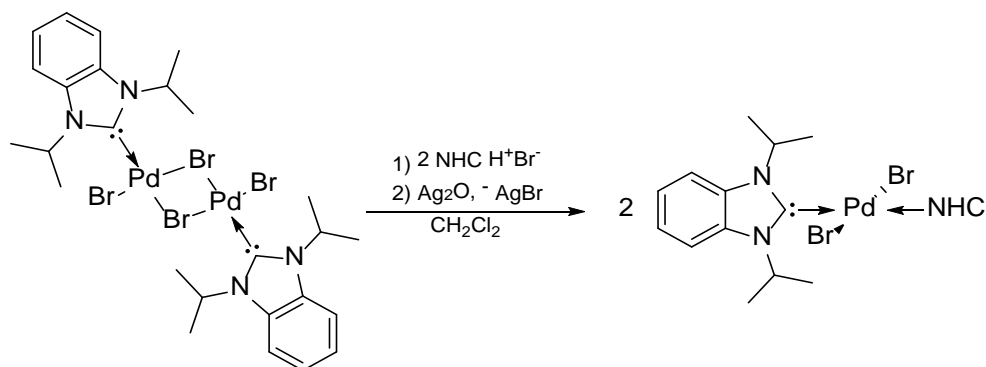


Figure 1.39: Synthesis of $\text{trans-}[\text{PdBr}_2(\text{}^i\text{Pr}_2\text{-bimy})\text{NHC}]$ complex.^[129]

Different ligands such as imidazoles, phosphines and *N*-heterocyclic carbenes have been measured using this method.

The best information about the compounds properties could be collected using a combination of the presented methods.

pK_a -Measurements

In this part I will, for the sake of completeness, outline the methods used to measure the pK_a value

of NHC salts. The Knowledge about the pK_a of the NHC salt which can be converted into the carbene in situ is advantageous. Whenever comparing pK_a values it is useful to notice the conditions these pK_a were measured because they are temperature and solvent dependent. Even though pK_a values have been measured for a broad range of compounds many known NHCs still lack this information. There are different methods to obtain the pK_a which will be shortly presented hereafter.

The deuterium method is used to determine the equilibrium constant.^[130] The method uses a particular reaction of the hydroimidazolium salt with deuterated water. The deuterium exchange reaction of the C2-proton of the imidazolium cation leads to an equilibrium state. Where mainly three compounds could be found in solution, from which one is the deuterated imidazolium cation (Figure 1.40, red). The deuterium exchange is hereby monitored by $^1\text{H-NMR}$ spectroscopy in buffered deuterated water (D_2O).

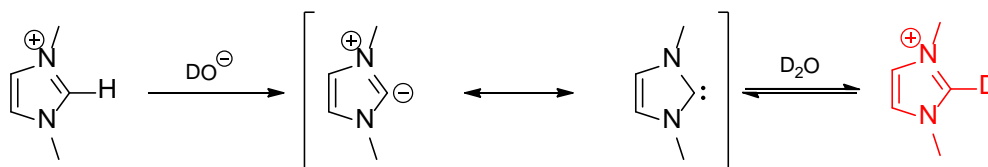


Figure 1.40: Deuterium Method for pK_a measurements.

The data is then used to obtain the pK_a values for ionization of these cations. Another process, which could be followed via $^1\text{H-NMR}$ spectroscopy, and therefore named NMR Method^[131], is the deprotonation ability of the carbene. Typical acidic hydrocarbons with known pK_a values are deprotonated by the compound of interest. The NMR signals can be integrated and related to each other to give the desired pK_a value.

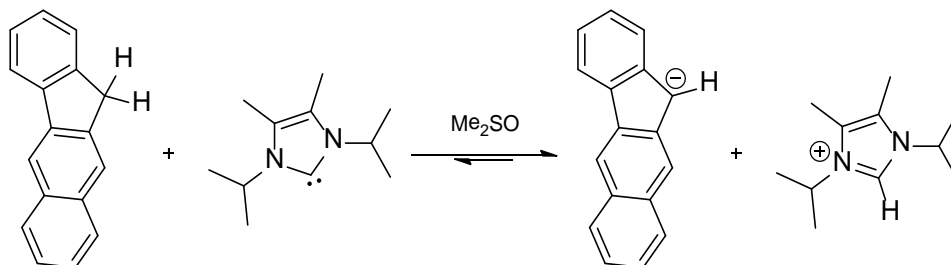


Figure 1.41: Reaction of 2,3-benzofluorene with 1,3-diisopropyl-4,5-dimethylimidazol-2-ylidene in dimethyl sulfoxide.

A further routinely used method to determine the pK_a value of an imidazolium moiety is called overlapping indicator method and uses UV/Vis spectroscopy.^[132] With this method the differences of the equilibrium acidity of the unknown acid relative to that of the indicator acid is measured by monitoring the changes of the UV/Vis absorption of the indicator or the unknown acid during the titration against each other.

At last computational methods could be used to determine the pK_a values of chemical compounds.^[133] In 2004 Yates *et al.* developed a computational method to determine highly accurate pK_a values.^[112] These calculations require a large amount of computational resources and time. After an initial geometry optimisation and frequency calculation, single point energies were calculated at three different levels of theory.

1.6. Scope

NHC ligands aroused major interests in catalysis during the last three decades. Furthermore, new carbon donor ligand design by the functionalization of NHCs evolved as an interesting research field, aiming at tailored electronic and steric properties of NHCs. During my master thesis I synthesised silyl-bridged NHBCs. Until now diarylsilicon bridged NHCs could only be synthesised carrying the carbene centre at the C2-position of the NHC moieties. These ligands feature an interesting scaffold for metal complexation in general may also enable the synthesis of bis-abnormal carbene complexes *via* an indirect deprotonation-protonation process that has been recently applied to mono-MIC iron and cobalt complexes.^[134]

The NHBCs to aNHBCs conversion should in principle be favoured due to the chelating effect offered by potentially bidentate ligands. However, such a conversion with NHBCs could not be observed with transition metals. Nickeldichloride, copperchloride, tris(triphenylphosphine)-rutheniumdichloride, tris(triphenylphosphine)rhodiumchloride, and palladiumdichloride were used in this experiments. Alternatively, protecting the carbene (C2) position of NHBCs with an aryl group and subsequent deprotonation should lead to the formation of aNHBCs

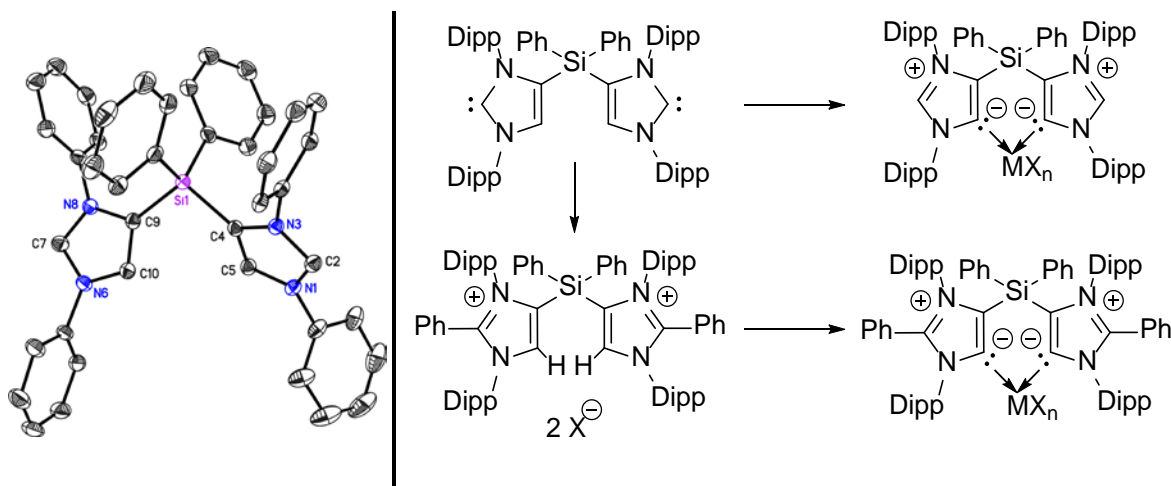


Figure 1.42: Diarylsilicon-bridged-NHBC compound (left); Aimed conversion of carbene centres (right).

Therefore, the development of a new synthesis strategy towards unconventional carbene ligands became necessary. Our major aim was to establish a synthetic strategy that would enable the efficient blocking of the C2-position with aryl substituents. The C2-blocking should be performed with an aryl compound, such as a phenyl group, to gain more electronic stabilisation. Afterwards the free MIC should be generated *via* deprotonation. Having these compounds in hand further reactions towards MIC transition metal complexes should be done. All new prepared compounds should be analysed and investigated focusing on their properties. Moreover, these complexes should be compared to well-known NHC compounds, which are often used in a large variety of catalytic reactions.

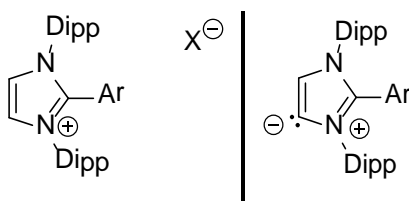


Figure 1.43: C2-arylated imidazolium salt (left); Free MIC with an unsubstituted C4-position (right).

With this work I would like to contribute some information of properties and catalytic activities of new unconventional NHC ligands and complexes to this extraordinary interesting research field.

2. Results and Discussion

2.1. The Synthesis of the *N*-Heterocyclic Carbene IPr

The 1,3-bis(2,6-diisopropylphenyl)imidazol-2-ylidene (IPr) (**1**) is a frequently used and extensively investigated nNHC. It was first reported by *Arduengo et al.* in 1999.^[135] Compound **1** is one of the most analysed NHCs known. Indeed, this NHC (**1**) is commercially available (Sigma-Aldrich: for 120 € per gram), indicating the importance and demand of **1**.^[136] Therefore, the IPr was an obvious choice for this work. Moreover, **1** can be readily prepared in large scale by literature procedures.^[137]

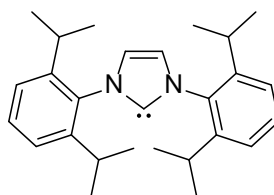


Figure 2.1: Lewis structure of IPr.

NHC **1** was prepared according to an adapted literature procedure.^[137] The first step in the synthesis of **1** is a condensation reaction of glyoxal with two equivalents of diisopropylaniline in the presence of a catalytically amount of formic acid which lead to the formation of a diazabutadiene (Figure 2.2, top). The crude product was washed with methanol and then dried to yield the analytical pure diazabutadiene in good yields of 85%. Even for up-scaled reactions starting with ~200 g diisopropylaniline a yield of 71% was obtained. The condensation is a rapid exothermic conversion of the starting materials after the catalysed initiation of the reaction.

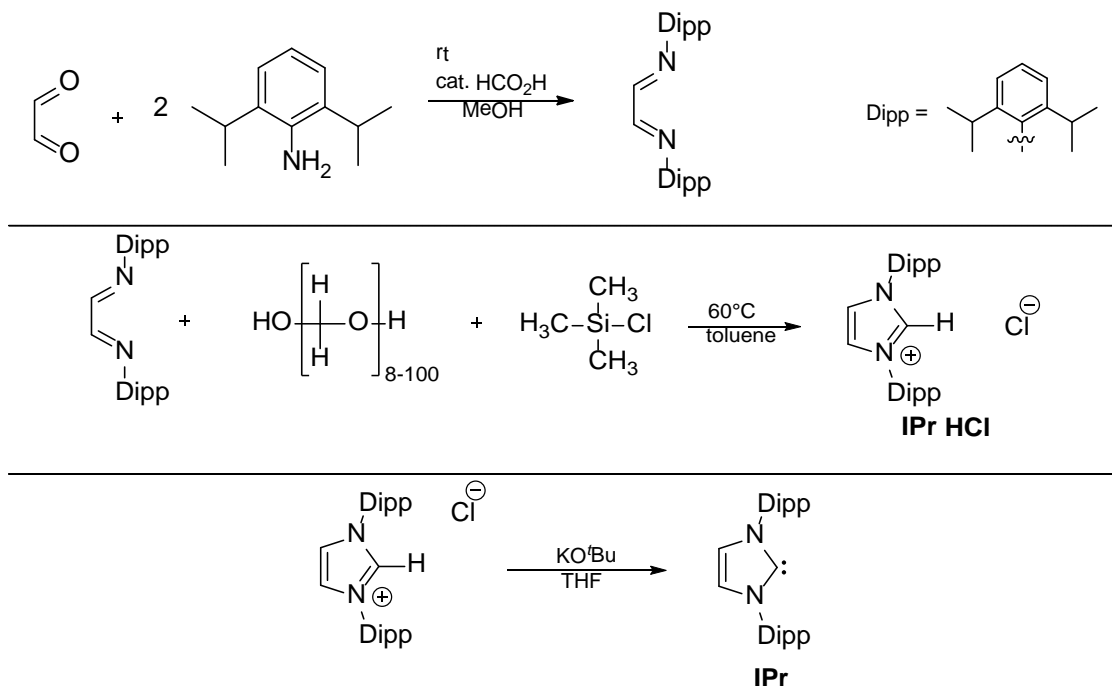


Figure 2.2: Reaction sequence yielding the diazabutadiene (top). 6 π electrocyclisation towards IPr·HCl (middle). Salt elimination reaction of IPr·HCl with KOtBu. (bottom)

In a 6π electrocyclisation of the obtained diazabutadiene with paraformaldehyde and chlorotrimethylsilane in 60°C warm toluene to yield the 1,3-bis(2,6-diisopropylphenyl) imidazolium chloride (IPr·HCl) (Figure 2.2, middle). The resulting suspension was filtered and washed with THF to obtain a white powder. The hydrochloride salt is stable and could be stored for years without decomposition. Finally IPr·HCl could be deprotonated in a salt elimination reaction with potassium *tert*-butoxide (KO^tBu) in THF using standard *Schlenk* techniques (Figure 2.2, bottom). The two white solids turn instantly brown. Filtering of the suspension afterwards leads to a brown solid in up to 91% yield. The carbene has to be stored under inert atmosphere in a flask or glove box. An approved method to minimise the risk of hydrolysis is to freshly prepare small batches for the following reactions instead of large batches, which have to be stored afterwards. Nonetheless **1** could be stored for months under inert atmosphere.

2.2. Functionalised bis-NHCs

Functionalization of NHCs is one of many methods of fine-tuning the properties of NHCs and opening a route to a new class of NHCs.^[35e, 43h, 119, 138] The perspective of direct access to functionalised NHCs from an NHC, especially with p-Block moieties is tremendous since it enables the innovative synthesis of new ligands. Phosphaalkene functionalised imidazole-2-ylidene were first observed by *Gates et al.*^[138a] Furthermore *Bertrand et al.* were able to develop a method to synthesise C4-substituted imidazole-2-ylidene only by deprotonation of a C2-substituted imidazolium salt.^[119, 138c] Functionalisation of an NHC has also been achieved with a silylene (IPrSiCl₂), when treated with adamantyl azide.^[43h] *Robinson et al.* followed a new route to a lithiated NHC, which led to easier access of a new ligand scaffold with remarkable properties and applications.^[35e] *Streubel et al.* could show that the reaction of 1-methyl-3-*tert*-butyl-imidazole-2-thione and *n*-butyllithium (*n*-Buli) in the presence of a phosphine affords a phosphine bridged di-thione. Unfortunately, the reaction of the di-thione with potassium metal does not lead to the phosphine-bridged NHBC but to a zwitterionic imidazolium phosphanide. Functionalised mono NHC compounds could be prepared before my investigations during the master thesis. But at that time no NHBC has been synthesised, what leads my focus on this type of compounds. Investigations in our group were focused on functionalised NHCs. Monomeric and dimeric structures could be synthesised.^[139] The aim was to connect two imidazole moieties *via* the C4 backbone carbon atom with a diarylsilyl spacer. NHBC (**4**) has been prepared in almost quantitative yield treating lithiated IPr (**2**) with an appropriate dihalosilane (Figure 2.3).

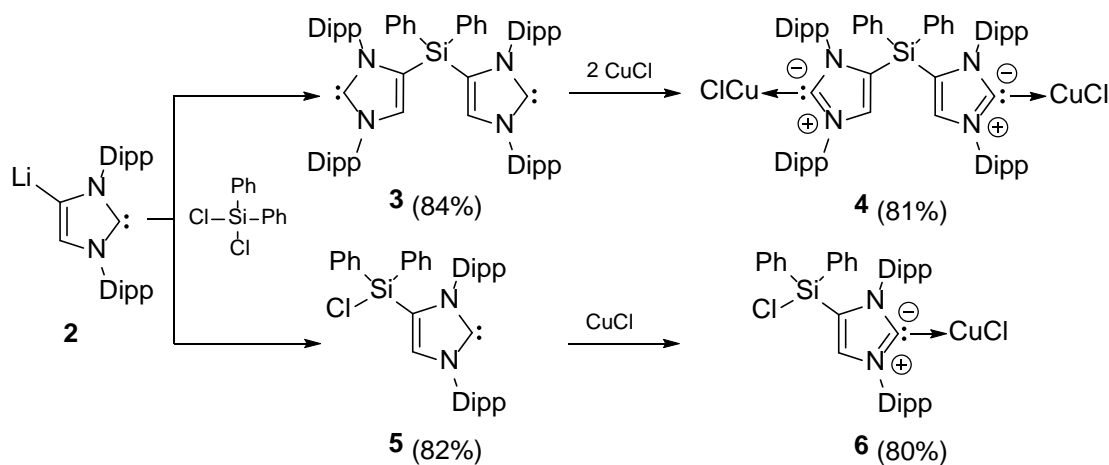


Figure 2.3: Synthesis of the NHBC, C4 functionalised NHC and its copper complex.

Furthermore, I could obtain the CuCl complexes of these functionalised NHCs. They are colourless, moisture sensitive crystalline solids which are soluble in THF and dichloromethane (DCM). The formation of **5** and **6** is supported by the appearance of the corresponding molecular ion peak in the EI-mass spectrum. Moreover, X-ray crystal structures could be obtained for compound **4** and **6**. Complex **4** crystallises in the orthorhombic space group *Pna*2₁. The molecular structure of **4** shows that each carbene centre coordinates one copper chloride moiety (Figure 2.4, left). The carbene copper distance of 1.89(5) Å and the C–Cu–Cl angle of 174.14° (av.) are consistent with other reported NHC-copper complexes. The Cu–Cl bond length of 2.11 Å (av.) may be assigned for terminal

CuCl .^[68b, 138c, 140] The four fold coordination of the silicon atom shows distorted tetrahedral geometry with a significant decrease of the C4–Si1–C9 bond angle of $98.63(14)^\circ$. Compound **6** crystallises in the monoclinic space group $P21/c$. The molecular structure of **6** shows a distorted linear geometry with a C2–Cu1–Cl1 bond angle of $174.02(5)^\circ$ (Figure 2.4, right). As expected for these metal complexes the N–C–N bond angle increases by 2.9° (av.).

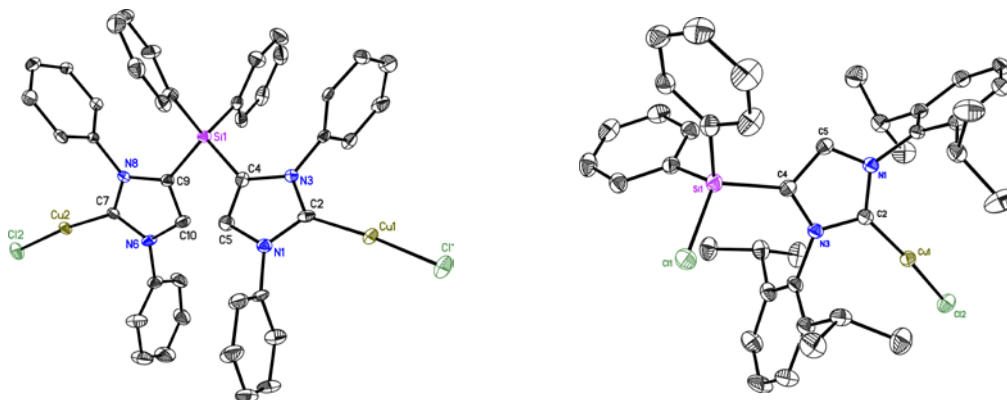


Figure 2.4: Molecular structure of NHBC copper complex (**4**)(left) and the C4 functionalised NHC copper complex (**6**)(right). Isopropyl groups for **4** and hydrogen atoms for **4** and **6** have been omitted for clarity. Anisotropic displacement parameters are depicted at the 50% probability level.

This bridged NHBC copper complex could potentially be used in catalysis although no experiments have been done until now. Furthermore, the ligand framework is of particular interest because of the steric bulk and two potential carbene centres at the backbone to gain a pincer type ligand. The synthetic problem that has to be solved is the blocking of the C2-positions of both sides and the subsequent deprotonations of the backbone carbene atoms have to be achieved. These reaction sequences will most certainly direct to a salt formation in the ligand metal complex, what is beneficial for catalyst storage and handling. On that score synthetic strategies have been developed to block the C2-position, which will be presented hereafter.

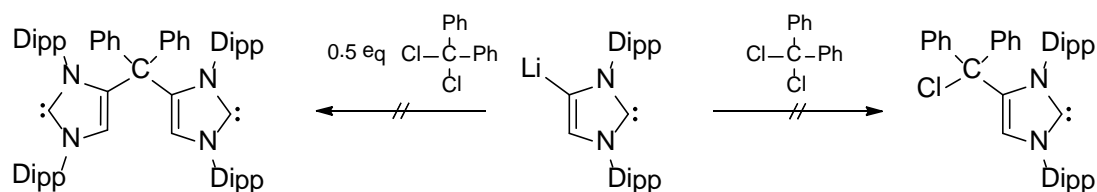


Figure 2.5: Unsuccessful reaction of Li-IPr with different equivalents of dichlorodiphenylmethane.

Further experiments have been done trying to synthesise carbon bridged NHCs. These reactions were performed following the same procedure as reported for the silicon bridged compounds but used dichlorodiphenylmethane as bridging moiety. Approaches to synthesise the functionalised NHC and the NHBC have been done, but unfortunately these reaction pathways did not afford the desired compounds. One reason could be the more strained C–(CPh₂)–C angle due to the shorter C–CPh₂ bond length (1.54 Å) compared to the C–SiPh₂ bond length (1.87 Å). The same reaction was performed with diiodomethane due to the less steric bulk carried by the methane moiety.

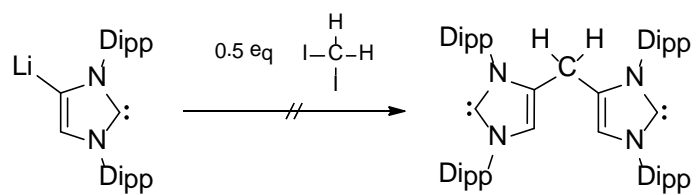


Figure 2.6: Unsuccessful reaction of Li-IPr with diiodomethane.

This would reduce the strain of the bridged IPr moieties and could therefore give the compound more degrees of freedom which could be beneficial for metal coordination. Unfortunately, no product could be isolated.

2.3. Palladium-Catalysed C2-Arylation of a nNHC

In order to block the C2-position of a nNHC initial tests have been performed with aryl halides (Figure 2.7).

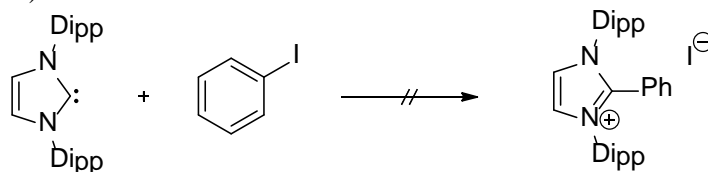


Figure 2.7: Reaction of IPr with phenyl iodide without any catalyst.

The used phenyl groups have enhanced stability compared to aliphatic groups. Moreover, phenyl groups are resistant against oxidation and reduction and deliver a steric bulk, which is also useful in order to shield the backbone carbon atoms. Another feature of an aryl halide is the high electrophilic character, which can lead to a nucleophilic attack of the nNHC. The reaction of phenyl iodide and IPr in toluene only resulted in the isolation of the starting materials. First approaches have been made using catalytically amounts of copper iodide as a catalyst in 1,4-dioxane at refluxing conditions. This route was also unsuccessful as only starting materials could be detected.

Another attempt was made by trying to increase the electrophilic character of the phenyl ring. Therefore, diphenyliodonium triflate was synthesised following literature procedure (Figure 2.8).^[141]

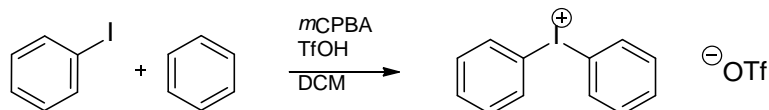


Figure 2.8: Synthesis of diaryliodonium triflate.

The oxidant *meta*-chloroperoxybenzoic acid (*m*CPBA) was used in a one pot reaction with benzene, phenyl iodide and triflic acid (TfOH) in DCM at room temperature to obtain the hypervalent diaryl- λ^3 -iodane salt. In this reaction *m*CPBA is used to initially oxidise the phenyl iodide to iodine (III) followed by a ligand exchange to yield the desired product. This compound is highly electron deficient and should therefore be a superb arylating agent.^[142] Reactions of IPr and the diphenyliodonium reagent were performed in toluene at room temperature and under refluxing conditions. Unfortunately, under the investigated conditions no reaction took place. Nevertheless, at least the crystal structure of diphenyliodonium triflate could be determined for the first time (Figure 2.9).

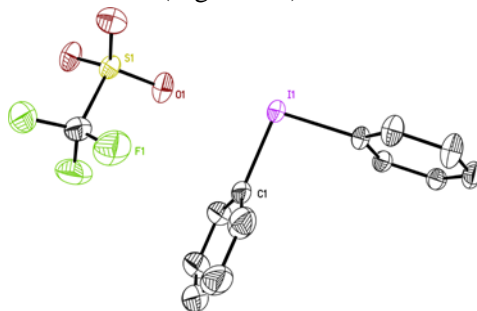


Figure 2.9: Crystal structure of diphenyliodonium triflate. Hydrogen atoms are omitted for clarity. Anisotropic displacement parameters are depicted at the 50% probability level.

Diaryliodonium derivatives with various anions have been measured in the past.^[143] In contrast to the compounds with halide anions the diphenyliodonium triflate forms a monomeric structure. The previously measured X-ray structures of diaryliodonium chloride, bromide and iodide by *Alcock* and *Countryman* were dimers.^[143a] The first synthesis of the (σ -aryl)palladium complex was reported by *Grushin* and *Marshall*, which was stabilised by a NHC and a triphenylphosphine (Figure 2.10).^[144]

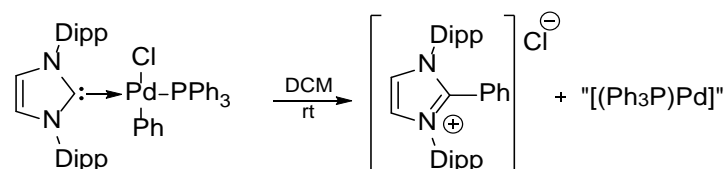
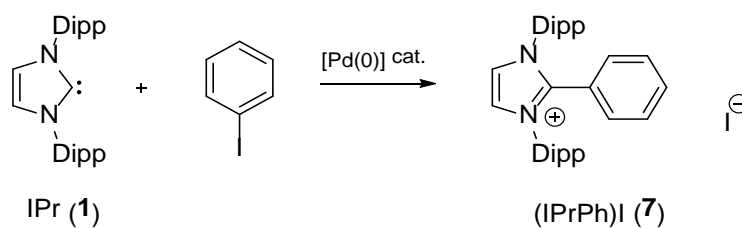


Figure 2.10: First (σ -aryl)palladium complex undergoing C–C reductive elimination of 2-phenylimidazolium salt.^[144]

They also report a solid precipitate after several hours and identified it as phenyl substituted IPr. Their serendipitous result enabled the first NMR measurements as well as X-ray diffraction experiments of the desired compound.

A novel catalytic and atom economic synthesis of MIC precursors by the direct C2-arylation could be achieved in this work (Table 2-1).^[68c]

Table 2-1: Direct catalytic C2-arylation of IPr. ([Pd(0)] = [Pd₂(dba)₃]). Reaction condition optimization for the reaction of IPr with PhI.



Entry	Time [h]	Temp [°C]	Solvent	Catalyst [mol%] ^[a]	Yield ^[b]
1	48	25	<i>o</i> -xylene	-	0
2	10	145	<i>o</i> -xylene	-	0
3	48	25	1,4-dioxane	-	0
4	10	102	1,4-dioxane	-	0
5	24	25	1,4-dioxane	1	16
6	2	102	1,4-dioxane	1	72
7	4	102	1,4-dioxane	0.5	92
8	3	102	1,4-dioxane	0.5	76
9	2	102	1,4-dioxane	0.1	2
10	48	25	<i>o</i> -xylene	1	18
11	2	145	<i>o</i> -xylene	1	81
12	2	70	THF	1	27
13	48	25	THF	1	0
14	48	25	Toluene	1	22
15	2	110	Toluene	1	75

[a] catalyst = [Pd₂(dba)₃]; [b] yield of isolated product.

If IPr (**1**) is treated with aryl iodide in the presence of 0.5 mol% of tris(dibenzylideneacetone)dipalladium(0) ([Pd₂(dba)₃]) as a precatalyst the corresponding C2-arylated 1,3-

bis(2,6-diisopropylphenyl)-2-phenyl-1*H*-imidazolium iodide ((IPrPh)I, **7**) can be obtained in good yields. (IPrPh)I is air and moisture stable and can therefore be stored easily without any additional precautions. The purification of the products can be performed by filtration because they are insoluble in *o*-xylene. Starting material and most of the catalyst remain in the solution. The crude product was extracted with DCM to obtain the analytically pure product. Equimolar ratio of carbene and phenyl iodide and 1 mol% of palladium catalyst was reacted in *o*-xylene to give a yield of 81% (Table 2-1).

Following this result reaction conditions were investigated to find the optimal reaction settings (Table 2-1). Different reaction times, temperatures and catalyst loadings as well as solvents have been tested. The exchange to the lower boiling solvent 1,4-dioxane results in almost similar results. The yield decreased under refluxing conditions by about 9%. At room temperature it could be shown, that the reaction proceeds but with highly reduced yields down to 16%. The same reaction was tested further in the more polar solvent THF and in the less polar solvent toluene. The yield of the reaction in boiling toluene is comparable to the reaction in 1,4-dioxane. Only the reaction in boiling THF provided significantly lower yields in the same time. At room temperature the tendency of decreasing yield is independent of the solvent. All reactions show decreased yields from 22% for toluene (48 h), 18% for *o*-xylene (48 h), 16% for 1,4-dioxane (24 h) and just hydrolysed product for THF (48 h). Furthermore, blank tests in *o*-xylene and 1,4-dioxane have been performed with the anticipated result of absolutely no conversion. These results give rise to the conclusion that this palladium catalysed reaction needs a certain activation energy in terms of temperature. A closer look at the solvent properties supports this conclusion as *o*-xylene with the highest boiling point (144°C) delivers the best yield at the boiling point followed by toluene (110°C), 1,4-dioxane (101°C) and at last THF (66°C).

2.3.1. Coordinating and Non-Coordinating Anions

Iodide as an anion is a mild reducing agent and could easily be oxidised to iodine. In order to prevent this redox chemistry of the prepared salts the iodide should be exchange for non-redox active and non-coordinating anions. Considering that halide anions are mainly coordination anions it could be beneficial to exchange the iodine anion not only because of its redox activity. Non-coordinating anions like tetrafluoroborate or hexafluorophosphate enable better solubility in organic solvents for the following deprotonation step. Moreover, these complex anions are less nucleophilic and less basic compared to halides.

Anion exchange reactions are widely known in organic chemistry. Typically, a silver salt carrying the desired anion is reacted with the salt of interest because silver salts, especially silver halides have very low solubility products. Basic requirement is that the solubility product of silver and the compound's anion is lower than the solubility product of the silver salt itself. In this particular case NaBF₄, KPF₆ and KOTf were used for the anion exchange for sustainability reasons as shown in Table 2-2.

Table 2-2: Comparison of purchase costs of different salts from Sigma-Aldrich. ^[145]

Compound	AgPF ₆	KPF ₆	AgBF ₄	NaBF ₄	AgOTf	NaOTf	KOTf
Prize	58,30 €	0,66 €	28,40 €	1,29 €	25.00 €	9.36 €	6.98 €

The anion exchange reactions were carried out at room temperature in a biphasic solvent mixture in the ratio of 3:2 (DCM: water). The mixture was stirred for one day before the phases were separated. The organic phase was dried further with magnesium sulphate (MgSO_4), then filtered and concentrated under reduced pressure. The compounds $(\text{IPrPh})\text{BF}_4$ (**8**), $(\text{IPrPh})\text{PF}_6$ (**9**) and $(\text{IPrPh})\text{OTf}$ (**10**) could be synthesised in good yields up to 86%. Furthermore $(\text{IPrPh})\text{Br}$ (**20**) could be prepared, which will be explained in chapter 2.4. The resonances of all compounds could be found with identical shifts, except for the backbone hydrogen atoms. The eight methyl groups of the *isopropyl* functionality could be found as two doublets at high field with a shift of 1.04 and 1.27 ppm. The four corresponding *ipso* protons show a discrete septet at 2.43 ppm. Furthermore, a doublet at 7.36 ppm and a triplet at 7.61 ppm describe the *meta* and *para* positions of the Dipp ligand. The resonances of the phenyl group appear as three sets of multiplets. A doublet of doublets at 6.96 ppm, a triplet at 7.26 ppm and another triplet at 7.44 ppm complete the spectrum. The ^1H -NMR spectra show significant shifting for the backbone ($\text{C}4/\text{C}5$) proton singlet resonances towards higher field for all compounds. The bromine ligand shows a shift at 8.29 ppm compared to the iodine ligand at 8.07 ppm followed by the triflate- (7.97 ppm), tetrafluoroborate- (7.88 ppm) and hexafluorophosphate ligands (7.76 ppm).

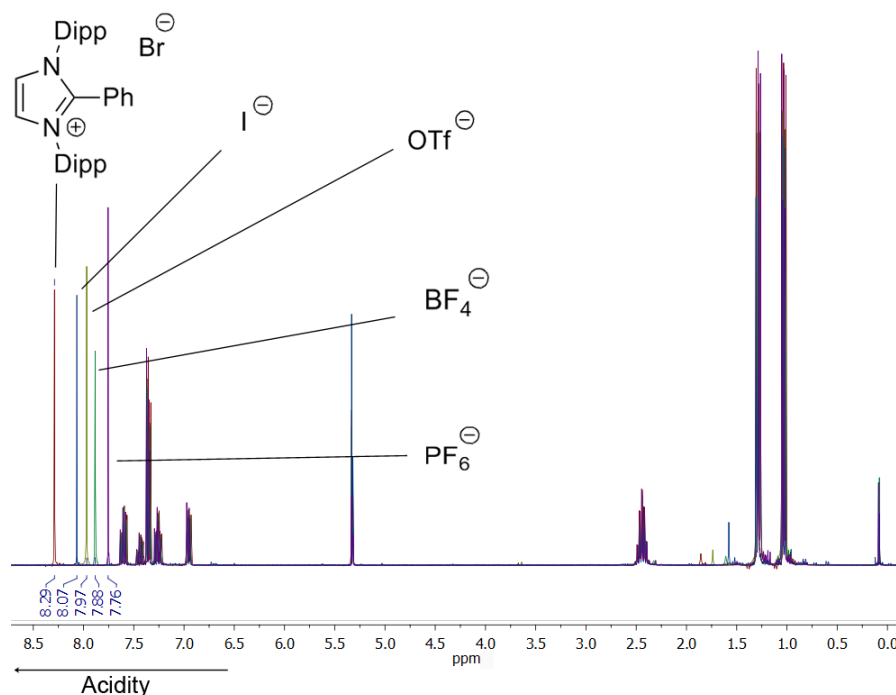


Figure 2.11: Superimposed ^1H -NMR spectra of the five $(\text{IPrPh})\text{X}$ compounds in CD_2Cl_2 . $\text{X} = \text{Br}^-$, I^- , OTf^- , BF_4^- , PF_6^- .

The shifting of the backbone singlet resonance results from the different electronic influences of the counterions. Bromine and iodine are supposed to be coordinating anions which results in a low field shift. Triflate, tetrafluoroborate and hexafluorophosphate are known to be non-coordinating anions. Correlating the chemical shift of the backbone hydrogen atoms of these five compounds with the acidity of the hydrogen atoms it could be stated that the bromine compound is the most acidic and the hexafluorophosphate compound the least acidic.

We could show with ^{19}F - ^1H -2D heteronuclear *Overhauser* enhancement spectroscopy experiments (HOESY) that in all three cases coupling between the fluorine and the hydrogen atoms could be observed. This proves at least a partial coordination of the anion. Furthermore,

^1H -NMR experiments have been done using different concentrations of the sample to evaluate, if a coordination of the anion is present. In case of coordinating anions one should observe a high field shift going to lower concentrations due to the lower probability of interactions.

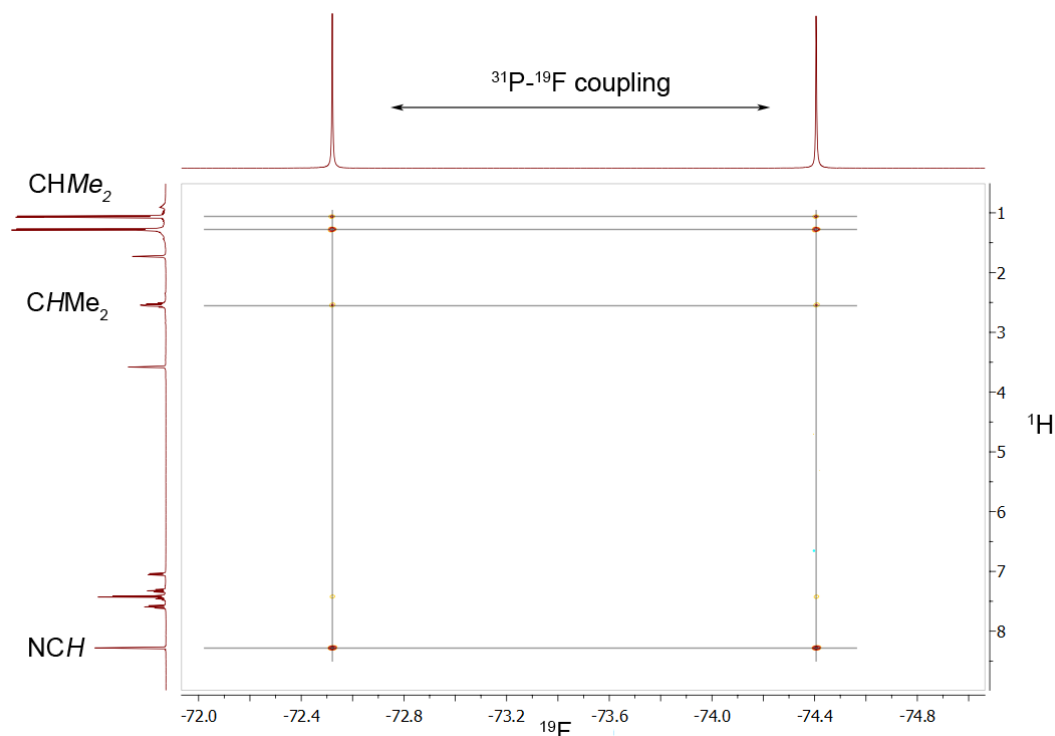


Figure 2.12: Exemplary ^{19}F - ^1H -HOESY spectrum of $(\text{IPrPh})\text{PF}_6$ in $\text{THF-}d_8$.

Furthermore, diffusion-ordered spectroscopy (DOSY) experiments have been done to evaluate the coordination behaviour of those five anions to the ligand. It was assumed that a coordination of the anion would lead to larger diffusion coefficients and therefore higher molecular weights determined with the ECC-MW estimation method developed by *R. Neufeld* and pursued by *S. Bachmann* in our workgroup.^[146] External calibration curves (ECC) have been used to determine the molecular weight of the five salts. For the method to work an internal reference has to be added to the sample to get a normalised diffusion coefficient, which can be used to overcome the inherent errors when comparing DOSY experiments (diversities in temperature, concentration, viscosity, NMR-device properties, etc.). For the measurements the reference molecule adamantane was added to the samples.

Furthermore, the method includes different ECCs for the shape of the molecule. Compact spheres (CS), dissipated spheres and ellipsoids (DSE) and expanded discs (ED) could be distinguished, which led to lower standard deviations of the ECCs. If the shape of a molecule is not clear a merged calibration curve can be used to determine the molecular weight but with a higher standard deviation. The shape of the measured molecules was considered to be associated to the DSE shape following the classification suggested by *Neufeld*. One issue with this method is the high molecular weight of the investigated compounds, if a coordinated anion is considered. The method was developed for compounds with molecular weights from 70 to 600 g/mol. The molecular weight of $(\text{IPrPh})\text{OTf}$ and $(\text{IPrPh})\text{PF}_6$ lie marginally above these values, wherefore the results have to be interpreted with care.

Table 2-3: Measured and calculated molecular weights and their standard deviations for the five salts using the ECC-DOSY method developed by *Neufeld and Bachmann*.

	Compound	MW [g/mol]	ΔMW_{DSE} [%]	MW_{Merge} [g/mol]	ΔMW_{Merge} [%]	$MW_{Calc.}$ [g/mol]
without anion	(IPrPh)Br	597.20	28.35	664.13	42.73	465.30
with anion			9.54		21.81	
without anion	(IPrPh)I	557.28	19.77	616.33	32.46	465.30
with anion			5.90		4.07	
without anion	(IPrPh)OTf	570.49	22.61	632.12	35.85	465.30
with anion			7.13		2.90	
without anion	(IPrPh)BF ₄	579.84	24.62	643.31	38.26	465.30
with anion			5.02		16.52	
without anion	(IPrPh)PF ₆	571.70	22.87	633.57	36.16	465.30
with anion			6.38		3.75	

Nevertheless, all results show a tendency towards coordinating aggregates even though most values are over interpreted. Following the results of *Bachmann et al.* a deviation of 14% could be tolerated for measurements in DCM. Those results fall into this given empirical error region. It is likely that all anions coordinate to a certain extent and molecular weights in between the values of the coordinated complex and the free cation are expected.

Another reason for the overestimated values could lie in DOSY experiment. ECCs possible inclusions of solvent in the cavities of the (IPrPh)I molecule or “free space” cannot be distinguished (Figure 2.13). The diffusion coefficients of molecules with or without these possible inclusions could ensure overestimated diffusion values, which again result in higher molecular weights. Unfortunately, it is not possible to prove the assumptions with this method until now.

**Figure 2.13:** Spacefill model of (IPrPh)I. Top view (left), side view (middle), bottom view (right).

2.3.2. Crystal Structures of IPrPhX Salts

Almost all discussed compounds could be crystallised. Crystals could be grown from saturated acetone (**7**) or DCM (**8**, **9** and **10**) solution *via* a slow solvent evaporation procedure. In case of compound **7**, two different coloured crystals, red crystals (**7b**) as impurity and

colourless crystals (**7a**) have been found in the same sample. These two different crystals contain different anions. The red crystal could be identified as the C2-arylated imidazolium cation with a palladium trichloride and the colourless compound contains iodide as anion. **7b** crystallises in the monoclinic space group $P2_1/n$ with one molecule in the asymmetric unit (Figure 2.14) and **7a** in the triclinic space group $P1$ with one molecule in the asymmetric unit (Figure 2.14). The two structures differ by the anion and the rotation of the phenyl group by 6.7° . In addition, **7b** shows a disordered *isopropyl* group with a site occupation factor of 0.55(3).

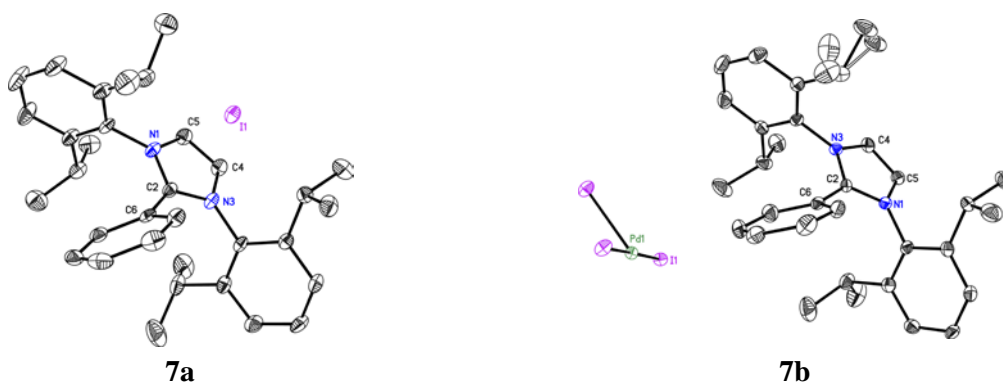


Figure 2.14: Crystal structures of compounds **7a** and its impurity **7b**. Hydrogen atoms have been omitted for clarity. Anisotropic displacement parameters are depicted at the 50% probability level.

(Figure 2.15) and compound **9** crystallises in the monoclinic space group and $P2_1/n$ with one molecule in the asymmetric unit. Compound **8** crystallises in the monoclinic space group $P2_1/m$ with one half of the molecule in the asymmetric unit (Figure 2.15)

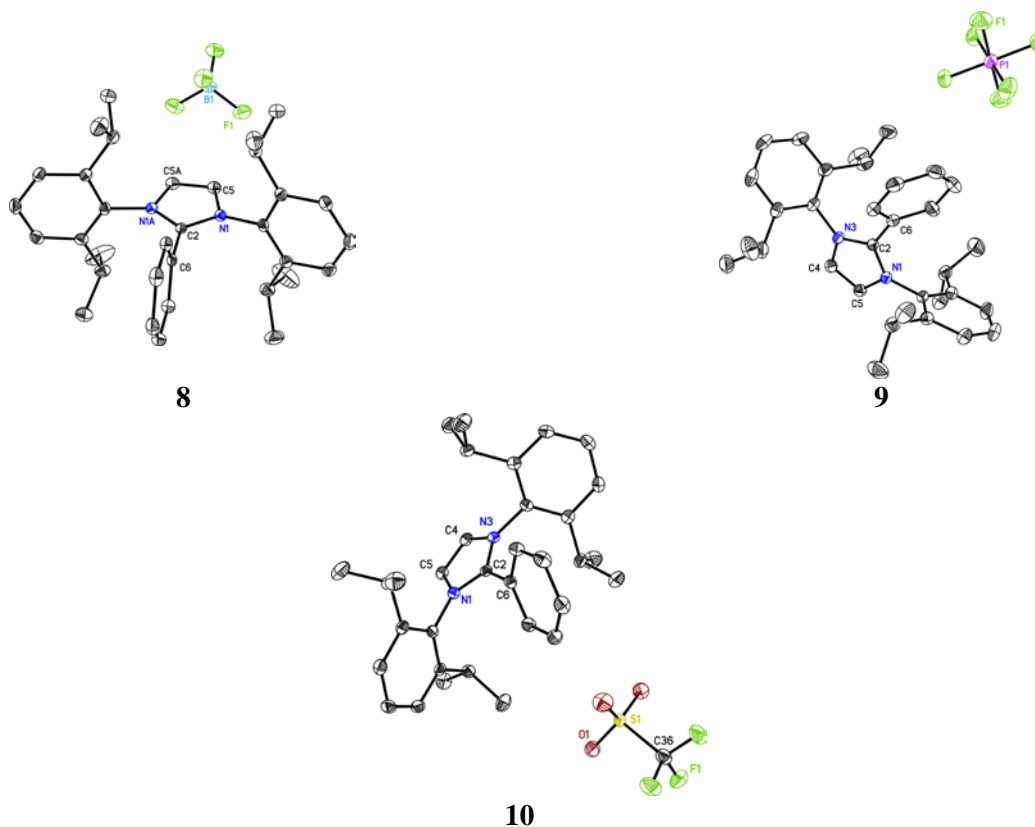


Figure 2.15: Crystal structures of compounds **8**, **9** and **10**. Hydrogen atoms have been omitted for clarity. Anisotropic displacement parameters are depicted at the 50% probability level.

Compound **10** crystallises in the monoclinic space group and $P2_1/c$ with one molecule in the asymmetric unit (Figure 2.15). Crystals from compound **20** could not be grown by the end of this work.

Table 2-4: Selected bond lengths [Å] and angles [°] of the four (IPrPh)X salts (**7a**, **7b**, **8**, **9**, **10**). *Symmetry generated.

	7a	7b	8	9	10
N1–C2	1.349(2)	1.346(4)	1.344(1)	1.351(2)	1.345(2)
N1A–C2/N3–C2	1.345(2)	1.348(4)	1.344(1)*	1.348(2)	1.349(2)
N1–C5	1.381(2)	1.380(4)	1.385(1)	1.382(2)	1.387(2)
N3–C4	1.384(2)	1.383(4)	-	1.383(2)	1.383(2)
C4–C5/C5–C5A	1.347(3)	1.348(4)	1.351(2)*	1.349(2)	1.346(2)
N1–C2–N1A/N1–C2–N3	106.96(2)	107.0(2)	107.3(1)*	106.8(1)	107.1(1)
N1–C2–C6–C7	61.1(2)	54.6(4)	89.7(2)	53.6(2)	51.0(2)

The imidazole moiety of the five structures is very similar with respect to the bond lengths and angles. The bonds N1–C2 and N3–C2 which carry the positive charge is partly a double bond and show bond length from 1.344(1) Å to 1.351(2) Å, which is in good agreement of theoretical C–N-bond lengths between a single (1.47 Å) and a double bond (1.29 Å).^[147] Compound **8** shows a slightly different binding situation concerning the phenyl ring, which is orientated perpendicular to the imidazole moiety compared to an approximately 60° angle in compounds **7a**, **7b**, **9** and **10**.

2.3.3. Substrate Scope

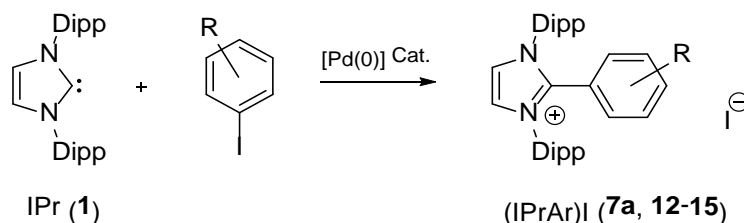


Figure 2.16: Palladium catalysed synthesis of C2-arylated NHC salts.

For investigation of the scope of the reactions according to Figure 2.16 alkyl-, methoxy-, ester-, nitro-, and amino substituted iodobenzenes have been tested. Table 2-5 summarises conditions and yield for this screening.^[68c]

Table 2-5: Scope of the C2-arylation of IPr with RC₆H₄X. [a] Time under reflux; [b] catalyst = [Pd₂(dba)₃]; [c] yield of isolated product; n.c. = no coupling product.

Entry	Time [h] ^[a]	R	X	Solvent	Catalyst [mol%] ^[b]	Yield [%] ^[c]
1	2	H	I	1,4-dioxane	1	72 (7a)
2	4	H	I	1,4-dioxane	0.5	92 (7a)
3	3	H	I	1,4-dioxane	0.5	76 (7a)
4	2	4-Me	I	<i>o</i> -xylene	1	80 (12)
5	3	2-Me	I	<i>o</i> -xylene	1	60 (13)
6	2	4-MeO	I	1,4-dioxane	1	74 (14)
7	2	4-MeOOC	I	1,4-dioxane	1	75 (15)
8	4	4-NO ₂	I	1,4-dioxane	1	n.c
9	4	4-NMe ₂	I	1,4-dioxane	1	n.c
10	4	H	Cl	1,4-dioxane	1	n.c
11	4	H	Br	1,4-dioxane	1	n.c

Compounds **12**, **14** and **15** were isolated in good yields (entries 4, 6 and 7). The treatment of compound **1** with 4-nitro- and 4-(*N,N*-dimethylamino)iodobenzene did not afford the anticipated products (entries 8 and 9). Coupling product **13** was synthesised in a rather low yield by reacting **1** with 2-iodotoluene, may be due to increased steric interference by the *o*-methyl group (entry 5). Under similar experimental conditions it was shown that, chloro- and bromobenzene are inactive (entries 10 and 11). Reasons for this behaviour can be found in the strength of the carbon halide bond which increases from iodine to fluorine in accordance to the concept of hard and soft acids and bases (HSAB). The fluorine atom as a hard base interact the most with the carbon atom as hard acid. The hardness of the used bases, in this case chlorine, bromine and iodine, decreases in this sequence. This trend in stability has been extensively examined e.g. by theoretical means. The bond energies for mono halogenated methane further underline these assumptions (bond energies [kcal] CH₃F = 107.0; CH₃Cl = 76.7; CH₃Br = 66.4; CH₃I = 52.6).

All air-stable C2-arylated imidazolium salts (**7a–15**) have been isolated as off-white solids. Compounds **7a–10** and **13–15** were utterly characterised by elemental analysis, NMR spectroscopy, and mass spectrometry. With the exception of **13**, the isopropyl groups of **7a**, **12–15** showed two sets of doublets for the methyl groups in the NMR spectra. The spectrum for compound **13** exhibits three sets of for the methyl protons of Me₂CH groups, with one of them ($\delta = 1.07$ ppm) appearing as a pseudo-triplet, due to the overlap of two expected doublets. The imidazole protons (at C4 and C5) in **12–15** appear as singlet in the range of 8.01–8.30 ppm. The EI mass spectra of **7**, **12–15** each show the molecular ion peak for the imidazolium moiety.

2.3.4. Crystal Structures of (IPrPh-R)I salts

Moreover, the molecular structures of **12–15** were determined by single crystal X-ray diffraction analysis.^[68c] The molecular structures of compounds **7a**, **12**, **14** and **15** exhibit similar structural features. Molecular structures of compound **12** and **13** are shown in Figure 2.17. The N1–C2–N3 bond angles range from 106.2–107.7°, which is comparable to those observed in unsubstituted 1,3-imidazolium salts.^[124, 148]

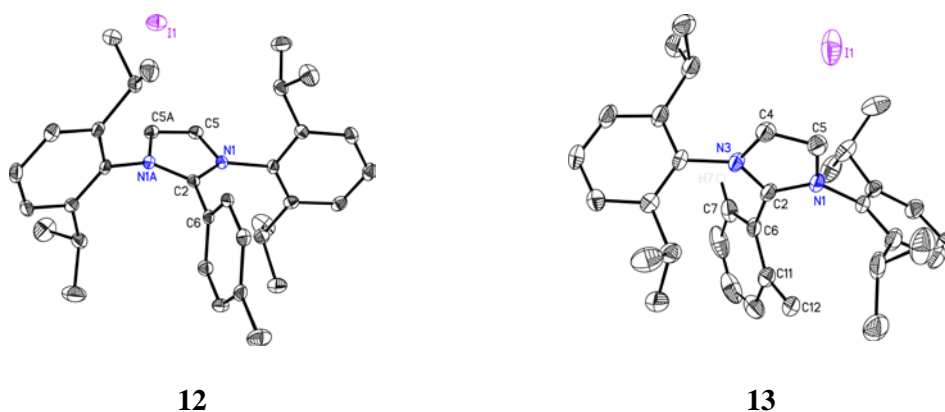


Figure 2.17: Crystal structures of compounds **12** and **13**. Hydrogen atoms have been omitted for clarity. Anisotropic displacement parameters are depicted at the 50% probability level.

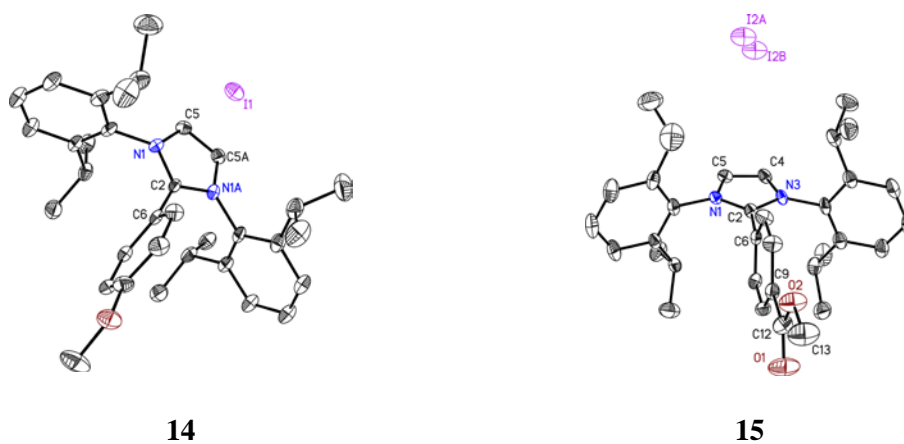


Figure 2.18: Crystal structures of compounds **14** and **15**. Hydrogen atoms have been omitted for clarity. Anisotropic displacement parameters are depicted at the 50% probability level.

All crystal structures give, with minor deviations, similar motifs (Figure 2.19). Almost all ligands at the imidazole are ordered in an approximately perpendicular fashion. Two exceptions show a slightly distorted motif. Compound **13** and (IPrPh)I. Structure **13** shows a twist of 58.3° for the C2-phenyl ring. Furthermore, the Dipp substituents are also twisted by 69.94° . For compound **7a** a twist of 59.2° of the C2-phenyl ring could be observe. However, the Dipp ligands are only twisted by 77.1° . This behaviour can be explained with the steric repulsion of the methyl group at the *ortho* position.

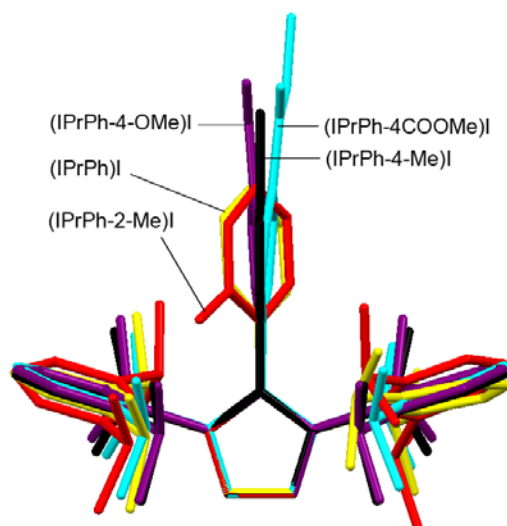


Figure 2.19: Overlay of the five synthesised structures **7a**, **12**, **13**, **14**, and **15**.

In Table 2-6 selected bond lengths and angles are listed, which show that all measured structures crystallise in the same motif. With an *ortho* substituted aryl halide the crystal structure could be twisted to some extent, whereas the different *para* substitution did not affect the approximately perpendicular orientation of the substituent. The possibility of changing the ligand orientation would be beneficial for further investigations.

Table 2-6: Selected bond lengths [\AA] and angles [$^\circ$] of the four (IPrPh)X salts (**12**, **13**, **14**, **15**).

	12	13	14	15**
N1–C2	1.345(2)	1.354(3)	1.344(2)	1.343(8)/ 1.327(9)
N1A–C2/N3–C2	1.345(2)*	1.349(3)	1.344(2)*	1.347(8)/ 1.345(9)
N1–C5	1.385(2)	1.377(3)	1.384(2)	1.393(7)/ 1.391(10)
N3–C4	-	1.382(3)	-	1.392(7)/ 1.389(9)
C4–C5/C5–C5A	1.345(3)*	1.346(4)	1.354(4)*	1.341(10)/ .338(11)
N1–C2–N1A/N1–C2–N3	107.2(2)*	106.6(2)	107.8(2)*	107.7(5)/ 108.1(6)
N1–C2–C6–C7	89.6(2)	58.3(3)	87.3(6)	87.6(8)/ 82.2(18)

*Symmetry generated. **Since there are two molecules in the asymmetric unit, both values are given.

Compounds **12–15** show that the palladium catalysed C2-arylation reaction is an efficient way to design a variety of new imidazolium salts, which could be used as precursors for MICs. The ability to tune the ligand (**1**) can be important to develop appropriate MICs for certain applications. Depending on the substituted aryl halide the electron density within the imidazolium moiety will change, influencing the acidity of the hydrogen atoms at the imidazole backbone carbon atoms C4 and C5. This is interesting for the generation of the MIC and its stabilisation after deprotonation.

The electron-releasing inductive effect increases the electron density in the imidazolium moiety, which lowers the acidity of its backbone hydrogen atoms. The electron withdrawing inductive effect decreases the electron density within the imidazolium moiety and therefore increases the acidity of the hydrogen atoms at the C4/C5 carbon atom. Mesomeric effects could not influence the CH-acidity since for mesomeric interaction, the C2-arylated phenyl ring has to be coplanar to

the imidazole moiety. The inductive effect can be observed through $^1\text{H-NMR}$ chemical shifts of the hydrogen atoms at the backbone carbon atoms. In solution one singlet can be assigned for the chemically equivalent hydrogen atoms. A shift towards lower field can be observed for the C2-substitution of 4-methoxyphenyl (8.01 ppm), 4-methylphenyl (8.02 ppm), 2-methylphenyl (8.11 ppm), phenyl (8.15 ppm) and 4-esterphenyl (8.30 ppm). All $^1\text{H-NMR}$ spectra were measured at 25°C in DCM and showed no impurities.

Unfortunately, until now it was not possible to isolate the free MIC from ligands **7a**, **12–15** and hence a conclusion about the stabilising effect of the C2-substituent cannot be given. Nevertheless, compounds **7a**, **12–15** are robust imidazolium salts. They can be stored without any precautions and are stable for months. Moreover, their high melting points indicate a tolerance against high temperatures. They could also be stored in solution without any recognisable decomposition. So far research has focused on IPr, preliminary tests with IMes and $t\text{Bu}$ proved unsuccessful. However, C2-arylation as described above should also be possible for these compounds and future attempts should target at this goal.

2.3.5. Proposed Catalytic Cycle

A proposed catalytic cycle to form compounds **7b/b** and **12–15** is given in Figure 2.20.^[68c]

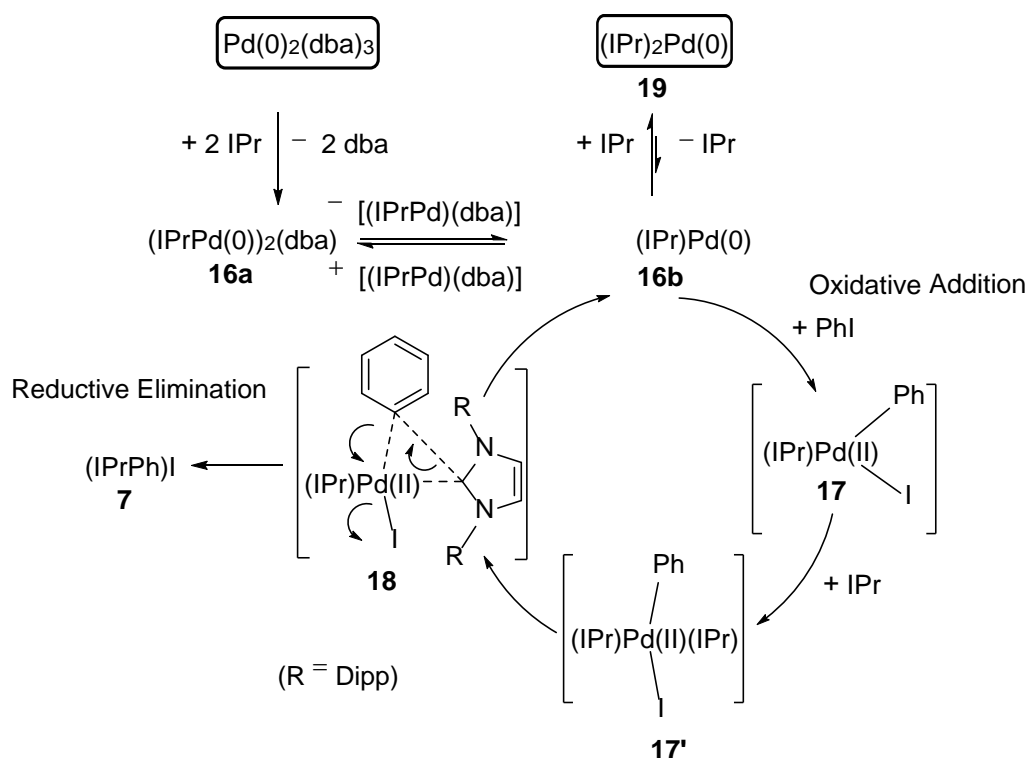


Figure 2.20: Proposed catalytic cycle for the C2-arylation of an nNHC.^[68c]

As precatalyst $[\text{Pd}_2(\text{dba})_3]$ was used as the commercially available source of Pd(0). Studies have shown that substitution of “dba” with a two-electron donor auxiliary ligand (L) leads to $[(\text{LPd})_2(\text{dba})]$ -type species.^[149] At higher temperature, $[(\text{LPd})_2(\text{dba})]$ generates a catalytically active monoligated L-Pd(0) species, which readily undergoes oxidative addition with an aryl halide.^[96b, 150] Therefore, formation of $[(\text{IPrPd})_2(\text{dba})]$ (**16a**) by reaction of $[\text{Pd}_2(\text{dba})_3]$ with IPr

seems reasonable. At high temperatures, **16a** yields the reactive monoligated [(IPr)Pd] compound (**16b**). The following oxidative addition step of iodobenzene with **16b** would give species **17**. The coordination by a second molecule of IPr may stabilise species **17** to yield species **17'**. The reductive elimination (RE) step *via* a concerted transition state **18** may afford the C2-arylated product (**7**) and regenerate [(IPr)Pd] (**16b**).^[151]

To examine the validity of the proposed cycle, catalytic activity of the bis-NHC-Pd(0) compound [(IPr)₂Pd] (**19**) was tested. [(IPr)₂Pd] was prepared by treating [(IPr)₂PdCl₂] in THF with KC₈. Although, compound **19** was found to be an active catalyst, the reaction of IPr with PhI to yield **7a** was rather slow. This further supports the involvement of **16a**, featuring a rather labile ligand (dba), in readily supplying the active catalyst **16b**. This catalytic cycle shows a novelty, in respect to the mechanism and the involvement of the IPr. To the best of our knowledge, the presented reaction is the first in which IPr acts as a catalyst ligand and reactant.

Finally, it could be shown that a catalyst recycling is possible. A standard reaction was performed and the resulting catalyst mixture was collected and combined with fresh carbene and phenyl iodide. In Table 2-7 the results of the catalyst recycling reaction are presented. In the first cycle 81% yield could be obtained as well as for the decreases significantly after the second cycle still 50% of **7** could be isolated. In the second cycle 80% could be obtained followed by a yield reduction of 30% in the third cycle. Even after the fourth cycle 50% yield could be isolated, which shows that Pd₂(dba)₃ is a very sufficient catalyst.

Table 2-7: Catalyst recycling for the reaction of compound **1** with PhI to species **7** by using 1 mol% of precatalyst.

Cycle	IPr (mmol)	PhI (mmol)	Yield (g, %)	Time
1	3.35	3.38	1.60, 81	2
2	3.35	3.35	1.51, 80	2
3	3.35	3.35	1.00, 50	2
4	3.35	3.35	0.99, 50	2

Under the presented conditions a turnover number of 257 could be reached. So far no further investigation on catalyst deactivation has been made.

2.4. Nickel-Catalysed C2-Arylation of an nNHC

Finding alternatives to precious heavy metals is an important step forward for addressing the current sustainability issues. Nickel based catalysts have shown a remarkable reactivity in a variety of coupling reactions^[152] and also hold promises in new challenging transformations. It should however be noted that the mechanism of Ni-catalysed reactions is significantly different than that of Pd-catalysed transformations. Therefore, the choice of reactants and reaction conditions plays an enormous role of the scope of reactions.

Nickel is the smaller homologue of palladium and seems to have all the attributes to also catalyse the direct C2-arylation reaction. With respect to the abundances of the elements and the price of the precatalysts, it is advantageous to use Nickel (Ni on earth are estimated to $1.69 \cdot 10^4$ and palladium to 0.88 ppmw.^[153]). One gram of nickel bromide cost 2.8 € compared to 66.1 € for of $\text{Pd}_2(\text{dba})_3$.^[154]

Nickel (II) halides are often used as precatalyst or catalyst in different types of reactions.^[155] Phosphine substituted nickel (II) chloride is for example used in *Suzuki-Miyaura* arylations. Many cross coupling reactions are actually catalysed by using nickel (II) halides or neutral ligand substituted nickel (II) halides.^[156] Furthermore many reactions are catalysed by using the nickel(0) compound, nickel dicyclooctadiene. *Radius et al.* published a di-NHC Ni(0) compound that can be applied in *Suzuki-Miyaura* cross-coupling reactions.^[157] The starting material is also react with phenyl halides to yield a C2-arylated NHC cation and an anionic nickel component of the type $[\text{NiBr}_2\text{X}_2]^{2-}$.

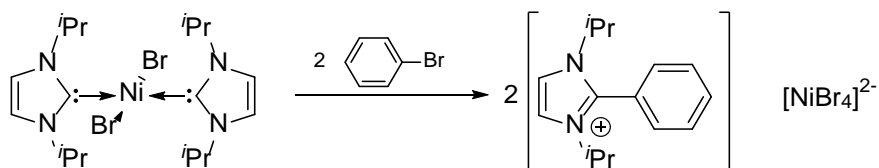


Figure 2.21: Synthesis of ⁱPrIM salt by *Radius et al.*

The NHC in this case is the *N,N*-isopropyl substituted imidazolium-2-ylidene (ⁱPrIm), but also other para-substituted aryl halides have been synthesised.^[157] This reaction was classified as a catalyst deactivation reaction. *Radius et al.* could proof that under their reaction condition slow catalyst crumbling takes place. A test reaction with excess of different aryl halides led to several different substituted C2-arylated imidazolium salts. The stoichiometric reaction conditions to obtain good yields are pretty harsh and the reaction took at least several days. Fluorobenzene and chlorobenzene did not react at all.

In view of this, it becomes clear that a systematic study is highly desired to achieve further mechanistic understanding of Ni-catalysed reactions as well as developing more efficient Ni-based catalysts. In this context, we decided to investigate NHC-Ni complexes for developing catalytic methods for C2-arylation of NHCs.

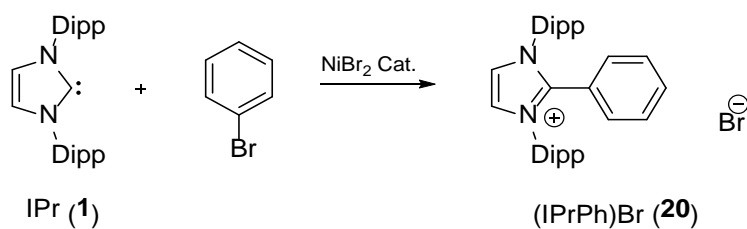


Figure 2.22: First nickel catalysed C2-arylation of an nNHC.

Following these results, a range of reactions has been done as shown in Table 2-8. The reactions were performed in analogy to the palladium catalysed C2-arylation reaction^[68c] but with 10mol% catalyst loading, NiBr₂ as catalyst and phenyl bromide as reactant. The typically used solvents *o*-xylene, 1,4-dioxane, THF and toluene have been tested at room temperature and under refluxing conditions. The progress of the reaction can be followed visibly because the product is not soluble in the used solvents and precipitates out as it forms. Reactions at rt were stopped after 24 h due to no conversion. A small amount of residue was formed and identified as (IPr·HBr). This may be due to slow hydrolysis of IPr. The reason for the hydrolysis is so far not clear. Using *o*-xylene as the solvent with the highest boiling point 37% product yield could be reached after 4h. A slow increase in yields (45%) can be observed for longer reactions times (12h). In toluene no conversion was observed regardless of reaction temperature. However, in refluxing THF 27% yield could be isolated after 12h. In boiling 1,4-dioxane 34% yield could be reached after the same time.

In the beginning, a 10 mol% of the catalyst loading was selected. Following the good yields of the reaction in *o*-xylene the catalyst loading was first decreased to 5 mol% and then to 1 mol%. The yield decreased slightly using 5 mol% of NiBr₂ under refluxing conditions for a similar time interval of 12 h. A catalyst loading of 1mol% leads to a lower yield of 29% even after a longer reaction time of 48 h.

Table 2-8: Reaction condition optimization for the reaction of IPr with PhBr. [a] catalyst = [NiBr₂]; [b] yield of isolated product; n.c. = no coupling product.

Entry	Time[h]	Temp [°C]	Solvent	Catalyst [mol%] ^[a]	Yield ^[b]
1	24	25	<i>o</i> -xylene	10	n.c.
2	4	145	<i>o</i> -xylene	10	36
3	12	145	<i>o</i> -xylene	10	45
4	24	25	1,4-dioxane	10	n.c.
5	12	102	1,4-dioxane	10	34
6	24	25	THF	10	n.c.
7	12	70	THF	10	27
8	24	25	toluene	10	n.c.
9	12	110	toluene	10	n.c.
10	12	145	<i>o</i> -xylene	5	40
11	12	145	<i>o</i> -xylene	1	12
12	48	145	<i>o</i> -xylene	1	29
13	48	145	<i>o</i> -xylene	5	42

In summary it can be stated that more energy is needed to break the bromine carbon bond to enable the oxidative addition step. A further possibility, through which one could possibly obtain higher yields, could be a pressurised reaction at high pressure enabling higher boiling points.

2.4.1. Substrate Scope

To investigate the substrate scope reactions with alkyl- and methoxy- substituted bromobenzenes have been tested (Figure 2.23).

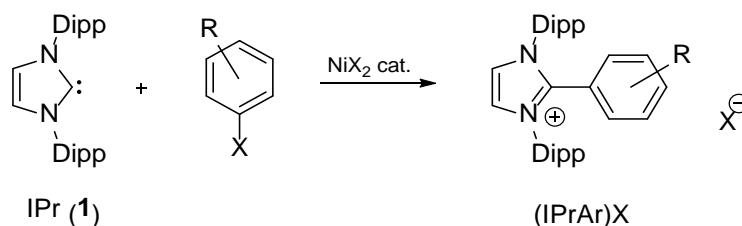


Figure 2.23: Nickel catalysed synthesis of C2-arylated NHC salts.

Table 2-9 entry 1–3 show the dependence of catalyst loading for the synthesis of (IPrPh)Br. The yield decreases inconsiderable from 45% with a catalyst loading of 10mol% to 40% with a catalyst loading of 5mol%. All other reaction parameters were maintained same.

The reaction of various substituted aryl halides have been tested as substrates (Table 2-9 entry 4–8). The methoxy and the *para*-methyl substituted phenyl bromide delivered the desired products in good to excellent (up to 82%) yield. Notably, di-substituted and *ortho*-substituted phenyl bromides did not undergo C–C coupling reactions under similar conditions (Table 2-9 entry 5, 7–8).

Table 2-9: Scope of the C2-arylation of IPr with RC₆H₄X.

Entry	Time[h] ^[a]	R	X	Solvent	Catalyst [mol%] ^[b]	Yield [%] ^[c]
1	12	H	Br	<i>o</i> -xylene	10	45 (20)
2	12	H	Br	<i>o</i> -xylene	5	40 (20)
3	12	H	Br	<i>o</i> -xylene	1	12 (20)
4	6	4-Me	Br	<i>o</i> -xylene	7	82 (21)
5	12	2-Me	Br	<i>o</i> -xylene	10	n.c.
6	5	4-MeO	Br	<i>o</i> -xylene	6	62 (22)
7	5	3,4-Me	Br	<i>o</i> -xylene	1	n.c.
8	24	2,6-Me	Br	1,4-dioxane	7	n.c.
9	12	H	I	<i>o</i> -xylene	10	62 (7a)
10	12	H	Cl	<i>o</i> -xylene	10	n.c.
11	72	H	Cl	1,4-dioxane	14	n.c.
12	24	4-Me	Cl	1,4-dioxane	11	n.c.

[a] Time under reflux.; [b] catalyst = [NiX₂], If an aryl bromide is used the complementary bromine nickel salt is used, analogously aryl iodides and chlorides were converted with NiI₂ and NiCl₂, respectively.; [c] yield of isolated product; n.c. = no coupling product.

P-toluene bromide did react with IPr and 7mol% catalyst loading to give the desired product in 82% yield after 6 h under refluxing conditions (Table 2-9 entry 4). Slightly lower yield (62%) was found for the reaction of *para*-bromoanisole with IPr and 6 mol% catalyst after 5 h. Furthermore,

different nickel(II) halides were. Nickel(II) iodide (10mol%) was successful in the reaction of IPr with phenyl iodide. After a reaction time of 12 h 62% yield could be obtained. The same reaction was performed using phenyl chloride and nickel (II) chloride as catalyst, but did not yield any product. In conclusion, the Ni-based catalysis works for the C2-arylation of an NHC and the use of nickel iodide and aryl iodides gives the best results.

2.4.2. Crystal Structures of (IPrPhR)Br

The molecular structures of **21** and **22** were determined by single crystal X-ray diffraction analysis. The molecular structures of compounds **21** and **22** exhibit similar structural features. The molecular structure of compound **21** crystallises in the triclinic space group *P*-1 with two molecules in the asymmetric unit.

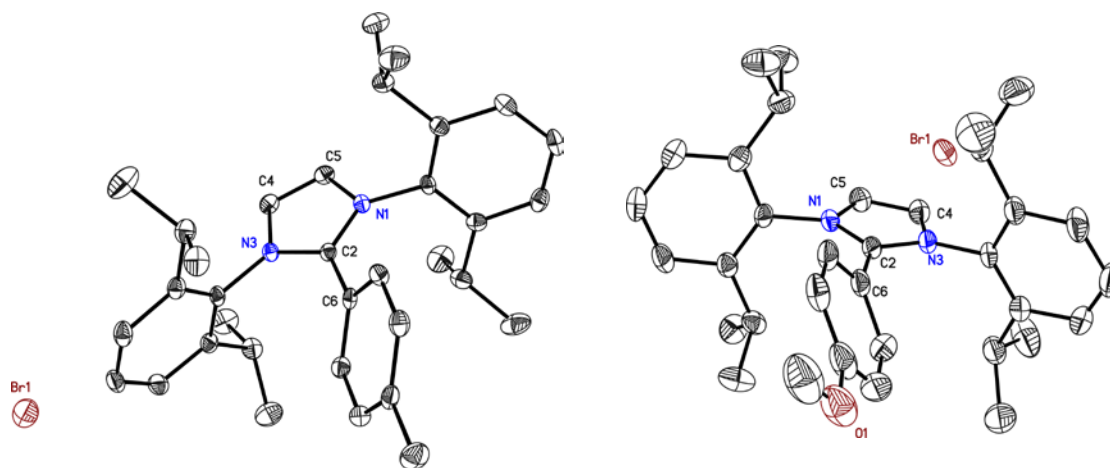


Figure 2.24: Crystal structure of **21** (left) and **22** (right). Hydrogen atoms are omitted for clarity.

The samples contain water molecules in the crystal. Residual electron density represents disordered water molecules. A further refinement of the water molecules does not lead to satisfying results. It has to be mentioned that the adequate description of the solvent molecules in the crystal structure is not meaningful; however, the refinement of the desired compounds **21** and **22** seems utterly acceptable.

2.4.3. Proposed Catalytic Cycle

A proposed catalytic cycle to form compounds **7a**, **20–23** is given in Table 2-9.

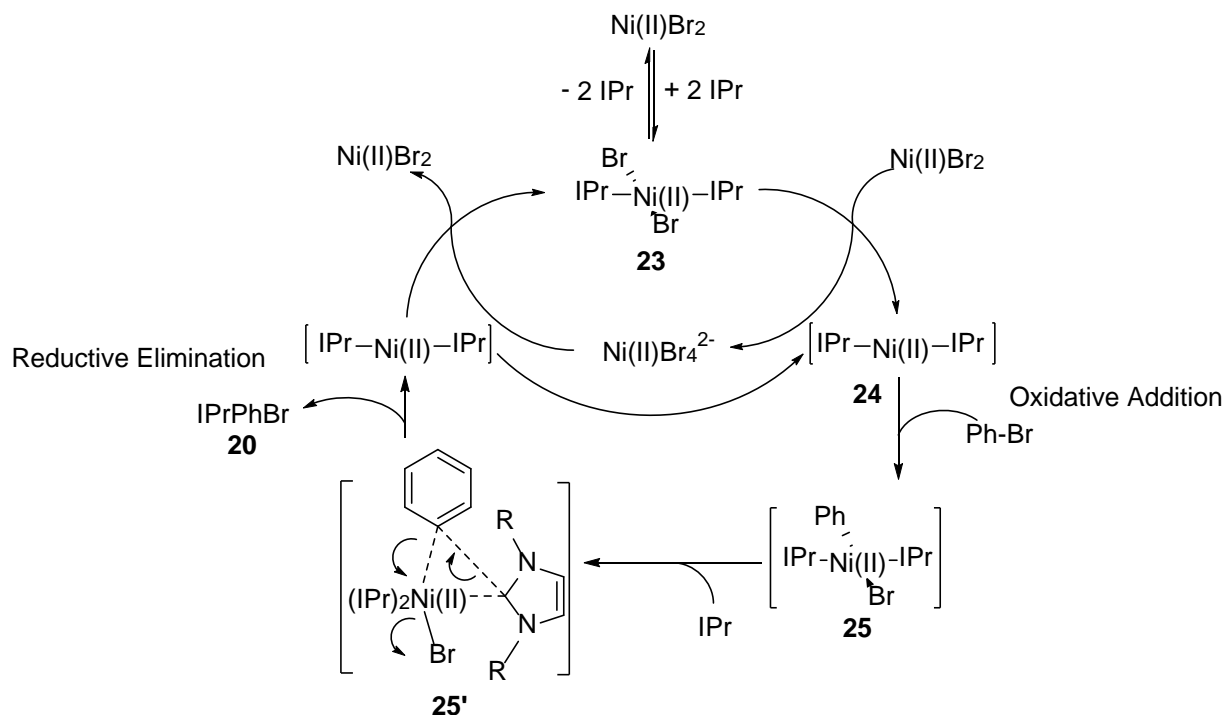


Figure 2.25: Proposed catalytic cycle for the nickel catalysed C2-arylation.

A typical case of nickel bromide as pre-catalyst is shown. With excessive IPr, $[(\text{IPr})_2\text{Ni}(\text{II})]\text{Br}_2$ (**23**) can be formed, which at higher temperature may react with the second nickel dibromide species to generate nickel tetrabromide and $[(\text{IPr})_2\text{Ni}(\text{II})]$ (**24**). Compound **24** can undergo oxidative addition with phenyl bromide to give $[(\text{IPr})_2\text{Ni}(\text{II})\text{Ph}]\text{Br}$ (**25**). The reductive elimination step *via* a concerted transition state **25'** would lead to the C2-arylated product (**7**) along with **24**. The catalytic active species in this cycle is believed to be the $[(\text{IPr})_2\text{Ni}(\text{II})]$ compound. Literature precedents indicate the disproportionation of NHC-species like **25** into corresponding imidazolium salts.

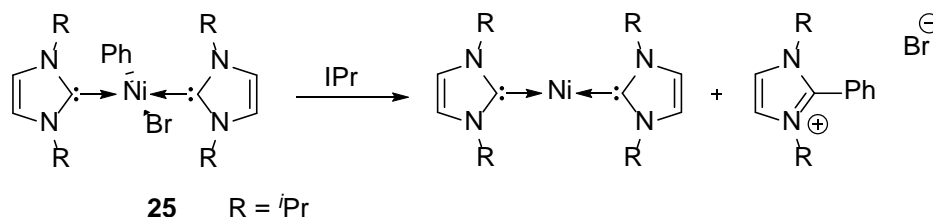


Figure 2.26: Disproportionation of NHC-species **25** leads to the formation of aryl imidazolium salts.

Our products are off-white solids. These results extend the range of C2-arylated imidazolium salts which could readily be prepared and reduces the cost by using nickel instead of palladium.

2.5. Electronic and Steric Properties of MICs and their precursors

2.5.1. Calculation of Tolman Electronic Parameter (TEP)

The detail understanding of the electronic and steric properties of ligands is essential to estimate their ability for catalytic applications. One of the most established methods for the determination of the electron donor ability of ligands is the Tolman Electronic Parameter (TEP) method (chapter 1.5). Experimental and calculated values are known for a variety of ligand systems. Herein, the reported values (entry 1–9) are compared with the calculated values of the synthesised compounds (entry 10–14).

Table 2-10: Calculated and experimentally determined TEPs for selected NHCs and those presented in this work. Experimental values of entry 1-9 for the complexes (NHC)IrCl(CO)₂ and (NHC)Ni(CO)₃ were reported in a review article by *Nolan et al.*^[124] DFT calculated values for entry 1-6 have been reported by *Gusev*.^[158] The values have a maximum deviation of 2.5 cm⁻¹.

Entry	NHC	(NHC)IrCl(CO) ₂ [cm ⁻¹]	(NHC)Ni(CO) ₃ [cm ⁻¹]	DFT calculation[cm ⁻¹]	
1	SIPr	2051.1	2052.2	2051.5	
2	SIMes	2050.8	2051.5	2051.5	
3	I ^t Bu	2048.9	n/a	2050.6	
4	IMes	2049.6	2050.7	2050.6	
5	IPr	2050.2	2051.5	2050.5	
6	IAd	2048.3	n/a	2045.8	
7	IPr-2,4-Ph	2038.4	n/a	n/a	
8	IPr-2-Ph-4-(Ph-4-OMe)	2039.2	n/a	n/a	
9	IPr-2-Ph-4-(Ph-4-Me)	2038.3	n/a	n/a	
10	(IPrPh-2-Me)(13)	n/a	n/a	2051.9*	2137.4 [#]
11	(IPrPh-4-Me)(12)	n/a	n/a	2052.6*	2138.4 [#]
12	(IPr-4-OMe)(14)	n/a	n/a	2051.2*	2141.6 [#]
13	(IPrPh-4-CO ₂ Me)(15)	n/a	n/a	2052.7*	2141.3 [#]
14	(IPrPh)(7)	n/a	n/a	2040.1**	
				2052.2*	2138.7 [#]

*Values for entry 10–14 are calculated with the BP86/def2-SVP functional.

[#]Values for entry 10–14 are calculated with the B3LYP/def2-SVP functional. The standard deviation for both calculations is around 1 cm⁻¹.

**Value for entry 14 was calculated following the instructions by *Gusev* to establish comparability.

In Table 2-10 some representative NHCs (entry 1–6), MICs (entry 7–9) and the synthesised compounds from this work (entry 10–14) are shown. DFT calculations were carried out according to *Gusev*, which allows extracting a comparison of the TEP values. *Gusev* calculated the TEP for 76 NHCs with the same DFT method and supported his results with experimental data. Furthermore, experimentally determined IR values are presented in order to classify the recent results.^[158] Imidazolidinylidenes show larger TEP values than imidazolylidene and are therefore less electron donating ligands. MICs (Table 2-10, entry 7–9) show exceptionally smaller TEP values and are therefore more electron donating compounds. Entry 14 shows a TEP (calc.) value of 2040.1 cm⁻¹ and is therefore a slightly weaker donor compared to MICs (entry 7–9), however a stronger donor than nNHCs (entry 1–6). An additional substituent at the C2-position (entry 14) or

at the C2- and C4-position (entry 7–9) leads to increased electron density in the zwitterionic imidazole moiety. The more substituents with a positive inductive effect are bound to the imidazole moiety the more electron rich are the compounds which leads to a lower TEP value. The prepared ligand is an effective electron donor but due to the two backbone H-atoms maybe not stable enough to isolate the free MIC. The calculated TEP values for entry 10–13 have to be handled with care. The first value was calculated with the BP86 DFT-functional and the second was calculated with B3LYP. Between these calculations are great differences, which could be seen comparing the values 2051.85 (BP86) and 2137.4 cm^{-1} (B3LYP) for entry 10. As not enough compounds have been compared using those calculation strategies, these compounds could not be classified concerning their donor ability. But a comparison between entries 10–13 could be done and within the standard deviation of 1 cm^{-1} the substituent at the phenyl ring seems to make no significant difference for the donor strength. Comparing the backbone CH-shift of C2- and C4-substituted NHCs a significant difference can be observed. It is likely to see that a substitution at the C4-position has more influence on the acidity of the C5 H-atom. The backbone protons of (IPrPh)I and IPr·HCl show a $^1\text{H-NMR}$ resonance in the range of 8.0–8.3 ppm. The C2-proton of IPr·HCl has a resonance at 10.1 ppm, which is in much lower field and therefore much more acidic than the backbone protons. Furthermore, the adjacent hydrogen atom and the carbene could switch among each other. This is not possible for the nNHC due to the adjacent threefold coordinated nitrogen atoms.

Coincidentally Dipp Migration

Attempts for the preparation of the nickel tricarbonyl and the iridium dicarbonyl chloride NHC compounds were made to experimentally investigate the CO stretching vibration (i.e., TEPs). Unfortunately, these efforts were not successful. The reaction of $\text{Ni}(\text{COD})_2$ with the MIC could just be performed *in situ* due to the instability of the free MIC.

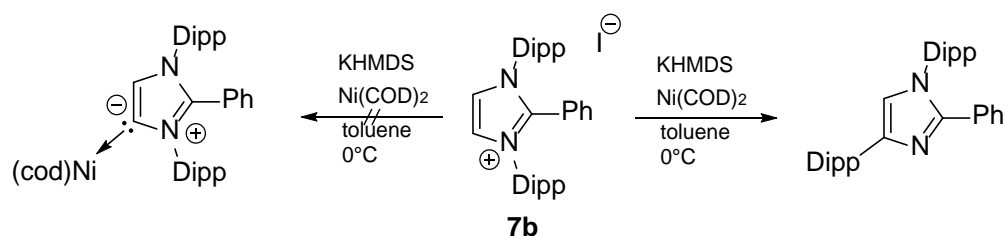


Figure 2.27: Reaction of **7a** with KHMDS and nickel cyclooctadiene led to a Dipp N-C migration.

As known from earlier reports a migration of the C2-bound substituent to the C4-backbone position is likely to happen.^[43h, 119, 138a] Surprisingly, a migration of the Dipp substituent of the nitrogen atom to the C4-backbone position has been so far not observed.

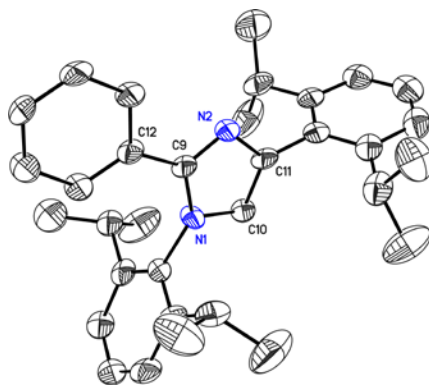


Figure 2.28: Migration of Dipp ligand from the nitrogen to the backbone of the imidazole moiety. The data of this crystal structure is below our internal quality standards and is therefore not further discussed but should illustrate the unexpected result.

The synthesis of the iridium complex also did not lead to the desired compound. The $[\text{Ir}(\text{COD})\text{Cl}]$ dimer could be synthesised according to literature.^[31] Unfortunately, the $[(\text{NHC})\text{Ir}(\text{CO})_2\text{Cl}]$ complex could not be prepared due to the instability of the free carbene.

2.5.2. NMR Measurements

On comparing the ^1H - and ^{13}C -NMR chemical shift values of the five different C2-arylated imidazolium salts, it becomes obvious that the substitution of the initial aryl halide exert an influence on the backbone H-atoms of the imidazole moiety (Table 2-11). As discussed for compounds **7–10** the C4/C5 backbone shift can be correlated with the CH acidity. The further their downfield shift the higher the acidity. This gives us the possibility to synthesise new C2-arylated compounds with other substituents and tune the acidity as needed.

Table 2-11: ^1H - and ^{13}C - NMR shifts of the backbone hydrogen- and carbon- atoms respectively of compounds **7, 12–15**.

	^1H -NMR shifts of the backbone H-atoms [ppm]	^{13}C -NMR shifts of the backbone C-atoms [ppm]
(IPrPh-4-OMe)I(14)	8.01	126.52
(IPrPh-4-Me)I (12)	8.02	126.71
(IPrPh-2-Me)I(13)	8.11	127.16
(IPrPh)I(7)	8.15	127.09
(IPrPh-4-CO ₂ Me)I(15)	8.30	127.85

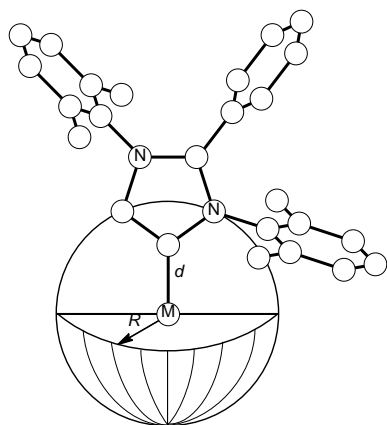
Compound **15** is therefore the most acidic compound compared to the other synthesised compounds.

2.5.3. Percent Buried Volume Calculation

To investigate the ligand environment further occupation calculations with the program SambVca for all precursor salts and the abnormal copper iodide complex were made.^[32] X-ray diffraction data was used for the calculation of %Vol_{bur}. The input .xyz files were manipulated in a way that the C4-position of the imidazole moiety was deprotonated. With the purpose of comparing optimised values (%Vol_{bur,opt}) with the crystallographic data, the crystal structure was geometry optimised by Avogadro^[159] using the MMFF94 force field. Furthermore default values suggested

by Cavallo *et al.* were used for the calculation.^[32] Not surprisingly, the values for both cases show the same tendency. The substituent has just a very little influence on the %Vol_{bur}. Four out of five aryl halides are *para* substituted and have a minor impact on the strain of the Dipp ligand, which occupies the carbene sphere. The *ortho* substituted aryl halide shows the highest %Vol_{bur} which can be explained by the steric effect of the *ortho* methyl group on the Dipp ligand. One Dipp ligand is not involved in the occupation of the coordination sphere which generally leads to smaller %Vol_{bur} values compared to nNHCs. Due to the expanded N–C–N angle one Dipp ligand is pushed into the coordination sphere.

Table 2-12: %Vol_{bur} values for selected compound and a schematic representation of the buried volume..



Compound	%V _{bur}	%V _{bur} opt
(IPrPh-2-Me)I	35.6	33.4
(IPrPh)I	33.9	31.7
(IPrPh-4-Me)I	32.3	31.4
(IPrPh-4-CO ₂ Me)I	32.1	31.2
(IPrPh-4-OMe)I	31.1	30.3
[(IPrPh)Cu]I	30.3	-
[(IPrPh)Cu]I, 1.897	33.3	-
IPr	33.6	-

In terms of sterics, C2-arylated compounds do not differ much from a nNHCs. Comparing IPr with the (IPrPh)I compound, the %Vol_{bur} value just differs by 0.3% which is negligible. The different reactivity of compound **7a** towards deprotonation and the problems of isolating the MIC IPrPh allow for the conclusion that the acidity of the backbone protons plays a major role in terms of reactivity.

2.6. Coin Metal Complexes of (IPrPh)I (**7a**)

Among a variety of routes to NHC-metal complexes, trans-metallation with silver or copper complexes has found to be the most convenient, as these complexes can be directly prepared from the air stable imidazolium salts.^[7, 86, 96, 100b, 101c, 124, 148, 160] Therefore, the suitability of the C2-arylated imidazolium salts **7a**, **12–15** to deliver the desired MIC-copper complexes was evaluated. Treatment of a 1:1 mixture of the MIC-precursor **7a** and CuI with KN(SiMe₃)₂ afforded the MIC-copper complex [(IPrPh)Cu]I (**26**) as a yellowish solid in 91% yield (Figure 2.29).^[68c]

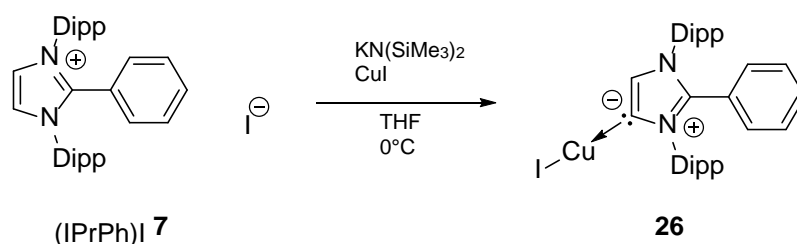


Figure 2.29: Synthesis of MIC-copper complex **26**.

The ¹H-NMR spectrum of **26** clearly indicates the deprotonation of **7a** with KN(SiMe₃)₂ to form the imidazole-4-ylidene. The remaining imidazole proton at the C5 position appears as a singlet at $\delta = 6.99$ ppm. Compound **26** shows three sets of signals for the methyl protons of the isopropyl groups. The EI mass spectrum of **26** exhibits the molecular ion [(IPrPh)CuI]⁺ peak at 654 amu. Elemental analysis, NMR spectroscopy, and mass spectral studies confirm the structure of **26**. Alternatively, compound **26** was also prepared by treatment of **7b** with CuCl and KN(SiMe₃)₂.

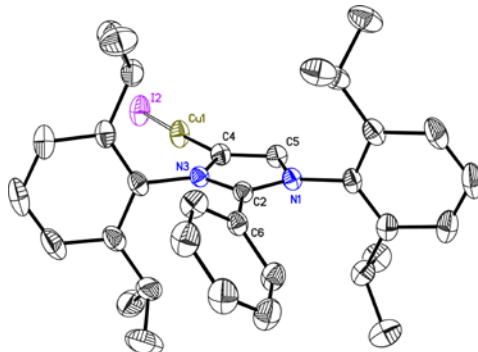


Figure 2.30: Molecular structure of MIC-copper complex [(IPrPh)CuI] (**26**). **26** was refined with 60% of iodine and 40% of chlorine occupancies. Hydrogen atoms and the chlorine disorder have been omitted for clarity. Anisotropic displacement parameters are depicted at the 50% probability level.

Colourless crystals were grown from a saturated toluene solution at room temperature which exhibited ¹H- and ¹³C-NMR resonances indistinguishable from those shown by the compound **26** prepared by using CuI. Single-crystal X-ray diffraction unequivocally supported the formation of complex **26**, the molecular structure of **26** shows disorder. The structure of **26** was refined with 60% of iodide and 40% of chloride occupancies, suggesting the formation of chloro as well as iodo derivatives of [(IPrPh)CuX] (X = Cl or I), which crystallise together. The disordered solvent molecules and halogen atoms were modelled and refined. Both N3–C4 and C4–C5 bonds are elongated compared to the free ligand. The N3–C4–C5 bond angle in **26** (103.3°) is decreased by 4°. These features are comparable to those of NHCs and their metal complexes.^[124, 148] This

accounts for the increased s-character at the C4 carbon atom in **26**. The N1–C2–N3 bond angle remains essentially the same.

Dimeric NHC copper complexes have been prepared in the past by the two groups of *Nolan* and *Gall*.^[161] Tetrakis(acetonitrile)copper(I) was used as copper source and treated with different azolium salts in the presence of sodium *tert*-butoxid to yield the corresponding [Cu(NHC)₂]X complexes. NHC salts with the tetrafluoroborate and hexafluorophosphate anions were used in this synthesis.

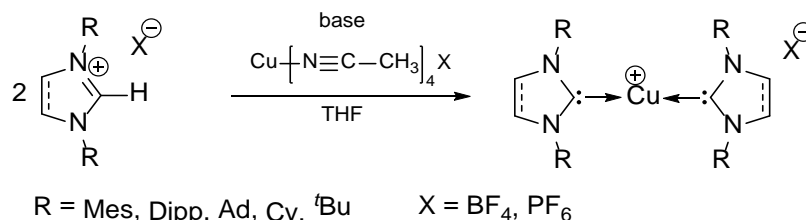


Figure 2.31: Synthesis of bis-NHC copper complexes by *Nolan et al.*

Another way to synthesise bis NHC copper complexes is a decarboxylation reaction in the presence of a copper salt. Therefore, the *N*-heterocyclic caboxylates have to be prepared by deprotonation of the azolium salt followed by a carbene quenching with carbon dioxide.

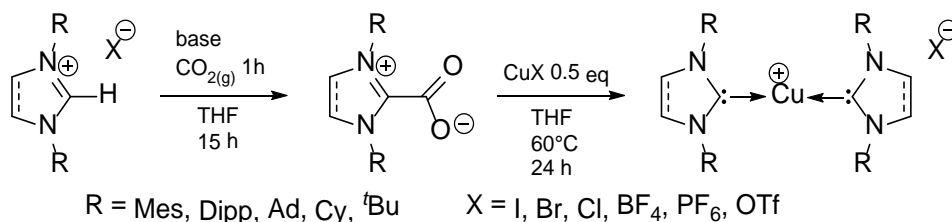


Figure 2.32: Synthesis of bis-NHC copper complexes by *Gall et al.*

The presented bis-NHC Cu complexes are very active catalysts in the 1,3-dipolar Huisgen cycloaddition (click chemistry) and hydrosilylation reactions.

In order to possibly improve the catalytic activity of bis-NHC-Cu-complexes a MIC moiety was introduced into the complex. Therefore, (IPrPh)I was deprotonated in the presence of CuI at 0°C to form (IPrPh)CuI. The resulting compound was then reacted with IPr to form the bis-MIC-Cu-complex [(IPrPh)Cu(IPr)]I.

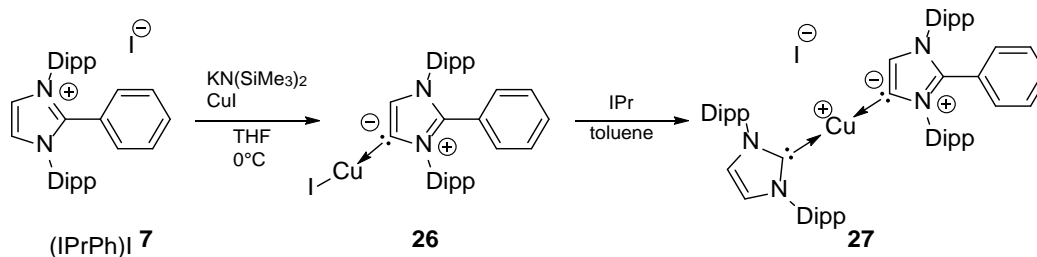


Figure 2.33: Synthesis of a mixed nNHC-MIC-Cu-complex.

The ¹H-NMR spectrum shows the two backbone singlets from which the two IPr backbone hydrogen atoms (7.75 ppm) are lowfield shifted. The C5 hydrogen atom at the MIC moiety shows a resonance at 6.51 ppm. Furthermore, from the heteronuclear single quantum correlation spectroscopy experiment (HSQC), three sets of multiplets representing the asymmetrical

environment of the Dipp ligands could be assigned. Two multiplets at 2.21 and 2.33 ppm belong to the MIC moiety and the third septet at 2.58 ppm represents the Dipp groups of the IPr moiety. The ESI mass spectrometry shows the molecular ion peak of the cation at $[\text{IPrPhCuIPr}]^+$ 915.5 amu. Suitable crystals for X-ray diffraction experiments could be grown from a DCM/toluene mixture.

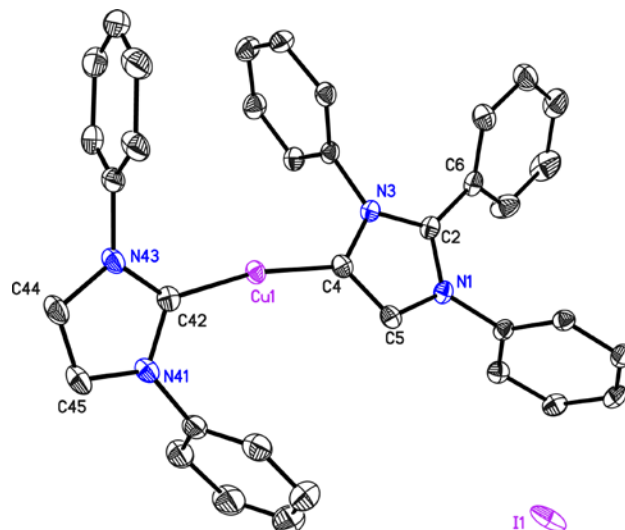


Figure 2.34: Molecular structure of bis MIC-copper complex $[\text{IPrPhCuIPr}]\text{I}$ (**27**). Hydrogen atoms and isopropyl groups have been omitted for clarity. Anisotropic displacement parameters are depicted at the 50% probability level

In comparison with crystal structures of two bis-nNHC-Cu-complexes reported by *Nolan et al.* the Cu–C bond length of 1.901 Å (Cu1–C4) and 1.904 Å (Cu1–C42) are comparable to the reported ones ($[(\text{IPr})_2\text{Cu}]\text{PF}_6$ Cu–C 1.938(5); $[(\text{IPr})_2\text{Cu}]\text{BF}_4$ Cu–C 1.939(18)).^[161a] The C4–Cu1–C42 angle of compound **26** is 168.45°, that is more bent than for the nNHC dimers which have an angle close to 180°. With the intention of changing the coordinating iodine anion to a non-coordinating anion an anion exchange reaction with sodium tetrafluoroborate was performed. $[\text{IPrPhCuIPr}]\text{BF}_4$ (**27b**) could be isolated in good yields of 70%.

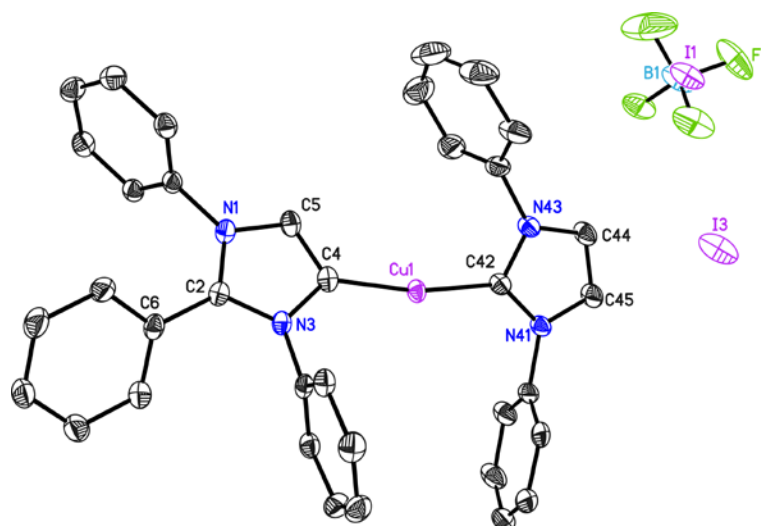


Figure 2.35: Molecular structure of bis MIC-copper complex $[\text{IPrPhCuIPr}]\text{BF}_4$ (**27a**). Hydrogen atoms and isopropyl groups have been omitted for clarity. Anisotropic displacement parameters are depicted at the 50% probability level

In order to generate a bis-MIC-Cu-complex, **7a** was treated with $\text{KN}(\text{SiMe}_3)_2$ and an sub stoichiometric amount of copper salt to yield **28** (Figure 2.36).

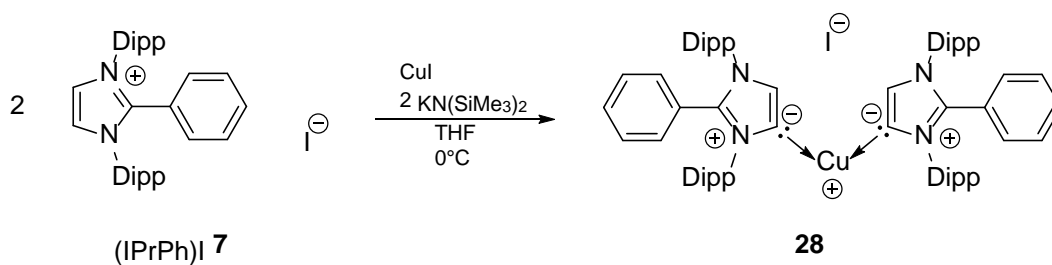


Figure 2.36: Synthesis of the bis-MIC-Cu-complex **25**.

The reaction was performed in THF for 2 h at 0°C. Afterwards the reaction was allowed to warm to room temperature and then filtered. The solvent was removed under reduced pressure and compound **28** was obtained in yields of 40%. The ¹H-NMR spectrum of compound **28** shows two overlapping sets of septets representing the *ipso*-hydrogen atoms of the isopropyl groups. The backbone hydrogen atoms could be assigned to a singlet at 7.08 ppm. Crystals could be grown from a saturated DCM solution. **28** crystallises in the hexagonal space group P6₃22 (Figure 2.37).

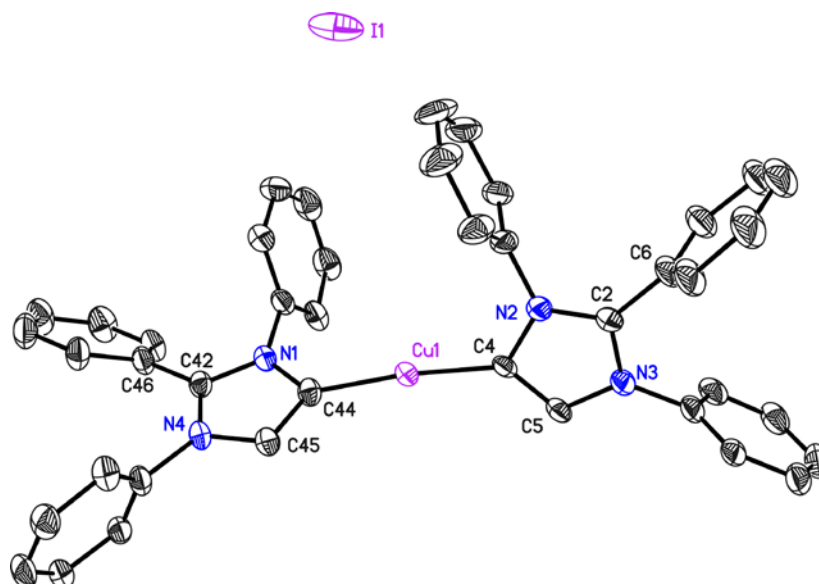


Figure 2.37: Crystal structure of **28**. Hydrogen and isopropyl groups have been omitted for clarity. Anisotropic displacement parameters are depicted at the 50% probability level.

The bond lengths in the crystal are in the same range then for their normal analogues. The Cu–C bond length lies in the range of 1.9 to 2.0 Å. Furthermore, it was tried to synthesise analogous silver complexes.

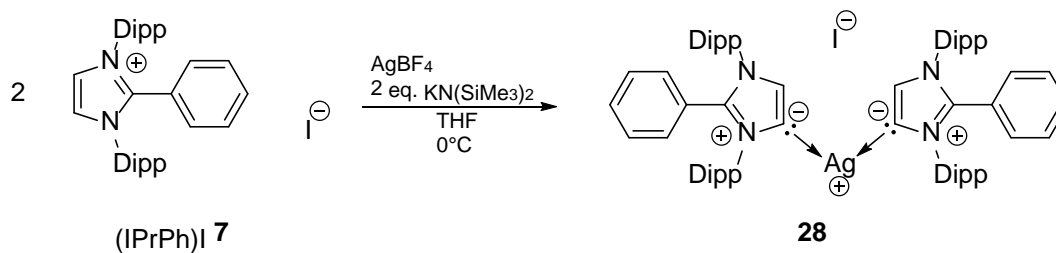


Figure 2.38: Synthesis of the bis-MIC-Ag-complex **28**.

The reaction of C2-blocked ligand in the presents of KHMDS as base and 0.5 equivalents of silver tetrafluoroborate led to the corresponding silver complex in 91 % yield. Crystals could be grown from a saturated DCM solution. **29** crystallises in the hexagonal space group $P6_322$.

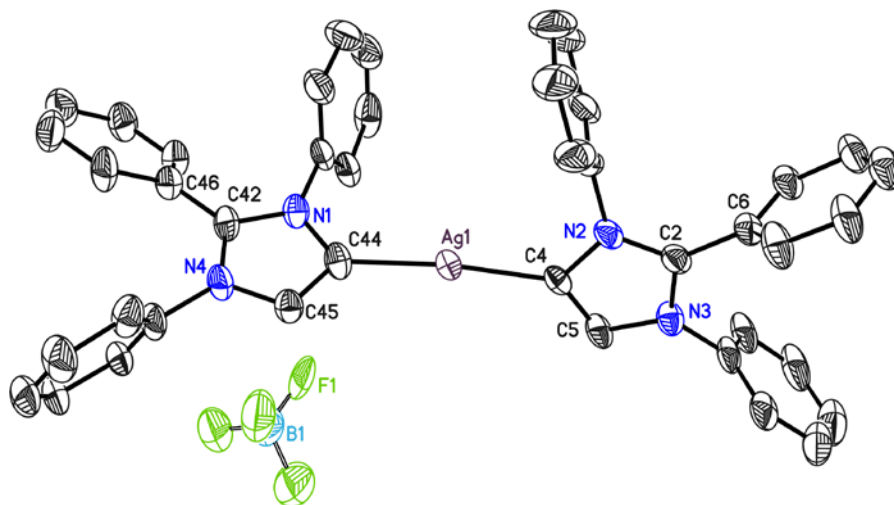


Figure 2.39: Crystal structure of **29**. Hydrogen and isopropyl groups have been omitted for clarity. Anisotropic displacement parameters are depicted at the 50% probability level.

The Ag—C bond lengths are comparable to literature in the range of 2.0–2.15 Å.

2.7. Application of Copper Catalysts (26–28) in Click Chemistry

NHC copper complexes are commonly used in catalysis. They can be divided into two classes: neutral mono-NHC and cationic bis-NHC derivatives. Some selected catalytic reactions are the boration- of alkenes^[162], allylic substitutions^[163], [3+2] cycloaddition (click chemistry)^[68b, 164] or hydrosilylations^[161a]. NHC copper complexes are very efficient as catalysts due to the tune ability of the NHC. NHCs can stabilise the copper halide and help to solve problems like catalyst crumbling or solubility. The catalytic activity of their MIC copper complex (1,3-bis(2,6-diisopropylphenyl)-2,4-diphenylimidazol copper (I) chloride) is outstanding.^[114a] Catalysts could be apply to at least 27 examples with not less than 73% isolated yield in maximal 5 hours reaction time. The reaction of benzyl azide with phenylacetylen yields 99% product in 20 minutes' time.

With a number of MIC-copper compounds in hand we decided to probe their catalytic activity for Copper(I)-catalysed Azide-Alkyne Cycloaddition (CuAAC) reactions. All three potential catalysts (26, 27, 28) have been tested in reactions using the same alkynes and azides in order to compare the catalytic activity.

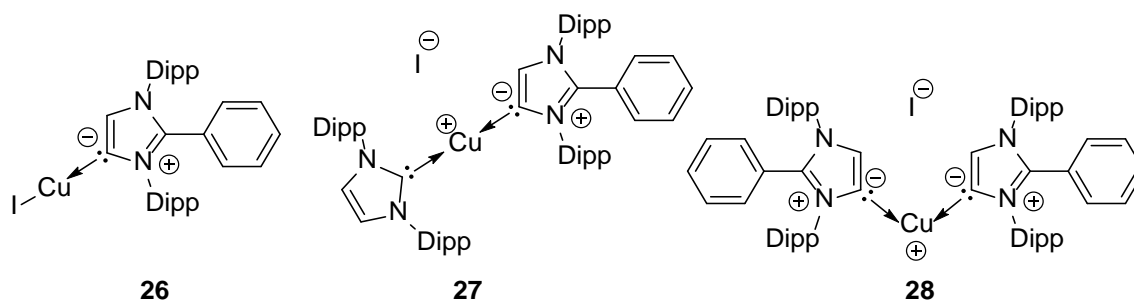


Figure 2.40: Copper complexes 26-28 used as catalysts in this work.

Table 2-13 summarises the reaction conditions (reaction times, used alkynes, catalysts and the conversion).

Table 2-13: Reactions performed to investigate the catalytic activity of the synthesised catalysts **26**, **27** and **28**.

Entry	Time[h]	R	Catalyst [1 mol%]	Conversion ^[a]
1	3	Ph	26	83
2	3	Ph	27	0
3	3	Ph	28	0
4	48	Ph	26	100
5	48	Ph	27	100
6	48	Ph	28	55
7	15	C ₂ H ₄ OH	26	100
8	15	C ₂ H ₄ OH	27	100
9	15	C ₂ H ₄ OH	28	80
10	15	C ₅ H ₄ N	26	100
11	15	C ₅ H ₄ N	27	100
12	15	C ₅ H ₄ N	28	83
13	15	Bu	26	100
14	15	Bu	27	26
15	15	Bu	28	8
16	15	C ₃ H ₆ OH	26	100
17	15	C ₃ H ₆ OH	27	100
18	48	C ₃ H ₆ OH	28	3

[a] The conversion was measured *via* ¹H-NMR spectroscopy.

Compound **26** appeared to be the most active catalyst in all reactions (entry 1, 4, 7, 10, 13, 16) with yield of 83–100%. It is shown that **26** is catalytically active independent of the substrate. In contrast to the reaction with **26**, the cycloaddition with **27** needs much longer reaction times (entry 2 and 5). After a reaction time of 3 h no conversion of the starting materials could be observed whereas after 48 h, all starting material is converted to the triazole. Compound **28** shows the least catalytic activity of the three copper complexes (entry 3 and 6). Even after 48 h just 55% of the starting materials were converted to the triazole. This activity ranking of the copper complex (**26** > **27** > **28**) is also shown for the other alkynes, even if generally the reaction time was increased to 15 h. The overall lowest catalytic activity was observed for the Bu-alkyne. **26** delivers complete conversion, while with **27** and **28** only 26% and 8% conversion could be reached respectively.

The mechanism of the copper catalytic [3+2] cycloaddition of alkynes and azides has been investigated by *Sharpless* and others. The catalytic cycle starts from the formation of the Cu(I) acetylide species (**29**) by the transformation of the catalyst with the alkyne. Upon the interaction of **29** with the azide the triazolide intermediate (**32**) was formed. Two further intermediates (**31** and **32**) could not be isolated, but there is evidence from extensive DFT calculations of their existence. (Figure 2.41).^[165]

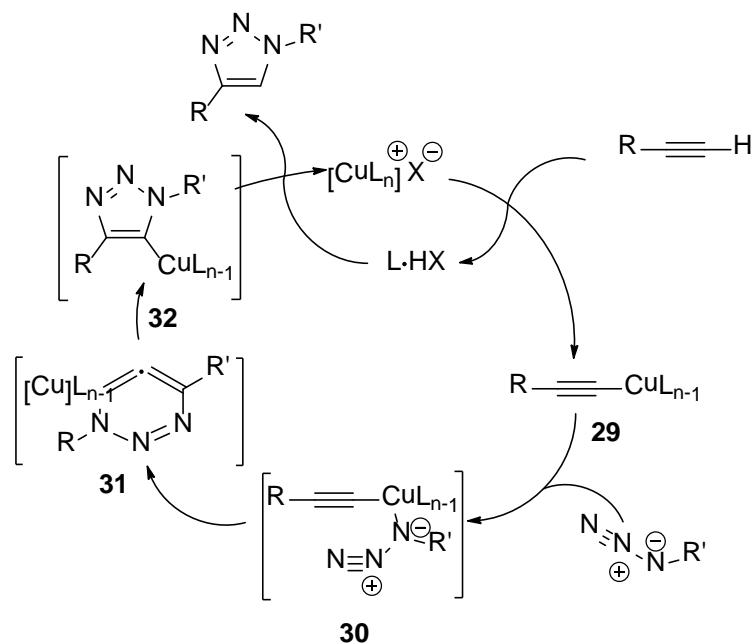


Figure 2.41: General mechanism for the copper-(I)-catalysed azide-alkyne cycloaddition.

Within these results, and the $^1\text{H-NMR}$ result from chapter 2.5, it could be argued, that a mono-ligated copper species is needed to form the acetylide. The formation of a mono-ligated copper species is achieved easier from **27** than from **28**. The second abnormal bound NHC in **28** is more difficult to remove, in comparison with the nNHC in **27**, to obtain the catalytic active mono-ligated NHC species. This is in accordance with the results of the reactions containing **27** and **28** as catalysts.

For further investigations the reaction conditions could be changed. Neat [3+2] cycloadditions containing nNHCs as catalyst show complete conversion in very short reaction times. Probably applied neat conditions will increase the yields and reduce the reaction times of the reaction using catalyst **26** and **27**.

2.8. Threefold Click Chemistry: Improved Procedure

One topic in our workgroup is currently concentrating on the synthesis of C₃-symmetric triazole ligands and their metal coordination. The basic reaction is a copper catalysed [3+2] cycloaddition of 1,1,1-tris(azidomethyl)ethane with three equivalents of alkyne (Figure 2.42).

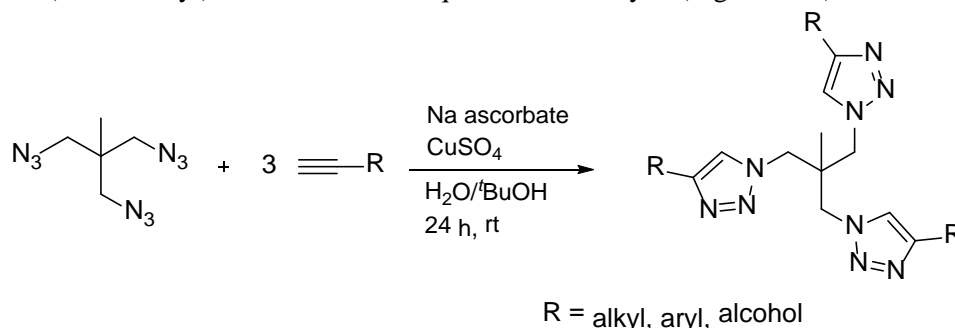


Figure 2.42: Synthesis of C₃-symmetric trisubstituted triazoles.

In this particular case the copper source is copper sulphate (CuSO₄). In the presence of a base in a solvent mixture of water and *tert*-butanol the reaction yields the desired trisubstituted triazole in 24 h at room temperature. The desired product precipitates from a cold pentane solution. A drawback of this standard procedure is the elaborate workup due to the presence of remaining copper in the reaction mixture. In view of metal complexes of the trisubstituted triazole ligand, copper residues have to be removed completely. The copper salt is good soluble in water and has to be extracted from the crude product with aqueous ammonia several times.

Using compound **26**, **27** or **28** as catalyst in this click reaction, the conversion can be performed in DCM at room temperature as discussed (Figure 2.43).

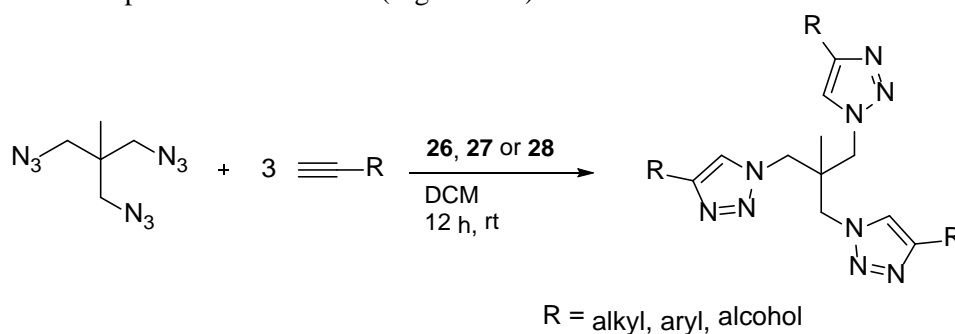


Figure 2.43: Synthesis of C₃-symmetric trisubstituted triazoles using copper complexes **26**, **27** and **28**.

To precipitate the product from the solution, cold pentane has to be added as mentioned before. The remaining solution can be filtered and washed with pentane to yield the pure product. A test on copper has been confirmed with aqueous ammonia to ensure no remaining copper in the product.

This improved procedure is sustainable and shortens the workup without reducing the yield. Reactions with different acetylenes could be performed following the same procedure. Herein phenylacetylene, 3-butyne-1-ol, 2-methyl-3-butyne-1-ol, 3,3-dimethyl-1-butyne and 1-pentyne were used to extend the scope of the application (Table 2-14). Measured ¹H-NMR data was compared to reported data.^[166]

Table 2-14: Alkyne-azide cycloaddition reaction performed with catalyst **26**, **27** and **28**.

Entry	Catalyst	Loading [mol%]	Alkyne	Yield [%]
1	IPhCuI	1	Phenylacetylene	99
2	(IPh) ₂ CuI	0.5	Phenylacetylene	91
3	(IPh) ₂ CuI	1	Phenylacetylene	79
4	[(IPh)Cu(IPr)]I	1	Phenylacetylene	76
5	IPhCuI	1	3-butyn-1-ol	65
6	IPhCuI	1	2-methyl-3-butyn-2-ol	74
7	IPhCuI	1	3,3-dimethyl-1-butyne	71
8	IPhCuI	1	1-Pentyne	87

Five 1,2,3-trisubstituted 1,2,3-triazoles could be synthesised using this modified procedure. It could be shown that all 1,2,3-trisubstituted 1,2,3-triazoles could be prepared in high to moderate yields using the different catalyst species **26**, **27** or **28**.

3. Conclusion and Outlook

Within this thesis, a novel synthetic access to C2-arylated imidazolium salts as precursors for MIC ligands was developed. The properties of the MIC precursors (**7a**, **8–10**, **12–15**) were investigated as well as their coin metal complexes (**26–28**, **33?**). Furthermore, the catalytic activity of the copper-NHC-complexes (**23–25**) examined.

The first catalytic C2-arylation of a NHC has been developed. Many examples could be synthesised (Figure 3.1).

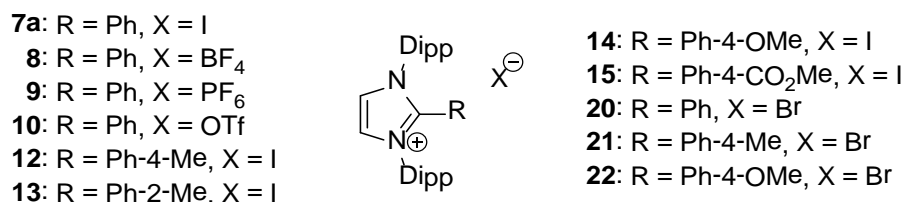


Figure 3.1: Synthesised C2-arylated NHCs as precursor for MICs.

Furthermore, the catalytic process could be optimised. It was found that the most beneficial conditions were to use 1 mol% of palladium catalyst in refluxing *o*-xylene for 2 h. The catalytic C2-arylation could also be performed using nickel halides as catalysts. The reactions however led to lower yields.

The synthesised compounds **7a**, **8–10** and **12–15** have been investigated with a particular emphasis on their electronic and steric properties. DOSY NMR measurements and others were used to find out that in all cases counter anions coordinate to the ligand to a certain extent. DFT calculations were made to evaluate the TEP for **7a**, **12–15**. It has been shown that the MIC is a stronger σ -donor compared to its nNHC counterparts. Furthermore, buried volume of compound **7a** and **12–15** have been calculated using the SambVca tool by *Cavallo et al.* Interestingly, it turns out that in the investigated cases the sterical demand of **7a** and **12–15** does not differ much from the known nNHCs.

In situ **7a** could successfully be deprotonated and reacted with Cu and Ag salts to yield compounds **26–28** (Figure 3.2).

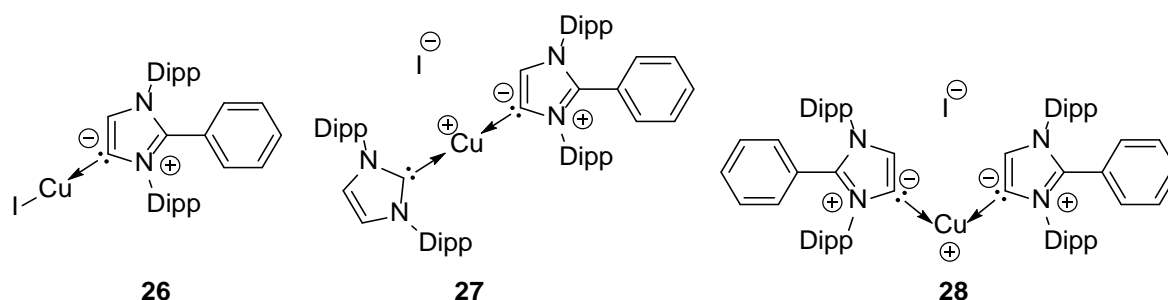


Figure 3.2: Synthesised MIC-Cu complexes **26–28**.

These Cu- and Ag-NHC complexes have been analysed and compared to their normal analogues. Moreover, the applicability of compounds **26–28** as catalyst in [3+2] cycloadditions has been evaluated. It could be verified that **26–28** catalysed the cycloaddition reaction. The most effective catalyst is, on this occasion the monomeric compound **26** followed by compound **27**.

Complexes **26–28** have also been applied in a [3+2] cycloaddition reaction for triazoles. The reaction towards triazolones typically uses CuSO_4 and sodium ascorbate in a solvent mixture of water and *tert*-butanol. The drawback of this reaction is the elaborate workup process, which include repeated washing with aqueous ammonia to remove all copper residues. With the use of the presented copper complexes **26–28** the reaction could be done in DCM which shortens the workup time. The purity of the desired 1,2,3-triazolone and therefore the absence of copper, could be verified with a copper analysis experiment.

Further work should be focused on the optimisation of the nickel catalysed C2-arylation as a sustainable and cheap alternative to the palladium catalysed reaction. An important and interesting work will be the investigation of the catalytic cycle involved. The knowledge of actual transition states is important to adjusted reaction conditions.

First reactions to investigate the catalytic activity of the copper complexes have been made. It is further necessary to expand the range of application for these kinds of compounds and to compare its activity with known catalysts.

Another desirable aim is the synthesis and characterisation of free MICs (Figure 3.3).

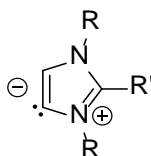


Figure 3.3: Desired free abnormal C2-arylated NHC.

In order to reach this goal, it could be beneficial to vary the substituents either at the nitrogen atom or at C2-position. If it could be managed to raise the acidity of the NHC backbone hydrogen atoms, one can be optimistic that the free MIC could be isolated.

C2-arylated NHCs allow functionalization at the backbone carbon atoms. A challenging task would be the introduction of another donor function *via* functionalization or the bridging of two NHC-moieties over the backbone carbon atoms (Figure 3.4).

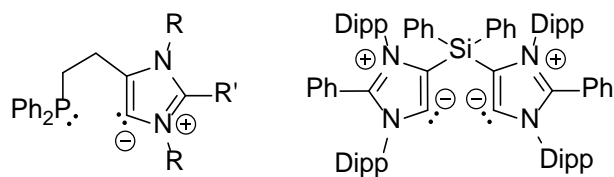


Figure 3.4: Proposed functionalisation of C2-arylated imidazolium salts.

These ligands featuring MIC moieties are believed to open new opportunities in organometallic chemistry as well as in catalysis.

4. Experimental Section

4.1. General Procedures

All reactions, except otherwise stated, were carried out with strict exclusion of air and moisture under nitrogen or argon atmosphere using modified *Schlenk*-techniques or in an argon dry box.^[167] All solvents were dried using standard laboratory procedures and were freshly distilled from sodium/potassium alloy (Et₂O, *n*-pentane, 1,4-dioxane, *o*-xylene), potassium (THF), sodium (*n*-hexane, toluene) or phosphorous pentoxide (DCM) prior to use. Solvents used for the synthesis were degassed according to standard laboratory procedures and stored over 3 Å molecular sieves (dried in vacuum at 300°C for 48 h). All employed reactants were commercially available or reproduced according to the given literature procedure.

4.2. Analytical Methods

4.2.1. Mass Spectrometry

EI-spectra were recorded with a *MAT 95* device (EI-MS: 70 eV). ESI-spectra were recorded either with a micrOTOF (ESI-TOF-MS) mass spectrometer (*Bruker Daltronik*) or a maXis (ESI-QTOF-MS) mass spectrometer (*Bruker Daltronik*). The measurements were performed by the *central analytic unit of the institute of organic and biomolecular chemistry* at the Georg-August University Göttingen. Peaks are given as a mass to charge ratio (*m/z*) of the fragment ions, based on the molecular mass of the isotopes with the highest natural abundance (¹H, ¹²C, ¹⁴N, ¹⁶O, ¹⁹F, ²⁸Si, ³²S, ³⁵Cl, ⁶³Cu, ^{79/81}Br, ¹⁰⁷Ag, ¹²⁷I).

4.2.2. NMR Spectroscopy

Samples were prepared and filled in NMR-tubes inside an argon dry box or when the compound was air and moisture stable no precautions were taken, instead of self-protection (gloves, goggles, labcoat). The NMR-tube was sealed to exclude any impurities. Spectra were recorded at room temperatures with a *Bruker Avance 300*, *Bruker Avance 400*, or a *Bruker Avance 500* NMR spectrometer. All chemical shifts δ are given in ppm, relative to the residual proton signal of the deuterated solvent.^[168] Assignments of the shifts were controlled by two-dimensional correlation spectra (heteronuclear single quantum correlation (HSQC)-, heteronuclear multiple bond correlation (HMBC)- and correlation spectroscopy (COSY) experiments). The shifts of the ¹⁵N-NMR signals were recorded in a ¹⁵N, ¹H-HMBC experiment.

4.2.3. Elemental Analysis

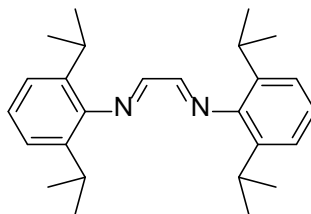
Elemental analysis was performed as a combustion analysis by the *Analytical Laboratory of the Institute of Inorganic Chemistry* at the Georg-August-Universität Göttingen with an *elementar vario EL III* device. The inclusion of argon, from canning in an argon dry box, led to systematic errors.

4.2.4. Computational studies

DFT calculation of the TEP value was performed by Thorsten Teuteberg from the workgroup of Prof. Ricardo Mata at the University of Göttingen.^[158, 169]

4.3. Synthesis and Characterisation

4.3.1. Synthesis of bis(2,6-diisopropylphenyl)diazabutadiene



In a one litre round bottom flask 2,6-diisopropylaniline (94.0 g, 0.52 mol), glyoxal (15.7 g, 0.27 mol) and methanol (500 mL) was added. Some drops of formic acid were applied as catalyst. The reaction mixture was stirred overnight and the precipitate was filtered afterwards. The crude product was washed with methanol and the solvent was removed in vacuum to yield the desired compound as yellow solid (84.7 g, 83%).

Empirical formula: C₂₆H₃₆N₂

Molecular weight: 376.29 g/mol

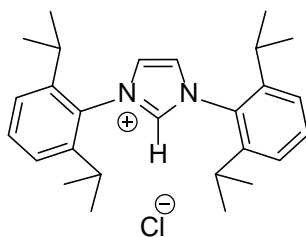
Yield: 84.7 g, 225.1 mmol, 83%.

¹H-NMR (300.13 MHz, THF-*d*₈): δ 1.21 (d, *J* = 6.9 Hz, 24H, H_{CM_e2}), 2.94 (sept, *J* = 6.9 Hz, 4H, CH_{Me2}), 7.21–7.16 (m, 6H, *m*-C₆H₃, *p*-C₆H₃), 8.10 (s, 2H, NCH) ppm.

¹³C{¹H}-NMR (75.47 MHz, THF-*d*₈): δ 23.5 (H_{CM_e2}), 28.2 (H_{CM_e2}), 123.3 (*m*-C₆H₃), 125.3 (*p*-C₆H₃), 136.9 (*o*-C₆H₃), 148.2 (*ipso*-C₆H₃), 163.3 (NCH) ppm.

Reference: ^[137a]

4.3.2. Synthesis of 1,3-bis(2,6-diisopropylphenyl)imidazolium chloride (IPr·HCl)



N,N'-(2,6-diisopropylphenyl)-1,4-diaza-1,3-butadiene (50 g, 0,13 mol) was dissolved in toluene (500 mL). Paraformaldehyde (3.9 g, 0,13 mol) was added and the reaction mixture was heated to 60°C. Subsequent slowly addition of trimethylsilylchlorid (16.5 mL, 0,13 mol) the reaction mixture was allowed to cool down to room temperature. The reaction mixture was stirred for 3 days the precipitate was filtered and washed three times with THF. The volatiles were evaporated under vacuum and the desired compound was obtained as off white solid (50.8 g, 92%).

Empirical formula: C₂₇H₃₈ClN₂

Molecular weight: 425.05 g/mol

Yield: 50.8 g, 120 mmol, 92%.

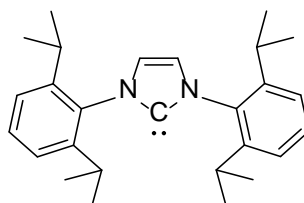
¹H-NMR (300.13 MHz, THF-*d*₈): δ 1.25 (d, *J* = 6.9 Hz, 12H, CHMe₂), 1.29 (d, *J* = 6.9 Hz, 12H, CHMe₂), 2.45 (sept, *J* = 6.9 Hz, 4H, CHMe₂), 7.34 (d, *J* = 7.8 Hz, 4H, *m*-C₆H₃), 7.57 (t, *J* = 7.8 Hz, 2H, *p*-C₆H₃), 8.14 (d, *J* = 1.5 Hz, 2H, NCH), 10.12 (s, 1H, NCHN) ppm.

¹³C{¹H}-NMR (75.47 MHz, THF-*d*₈): δ 23.9 (s, 4C, CHMe₂), 25.0 (s, 4C, CHMe₂), 29.7 (s, 4C, CHMe₂), 125.1 (s, 4C, *m*-C₆H₃), 126.1 (s, 2C, NCH), 130.6 (s, 2C, *ipso*-C₆H₃), 132.5 (s, 2C, *p*-C₆H₃), 141.2 (s, 1C, NCHN), 145.7 (s, 4C, *o*-C₆H₃) ppm.

Reference: ^[137a]

4.3.3. Synthesis of 1,3-bis(2,6-diisopropylphenyl)imidazole-2-ylidene

(IPr) (1)



THF (250 mL) was added to a mixture of IPr·HCl (30.0 g, 70.7 mmol) and potassium *tert*-butoxid (7.9 g, 70.7 mmol) at room temperature. The reaction mixture was stirred for 6 ½ h and the solution was filtered through a plug of Celite®. The volatiles were removed under vacuum and the desired carbene was obtained as brown solid (25.0 g, 91%).

Empirical formula: C₂₇H₃₆N₂

Molecular weight: 388.59 g/mol

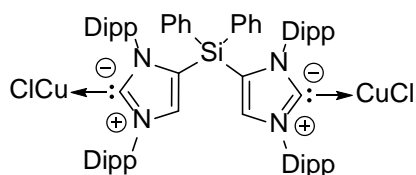
Yield: 25.0 g, 64.3 mmol, 91%.

¹H-NMR (300.13 MHz, THF-*d*₈): δ 1.16 (d, *J* = 6.9 Hz, 12H, CHMe₂). 1.20 (d, *J* = 6.9 Hz, 12H, CHMe₂), 2.82 (sept, *J* = 6.9 Hz, CHMe₂), 7.18 (s, 2H, NCH), 7.25 (d, *J* = 7.2 Hz, 4H, *m*-C₆H₃), 7.36 (t, *J* = 6.6 Hz, 2H, *p*-C₆H₃).

¹³C{¹H}-NMR (75.47 MHz, THF-*d*₈): δ 23.9 (s, 4C, CHMe₂), 25.0 (s, 4C, CHMe₂), 29.4 (s, 4C, CHMe₂), 122.6 (s, 4C, *m*-C₆H₃), 124.1 (s, 2C, NCH), 129.3 (s, 2C, *ipso*-C₆H₃), 139.8 (s, *o*-C₆H₃), 146.9 (s, 4C, *o*-C₆H₃) ppm.

Reference: ^[137a]

4.3.4. Synthesis of bis(1,3-bis(2,6-diisopropylphenyl)-4-diphenylsilane-5-hydro-1*H*-imidazol)-copper chloride $\text{Ph}_2\text{Si}[(\text{IPr}^{\text{H}})\text{CuCl}]_2$ (**4**)



To a *Schlenk* flask containing $\text{Ph}_2\text{Si}(\text{IPr}^{\text{H}})_2$ (0.52 g, 0.54 mmol) and CuCl (0.11 g, 1.11 mmol) was added 20 mL of THF. The resulting suspension was stirred overnight at room temperature. Removal of the volatiles under vacuum afforded an off-white solid, which was washed with (2 x 20 mL) *n*-hexane. The residue was dissolved in 5 mL of DCM and combined with 10 mL of *n*-hexane. The solution was stored at -35°C to obtain colourless crystals of **4** in 81% (0.51 g) yield.

Empirical formula: $\text{C}_{66}\text{H}_{80}\text{Cl}_2\text{Cu}_2\text{N}_4\text{Si}$

Molecular weight: 1155.45 g/mol

Yield: 510mg, 0.44 mmol, 81%.

$^1\text{H-NMR}$ (300.13 MHz, CD_2Cl_2): δ 0.50 (d, 12H, $J = 6.63$ Hz, HCMe_2), 1.14 (d, 12H, $J = 6.79$ Hz, HCMe_2), 1.31 (m, 24H, HCMe_2), 2.18 (sept, 4H, $J = 6.77$ Hz, HCMe_2), 2.64 (sept, 4H, $J = 6.88$ Hz, HCMe_2), 6.85 (m, 8H, *o*-, *m*- C_6H_5), 7.08 (m, 4H, $J = 7.70$ Hz, *m*- C_6H_3), 7.31 (t, 2H, $J = 6.99$ Hz, *p*- C_6H_3), 7.19 (t, 2H, $J = 7.79$ Hz, *p*- C_6H_5), 7.41 (d, 4H, $J = 7.76$ Hz, *m*- C_6H_3), 7.50 (s, 2H, NCH), 7.61 (t, 2H, $J = 7.77$ Hz, *p*- C_6H_3) ppm.

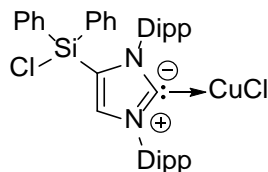
$^{13}\text{C}\{^1\text{H}\}$ -NMR (75.47 MHz, CD_2Cl_2): δ 21.42 (HCMe_2), 24.44, 24.90, 27.21, 29.18 (HCMe_2), 29.39, 124.27 (C_6H_5 , C_6H_3), 124.90, 126.49, 128.72, 129.58, 131.17, 131.26, 131.33, 134.27, 134.48, 134.88, 136.48, 145.69, 146.02, 186.27 (NCN) ppm.

$^{29}\text{Si}\{^1\text{H}\}$ -NMR (59 MHz, CD_2Cl_2): δ -30.10 ppm.

Elemental analysis (found (calc.) [%]): C 67.50 (68.61), H 6.85 (6.98), N 4.91 (4.85).

EI-MS: m/z : 1154.3 $[\text{M}]^+$, 1054.5 $[\text{M}-\text{CuCl}]^+$, 956.6 $[\text{M}-2 \text{CuCl}]^+$.

4.3.5. Synthesis of [4-(chlorodiphenylsilyl)-1,3-bis(2,6-diisopropylphenyl)-imidazole-2-ylidene] copper(I) chloride [Ph₂(Cl)Si(IPr)Cu]Cl (6)



To a 100 mL *Schlenk* flask equipped with SiPh₂Cl(IPr^H) (360 mg, 0.6 mmol) and anhydrous CuCl (60 mg, 0.6 mmol) was added 50 mL toluene and stirred overnight. Filtration through Celite® afforded yellowish solution, which was concentrated (20 mL) under vacuum and stored at 0°C to yield colourless crystals (335 mg, 80%).

Empirical formula: C₃₉H₄₅Cl₂CuN₂Si

Molecular weight: 704.33 g/mol

Yield: 335 mg, 0.50 mmol, 80%.

¹H NMR (300.13 MHz, THF-*d*8): δ 0.75 (d, 6H, *J* = 6.81 Hz, H_{CMe₂}), 1.26 (d, 6H, *J* = 3.99 Hz, H_{CMe₂}), 1.28 (d, 6H, *J* = 4.07 Hz, H_{CMe₂}), 1.32 (d, 6H, *J* = 6.88 Hz, H_{CMe₂}), 2.41 (sept, 2H, *J* = 6.81 Hz, H_{CMe₂}), 2.69 (sept, 2H, *J* = 6.90 Hz, H_{CMe₂}), 7.19 (d, 2H, *J* = 7.83 Hz, *m*-C₆H₃), 7.35–7.52 (m, 15H, C₆H₅, C₆H₃), 7.89 (s, 1H, NCH) ppm.

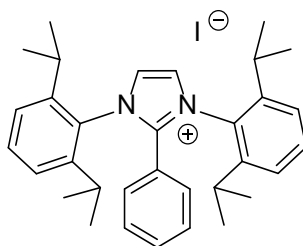
¹³C{¹H}-NMR (75.47 MHz, THF-*d*8): δ 22.20 (H_{CMe₂}), 24.13, 24.34, 24.91, 25.10 (H_{CMe₂}), 27.07, 29.92, 30.14, 125.05 (C₆H₅, C₆H₃), 125.08, 125.79, 129.35, 129.45, 131.41, 131.56, 131.70, 135.96, 137.38, 146.63 (*ipso*-C₆H₃), 147.02, 186.82 (NCN) ppm.

²⁹Si{¹H}-NMR (59 MHz, THF-*d*8): δ -10.95 ppm.

Elemental analysis (found (calc.) [%]): C 66.95 (66.51), H 6.25 (6.44), N 3.88 (3.98).

MS (ED): *m/z*: 703.9[M]⁺, 603.1 [M–CuCl]⁺, 387.28 [IPr].

4.3.6. Synthesis of 1,3-bis(2,6-diisopropylphenyl)-2-phenyl-imidazolium iodide (IPrPh)I (7)



To a 100 mL *Schlenk* flask equipped with IPr (1) (1.30 g, 3.35 mmol) and $\text{Pd}_2(\text{dba})_3$ (31 mg, 0.035 mmol, 1 mol%) was added 50 mL of *o*-xylene. Iodobenzene (683 mg, 3.35 mmol) was added and the reaction mixture was heated under reflux for 2 h. The precipitate was filtered and washed with 20 mL of toluene. Removal of the volatiles under vacuum afforded an off-white solid, which was extracted with 20 mL of dichloromethane to obtain analytically pure product (IPrPh)I (7) in 81% (1.60 g) yield. Suitable single crystals of 7 for X-ray diffraction analysis were grown from a saturated acetone solution at room temperature with slow evaporation of acetone.

Empirical formula: $\text{C}_{33}\text{H}_{41}\text{N}_2\text{I}$

Molecular weight: 592, 60 g/mol

Yield: 1.60 g, 2.70 mmol, 81%.

^1H -NMR (300.13 MHz, CD_2Cl_2): δ 1.03 (d, $J = 6.8$ Hz, 12H, $\text{H}\text{C}\text{M}\text{e}_2$), 1.30 (d, $J = 6.8$ Hz, 12H, $\text{H}\text{C}\text{M}\text{e}_2$), 2.45 (sept, $J = 6.8$ Hz, 4H, $\text{H}\text{C}\text{M}\text{e}_2$), 6.96 (d, $J = 7.5$ Hz, 2H, *o*- C_6H_5), 7.26 (t, $J = 7.9$ Hz, 2H, *m*- C_6H_5), 7.36 (d, $J = 7.9$ Hz, 4H, *m*- C_6H_3), 7.45 (t, $J = 7.6$ Hz, 1H, *p*- C_6H_5), 7.61 (t, $J = 7.8$ Hz, 2H, *p*- C_6H_3), 8.15 (s, 2H, NCH) ppm.

$^{13}\text{C}\{^1\text{H}\}$ -NMR (75.47 MHz, CD_2Cl_2): δ 22.84 ($\text{H}\text{C}\text{M}\text{e}_2$), 25.86($\text{H}\text{C}\text{M}\text{e}_2$), 29.97 ($\text{H}\text{C}\text{M}\text{e}_2$), 120.79 (*ipso*- C_6H_5), 125.97 (*m*- C_6H_3), 127.09(NCH), 129.71 (*o*- C_6H_5), 129.95 (*m*- C_6H_5), 130.37(*ipso*- C_6H_3), 132.98 (*p*- C_6H_3), 133.62 (*p*- C_6H_5), 145.30(*o*- C_6H_3), 146.30 (NCN, only seen in HMBC) ppm.

Elemental analysis (found (calc.) [%]): C 66.67 (66.88), H 6.77 (6.97), N 4.71 (4.73).

EI-MS m/z [%]: 465.3 [M-I]⁺.

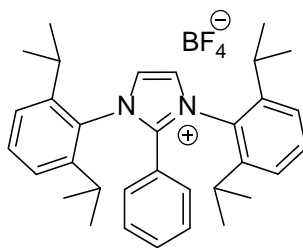
Mp: 280°C.

4.3.7. Large Scale Synthesis of (7)

A 150 mL 1,4-dioxane solution of **1** (17.45 g, 44.90 mmol) and Pd₂(dba)₃ (0.20 g, 0.22 mmol, 0.5 mol%) was stirred at room temperature for 10 min. To the brown reaction mixture was added 5.0 mL of iodobenzene (9.16 g, 44.88 mmol) and boiled under reflux (102°C) for 4 h with constant stirring. Heating was stopped and the resulting suspension was allowed to cool to room temperature. Off-white solid was isolated by filtration, washed with Et₂O (2 x 20 mL), and dried under vacuum to yield **7** (24.5 g, 92%).

Treatment of a *o*-xylene (145°C) solution of **1** (8.90 g, 22.90 mmol) with iodobenzene (2.56 mL, 23.19) in the presence of 0.5 mol% of Pd₂(dba)₃ (0.10 g, 0.11 mmol) afforded 88% (11.90 g) of **7** after 4 h.

4.3.8. Synthesis of 1,3-bis(2,6-diisopropylphenyl)-2-phenyl-imidazolium tetrafluoroborate (IPrPh)BF₄ (8)



To a 100 mL *Schlenk* flask equipped with **7a** (5.0 g, 8.4 mmol) and NaBF₄ (0.31 g, 8.4 mmol) was added 30 mL of DCM. Water (20 mL) was added and the reaction mixture was stirred for 24 h. The phases were separated and the organic layer was dried over MgSO₄. Removal of the volatiles under vacuum afforded a brown solid in 86% (4.0 g) yield.

Empirical formula: C₃₃H₄₁BF₄N₂

Molecular weight: 552.51 g/mol

Yield: 4.00 g, 7.24 mmol, 86%.

¹H-NMR (300.13 MHz, CD₂Cl₂): δ 1.03 (d, *J* = 6.9 Hz, 12H, HCMe₂), 1.29 (d, *J* = 6.8 Hz, 12H, CHMe₂), 2.46 (sept, *J* = 6.9 Hz, CHMe₂), 6.96 (dd, *J* = 8.4 Hz, 2H, *m*-C₆H₅), 7.26 (t, *J* = 7.9 Hz, 2H, *o*-C₆H₅), 7.36 (d, *J* = 7.9 Hz, 4H, *m*-C₆H₃), 7.44 (t, *J* = 7.6 Hz, 1H, *p*-C₆H₅), 7.61 (t, *J* = 7.8 Hz, 2H, *p*-C₆H₃), 7.95 (s, 2H, NCH) ppm.

¹³C{¹H}-NMR (75.47 MHz, CD₂Cl₂): δ 22.8 (HCMe₂), 25.7 (HCMe₂), 29.9 (HCMe₂), 120.7 (*ipso*-C₆H₅), 125.9 (*m*-C₆H₃), 126.8 (NCH), 129.6 (*o*-C₆H₅), 129.9 (*m*-C₆H₅), 130.3 (*ipso*-C₆H₃), 132.9 (*p*-C₆H₃), 133.5 (*p*-C₆H₅), 145.2 (*ipso*-C₆H₃), 145.9 (NCN) ppm.

¹¹B-NMR (96.3 MHz, CD₂Cl₂): δ -1.06 (s, 1B) ppm.

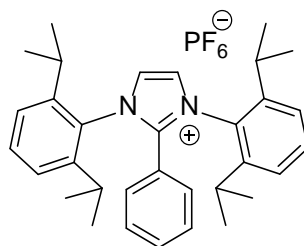
¹⁹F-NMR (282.3 MHz, CD₂Cl₂): δ -153.1 (s, 4F, B) ppm.

Elemental analysis (found (calc.) [%]): C 70.94 (71.74), H 7.70 (7.48), N 4.94 (5.07)

ESI-MS *m/z* [%]: 465.3 [M- BF₄]⁺.

Mp.: 297°C.

4.3.9. Synthesis of 1,3-bis(2,6-diisopropylphenyl)-2-phenyl-imidazolium hexafluorophosphate (IPrPh)PF₆ (9)



To a 100 mL *Schlenk* flask equipped with **7a** (5.0 g, 8.4 mmol) and KPF₆ (1.55 g, 8.4 mmol) was added 30 mL of DCM. Water (20 mL) was added and the reaction mixture was stirred for 24 h. The phases were separated and the organic layer was dried over MgSO₄. Removal of the volatiles under vacuum afforded a brown solid in 87% (4.43 g) yield.

Empirical formula: C₃₃H₄₁PF₆N₂

Molecular weight: 610.67 g/mol

Yield: 4.43 g, 7.25 mmol, 87%.

¹H-NMR (300.13 MHz, CD₂Cl₂): δ 1.04 (d, *J* = 6.8 Hz, HCMe₂), 1.27 (d, *J* = 6.8 Hz, HCMe₂), 2.43 (sept, *J* = 6.8 Hz, CHMe₂), 6.96 (dd, *J* = 8.4 Hz, *m*-C₆H₅), 7.26 (t, *J* = 7.9 Hz, *o*-C₆H₅), 7.36 (d, *J* = 7.9 Hz, *m*-C₆H₅), 7.44 (t, *J* = 7.6 Hz, *p*-C₆H₅), 7.61 (t, *J* = 7.8 Hz, *p*-C₆H₃), 7.74 (s, 2H, NCH) ppm.

¹³C{¹H}-NMR (75.47 MHz, CD₂Cl₂): δ 22.8 (HCMe₂), 25.7 (HCMe₂), 30.0 (HCMe₂), 120.7 (*ipso*-C₆H₅), 126.0 (*m*-C₆H₃), 126.4 (NCH), 129.7 (*o*-C₆H₅), 130.0 (*m*-C₆H₅), 130.4 (*ipso*-C₆H₃), 133.0 (*p*-C₆H₃), 133.7 (*p*-C₆H₅), 145.3 (*ipso*-C₆H₃), 146.2 (NCN) ppm.

³¹P-NMR (121.5 MHz, CD₂Cl₂): δ -144.5 (sept, ¹*J*_{PF} = 710.4 Hz) ppm.

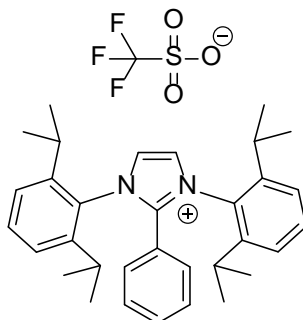
¹⁹F-NMR (282.3 MHz, CD₂Cl₂): δ -73.2 (d, ¹*J*_{PF} = 711.6 Hz) ppm.

Elemental analysis (found (calc.) [%]): C 64.73 (64.91), H 7.20 (6.77), N 4.37 (4.59).

ESI-MS *m/z* [%]: 465.3 [M- PF₆]⁺.

Mp.: 241°C.

4.3.10. Synthesis of 1,3-bis(2,6-diisopropylphenyl)-2-phenylimidazolium triflate (IPrPh)CF₃SO₃ (10)



To a 100 mL *Schlenk* flask equipped with **7** (1.0 g, 1.69 mmol) and KCF₃SO₃ (318 mg, 1.69 mmol) was added 30 mL of DCM. Water (20 mL) was added and the reaction mixture was stirred for 24 h. The phases were separated and the organic layer was dried over MgSO₄. Removal of the volatiles under vacuum afforded a brown solid in 40% (410 mg) yield.

Empirical formula: C₃₄H₄₁F₃N₂O₃S

Molecular weight: 614.28 g/mol

Yield: 410 mg, 0.67 mmol, 40%.

¹H-NMR (300.13 MHz, CD₂Cl₂): δ 1.03 (d, *J* = 6.8 Hz, HCMe₂), 1.28 (d, *J* = 6.8 Hz, HCMe₂), 2.44 (sept, *J* = 6.9 Hz, CHMe₂), 6.95 (dd, *J* = 8.6 Hz, *m*-C₆H₅), 7.26 (t, *J* = 8.0 Hz, *o*-C₆H₅), 7.35 (d, *J* = 7.9 Hz, *m*-C₆H₃), 7.44 (t, *J* = 7.8 Hz, *p*-C₆H₅), 7.60 (t, *J* = 7.8 Hz, *p*-C₆H₃), 7.97 (s, 2H, NCH) ppm.

¹³C{¹H}-NMR (75.47 MHz, CD₂Cl₂): δ 22.81 (HCMe₂), 25.69 (HCMe₂), 29.95 (HCMe₂), 120.80 (*ipso*-C₆H₅), 125.94 (*m*-C₆H₃), 126.88 (NCH), 129.70 (*o*-C₆H₅), 129.93 (*m*-C₆H₅), 130.40 (*ipso*-C₆H₃), 132.94 (*p*-C₆H₃), 133.57 (*p*-C₆H₅), 145.30 (*ipso*-C₆H₃), 146.01 (NCN) ppm.

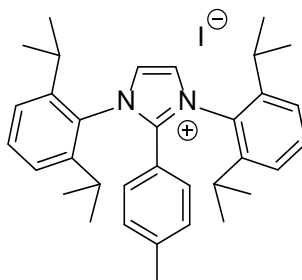
¹⁹F-NMR (282.3 MHz, CD₂Cl₂): δ -78.9 ppm.

Elemental analysis (found (calc.) [%]): C 65.70 (66.43), H 6.81 (6.72), N 4.51 (4.56).

ESI-MS m/z [%]: 465.3 [M-CF₃SO₃]⁺; 149.0 [M-IPrPh]⁻.

Synthesis of 12–15: Compounds **12–15** were prepared by employing the similar protocol as discussed for **7**. Detail of the reactants used, analytical data, and NMR spectroscopic data are given below.

4.3.11. Synthesis of 1,3-bis(2,6-diisopropylphenyl)-2-(*p*-tolyl)-imidazolium iodide (IPrPh-4-Me)I (**12**)



Reactants: IPr (**1**) (4.00 g, 10.29 mmol), 4-MeC₆H₄I (2.25 g, 10.32 mmol), Pd₂(dba)₃ (0.09 g, 1 mol%).

Empirical formula: C₃₄H₄₃IN₂ **Molecular weight:** 606.62 g/mol

Yield: 5.00 g, 8.24 mmol, 80%.

¹H-NMR (300.13 MHz, CD₂Cl₂): δ 1.03 (d, *J* = 6.8 Hz, 12H, H_{CMe₂}), 1.30 (d, *J* = 6.8 Hz, 12H, H_{CMe₂}), 2.23 (s, 3H, C₆H₄Me), 2.43 (sept, *J* = 6.9 Hz, 4H, H_{CMe₂}), 6.82 (d, *J* = 8.4 Hz, 2H, *o*-C₆H₄Me), 7.03 (d, *J* = 8.7 Hz, 2H, *m*-C₆H₄Me), 7.35 (d, *J* = 7.8 Hz, 4H, *m*-C₆H₃), 7.61 (t, *J* = 7.8 Hz, 2H, *p*-C₆H₃), 8.02 (s, 2H, NCH) ppm.

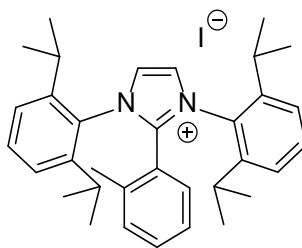
¹³C{¹H}-NMR (75.47 MHz, CD₂Cl₂): δ 21.76 (C₆H₄Me), 22.86 (H_{CMe₂}), 25.80 (H_{CMe₂}), 29.94 (H_{CMe₂}), 117.73 (*ipso*-C₆H₄Me), 125.94 (*m*-C₆H₃), 126.71(NCH), 129.52 (*o*-C₆H₄Me), 130.59 (*m*-C₆H₄Me), 132.89 (*p*-C₆H₃), 144.9 (*p*-C₆H₄Me), 145.30 (*ipso*-C₆H₃), 146.40 (NCN) ppm.

Elemental analysis (found (calc.) [%]): C 67.30 (67.32), H 6.94 (7.14), N 4.59 (4.62).

ESI-MS *m/z* [%]: 465.3 [M- I]⁺.

Mp.: 245°C.

4.3.12. Synthesis of 1,3-bis(2,6-diisopropylphenyl)-2-(*o*-tolyl)-imidazolium iodide (IPrPh-2-Me)I (13)



Reactants: IPr (1) (1.30 g, 3.35 mmol), 2-MeC₆H₄I (730 mg, 3.35 mmol), Pd₂(dba)₃ (31 mg, 1 mol %).

Empirical formula: C₃₄H₄₃IN₂

Molecular weight: 606.62 g/mol

Yield: 1.18 g, 1.94 mmol, 58 %.

¹H-NMR (300.13 MHz, CD₂Cl₂): δ 1.07 (t, *J* = 6.6 Hz, 12H, HCMe₂), 1.24 (d, *J* = 6.8 Hz, 6H, HCMe₂), 1.32 (d, *J* = 6.8 Hz, 6H, HCMe₂), 2.00 (s, 3H, C₆H₄Me), 2.42 (sept, *J* = 6.9 Hz, 2H, CHMe₂), 2.58 (sept, *J* = 6.9 Hz, 2H, CHMe₂), 6.94 (d, *J* = 6.9 Hz, 1H, *o*-C₆H₄Me), 7.15–7.08 (m, 2H, *m*-C₆H₄Me), 7.32–7.28 (m, 5H, *p*-C₆H₄Me, *m*-C₆H₃), 7.55 (t, *J* = 7.8 Hz, 2H, *p*-C₆H₃), 8.11 (s, 2H, NCH) ppm.

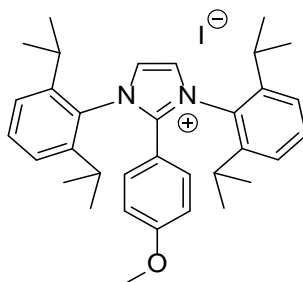
¹³C{¹H}-NMR (75.47 MHz, CD₂Cl₂): δ 20.84 (C₆H₄Me), 22.44 (HCMe₂), 22.69 (HCMe₂), 26.50 (HCMe₂), 26.85 (HCMe₂), 29.89 (CHMe₂), 30.21 (CHMe₂), 120.29 (*ipso*-C₆H₄Me), 125.72 (*m*-C₆H₄Me), 126.05 (*m*-C₆H₃), 126.83 (*m*-C₆H₄Me), 127.16 (NCH), 130.27 (*ipso*-C₆H₃), 132.01 (*o*-C₆H₄Me), 132.11 (*m*-C₆H₄Me), 132.82 (*p*-C₆H₃), 133.50 (*p*-C₆H₄Me), 139.04 (*o*-C₆H₄Me), 145.05 (*o*-C₆H₃), 145.43 (*o*-C₆H₃), 147.60 (NCN, only seen in HMBC) ppm.

Elemental analysis (found (calc.) [%]): C 66.86 (67.32), H 7.17 (7.14), N 4.55 (4.62).

ESI-MS *m/z* [%]: 479.3 [M- I]⁺.

Mp.: 285°C.

4.3.13. Synthesis of 1,3-bis(2,6-diisopropylphenyl)-2-(4-methoxyphenyl)-imidazolium iodide (IPrPh-4-OMe)I (14)



Reactants: IPr (1) (1.30 g, 3.35 mmol), 4-MeO-C₆H₄I (784 mg, 3.35 mmol), Pd₂(dba)₃ (31 mg, 1 mol%).

Empirical formula: C₃₄H₄₃IN₂O

Molecular weight: 622.62 g/mol

Yield: 1.54 g, 2.47 mmol, 74%.

¹H-NMR (300.13 MHz, CD₂Cl₂): δ 1.04 (d, *J* = 6.8 Hz, 12H, HCMe₂), 1.29 (d, *J* = 6.8 Hz, 12H, HCMe₂), 2.44 (sept, *J* = 6.9 Hz, 4H, HCMe₂), 3.71 (s, 3H, OMe), 6.71 (d, *J* = 9.2 Hz, 2H, *o*-C₆H₄OMe), 6.85 (d, *J* = 9.2 Hz, 2H, *m*-C₆H₄OMe), 7.37 (d, *J* = 7.9 Hz, 4H, *m*-C₆H₃), 7.62 (t, *J* = 7.8 Hz, 2H, *p*-C₆H₃), 8.01 (s, 2H, NCH) ppm.

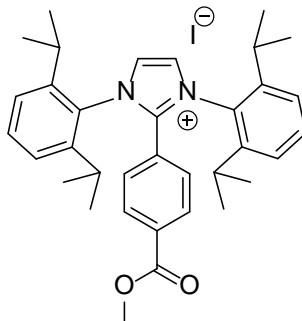
¹³C{¹H}-NMR (75.47 MHz, CD₂Cl₂): δ 22.87(HCMe₂), 25.69 (HCMe₂), 29.90(CHMe₂), 56.25 (OMe), 112.34 (*ipso*-C₆H₄OMe), 115.42 (*o*-C₆H₄OMe), 125.98 (*p*-C₆H₃), 126.52 (NCH), 130.64 (*ipso*-C₆H₃), 131.45 (*m*-C₆H₄OMe), 132.86 (*m*-C₆H₃), 145.30 (*o*-C₆H₃), 146.23 (NCN), 163.43 (*p*-C₆H₄OMe) ppm.

Elemental analysis (found (calc.) [%]): C 65.67 (65.59), H 6.70 (6.96), N 4.57 (4.50).

ESI-MS *m/z* [%]: 494.3 [M- I]⁺.

Mp.: 302°C.

4.3.14. Synthesis of 1,3-bis(2,6-diisopropylphenyl)-2-(4-(methoxycarbonyl) phenyl)-imidazolium iodide (IPrPh-4-CO₂Me)I (15)



Reactants: IPr (1) (1.30 g, 3.35 mmol), 4-MeO₂CC₆H₄I (880 mg, 3.35 mmol), Pd₂(dba)₃ (31 mg, 1 mol%).

Empirical formula: C₃₅H₄₃IN₂O₂

Molecular weight: 650.63 g/mol

Yield: 1.49 g, 2.29 mmol, 68%.

¹H-NMR (300.13 MHz, CD₂Cl₂): δ 1.03 (d, *J* = 6.8 Hz, 12H, HCMe₂), 1.30 (d, *J* = 6.8 Hz, 12H, HCMe₂), 2.42 (sept, *J* = 6.6 Hz, 4H, CHMe₂), 3.82 (s, 3H, CO₂Me), 7.03 (d, *J* = 8.8 Hz, 2H, *o*-C₆H₄CO₂Me), 7.35 (d, *J* = 7.9 Hz, 4H, *m*-C₆H₃), 7.61 (t, *J* = 7.8 Hz, 2H, *p*-C₆H₃), 7.87 (d, *J* = 8.8 Hz, 2H, *m*-C₆H₄CO₂Me), 8.30 (s, 2H, NCH) ppm.

¹³C{¹H}-NMR (75.47 MHz, CD₂Cl₂): δ 22.83 (CHMe₂), 25.84 (CHMe₂), 29.94 (CHMe₂), 53.17 (CO₂Me), 125.82 (*ipso*-C₆H₄CO₂Me), 126.01(*m*-C₆H₃), 127.85 (NCH), 129.83 (*o*-C₆H₄CO₂Me), 130.10 (*ipso*-C₆H₃), 130.62 (*m*-C₆H₄CO₂Me), 133.12 (*p*-C₆H₃), 134.41(*p*-C₆H₄CO₂Me), 144.68 (NCN), 145.18 (*o*-C₆H₃), 165.25 (CO₂Me) ppm.

Elemental analysis (found (calc.) [%]): C 64.33 (64.61), H 6.75 (6.66), N 4.45 (4.31).

ESI-MS m/z [%]: 527.2 [M- I]⁺.

Mp.: 359°C.

4.3.15. Reaction Optimisation

Detail of the reaction optimization is given in Table 4-1.

Table 4-1: Reaction details for the reaction optimization.

Entry	IPr (1) (g, mmol)	PhI (g, mmol)	Solvent	Catalyst; Pd ₂ (dba) ₃ (mg/ mol %)	Temp. (°C)	Time (h)	Yield (g, %)
1	1.30, 3.35	0.69, 3.38	<i>o</i> -xylene	-	25	48	-
2	1.30, 3.35	0.69, 3.38	<i>o</i> -xylene	-	145	10	-
3	1.30, 3.35	0.69, 3.38	1,4-dioxane	-	25	48	-
4	1.30, 3.35	0.69, 3.38	1,4-dioxane	-	102	10	-
5	0.5, 1.29	0.26, 1.27	1,4-dioxane	12/ 1	25	2	0.12, 16
6	0.65, 1.67	0.34, 1.66	1,4-dioxane	16/ 1	102	2	0.71, 72
7	1.30, 3.35	0.69, 3.38	1,4-dioxane	16/ 0.5	102	3	1.50, 76
8	17.45, 44.90	9.16, 44.88	1,4-dioxane	200/ 0.5	102	4	24.5, 92
9	1.30, 3.35	0.69, 3.38	1,4-dioxane	3/ 0.1	102	2	0.04, 2
10	0.5, 1.29	0.26, 1.27	<i>o</i> -xylene	12/ 1	25	48	0.14, 18
11	1.30, 3.35	0.69, 3.38	<i>o</i> -xylene	31/ 1	145	2	1.60, 81
12	0.65, 1.67	0.34, 1.66	THF	16/ 1	70	2	0.27, 27
13	0.5, 1.29	0.26, 1.27	toluene	12/ 1	25	48	0.17, 22
14	0.65, 1.67	0.34, 1.66	toluene	16/ 1	110	2	0.74, 75

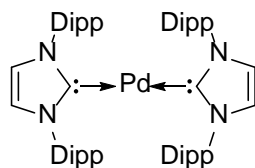
4.3.16. Recycling of the Catalyst

A 50 mL *o*-xylene solution of **1** (1.30 g, 3.35 mmol), Pd₂(dba)₃ (31 mg, 0.035 mmol, 1 mol%), and iodobenzene (0.69 mg, 3.38 mmol) was stirred under reflux for 2 h. The resulting suspension was allowed to come to room temperature. Filtration through a frit afforded brown filtrate. The off-white residue was extracted in dichloromethane after washing with Et₂O and dried under vacuum to obtain **7** (81%, Table 4-2).

To the brown filtrate was added **1** (1.30 g, 3.35 mmol) and iodobenzene (0.68 mg, 3.33 mmol). The reaction mixture was refluxed for 2 h and then brought to the room temperature. Insoluble product was isolated, dried, and characterized as **7** (80%). The filtrate was re-employed for the next cycle. The results of the four cycles are summarized in the Table 4-2.

Table 4-2: Catalyst recycling for the reaction of **1** with PhI to **7**.

Cycle	IPr (mmol)	PhI (mmol)	Yield (g, %)	Time
1	3.35	3.38	1.60, 81	2
2	3.35	3.35	1.51, 80	2
3	3.35	3.35	1.00, 50	2
4	3.35	3.35	0.99, 50	2

4.3.17. Modified Method for the Synthesis of (IPr)₂Pd (19)

To a 100 mL *Schlenk* flask equipped with (IPr)₂PdCl₂ (1.0 g, 1.05 mmol) and KC₈ (283 mg, 2.1 mmol) was added 40 mL of precooled (-30°C) THF. The reaction mixture was slowly brought to room temperature and stirred overnight. Removal of the volatiles under vacuum afforded **19** as a brown solid, which was extracted with 20 mL of toluene.

Yield: 687 mg (74%).

¹H-NMR (300 MHz, C₆D₆): δ 1.12 (d, *J* = 6.9 Hz, 24H, HCMe₂), 1.21 (d, *J* = 6.9 Hz, 24H; HCMe₂), 2.88 (sept, *J* = 6.9 Hz, 8H; HCMe₂), 6.27 (s, 4H; NCH), 7.09 (d, *J* = 7.7 Hz, 8H, *m*-C₆H₃), 7.30 (t, *J* = 7.7 Hz, 4H, *p*-C₆H₃) ppm.

¹³C{¹H}-NMR (75 MHz, C₆D₆): δ 24.08 (HCMe₂), 25.16 (HCMe₂), 28.72 (HCMe₂), 125.25 (NCH), 123.43 (*m*-C₆H₃), 128.61 (*p*-C₆H₃), 139.17 (*ipso*-C₆H₃), 146.08 (*o*-C₆H₃), 199.31 (NCN) ppm.

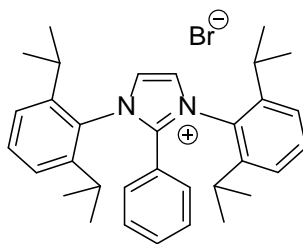
Mp.: 253°C.

Reference: ^[170]

4.3.18. Reaction of IPr and PhI with 1 mol% of (IPr)₂Pd

To a *Schlenk* flask containing IPr (**1**) (1.27 g, 3.27 mmol) and (IPr)₂Pd (30 mg, 1 mol%) was added iodobenzene (0.36 mL, 3.27 mmol) and 30 mL of 1,4-dioxane. The resulting reaction mixture was stirred under reflux for 3 h. White precipitate was isolated by filtration and washed with 10 mL of toluene. Removal of the volatiles under vacuum afforded compound **7a** as a white solid (0.72 g, 37%).

4.3.19. Synthesis of 1,3-bis(2,6-diisopropylphenyl)-2-phenylimidazolium bromide (IPrPh)Br (**20**)



To a 100 mL *Schlenk* flask equipped with IPr (**1**) (500 mg, 1.28 mmol) and NiBr₂ (28 mg, 0.13 mmol, 10 mol%) was added 25 mL of *o*-xylene. bromobenzene (261 mg, 1.28 mmol) was added and the reaction mixture was heated under reflux for 24 h. The precipitate was filtered and removal of the volatiles under vacuum afforded an off-white solid, which was extracted with 20 mL of dichloromethane to obtain analytically pure product (IPrPh)Br (**20**) in 36% (250 mg) yield.

Empirical formula: C₃₃H₄₁BrN₂

Molecular weight: 545.60 g/mol

Yield: 250 mg, 0.46 mmol, 36%.

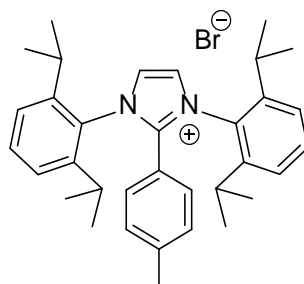
¹H-NMR (300.13 MHz, THF-*d*₈): δ 1.02 (d, *J* = 6.8 Hz, 12H, CHMe₂), 1.30 (d, *J* = 6.8 Hz, 12H, CHMe₂), 2.45 (sept, *J* = 6.9 Hz, 4H, CHMe₂), 6.94 (d, *J* = 8.0 Hz, 4H, *o*-C₆H₅), 7.25 (t, *J* = 8.0 Hz, 2H, *m*-C₆H₅), 7.34 (d, *J* = 7.8 Hz, 1H, *m*-C₆H₃), 7.43 (t, *J* = 8.2 Hz, 1H, *p*-C₆H₅), 7.59 (t, *J* = 8.2 Hz, 2H, *p*-C₆H₃), 8.32 (s, 2H, NCH) ppm.

¹³C{¹H}-NMR (75.47 MHz, THF-*d*₈): δ 22.82 (HCMe₂), 25.82(HCMe₂), 29.95 (HCMe₂), 120.93 (*ipso*-C₆H₅), 125.90 (*m*-C₆H₃), 127.33(NCH), 129.74 (*o*-C₆H₅), 129.87 (*m*-C₆H₅), 130.46(*ipso*-C₆H₃), 132.87 (*p*-C₆H₃), 133.46 (*p*-C₆H₅), 145.34(*o*-C₆H₃), ppm.

Elemental analysis (found (calc.) [%]): C 71.25 (72.65), H 7.66 (7.57), N 4.76 (5.13).

ESI-MS m/z [%]: 465.3 [M-Br]⁺.

4.3.20. Synthesis of 1,3-bis(2,6-diisopropylphenyl)-2-(*p*-tolyl)-imidazolium bromide (IPrPh-4-Me)Br (**21**)



To a 100 mL *Schlenk* flask equipped with IPr (**1**) (500 mg, 1.28 mmol) and NiBr₂ (20 mg, 0.09 mmol, 7 mol%) was added 40 mL of 1,4-dioxane. 1-bromo-4-methylbenzene (220 mg, 1.28 mmol) was added and the reaction mixture was heated under reflux for 6 h. The precipitate was filtered and removal of the volatiles under vacuum afforded an off-white solid, which was extracted with 20 mL of DCM to obtain analytically pure product (IPrPh)Br (**21**) in 82% (590 mg) yield.

Empirical formula: C₃₄H₄₃BrN₂

Molecular weight: 558.26 g/mol

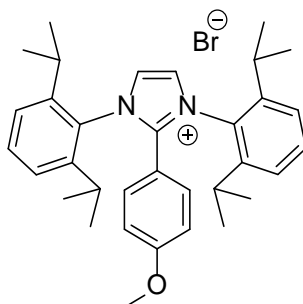
Yield: 590 mg, 1.05 mmol, 82%.

¹H-NMR (300.13 MHz, THF-*d*₈): δ 1.02 (d, *J* = 6.9 Hz, 12H, CHMe₂), 1.28 (d, *J* = 6.8 Hz, 12H, CHMe₂), 2.23 (s, 3H, C₆H₄Me), 2.43 (sept, *J* = 6.8 Hz, 4H, CHMe₂), 6.81 (d, *J* = 8.4 Hz, 4H, *o*-C₆H₄), 7.05 (d, *J* = Hz, 2H, *m*-C₆H₄), 7.34 (d, *J* = 1.5 Hz, 4H, *m*-C₆H₃), 7.59 (t, 2H, *p*-C₆H₃), 8.19 (s, 2H, NCH) ppm.

¹³C{¹H}-NMR (75.47 MHz, THF-*d*₈): δ 21.69 (C₆H₄Me), 22.79 (CHMe₂), 25.72 (CHMe₂), 29.66 (s, 2C, *ipso*-C₆H₄Me), 29.87 (*ipso*-C₆H₃), 117.82 (C₆H₄Me), 125.14 (*m*-C₆H₃), 126.83 (NCH), 129.49 (*o*-C₆H₄), 130.49 (*m*-C₆H₄), 132.75 (*p*-C₆H₃), 144.80 (*p*-C₆H₄), 145.30 (*o*-C₆H₃), 146.16 (NCN) ppm.

EI-MS *m/z* [%]: 465.3 [M-Br]⁺.

4.3.21. Synthesis of 1,3-bis(2,6-diisopropylphenyl)-2-(4-methoxyphenyl)-imidazolium bromide (IPrPh-4-OMe)Br (22)



To a 100 mL *Schlenk* flask equipped with IPr (**1**) (613 mg, 1.58 mmol) and NiBr₂ (20 mg, 0.09 mmol, 6 mol%) was added 20 mL of *o*-xylene. 1-bromo-4-methoxybenzene (295 mg, 1.58 mmol) was added and the reaction mixture was heated under reflux for 5 h. The precipitate was filtered and removal of the volatiles under vacuum afforded an off-white solid, which was extracted with 20 mL of dichloromethane to obtain the product (IPrPh)Br (**22**) in 62% (560 mg) yield.

Empirical formula: C₃₄H₄₃BrN₂O

Molecular weight: 575.63 g/mol

Yield: 560 mg, 0.98 mmol, 62%.

¹H-NMR (300.13 MHz, CD₂Cl₂): δ 1.02 (d, *J* = 6.8 Hz, 12H, HCMe₂), 1.27 (d, *J* = 6.8 Hz, 12H, HCMe₂), 2.44 (sept, *J* = 6.6 Hz, 4H, HCMe₂), 3.70 (s, 3H, OMe), 6.70 (d, *J* = 9.0 Hz, 2H, *o*-C₆H₄OMe), 6.84 (d, *J* = 9.0 Hz, 2H, *m*-C₆H₄OMe), 7.35 (d, *J* = 7.8 Hz, 4H, *m*-C₆H₃), 7.62 (t, *J* = 7.8 Hz, 2H, *p*-C₆H₃), 8.17 (s, 2H, NCH) ppm.

¹³C{¹H}-NMR (75.47 MHz, CD₂Cl₂): δ 22.82(HCMe₂), 25.63 (HCMe₂), 29.83(CHMe₂), 56.17 (OMe), 112.45 (*ipso*-C₆H₄OMe), 115.31 (*o*-C₆H₄OMe), 125.87 (*p*-C₆H₃), 126.70 (NCH), 130.67 (*ipso*-C₆H₃), 131.42 (*m*-C₆H₄OMe), 132.72 (*m*-C₆H₃), 145.30 (*o*-C₆H₃), 146.29 (NCN), 163.30 (*p*-C₆H₄OMe) ppm.

ESI-MS *m/z* [%]: 495.3 [M-Br]⁺.

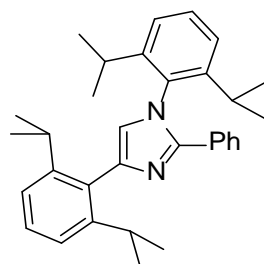
4.3.22. Reaction Optimisation

In order to optimise the reaction conditions a whole string of reactions have been made

Entry	IPr (1) (g, mmol)	PhBr (g, mmol)	Solvent	Catalyst; NiBr ₂ (mg/ mol %)	Temp. (°C)	Time (h)	Yield (g, %)
1	0.50, 1.28	0.21, 1.34	<i>o</i> -xylene	28/ 10	25	24	-
2	0.75, 1.93	0.32, 2.02	<i>o</i> -xylene	43/ 10	145	12	0.48, 45
3	0.50, 1.28	0.21, 1.34	<i>o</i> -xylene	14/ 5	145	12	0.28, 40
4	0.50, 1.28	0.21, 1.34	<i>o</i> -xylene	3/ 1	145	48	0.20, 29
5	0.50, 1.28	0.21, 1.34	<i>o</i> -xylene	3/ 1	145	12	-
6	0.50, 1.28	0.21, 1.34	<i>o</i> -xylene	14/ 5	145	48	0.29, 42
7	0.50, 1.28	0.21, 1.34	THF	28/ 10	25	24	-
8	0.50, 1.28	0.21, 1.34	THF	28/ 10	70	12	0.90, 27
9	0.50, 1.28	0.21, 1.34	toluene	28/ 10	25	24	-
10	0.50, 1.28	0.21, 1.34	toluene	28/ 10	110	12	-
11	0.50, 1.28	0.21, 1.34	1,4-dioxane	28/ 10	25	24	-
12	0.50, 1.28	0.21, 1.34	1,4-dioxane	28/ 10	102	12	0.24, 34
12	0.50, 1.28	0.21, 1.34	THF	16/ 1	70	2	0.27, 27

Entry	IPr (1) (g, mmol)	PhX (g, mmol)	Solvent	Catalyst; (mg/ mol %)	Temp. (°C)	Time (h)	Yield (g, %)
13	0.50, 1.28	I, (0.21, 1.34)	<i>o</i> -xylene	NiI ₂ (40/ 10)	145	12	0.47,
14	0.50, 1.28	Cl (0.14, 1.28)	<i>o</i> -xylene	NiCl ₂ (17/10)	145	12	-

4.3.23. Coincidental synthesis of 1,4-bis(2,6-diisopropylphenyl)-2-phenyl-1*H*-imidazole



Empirical formula: C₃₃H₄₀N₂

Molecular weight: 464.68 g/mol

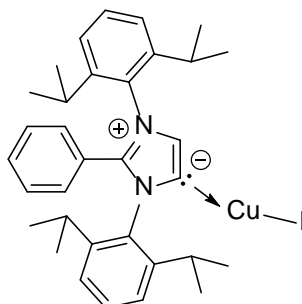
To a 100 mL *Schlenk* flask equipped with IPrPhI (**7**) (1 g, 1.69 mmol), KHMDS (338 mg, 1.69 mmol) and NiCOD₂ (464 mg, 1.69 mmol) was added 30 mL of precooled (0°C) toluene. The reaction mixture stirred for 1 h at 0°C. Afterwards the reaction mixture was allowed to warm to rt and stirred overnight. The solution was filtered and removal of the volatiles under vacuum afforded a brownish solid as product in 35 % (275 mg) yield.

Yield: 275 mg, 0.59. mmol, 35%.

¹H-NMR (300.13 MHz, CD₂Cl₂): δ 1.01 (dd, *J* = 6.9 Hz, 12H, HCMe₂), 1.16 (d, *J* = 6.9 Hz, 6H, HCMe₂), 1.19 (d, *J* = 6.9 Hz, 12H, HCMe₂), 2.70 (sept, *J* = 7.0 Hz, 2H, HCMe₂), 3.17 (sept, *J* = 7.0 Hz, 2H, HCMe₂), 6.97 (s, 1H, NCH), 7.14-7.21 (m, 5H,), 7.27-7.35 (m, 3H,), 7.46-7.54 (m, 3H,) ppm.

¹³C{¹H}-NMR (75.47 MHz, CD₂Cl₂): δ 23.18, 24.77, 25.49 (CHMe₂), 29.54, 31.44 (CHMe₂), 122.97, 123.93 (NCH), 125.31, 127.89, 128.73, 128.90, 129.08, 130.85, 132.24, 133.94, 136.06, 140.52, 146.80, 146.96, 149.49 (C₆H₃, C₆H₅) ppm.

4.3.24. Synthesis of [1,3-bis(2,6-diisopropylphenyl)-2-phenyl-imidazol-4-ylidene] copper(I) iodide (IPrPh)CuI (**26**) from CuI



To a 100 mL *Schlenk* flask equipped with (IPrPh)I (**7**) (1.0 g, 1.69 mmol), KN(SiMe₃)₂ (337 mg, 1.69 mmol), and CuI (321 mg, 1.69 mmol) was added 30 mL of pre-cooled THF at 0°C. The reaction mixture was brought to room temperature and further stirred overnight. Filtration through a plug of Celite® afforded clear solution. The volatiles were removed under vacuum to obtain off-white solid, which was washed with 20 mL of *n*-hexane and dried to yield **23** (1.01 g, 91%).

Empirical formula: C₃₃H₄₀N₂CuI

Molecular weight: 655.13 g/mol

Yield: 1.01 g, 1.54. mmol, 91%.

¹H-NMR (300.13 MHz, CD₂Cl₂): δ 1.01 (dd, *J* = 6.6 Hz, 12H, H_{CM_e2}), 1.24 (d, *J* = 6.5 Hz, 6H, H_{CM_e2}), 1.40 (d, *J* = 6.5 Hz, 6H, H_{CM_e2}), 2.57 (m, 4H, H_{CM_e2}), 6.91 (d, 2H, *o*-C₆H₅), 6.99 (s, 1H, NCH), 7.12 (t, 2H, *m*-C₆H₅), 7.26 (m, 5H, *p*-C₆H₅, *m*-C₆H₃), 7.49 (t, 2H, *p*-C₆H₃) ppm.

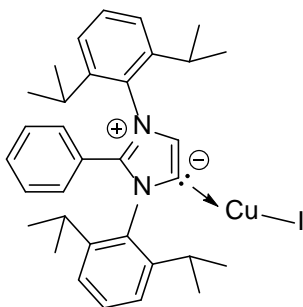
¹³C{¹H}-NMR (75.47 MHz, CD₂Cl₂): δ 22.83, 22.91 (H_{CM_e2}), 26.01, 26.29 (H_{CM_e2}), 29.40, 29.50 (H_{CM_e2}), 124.98, 125.26 (*m*-C₆H₃), 129.04 (*m*-C₆H₅), 129.59 (*o*-C₆H₅), 130.24 (NCH), 130.92 (NCCuI), 131.39 (*p*-C₆H₃), 131.54 (*p*-C₆H₅), 135.98 (*o*-C₆H₃), 145.42 (*ipso*-C₆H₅), 145.68 (*ipso*-C₆H₃) ppm.

Elemental analysis (found (calc.) [%]): C 60.06 (60.50), H 6.48 (6.15), N 4.67 (4.31).

ESI-MS m/z [%]: 654.0 [{M}]⁺, 527.2 [M-I]⁺, 465.3 [M-CuI]⁺.

Mp.: 215°C.

4.3.25. Synthesis of [1,3-bis(2,6-diisopropylphenyl)-2-phenylimidazol-4-ylidene] copper(I) iodide (IPrPh)CuI (**26b**) from CuCl



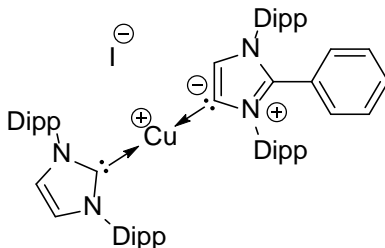
Treatment of a mixture of (IPrPh)I (**7a**) (510 mg, 0.86 mmol) and CuCl (172 mg, 0.86 mmol) with KN(SiMe₃)₂ (172mg, 0.86 mmol), under similar experimental conditions as discussed for the compound **23**, afforded compound (IPrPh)CuI (**23b**) (305 mg, 72%). Irrespective of the copper precursor (CuCl or CuI) used the product shows identical ¹H- and ¹³C-NMR signals, which indicates the formation of the (IPrPh)CuI (**23**) in both cases. However, the presence of the small amount of (IPrPh)CuCl can be seen in the EI-mass spectrum when CuCl was used. Suitable single crystals for X-ray diffraction analysis were grown from a saturated toluene solution at -30°C.

¹H-NMR (300 MHz, CD₂Cl₂): δ 1.01 (dd, *J* = 6.6 Hz, 12H, H_{CMe₂}), 1.24 (d, *J* = 6.8 Hz, 6H, H_{CMe₂}), 1.40 (d, *J* = 6.5 Hz, 6H, H_{CMe₂}), 2.57 (m, 4H, H_{CMe₂}), 6.91 (d, 2H, *o*-C₆H₅), 6.99 (s, 1H, NCH), 7.12 (t, 2H, *m*-C₆H₅), 7.27 (m, 5H, *p*-C₆H₅, *m*-C₆H₃), 7.48 (t, 2H, *p*-C₆H₃) ppm.

¹³C{¹H}-NMR (75 MHz, CD₂Cl₂): δ 22.83, 22.91 (H_{CMe₂}), 26.01, 26.29 (H_{CMe₂}), 29.40, 29.50 (H_{CMe₂}), 125.01, 125.25 (*m*-C₆H₃), 129.02 (*m*-C₆H₅), 129.62 (*o*-C₆H₅), 130.46 (NCH), 130.93 (NCCuI), 131.35 (*p*-C₆H₃), 131.52 (*p*-C₆H₅), 136.08 (*o*-C₆H₃), 145.45 (*ipso*-C₆H₅), 145.71 (*ipso*-C₆H₃) ppm.

ESI-MS: m/z: 654.0[(IPrPh)CuI]⁺, 562.2 [(IPrPh)CuCl]⁺, 527.2 [(IPrPh)CuI – I]⁺ / [(IPrPh)CuCl – Cl]⁺, 465.3 [(IPrPh)CuI – CuI/CuCl]⁺.

4.3.26. Synthesis of [(1,3-bis(2,6-diisopropylphenyl)-2-phenyl-imidazol-4-ylidene)-(1,3-bis(2,6-diisopropylphenyl)-imidazol-2-ylidene)] copper(I) iodide [(IPrPh)Cu(IPr)]I (**27**)



To a 100 mL *Schlenk* flask equipped with (IPrPh)CuI (**23**) (1.0 g, 1.53 mmol), and IPr (594 mg, 1.53 mmol) was added 20 mL of toluene. The reaction mixture was stirred at room temperature overnight. Filtration through a plug of Celite® afforded a clear solution. The volatiles were removed under vacuum to obtain the desired compound as brown solid (1.29 g, 81%).

Empirical formula: C₆₀H₇₆CuIN₄

Molecular weight: 1043.72 g/mol

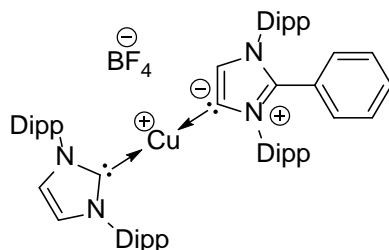
Yield: 1.29 g, 1.24 mmol, 81%.

¹H-NMR (300.13 MHz, THF-*d*8): δ 0.65 (d, *J* = 6.79 Hz, 6H, IPrPhCHMe₂), 0.82 (d, *J* = 6.86 Hz, 6H, IPrPhCHMe₂), 0.96 (d, *J* = 6.85 Hz, 6H, IPrPhCHMe₂), 1.10 (t, *J* = 6.65 Hz, 18H, IPrCHMe₂, IPrPhCHMe₂), 1.17 (d, 12H, *J* = 6.85 Hz, IPrCHMe₂) 2.08–2.26 (m, 2H, IPrPhCHMe₂), 2.28–2.37 (m, 2H, IPrPhCHMe₂), 2.58 (sept, *J* = 6.85 Hz, 4H, IPrCHMe₂), 6.51 (s, 1H, IPrPhNCH), 6.81 (d, *J* = 7.38 Hz, 2H, *o*-C₆H₅), 7.07–7.15 (m, 4H, *p*-C₆H₃), 7.25–7.37 (m, 8H, *m*-C₆H₃), 7.45–7.54 (m, 3H, *m-p*-C₆H₅) 7.75 (s, 2H, IPrNCH) ppm.

¹³C{¹H}-NMR (75.47 MHz, THF-*d*8): δ 22.81 (IPrPhCHMe₂), 22.94 (IPrPhCHMe₂), 24.48 (IPrCHMe₂), 25.34 (IPrCHMe₂, IPrPhCHMe₂), 26.29 (IPrPhCHMe₂), 29.73 (IPrCHMe₂), 29.83 (IPrPhCHMe₂), 30.05 (IPrPhCHMe₂), 123.67 (*o*-C₆H₃), 125.20 (*p*-C₆H₃), 125.58 (*p*-C₆H₃), 126.05 (*m*-C₆H₃), 126.08 (IPrNCH), 129.76 (*p*-C₆H₃), 129.98 (*o*-C₆H₅), 131.47, 131.81 (*m-p*-C₆H₅), 132.09 (IPrPhNCH), 132.48, 132.57, 136.02 (*o*-C₆H₃), 136.44, 145.17 (*o*-C₆H₃), 145.80, 145.89, 146.58 (*ipso*-C₆H₅), 159.53, 180.99 ppm.

ESI-MS m/z [%]: 915.5 [{M-I}]⁺, 465.3 [M-(IPr)CuI]⁺.

4.3.27. Synthesis of [(1,3-bis(2,6-diisopropylphenyl)-2-phenyl-imidazol-4-ylidene)-(1,3-bis(2,6-diisopropylphenyl)-imidazol-2-ylidene)] copper(I) tetrafluoroborate [(IPrPh)Cu(IPr)]BF₄ (27a**)**



To a *Schlenk* flask equipped with **27** (120 mg, 0.11 mmol) and NaBF₄ (13 mg, 8.4 mmol) was added 10 mL of DCM. Water (10 mL) was added and the reaction mixture was stirred for 24 h. The phases were separated and the organic layer was dried over MgSO₄. Removal of the volatiles under vacuum afforded a brown solid in 59% (65 mg) yield.

Empirical formula: C₆₀H₇₆CuBF₄N₄

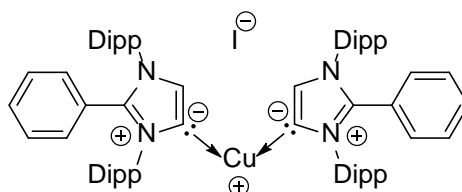
Molecular weight: 1003.62 g/mol

Yield: 65 mg, 0.65 mmol, 59%.

¹H-NMR (300.13 MHz, THF-*d*8): δ 0.68 (d, *J* = 6.88 Hz, 6H, IPrPhCHMe₂), 0.82 (d, *J* = 6.81 Hz, 6H, IPrPhCHMe₂), 0.98 (d, *J* = 6.88 Hz, 6H, IPrPhCHMe₂), 1.11-1.15 (m, 18H, IPrCHMe₂, IPrPhCHMe₂), 1.18-1.24 (m, 12H, IPrCHMe₂) 2.24 (m, 2H, IPrPhCHMe₂), 2.36 (m, 2H, IPrPhCHMe₂), 2.61 (m, 4H, IPrCHMe₂), 6.54 (s, 1H, IPrPhNCH), 6.84 (d, *J* = 7.84 Hz, 2H, *o*-C₆H₅), 7.05–7.17 (m, 4H, *p*-C₆H₃), 7.24–7.41 (m, 8H, *m*-C₆H₃), 7.45–7.55 (m, 3H, *m-p*-C₆H₅) 7.61 (s, 2H, IPrNCH) ppm.

The ¹H-NMR data are in good agreement with the reference data of compound **27**. The reaction was not repeated and therefore no further measurement than the x-ray diffraction experiment was done.

4.3.28. Synthesis of Bis[1,3-bis(2,6-diisopropylphenyl)-2-phenyl-imidazol-4-ylidene] copper(I) iodide [(IPrPh)₂Cu]I (28)



To a 100 mL *Schlenk* flask equipped with (IPrPh)I (**7**) (1.0 g, 1.69 mmol), KN(SiMe₃)₂ (337 mg, 1.69 mmol), and CuI (161 mg, 0.84 mmol) was added 30 mL of pre-cooled THF at 0°C. The reaction mixture was brought to room temperature and further stirred overnight. Filtration through a plug of Celite® afforded clear solution. The volatiles were removed under vacuum to obtain a brown solid, which was washed with 20 mL of *n*-pentane and dried to yield **25** (746 g, 40%).

Empirical formula: C₆₆H₈₀CuIN₄

Molecular weight: 1119.82 g/mol

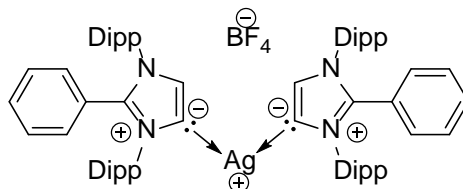
Yield: 746 mg, 0.67 mmol, 40%.

¹H-NMR (500.26 MHz, THF-*d*₈): δ 1.01(dd, *J* = 6.9 Hz, 24H, H_{CMe₂}), 1.12(d, *J* = 6.8 Hz, 12H, H_{CMe₂}), 1.22 (d, *J* = 6.8 Hz, 12H, H_{CMe₂}), 2.49–2.59 (m, 8H, H_{CHMe₂}), 6.91(d, *J* = 7.4 Hz, 4H, *o*-C₆H₃), 7.08 (s, 2H, NCH), 7.18(t, *J* = 7.5 Hz, 4H, *m*-C₆H₃), 7.23 (d, *J* = 7.8 Hz, 4H, *m*-C₆H₃), 7.30 (t, *J* = 7.5 Hz, 2H, *p*-C₆H₃), 7.38 (m, 6H, *m*-C₆H₃, *p*-C₆H₃), 7.54 (t, *J* = 7.8 Hz, 2H, *p*-C₆H₃) ppm.

¹³C{¹H}-NMR (125.76 MHz, THF-*d*₈): δ 22.89 (CH_{Me₂}), 22.95 (CH_{Me₂}), 25.90 (CH_{Me₂}), 26.38 (CH_{Me₂}), 29.91 (CH_{Me₂}), 30.08 (CH_{Me₂}), 124.07, 125.55, 125.94, 129.68 (*m*-C₆H₃), 130.10 (*o*-C₆H₃), 131.51 (*p*-C₆H₃), 131.73 (NCH), 132.18 (*p*-C₆H₃), 132.32 (*p*-C₆H₃), 132.43 (*o*-C₆H₃), 136.64 (*o*-C₆H₃), 145.71 (*ipso*-C₆H₃), 146.02 (*ipso*-C₆H₃), 161.03 (CCuC) ppm.

ESI-MS m/z [%]: 991.6 [{M-I}]⁺, 465.3 [M-(IPrPh)CuI]⁺.

4.3.29. Synthesis of Bis[1,3-bis(2,6-diisopropylphenyl)-2-phenylimidazol-4-ylidene] silver (I) tetrafluoroborate ([IPrPh)₂Ag(I)]BF₄ (29)



To a 100 mL *Schlenk* flask equipped with (IPrPh)BF₄ (**3**) (1.33 g, 2.4 mmol), KN(SiMe₃)₂ (480 mg, 2.40 mmol), and AgBF₄ (230 mg, 1.2 mmol) was added 30 mL of pre-cooled THF at 0°C. The reaction mixture was brought to room temperature and further stirred overnight. Filtration through a plug of Celite® afforded clear solution. The volatiles were removed under vacuum to obtain the desired compound as brown solid (1.2 g, 91%).

Empirical formula: C₆₆H₈₀AgBF₄N₂

Molecular weight: 1124.07 g/mol

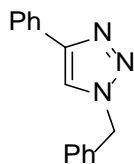
Yield: 1.2 g, 1.06 mmol, 86%.

¹H-NMR (300.13 MHz, CD₂Cl₂): δ 1.12–0.88 (m, 24H, CHMe₂), 1.41–1.14 (m, 24H, CHMe₂), 2.66–2.47 (m, 8H, CHMe₂), 6.92 (dbr, *J* = 9.1 Hz, 4H, *m*-C₆H₃), 7.23–7.10 (m, 4H, *m*-C₆H₃), 7.30–7.24 (m, 4H, *p*-C₆H₃), 7.34 (d, *J* = 7.5 Hz, 4H, *o*-C₆H₅), 7.40 (s, 2H, NCH), 7.50 (t, *J* = 7.8 Hz, 1H, *p*-C₆H₅) ppm.

¹³C{¹H}-NMR (75.47 MHz, CD₂Cl₂): 22.90 (CHMe₂), 25.76 (CHMe₂), 26.28 (CHMe₂), 29.78 (CHMe₂), 30.05 (CHMe₂), 124.17, 125.56 (*m*-C₆H₃), 125.86 (*p*-C₆H₃), 129.62 (*m*-C₆H₃), 130.14(*m*-C₆H₅), 131.58 (*o*-C₆H₅), 132.13 (*p*-C₆H₅), 145.76 (*ipso*-C₆H₅), 146.03(*ipso*-C₆H₅).

ESI-MS *m/z* [%]: 1037.5 [M-BF₄]⁺, 465.3 [M-(IPrPh)AgBF₄]⁺.

4.3.30. Synthesis of 1-benzyl-4-phenyl-1*H*-1,2,3-triazol (30)



Phenylacetylene (0.41 mL, 3.75 mmol) and benzyl azide (0.5 g, 3.75 mmol) was added to a solution of a catalyst in DCM (10 mL). The reaction mixture was stirred for 3 or 48 h. The conversion of the reactants was monitored by ¹H-NMR spectroscopy. The reaction mixture was filtered and all volatiles were removed under vacuum to obtain the product. Catalyst loadings, ¹H-NMR conversion and isolated yields are shown in the tables below.

Catalyst loading:	Conversion after 3 h	Isolated yield:
(IPrPh)CuI, 25 mg, 1 mol%	83 %	570 mg, 2.42 mmol, 65%.
(IPrPh)Cu(IPr)I, 39 mg, 1 mol%	0 %	-
(IPrPh) ₂ CuI, 42 mg, 1 mol%	0 %	-

Catalyst loading:	Conversion after 48 h	Isolated yield:
(IPrPh)CuI, 125 mg, 5 mol%	100 %	758 mg, 3.33 mmol, 89%.
(IPrPh)Cu(IPr)I, 196 mg, 5 mol%	100 %	610 mg, 2.59 mmol, 69%
(IPrPh) ₂ CuI, 210 mg, 5 mol%	55 %	350 mg, 1.48 mmol, 40%

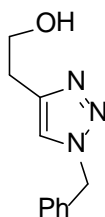
Empirical formula: C₁₅H₁₃N₃

Molecular weight: 235.28 g/mol

¹H-NMR (300.13 MHz, CDCl₃): δ 5.57 (s, 2H, CH₂Ph), 7.28-7.42 (m, 8H, CH₂Ph, C₆H₅), 7.67 (s, 1H, CN₃CH), 7.80 (dd, *J* = 8.3 Hz, 2H, C₆H₅) ppm.

¹³C{¹H}-NMR (75.47 MHz, CDCl₃): 54.32 (CH₂Ph), 119.61 (CN₃CH), 125.80, 128.15, 128.25, 128.87, 128.90, 129.25, 130.66, 134.81 (CH₂Ph, C₆H₅), 148.32 (CN₃CH) ppm.

Reference: ^[171]

4.3.31. Synthesis of 2-(1-benzyl-1*H*-1,2,3-triazol-4-yl)ethanol (31)

But-3yn-1-ol (0.29 mL, 3.75 mmol) and benzyl azide (0.5 g, 3.75 mmol) was added to a solution of a catalyst in DCM (10 mL). The reaction mixture was stirred for 15 h. The conversion of the reactants was monitored by $^1\text{H-NMR}$ spectroscopy. The reaction mixture was filtered and all volatiles were removed under vacuum to obtain the product. Catalyst loadings, $^1\text{H-NMR}$ conversion and isolated yields are shown in the table below.

Catalyst loading:	Conversion after 15 h	Isolated yield:
(IPrPh)CuI, 25 mg, 1 mol%	100 %	445 mg, 2.19 mmol, 58%
(IPrPh)Cu(IPr)I, 39 mg, 1 mol%	100 %	350 mg, 1.73 mmol, 46%.
(IPrPh) ₂ CuI, 42 mg, 1 mol%	80 %	304 mg, 1.50 mmol, 40%

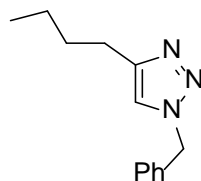
Empirical formula: C₁₁H₁₃N₃O

Molecular weight: 203.24 g/mol

$^1\text{H-NMR}$ (300.13 MHz, CDCl₃): δ 3.37 (dt, 4H, $J = 11.5, 6.0$ Hz C₂H₄OH), 5.46 (s, 2H, CH₂Ph), 7.22–7.26 (m, 2H, *o*-C₆H₅), 7.31–7.36 (m, 4H, *p*-C₆H₅, *m*-C₆H₅, CN₃CH) ppm.

$^{13}\text{C}\{^1\text{H}\}$ -NMR (75.47 MHz, CDCl₃): δ 53.95 (CH₂Ph), 61.22 (C₂H₄OH), 121.77 (CN₃CH), 127.97, 128.57, 128.98 (CH₂Ph), 134.73 (CN₃CH) ppm.

Reference: ^[172]

4.3.32. Synthesis of 1-benzyl-4-butyl-1*H*-1,2,3-triazol (32)

Hexin (0.43 mL, 3.75 mmol) and benzyl azide (0.5 g, 3.75 mmol) was added to a solution of a catalyst in DCM (10 mL). The reaction mixture was stirred for 15 h. The conversion of the reactants was monitored by ¹H-NMR spectroscopy. The reaction mixture was filtered and all volatiles were removed under vacuum to obtain the product. Catalyst loadings, ¹H-NMR conversion and isolated yields are shown in the table below.

Catalyst loading:	Conversion after 15 h	Isolated yield:
(IPrPh)CuI, 25 mg, 1 mol%	100 %	690 mg, 3.21 mmol, 85%.
(IPrPh)Cu(IPr)I, 39 mg, 1 mol%	26 %	96 mg, 0.45 mmol, 12%
(IPrPh) ₂ CuI, 42 mg, 1 mol%	8 %	-

Empirical formula: C₁₃H₁₇N₃

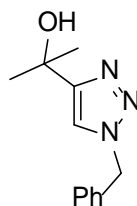
Molecular weight: 215.14 g/mol

¹H-NMR (300.13 MHz, CDCl₃): δ 0.90 (t, *J* = 7.3 Hz, 3H, C₄H₆Me), 1.35 (sext, 2H, *J* = 7.3 Hz, C₄H₆Me), 1.61 (pent, 2H, *J* = 7.3 Hz, C₄H₆Me), 2.67 (t, *J* = 8.1 Hz, 2H, C₄H₆Me), 5.47 (s, 2H, CH₂Ph), 7.17 (s, 1H, CN₃CH), 7.22–7.26 (m, 2H, *o*-CH₂Ph), 7.32–7.39 (m, 3H, *m-p*-CH₂Ph) ppm.

¹³C{¹H}-NMR (75.47 MHz, CDCl₃): δ 13.84 (C₄H₆Me), 22.35 (C₄H₆Me), 25.45 (C₄H₆Me), 31.55 (C₄H₆Me), 53.98 (CH₂Ph), 120.57 (CN₃CH), 127.97 (*m*-C₆H₅), 128.59 (*p*-C₆H₅), 129.05 (*o*-C₆H₅), 135.09 (*ipso*-C₆H₅), 148.98 (CN₃CH) ppm.

Reference: ^[172]

4.3.33. Synthesis of 2-(1-benzyl-1*H*-1,2,3-triazol-4-yl)propan-2-ol (33)



2-methylbut-3-yn-2-ol (0.37 mL, 3.75 mmol) and benzyl azide (0.5 g, 3.75 mmol) was added to a solution of a catalyst in DCM (10 mL). The reaction mixture was stirred for 15 or 48 h. The conversion of the reactants was monitored by ¹H-NMR spectroscopy. The reaction mixture was filtered and all volatiles were removed under vacuum to obtain the product. Catalyst loadings, ¹H-NMR conversion and isolated yields are shown in the tables below.

Catalyst loading:	Conversion after 15 h	Isolated yield:
(IPrPh)CuI, 25 mg, 1 mol%	100 %	740 mg, 3.48 mmol, 92 %.
(IPrPh)Cu(IPr)I, 39 mg, 1 mol%	100 %	620 mg, 2.85 mmol, 76 %.

Catalyst loading:	Conversion after 48 h	Isolated yield:
(IPrPh) ₂ CuI, 42 mg, 1 mol%	3 %	-

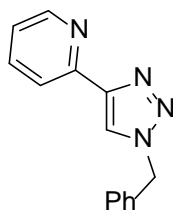
Empirical formula: C₁₂H₁₅N₃O

Molecular weight: 217.27 g/mol

¹H-NMR (300.13 MHz, CDCl₃): δ 1.60 (s, 6H, COHMe₂), 2.73 (s, 1H, OH), 5.48 (s, 2H, CH₂Ph), 7.24–7.30 (m, 2H, *o*-CH₂Ph), 7.34–7.39 (m, 4H, *m-p*-CH₂Ph, CN₃CH) ppm.

¹³C{¹H}-NMR (75.47 MHz, CDCl₃): δ 30.51 (CMe₂OH), 54.16 (CH₂Ph), 68.55 (CMe₂OH), 119.22 (NCHC), 128.19 (*o*-C₆H₅), 128.76 (*p*-C₆H₅), 129.15 (*m*-C₆H₅), 134.74 (NCHC) ppm.

Reference: ^[173]

4.3.34. Synthesis of 2-(1-benzyl-1*H*-1,2,3-triazol-4-yn)pyridine (34)

2-ethynylpyridine (0.41 mL, 3.75 mmol) and benzyl azide (0.5 g, 3.75 mmol) was added to a solution of a catalyst in DCM (10 mL). The reaction mixture was stirred for 15 h. The conversion of the reactants was monitored by $^1\text{H-NMR}$ spectroscopy. The reaction mixture was filtered and all volatiles were removed under vacuum to obtain the product. Catalyst loadings, $^1\text{H-NMR}$ conversion and isolated yields are shown in the table below.

Catalyst loading:	Conversion after 15 h	Isolated yield:
(IPrPh)CuI, 25 mg, 1 mol%	100%	710 mg, 3.00 mmol, 80%.
(IPrPh)Cu(IPr)I, 39 mg, 1 mol%	100%	690 mg, 2.92 mmol, 78%
(IPrPh) ₂ CuI, 42 mg, 1 mol%	83 %	600 mg, 2.54 mmol, 68%

Empirical formula: C₁₄H₁₂N₄

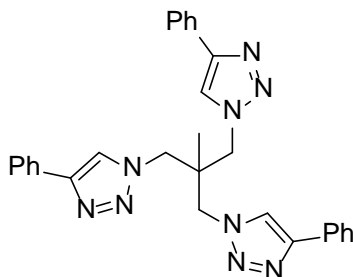
Molecular weight: 236.11 g/mol

$^1\text{H-NMR}$ (300.13 MHz, CDCl₃): δ 5.50 (s, 2H, CH₂Ph), 7.13 (ddd, 1H, $J = 7.4, 4.9, 1.1$ Hz, *p*-C₅H₄N), 7.23–7.34 (m, 5H, CH₂Ph), 7.68 (dt, $J = 7.7, 1.7$ Hz, 1H, *m*-C₅H₄N), 7.98 (s, 1H, CN₃CH), 8.08 (d, 1H, $J = 8.0$ Hz, *o*-C₅H₄N), 8.45 (d, $J = 4.9$ Hz, 1H, *m*-C₅H₄N) ppm.

$^{13}\text{C}\{^1\text{H}\}$ -NMR (75.47 MHz, CDCl₃): δ 54.46 (CH₂Ph), 120.30 (*p*-C₅NH₄), 122.01 (NCHC), 122.92 (*p*-C₅NH₄), 128.39 (*o*-C₆H₅), 128.92 (*p*-C₆H₅), 129.25 (*m*-C₆H₅), 134.45 (NCHC), 136.95 (*m*-C₅NH₄), 148.83 (*ipso*-C₆H₅), 149.42 (*m*-C₅NH₄), 150.34 (*ipso*-C₅NH₄) ppm.

Reference: ^[174]

4.3.35. Synthesis of 1,1'-(2-methyl-2-((4-phenyl-1H-1,2,3-triazol-1-yl)methyl)propane-1,3-diyl)bis(4-phenyl-1H-1,2,3-triazole)
 $C_2H_3(C_3H_3N_3(Ph))_3$ (35)



Phenylacetylene (0.84 mL, 7.68 mmol) and 1,3-diazido-2-(azidomethyl)-2-methylpropane (0.5 g, 2.54 mmol) was added to a solution of a catalyst in DCM (10 mL). The reaction mixture was stirred for 5 h. The solution was halved under vacuum and cold pentane was added. The product precipitates as a white solid. The solution was filtered and dried under vacuum to yield the pure product.

Catalyst loading:	Isolated yield:
(IPrPh)CuI, 17 mg, 1 mol%	1,27 g, 2.53 mmol, 99%.
IPrPhCuIPrI 26 mg, 1 mol%	1,28 g, 2.55 mmol, 99.7%
(IPrPh) ₂ CuI, 29 mg, 1 mol%	1.02 g, 2.03 mmol, 79 %

Summenformel: $C_{29}H_{27}N_9$

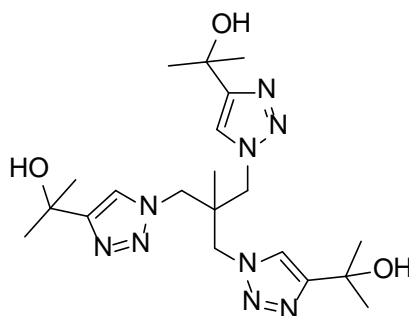
Molekulargewicht: 501.59 g/mol

¹H-NMR (300 MHz, THF-*d*8): δ , 0.96 (s, 3 H, CH₃), 4.64 (s, 6 H, (CH₂)₃), 7.27 (t, $J = 7.4$ Hz, 3H, *p*-C₆H₅), 7.38 (t, $J = 7.4$ Hz, 6H, *m*-C₆H₅), 7.91 (d, $J = 7.0$ Hz, 6H, *o*-C₆H₅), 8.54 (s, 3 H, C₂HN₃) ppm.

¹³C{¹H}-NMR (75.47 MHz, THF-*d*8): δ 19.43 ((CH₂)₃CMe), 42.21 ((CH₂)₃CMe), 54.46 ((CH₂)₃CMe), 123.76 (*ipso*-C₆H₅), 126.37 (*o*-C₆H₅), 128.65 (*p*-C₆H₅), 129.56 (*m*-C₆H₅), 132.23 (NCHC), 147.92 (NCHC) ppm.

ESI-MS *m/z* [%]: 524.2 [M+Na]⁺.

4.3.36. Synthesis of 1,1'-(2-methyl-2-((4-phenyl-1H-1,2,3-triazol-1-yl)methyl)propane-1,3-diyl)bis(4-phenyl-1H-1,2,3-triazole) (36)



2-methyl-3-butyn-2-ol (0.86 mL, 7.68 mmol) and 1,3-diazido-2-(azidomethyl)-2-methylpropane (0.5 g, 2.56 mmol) was added to a solution of a catalyst IPrPhCuI 17 mg, 1 mol% in DCM (20 mL). The reaction mixture was stirred for 5 h. The solution was halved under vacuum and cold pentane was added. The product precipitates as a white solid. The solution was filtered and dried under vacuum to yield the pure product.

Summenformel: C₂₂H₃₃N₉O₃

Molekulargewicht: 447.53 g/mol

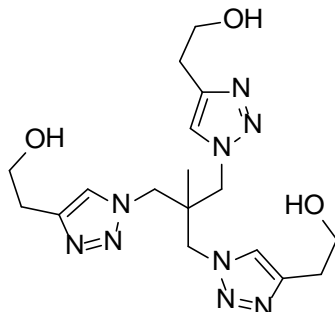
Yield: 850 mg, 1.89 mmol, 74%

¹H-NMR (300 MHz, THF-*d*8): δ 7.97 (s, 3 H, C₂H₃N₃), 4.39 (s, 6H, (CH₂)₃), 4.30 (s, 3H, OH), 1.53 (s, 18H, C₃H₆OH), 0.79 (s, 3 H, CH₃) ppm.

¹³C{¹H}-NMR (75.47 MHz, THF-*d*8): δ 19.49 (CH₂)₃CMe), 31.29 ((CH₃)₂COH), 42.07 ((CH₂)₃CMe₃), 54.16 (CH₂)₃CMe₃), 68.46 ((CH₃)₂COH), 123.15 (NCHC), 157.21 (NCHC) ppm.

ESI-MS m/z [%]: 470.3 [M+Na]⁺.

4.3.37. Synthesis of 2,2'-(1,1'-(2-((4-(2-hydroxyethyl)-1H-1,2,3-triazol-1-yl)methyl)-2-methylpropane-1,3-diyl)bis(1H-1,2,3-triazole-4,1-diyl))diethanol (37)



3-butyn-1-ol (0.58 mL, 7.68 mmol) and 1,3-diazido-2-(azidomethyl)-2-methylpropane (0.5 g, 2.56 mmol) was added to a solution of a catalyst IPrPhCuI 17 mg, 1 mol% in DCM (20 mL). The reaction mixture was stirred for 5 h. The solution was halved under vacuum and cold pentane was added. The product precipitates as a white solid. The solution was filtered and dried under vacuum to yield the pure product.

Summenformel: C₁₇H₂₇N₉O₃

Molekulargewicht: 405.45 g/mol

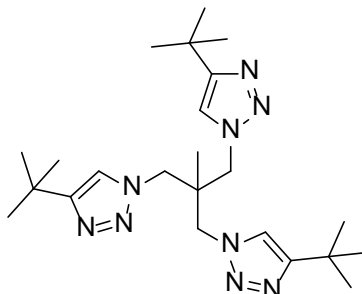
Yield: 680 mg, 1.68 mmol, 65%

¹H-NMR (300 MHz, DMSO-*d*6): δ 7.89 (s, 3 H, NCHC), 4.52 (s, 3H, OH), 4.32(s, 6H, (CH₂)₃CCH₃), 3.72 (s, 6H, (CH₂CH₂OH)₃), 2.84 (s, 6H, (CH₂CH₂OH)₃), 0.75 (s, 3H,(CH₂)₃CCH₃) ppm.

¹³C{¹H}-NMR (75.47 MHz, DMSO-*d*6): δ 18.66 (CH₂)₃CMe, 28.83 ((CH₂CH₂OH)₃), 40.58 (CMe₃), 52.75((CH₂)₃CCH₃), 60.36 ((CH₂CH₂OH)₃), 124.38 (NCHC), 144.61 (NCHC) ppm.

ESI-MS m/z [%]: 428.2 [M+Na]⁺.

4.3.38. Synthesis of 1,1'-(2-methyl-2-((4-neopentyl-1H-1,2,3-triazol-1-yl)methyl)propane-1,3-diyl)bis(4-(tert-butyl)-1H-1,2,3-triazole) (38)



3,3-dimethyl-1-butyne (0.95 mL, 7.68 mmol) and 1,3-diazido-2-(azidomethyl)-2-methylpropane (0.5 g, 2.56 mmol) was added to a solution of a catalyst (IPrPh)CuI 17 mg, 1 mol% in DCM (20 mL). The reaction mixture was stirred for 5 h. The solution was halved under vacuum and cold pentane was added. The product precipitates as a white solid. The solution was filtered and dried under vacuum to yield the pure product.

Summenformel: C₂₃H₃₉N₉

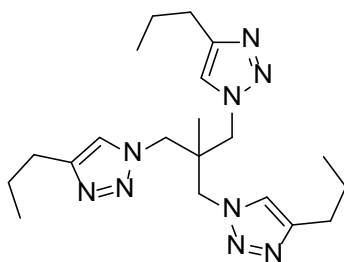
Molekulargewicht: 441.33 g/mol

Yield: 830 mg, 1.82 mmol, 71%

¹H-NMR (300 MHz, THF-*d*8): δ 7.91 (s, 3 H, C₂HN₃), 4.38 (s, 6H, (CH₂)₃), 1.35(s, 27H, CMe₃), 0.77 (s, 3H, CH₃) ppm.

¹³C{¹H}-NMR (75.47 MHz, CDCl₃): δ 19.33 (CH₂)₃CMe), 30.88 (CMe₃), 31.52 (CMe₃), 42.12 (CH₂)₃CMe), 54.09 ((CH₂)₃CMe), 122.46 (NCHC), 157.34 (NCHC) ppm.

ESI-MS m/z [%]: 464.3 [M+Na]⁺.

4.3.39. Synthesis of 1,1'-(2-methyl-2-((4-propyl-1H-1,2,3-triazol-1-yl)methyl)propane-1,3-diyl)bis(4-propyl-1H-1,2,3-triazole) (39)

1-Pentyn (0.76 mL, 7.68 mmol) and 1,3-diazido-2-(azidomethyl)-2-methylpropane (0.5 g, 2.56 mmol) was added to a solution of a catalyst (IPrPh)CuI 17 mg, 1 mol% in DCM (20 mL). The reaction mixture was stirred for 5 h. The solution was halved under vacuum and cold pentane was added. The product precipitates as a white solid. The solution was filtered and dried under vacuum to yield the pure product.

Empirical formula: C₂₀H₃₃N₉

Molecular weight: 399.29 g/mol

Yield: 886 mg, 2.21 mmol, 87%.

¹H-NMR (300 MHz, THF-*d*8): δ 7.93 (s, 3 H, C₂HN₃), 4.39 (s, 6H, (CH₂)₃), 2.67(t, *J* = 7.5 Hz, 6H, C₂H₄Me), 1.76–1.64 (m, 6H, C₂H₄Me), 0.97 (t, 9H, C₂H₄Me), 0.77 (s, 3H, Me) ppm.

¹³C{¹H}-NMR (75.47 MHz, THF-*d*8): δ 14.17 (C₂H₄Me), 19.36 ((CH₂)₃CMe), 23.63 (C₂H₄Me), 28.50 (C₂H₄Me), 42.16 ((CH₂)₃CMe), 53.98 ((CH₂)₃CMe), 124.58 (NCHC), 147.95 (NCHC) ppm.

ESI-MS *m/z* [%]: 422.3 [M+Na]⁺.

5. Crystallographic Section

5.1. Crystal Selection and Manipulation

If necessary, due to moisture and air sensitivity and crystal growing temperature, single crystals were selected from a *Schlenk* flask under argon atmosphere and covered with perfluorated polyether oil on a microscope slide, which was cooled with an inert gas flow (nitrogen, +25 °C – –100 °C) using the *X-TEMP2* device.^[175] An appropriate crystal was selected using a microscope equipped with polarization filter, mounted on the tip of a MiTeGen[®] MicroMount or glass fibre, fixed to a goniometer head and shock cooled by the crystal cooling device.

5.2. Data Collection and Processing

The compounds were measured using either an Incoatec microfocus source with mirror optics or on a rotating anode turbo X-ray source.^[176] Both are equipped with an APEX II CCD detector, mounted on a three-circle D8 goniometer, and mirrors as monochromator optics, which supplies very intense and brilliant MoK_α radiation ($\lambda = 0.71073 \text{ \AA}$). All crystals were centred optically using a video camera after being placed on the diffractometer.

The data collection strategy was calculated with the APEX plugin *COSMO*^[177] or entered by hand. Therefore, a test run (*matrix scan*) was recorded prior to each experiment to check the crystal quality, to get a rough estimate of the cell parameters, and to determine the optimum exposure time. All scans of the data collections were performed in an ω -scan mode with a step-width of 0.5° at fixed ϕ -angles.

The unit cell was indexed with the tools in the Bruker *APEX2* software suite.^[178] The intensities on the raw frames were integrated with *SAINT* 7.68a.^[178a] The orientation matrix was refined in several integration runs and the maximum resolution was adjusted so that only useable data with a maximum R_{int} of 0.20 were integrated.

The software *SADABS*^[179] was used for absorption correction and scaling. *TWINABS*^[180] was utilised in the cases of non-merohedral twins or split crystals. Both programs refine an empirical error function by symmetry-equivalent reflections. *XPREP* in various version up to 2015/1^[181] was used for the examination of data statistics and preliminary space group determination prior to the absorption correction, as this is crucial for a correct treatment. Finally, *XPREP* was used to setup the files for structure solution and refinement.

5.3. Structure Solution and Refinement

The structures were solved with direct methods using *SHELXS*.^[182] All refinements were performed on F^2 with *SHELXL-2012*^[183] implemented in the *SHELXLE-GUI*.^[184] All non-hydrogen-atoms were refined with anisotropic displacement parameters. The C-bonded hydrogen atoms were set on calculated positions and refined isotropically using a riding model with their U_{iso} values constrained equal to 1.5 times the U_{eq} of their pivot atoms for methyl carbon atoms and 1.2 times for all other carbon atoms. The N-bonded hydrogen atom coordinates were refined

freely from the residual density map and constrained to $1.5 U_{eq}$ of their pivot nitrogen atom. If not stated otherwise, the hydrogen bond lengths were restrained to a sensible value and the U_{iso} were constrained as mentioned above.

In the absence of restraints, the only data the structural model is refined against are the measured intensities in the form of squared structure factors. Structure factors are calculated from the atomic model and the so-calculated intensities are then compared with the measured intensities, and the best model is the one that minimises $M(p_i, k)$ (Eq. 6-1) using the weights w defined in Eq. 6-2.

$$\text{Eq. 6-1} \quad M(p_i, k) = \sum w [k|F_{obs}|^2 - |F_{calc}|^2]^2 = \min$$

(p_i : structural parameters; k : scale factor)

$$\text{Eq. 6-2} \quad w^{-1} = \sigma^2(F_{obs}^2) + (g1 \times P)^2 + g2 \times P \quad \text{with} \quad P = \left(\frac{\text{Max}(F_{obs}^2 + 2F_{calc}^2)}{3} \right)$$

The results of the refinements were verified by comparison of the calculated and the observed structure factors. Commonly used criteria are the residuals $R1$ (Eq. 6-3) and $wR2$ (Eq. 6-4).

$$\text{Eq. 6-3} \quad R1 = \frac{\sum |F_{obs}| - |F_{calc}|}{\sum |F_{obs}|}$$

$$\text{Eq. 6-4} \quad wR2 = \sqrt{\frac{\sum w(F_{obs}^2 - F_{calc}^2)^2}{\sum w(F_{obs}^2)^2}}$$

Additionally, the goodness of fit (GoF , S), a figure of merit showing the relation between deviation of F_{calc} from F_{obs} and the over-determination of refined parameters is calculated (Eq. 6-5).

$$\text{Eq. 6-5} \quad S = \sqrt{\frac{\sum (w(F_{obs}^2 - F_{calc}^2)^2)}{n-p}}$$

(n : number of reflections; p : number of parameters)

The residual densities from difference *Fourier* analysis should be low. Due to the model restrictions the residuals are normally found in the bonding regions. Higher residuals for heavy scatterers are acceptable as they arise mainly from absorption effects and *Fourier* truncation errors due to the limited recorded resolution range. The highest peak and deepest hole from difference *Fourier* analysis are listed in the crystallographic tables.

Additionally, the orientation, size and ellipticity of the ADPs show the quality of the model. Ideally, the ADPs should be oriented perpendicular to the bonds, be equal in size and show little ellipticity. All graphics were generated and plotted with the $xp^{[185]}$ program at the 50 % probability level.

5.4. Treatment of Disorder

Structures containing disordered fragments were refined using constraints and restraints. Constraints used within this work are, for example, the site occupation factor and the AFIX instruction, which defines and constrains rigid groups.

Mathematically, restraints are treated as additional experimental observations, thus increasing the number of data to refine against. In the presence of restraints, the minimization function changes as follows:

$$\text{Eq. 6-6} \quad M = \sum w(F_{obs}^2 - F_{calc}^2)^2 + \sum w_r(R_{target} - R_{calc})^2$$

The geometries of chemically equivalent but crystallographically independent fragments can be fitted to each other by distance restraints. Especially the 1,2 distances (bond lengths) and 1,3 distances (bond angles) are set to be equal within their effective standard deviations. This is helpful for refining disordered positions as the averaging of equivalent fragments implements chemical information and stabilises the refinement. Within this work, disordered moieties were refined using distance restraints (*SADI* and *SAME*) and anisotropic displacement parameter restraints (*SIMU*, *DELU* and *RIGU*).^[147]

5.5. Determined Structures

5.5.1. 1,3-bis(2,6-diisopropylphenyl)imidazole-2-yliden (IPr) (1)

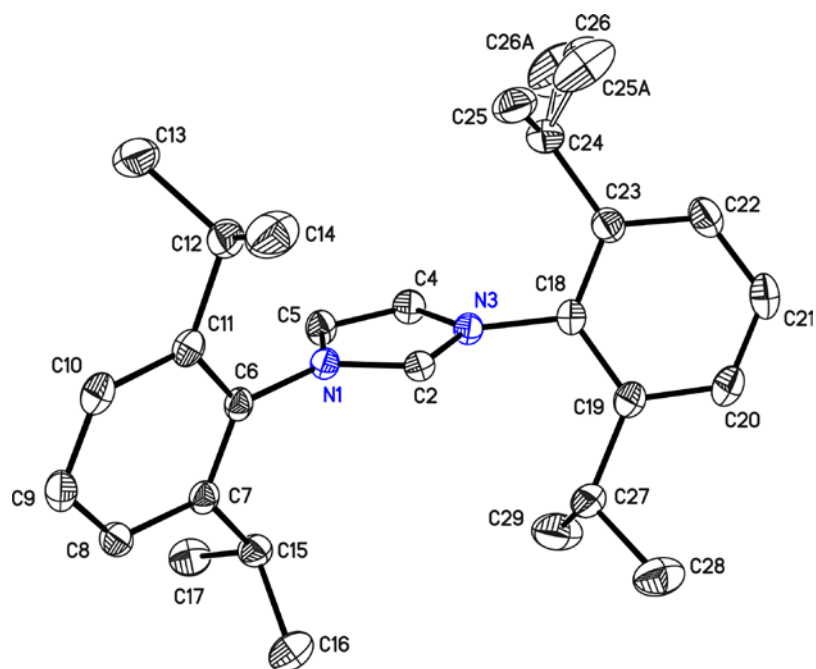


Figure 5.1: Asymmetric unit of IPr. The anisotropic displacement parameters are shown at the 50% probability level. Hydrogen atoms are omitted for clarity.

This structure was first reported by *Arduengo et al.* in 1999.^[135]

Structure code	SR_070_IPr	Z	4
Empirical formula	C ₂₇ H ₃₆ N ₂	Crystal dimensions [mm]	0.178 × 0.175 × 0.080
Formula weight [g/mol]	388.58	$\rho_{\text{calcd.}}$ [g/cm ³]	1.089
Sample temperature [K]	100(2)	μ [mm ⁻¹]	0.063
Wavelength [Å]	0.71073	<i>F</i> (000)	848
Crystal system	Monoclinic	Θ range [°]	1.959 to 25.384
Space group	<i>P</i> 2 ₁ / <i>c</i>	Reflections collected	47390
Unit cell dimensions [Å] and [°]		Unique reflections	4330
	<i>a</i> = 20.810(3)	<i>R</i> _{int}	0.0445
	<i>b</i> = 5.775(2)	Completeness to $\theta_{\text{full}} = 25.242^\circ$	100%
	<i>c</i> = 19.733(2)	restraints/parameters	86 / 291
	α = 90.0	GooF	1.096
	β = 92.36(2)	<i>R</i> 1(<i>I</i> > 2 σ (<i>I</i>))	0.0438
	γ = 90.0	<i>wR</i> 2 (all data)	0.1178
Volume [Å ³]	2369.5(9)	max. diff. peak/hole [e ⁻ Å ⁻³]	0.208 and -0.230

5.5.2. 1,3-bis(2,6-diisopropylphenyl)imidazoliumiodide (IPr·HI)

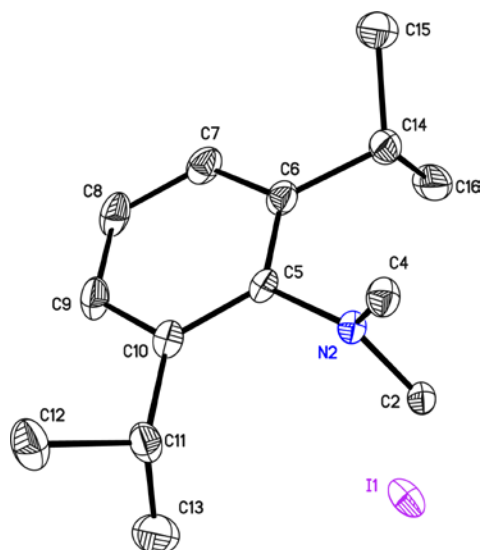


Figure 5.2: Asymmetric unit of IPr·HI. The anisotropic displacement parameters are shown at the 50% probability level. Hydrogen atoms are omitted for clarity.

This structure was first reported by *Curran et al.* in 2010.^[186] It was grown in the mother liquor of an unsuccessful reaction.

Structure code	SR_126	Z	4
Empirical formula	C ₂₇ H ₃₇ N ₂	Crystal dimensions [mm]	0.1 × 0.1 × 0.1
Formula weight [g/mol]	516.48	$\rho_{\text{calcd.}}$ [g/cm ³]	1.328
Sample temperature [K]	100(2)	μ [mm ⁻¹]	1.254
Wavelength [Å]	0.71073	F (000)	1064
Crystal system	Monoclinic	Θ range [°]	2.146 to 26.389
Space group	<i>Pccn</i>	Reflections collected	32743
Unit cell dimensions [Å] and [°]		Unique reflections	2650
a =	10.644(2)	R _{int}	0.0249
b =	12.791(2)	Completeness to $\theta_{\text{full}} = 25.242^\circ$	100%
c =	18.979(3)	restraints/parameters	0 / 141
$\alpha =$	90.0	Goof	1.044
$\beta =$	90.0	R1(I > 2 σ (I))	0.0234
$\gamma =$	90.0	wR2 (all data)	0.0680
Volume [Å ³]	2385.9(8)	max. diff. peak/hole [e·Å ⁻³]	0.612 and -0.737

5.5.3. 1,3-bis(2,6-diisopropylphenyl)imidazoliumiodide (IPr·HI*1,4-dioxane)

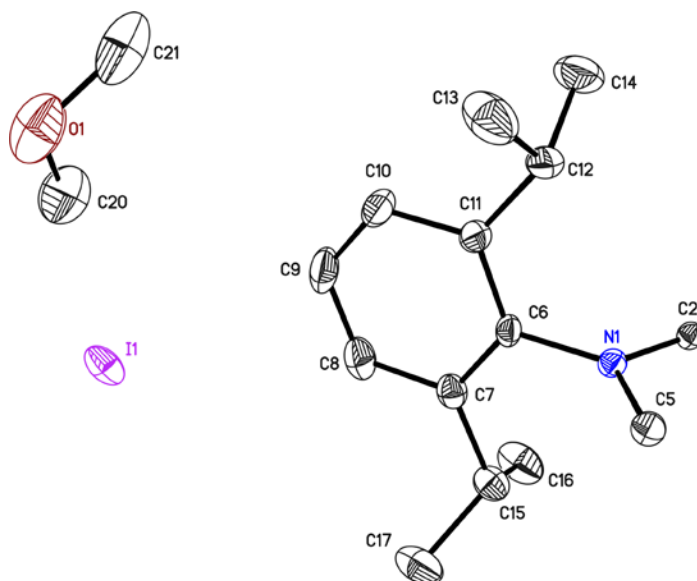


Figure 5.3: Asymmetric unit of IPr·HI. The anisotropic displacement parameters are shown at the 50% probability level. Hydrogen atoms are omitted for clarity.

This structure without co-crystallised solvent was first reported by *Curran et al.* in 2010.^[186] It was grown in the mother liquor of an unsuccessful reaction.

Structure code	SR_139	Z	4
Empirical formula	C ₃₁ H ₄₅ IN ₂ O ₂	Crystal dimensions [mm]	0.1 × 0.1 × 0.1
Formula weight [g/mol]	604.59	$\rho_{\text{calcd.}}$ [g/cm ³]	1.256
Sample temperature [K]	100(2)	μ [mm ⁻¹]	1.028
Wavelength [Å]	0.71073	$F(000)$	1256
Crystal system	Monoclinic	Θ range [°]	2.046 to 26.336
Space group	<i>C2/c</i>	Reflections collected	31670
Unit cell dimensions [Å] and [°]		Unique reflections	3247
	a = 22.403(3)	R_{int}	0.0208
	b = 9.428(2)	Completeness to $\theta_{\text{full}} = 25.242^\circ$	100%
	c = 17.029(2)	restraints/parameters	0 / 168
	$\alpha = 90.0$	GooF	1.081
	$\beta = 117.28(2)0$	$R1(I > 2\sigma(I))$	0.0265
	$\gamma = 90.0$	$wR2$ (all data)	0.0679
Volume [Å ³]	3196.7(10)	max. diff. peak/hole [e·Å ⁻³]	1.582 and -0.484

5.5.4. 4-(chlorodiphenylsilyl)-1,3-bis(2,6-diisopropyl-phenyl)-2,3-dihydro-1*H*-imidazole copper chloride
CuCl(IPr)SiPh₂Cl·toluene (6)

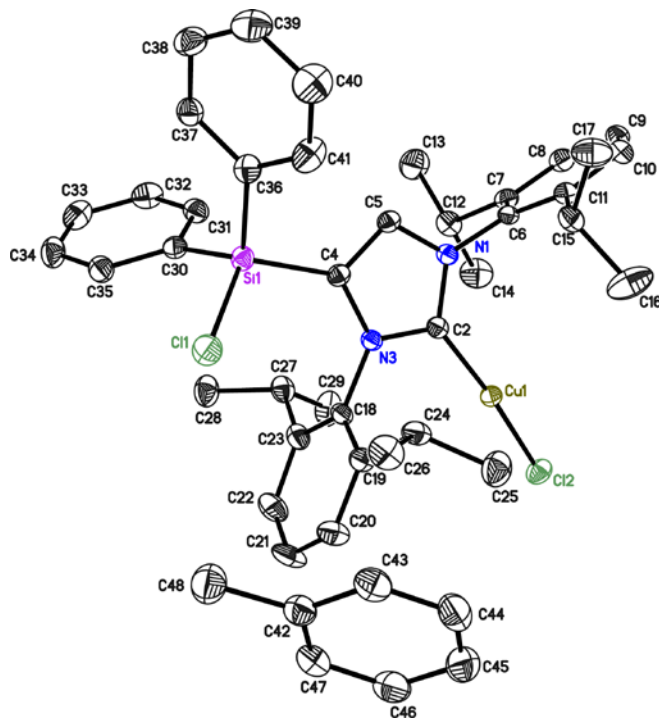


Figure 5.4: Asymmetric unit of compound **6**. The anisotropic displacement parameters are shown at the 50% probability level. Hydrogen atoms are omitted for clarity.

Published in: “*Synthesis and structural investigation of R₂Si (R = Me, Ph) bridged di-N-heterocyclic carbenes.*” R. S. Ghadwal, S. O. Reichmann, E. Carl, R. Herbst-Irmer, *Dalton Trans.* **2014**, *43*, 13704-13710.

CCDC number	982102		
Structure code	SOR_A_079	Z	4
Empirical formula	C ₄₆ H ₅₃ Cl ₂ CuN ₂ Si	Crystal dimensions [mm]	0.235 × 0.196 × 0.150
Formula weight [g/mol]	796.43	$\rho_{\text{calcd.}}$ [g/cm ³]	1.230
Sample temperature [K]	100(2)	μ [mm ⁻¹]	0.692
Wavelength [Å]	0.71073	<i>F</i> (000)	1680
Crystal system	Monoclinic	Θ range [°]	1.558 to 26.378
Space group	<i>P</i> 2 ₁ / <i>c</i>	Reflections collected	97304
Unit cell dimensions [Å] and [°]		Unique reflections	8799
	a = 11.380(2)	R _{int}	0.0519
	b = 15.471(2)	Completeness to $\theta_{\text{full}} = 25.242^\circ$	100%
	c = 24.676(3)	restraints/parameters	0 / 478
	$\alpha = 90.0$	Goof	1.036
	$\beta = 98.03(2)$	R1(I > 2 σ (I))	0.0288
	$\gamma = 90.0$	wR2 (all data)	0.0740
Volume [Å ³]	4301.9(11)	max. diff. peak/hole [e ⁻ ·Å ⁻³]	0.367 and -0.272

5.5.5. Bis(1,3-bis(2,6-diisopropylphenyl)-2,3-dihydro-1*H*-imidazol-4-yl)diphenylsilane-copper chloride $\text{Ph}_2\text{Si}[(\text{IPr})\text{CuCl}]_2$ (**4**)

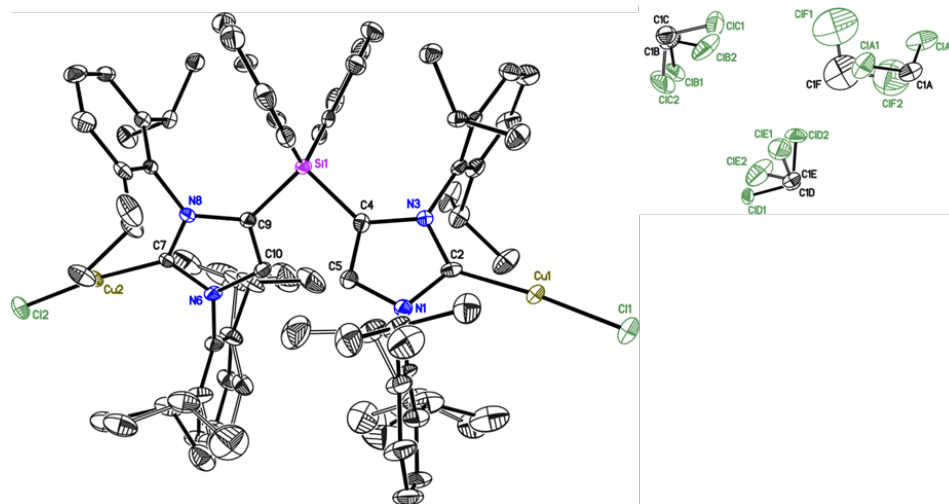


Figure 5.5: Molecular structure of $\text{Ph}_2\text{Si}[(\text{IPr})\text{CuCl}]_2$ (**4**) with three dichloromethane molecules in the asymmetric unit. Anisotropic displacement parameters are depicted at the 50% probability level. All hydrogen atoms are omitted for clarity. The dichloromethane molecules are disordered on the two positions each. The site occupation factor refine to 0.691(8), 0.717(5), 0.683(6)..

Published in: “*Synthesis and structural investigation of $R_2\text{Si}$ ($R = \text{Me}, \text{Ph}$) bridged di-*N*-heterocyclic carbenes.*” R. S. Ghadwal, S. O. Reichmann, E. Carl, R. Herbst-Irmer, *Dalton Trans.* **2014**, 43, 13704-13710.

CCDC number	982104	Z	4
Structure code	SR_Raj_287	Crystal dimensions [mm]	0.368 × 0.190 × 0.964
Empirical formula	$\text{C}_{69}\text{H}_{86}\text{Cl}_8\text{Cu}_2\text{N}_4\text{Si}$	$\rho_{\text{calcd.}}$ [g/cm^3]	1.327
Formula weight [g/mol]	1410.18	μ [mm^{-1}]	0.964
Sample temperature [K]	100(2)	$F(000)$	2944
Wavelength [Å]	0.71073	Θ range [°]	1.647 to 26.347
Crystal system	Orthorhombic	Reflections collected	226192
Space group	$Pna2_1$	Unique reflections	14390
Unit cell dimensions [Å]		R_{int}	0.0340
a =	24.735(3)	Completeness to $\theta_{\text{full}}=25.242^\circ$	100%
b =	11.999(2)	restraints/parameters	2847 / 1003
c =	23.789(2)	Goof	1.075
$\alpha =$	90°	$R1(I > 2\sigma(I))$	0.0352
$\beta =$	90°	$wR2$ (all data)	0.0968
$\gamma =$	90°	max. diff. peak/hole [$\text{e} \cdot \text{Å}^{-3}$]	0.824 and -0.561
Volume [Å ³]	7060.5(16)		

The molecular structure shows pseudo-symmetry. It can also be refined in space group $Pccn$, but then the results are much poorer (Table 5-1). To identify the correct space group we had a closer look at the weak reflection.^[187] A good figure of merit is the K value $K = |[F_0^2]|/|[F_C^2]|$ calculated as $K = |[F_0^2]|/|[F_C^2]|$ for reflections with low intensity (Table 5-2). In this case the K value for $Pna2_{(1)}$ does not deviate much from unity compared to the $Pccn$ model. Furthermore the R1 (%) value drops from 7.94 (in $Pccn$) down to 3.62 (in $Pna2_{(1)}$), indicating that the space group $Pna2_{(1)}$ fits best. Additionally the systematic absences of space group $Pccn$ are not fulfilled. (Table 5-3)

Table 5-1: K-value for the reflections with weakest intensity and R1 for all data for the two space groups *Pccn* and *Pna2₍₁₎*

	<i>Pccn</i>	<i>Pna2₍₁₎</i>
K for the reflections with weakest intensity	8.842	1.291
R1 all data [%]	8.19	3.73

Table 5-2 Abstract of the program XPREP –Reciprocal space exploration- Version 2013/2 for Windows.

Systematic absence exceptions:

	b--	c--	n--	21--	-c-	-a-	-n-	-21-	--a	--b	--n	--21
N	6535	6554	6487	72	3155	3196	3197	121	3149	3158	3165	127
N I>3s	2925	26	2941	9	1472	2166	2176	37	1466	1492	48	20
<I>	29.8	0.1	30.0	0.2	1.9	31.6	31.7	0.6	23.1	23.0	0.2	0.4
<I/s>	10.9	0.5	11.0	1.1	4.9	12.9	13.0	2.2	11.0	11.0	0.6	1.8

Table 5-3: Abstract of the program XPREP –Reciprocal space exploration- Version 2013/2 for Windows.

Identical indices and Friedel opposites combined before calculating R(sym)

Option	Space Group	No.	Type	Axes	CSD	R(sym)	N(eq)	Syst.	Abs.	CFOM
[A]	<i>Pna2₍₁₎</i>	#33	Non-cen	5	903	0.014	20848	2.2	4.9	5.73
[B]	<i>Pnma</i>	#62	centro	4	894	0.014	20848	2.2	4.9	2.64

In space group *Pna2₍₁₎* the structure crystallizes as a twin by inversion. The fractional contribution of the minor domain refines to 0.19(2). All solvent molecules are severely disordered. Although we tried to resolve the disorder, the results are not quit satisfying leading to still relatively high residual density. Trials with the SQUEEZE routine of the PLATON program package did not improve the model.^[188] The large non-solvent Ueq(max)/Ueq(min) ratio of 6.6 is caused by disorder of the isopropyl groups.

5.5.6. 1,3-bis(2,6-diisopropylphenyl)-2-phenyl-imidazolium palladium triiodide (IPrPh)PdI₃ (7b)

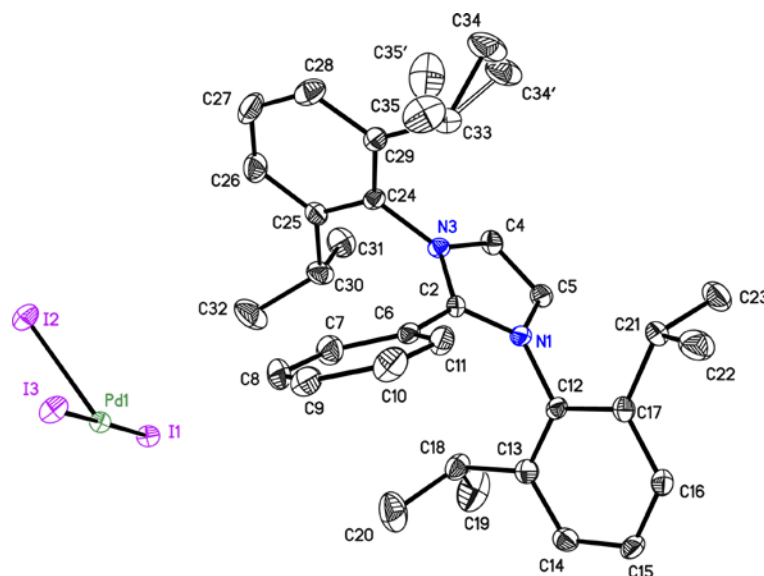


Figure 5.6: Asymmetric unit of compound **7b**. The anisotropic displacement parameters are shown at the 50% probability level. Hydrogen atoms are omitted for clarity. The isopropyl-moiety is disordered on two positions (*sof*: 0.552(30)).

Structure code	SOR-A-083	Z	4
Empirical formula	C ₃₃ H ₄₁ N ₂ I ₃ Pd	Crystal dimensions [mm]	0.08 × 0.12 × 0.10
Formula weight [g/mol]	952.78	$\rho_{\text{calcd.}}$ [g/cm ³]	1.764
Sample temperature [K]	100(2)	μ [mm ⁻¹]	3.121
Wavelength [Å]	0.71073	<i>F</i> (000)	1832
Crystal system	Monoclinic	Θ range [°]	1.711 to 26.480
Space group	<i>P</i> 2 ₁ / <i>n</i>	Reflections collected	57358
Unit cell dimensions [Å] and [°]		Unique reflections	74113
a =	12.103(2)	R _{int}	0.0460
b =	20.028(3)	Completeness to $\theta_{\text{full}} = 25.242^\circ$	100%
c =	15.122(2)	restraints/parameters	17 / 381
$\alpha =$	90.0	Goof	1.020
$\beta =$	101.82(2)	<i>R</i> 1(<i>I</i> > 2 σ (<i>I</i>))	0.0227
$\gamma =$	90.0	<i>wR</i> 2 (all data)	0.04866
Volume [Å ³]	3587.8(10)	max. diff. peak/hole [e·Å ⁻³]	0.618 and -0.473

5.5.7. 1,3-bis(2,6-diisopropylphenyl)-2-phenyl-imidazolium iodide (IPrPh)I (7a)

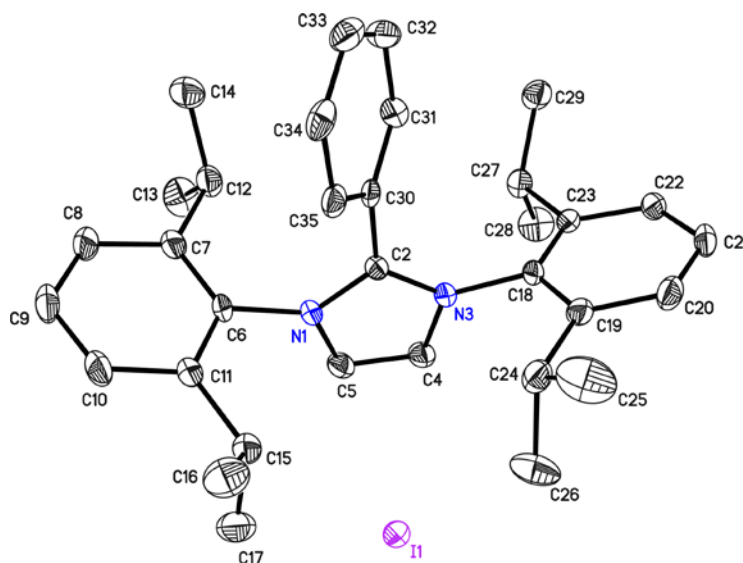


Figure 5.7: Asymmetric unit of compound **7a**. The anisotropic displacement parameters are shown at the 50% probability level. Hydrogen atoms are omitted for clarity.

Published in: “Palladium-Catalyzed Direct C2-Arylation of an N-Heterocyclic Carbene: An Atom-Economic Route to Mesoionic Carbene Ligands.” R. S. Ghadwal, S. O. Reichmann, R. Herbst-Irmer, *Chem. Eur. J.* **2015**, *21*, 4247-4251.

CCDC number	1017469		
Structure code	SOR-A-083_white	Z	2
Empirical formula	C ₃₃ H ₄₁ N ₂ I	Crystal dimensions [mm]	0.15 × 0.11 × 0.09
Formula weight [g/mol]	592.58	$\rho_{\text{calcd.}}$ [g/cm ³]	1.271
Sample temperature [K]	100(2)	μ [mm ⁻¹]	1.056
Wavelength [Å]	0.71073	F (000)	612
Crystal system	Triclinic	Θ range [°]	1.240 to 26.491
Space group	<i>P</i> -1	Reflections collected	56863
Unit cell dimensions [Å] and [°]		Unique reflections	6401
	a = 10.146(2)	R _{int}	0.0395
	b = 10.563(2)	Completeness to $\theta_{\text{full}} = 25.242^\circ$	100%
	c = 16.556(3)	restraints/parameters	0 / 333
	$\alpha = 82.81(2)$	Goof	1.062
	$\beta = 86.52(3)$	R1(I > 2 σ (I))	0.0233
	$\gamma = 61.56(2)$	wR2 (all data)	0.0503
Volume [Å ³]	1547.9(6)	max. diff. peak/hole [e·Å ⁻³]	0.513 and -0.571

5.5.8. 1,3-bis(2,6-diisopropylphenyl)-2-phenyl-imidazolium tetrafluoroborate (IPrPh)BF₄ (8)

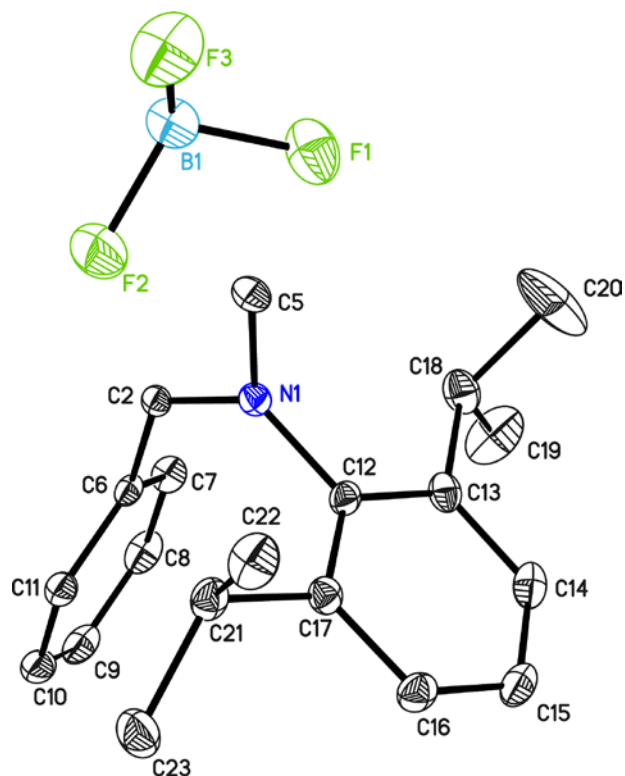


Figure 5.8: Asymmetric unit of compound **8**. The anisotropic displacement parameters are shown at the 50% probability level. Hydrogen atoms are omitted for clarity.

Structure code	SR_NG_6	Z	2
Empirical formula	C ₃₃ H ₄₁ BF ₄ N ₂	Crystal dimensions [mm]	0.305 × 0.201 × 0.172
Formula weight [g/mol]	552.49	$\rho_{\text{calcd.}}$ [g/cm ³]	1.242
Sample temperature [K]	100(2)	μ [mm ⁻¹]	0.089
Wavelength [Å]	0.71073	<i>F</i> (000)	588
Crystal system	Monoclinic	Θ range [°]	2.217 to 27.482
Space group	<i>P</i> 2 ₁ / <i>m</i>	Reflections collected	15691
Unit cell dimensions [Å]		Unique reflections	3474
a =	9.313(2)	<i>R</i> _{int}	0.0278
b =	17.270(3)	Completeness to $\theta_{\text{full}} = 25.242^\circ$	99.6%
c =	9.822(2)	restraints/parameters	0 / 200
$\alpha =$	90°	GooF	1.041
$\beta =$	110.70(2)°	<i>R</i> 1(<i>I</i> > 2 σ (<i>I</i>))	0.0407
$\gamma =$	90°	<i>wR</i> 2 (all data)	0.1027
Volume [Å ³]	1477.7(5)	max. diff. peak/hole [e ⁻ ·Å ⁻³]	0.270 and -0.388

5.5.9. 1,3-bis(2,6-diisopropylphenyl)-2-phenyl-imidazolium hexafluorophosphate (IPrPh)PF₆ (9)

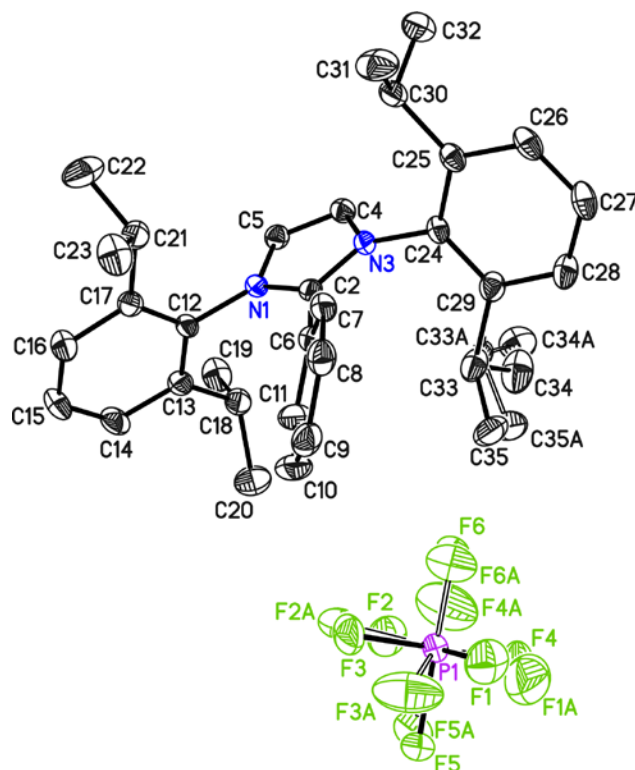


Figure 5.9: Asymmetric unit of compound **9**. The anisotropic displacement parameters are shown at the 50% probability level. Hydrogen atoms are omitted for clarity. The isopropyl-moiety is disordered on two positions (*sof*: 0.440(17)). The hexafluoro phosphate anion is disordered on two positions (*sof*: 0.925(2))

Structure code	SR_NG_X	Z	4
Empirical formula	C ₃₃ H ₄₁ F ₆ N ₂ P	Crystal dimensions [mm]	0.246 × 0.228 × 0.176
Formula weight [g/mol]	610.65	$\rho_{\text{calcd.}}$ [g/cm ³]	1.267
Sample temperature [K]	100(2)	μ [mm ⁻¹]	0.145
Wavelength [Å]	0.71073	<i>F</i> (000)	1288
Crystal system	Monoclinic	Θ range [°]	1.763 to 26.386
Space group	<i>P</i> 2 ₁ / <i>n</i>	Reflections collected	65146
Unit cell dimensions [Å]		Unique reflections	6539
	<i>a</i> = 13.508(2)	<i>R</i> _{int}	0.0324
	<i>b</i> = 13.745(2)	Completeness to $\theta_{\text{full}} = 25.242^\circ$	99.9%
	<i>c</i> = 17.630(3)	restraints/parameters	473 / 469
	α = 90°	Goof	0.894
	β = 101.97(2)°	<i>R</i> 1(<i>I</i> > 2 σ (<i>I</i>))	0.0351
	γ = 90°	<i>wR</i> 2 (all data)	0.0902
Volume [Å ³]	3202.1(9)	max. diff. peak/hole [e ⁻ ·Å ⁻³]	0.372 and -0.280

5.5.10.1,3-bis(2,6-diisopropylphenyl)-2-phenyl-imidazolium triflate (IPrPh)CF₃SO₃ (10)

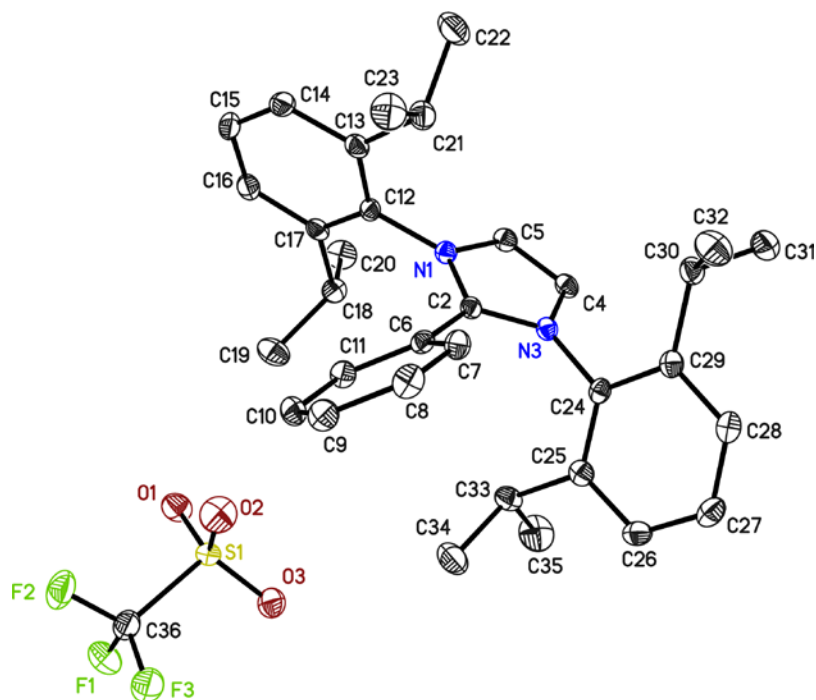


Figure 5.10: Asymmetric unit of compound **10**. The anisotropic displacement parameters are shown at the 50% probability level. Hydrogen atoms are omitted for clarity.

Structure code	SR_303	Z	4
Empirical formula	C ₃₄ H ₄₁ F ₃ N ₂ O ₃ S	Crystal dimensions [mm]	0.232 × 0.182 × 0.143
Formula weight [g/mol]	614.75	$\rho_{\text{calcd.}}$ [g/cm ³]	1.285
Sample temperature [K]	100(2)	μ [mm ⁻¹]	0.156
Wavelength [Å]	0.71073	<i>F</i> (000)	1304
Crystal system	Monoclinic	Θ range [°]	1.738 to 26.466
Space group	<i>P</i> 2 ₁ / <i>c</i>	Reflections collected	78299
Unit cell dimensions [Å]		Unique reflections	6538
	<i>a</i> = 11.742(2)	<i>R</i> _{int}	0.0377
	<i>b</i> = 13.656(2)	Completeness to $\theta_{\text{full}} = 25.242$	100%
	<i>c</i> = 19.859(3)	restraints/parameters	0 / 396
	α = 90°	GooF	1.066
	β = 93.90(2)°	<i>R</i> 1(<i>I</i> > 2 σ (<i>I</i>))	0.0356
	γ = 90°	<i>wR</i> 2 (all data)	0.0885
Volume [Å ³]	3177.0(9)	max. diff. peak/hole [e ⁻ ·Å ⁻³]	0.414 and -0.280

5.5.11.1,3-bis(2,6-diisopropylphenyl)-2-(*p*-tolyl)-imidazolium iodide (IPrPh-4-Me)I (12)

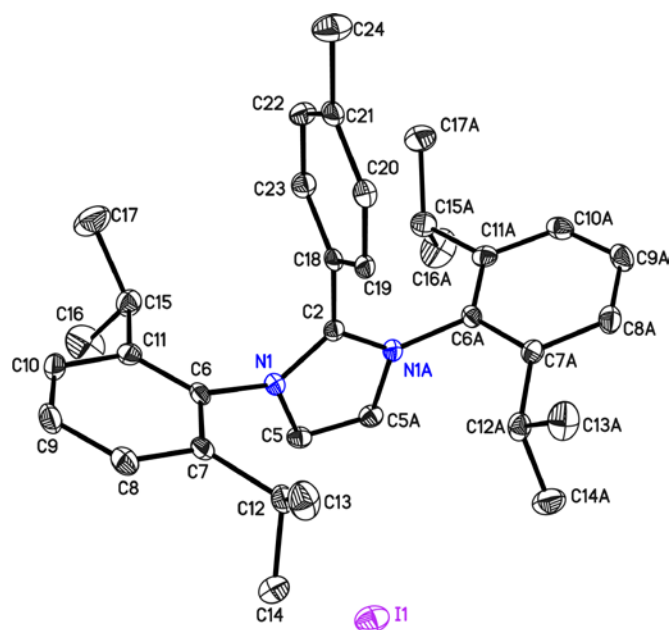


Figure 5.11: Asymmetric unit of compound **12**. The anisotropic displacement parameters are shown at the 50% probability level. Hydrogen atoms are omitted for clarity.

Published in: "Palladium-Catalyzed Direct C2-Arylation of an N-Heterocyclic Carbene: An Atom-Economic Route to Mesoionic Carbene Ligands." R. S. Ghadwal, S. O. Reichmann, R. Herbst-Irmer, *Chem. Eur. J.* **2015**, *21*, 4247-4251.

CCDC number	1017467	Z	2
Structure code	SR_Raj_Pd	Crystal dimensions [mm]	0.2 × 0.19 × 0.09
Empirical formula	C ₃₄ H ₄₃ N ₂ I	$\rho_{\text{calcd.}}$ [g/cm ³]	1.331
Formula weight [g/mol]	606.60	μ [mm ⁻¹]	1.082
Sample temperature [K]	100(2)	<i>F</i> (000)	628
Wavelength [Å]	0.71073	Θ range [°]	2.202 to 26.338
Crystal system	Monoclinic	Reflections collected	26916
Space group	<i>P</i> 2 ₁ / <i>m</i>	Unique reflections	3187
Unit cell dimensions [Å]		<i>R</i> _{int}	0.0318
a =	9.569(2)	Completeness to $\theta_{\text{full}} = 25.242$	99.9%
b =	17.103(3)	restraints/parameters	0 / 186
c =	9.832(2)	Goof	1.050
$\alpha =$	90°	<i>R</i> 1(<i>I</i> > 2 σ (<i>I</i>))	0.0215
$\beta =$	109.80(2)°	<i>wR</i> 2 (all data)	0.0491
$\gamma =$	90°	max. diff. peak/hole [e ⁻ ·Å ⁻³]	0.495 and -0.540
Volume [Å ³]	1514.0(5)		

5.5.12.1,3-bis(2,6-diisopropylphenyl)-2-(*p*-tolyl)-imidazolium iodide (IPrPh-2-Me)I (13)

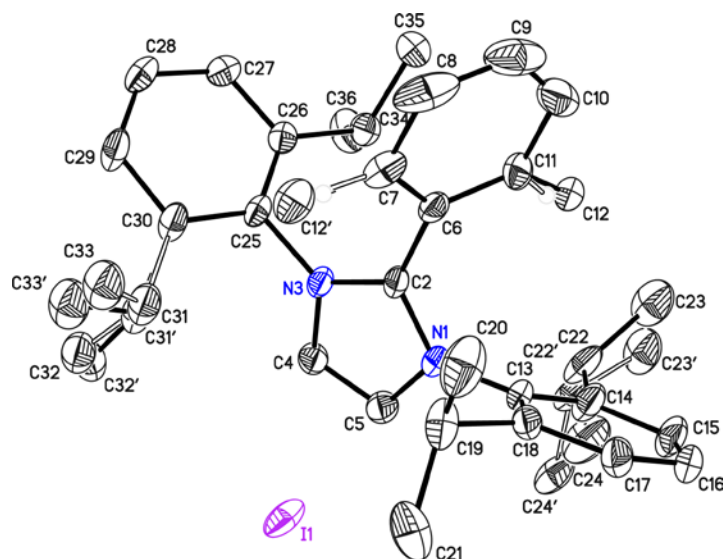


Figure 5.12: Asymmetric unit of compound **13**. The anisotropic displacement parameters are shown at the 50% probability level. Hydrogen atoms are omitted for clarity.

Published in: "Palladium-Catalyzed Direct C2-Arylation of an *N*-Heterocyclic Carbene: An Atom-Economic Route to Mesoionic Carbene Ligands." R. S. Ghadwal, S. O. Reichmann, R. Herbst-Irmer, *Chem. Eur. J.* **2015**, *21*, 4247-4251.

CCDC number	1017468		
Structure code	SOR-A-128	Z	4
Empirical formula	C ₃₄ H ₄₃ N ₂ I	Crystal dimensions [mm]	0.09 × 0.19 × 0.20
Formula weight [g/mol]	606.60	$\rho_{\text{calcd.}}$ [g/cm ³]	1.294
Sample temperature [K]	100(2)	μ [mm ⁻¹]	1.051
Wavelength [Å]	0.71073	<i>F</i> (000)	1256
Crystal system	Triclinic	Θ range [°]	1.833 to 26.397
Space group	<i>P</i> 2 ₁ / <i>n</i>	Reflections collected	82325
Unit cell dimensions [Å]		Unique reflections	6375
	<i>a</i> = 12.469(2)	<i>R</i> _{int}	0.0476
	<i>b</i> = 14.628(2)	Completeness to $\theta_{\text{full}} = 25.242^\circ$	100%
	<i>c</i> = 17.254(3)	restraints/parameters	382/406
	α = 90°	GooF	1.057
	β = 98.23(2)°	<i>R</i> 1(<i>I</i> > 2 σ (<i>I</i>))	0.0370
	γ = 90°	<i>wR</i> 2 (all data)	0.0763
Volume [Å ³]	3114.7(9)	max. diff. peak/hole [e ⁻ Å ⁻³]	1.697 and -1.782

5.5.13.1,3-bis(2,6-diisopropylphenyl)-2-(4-methoxyphenyl)-imidazolium iodide (IPrPh-4-OMe)I (14)

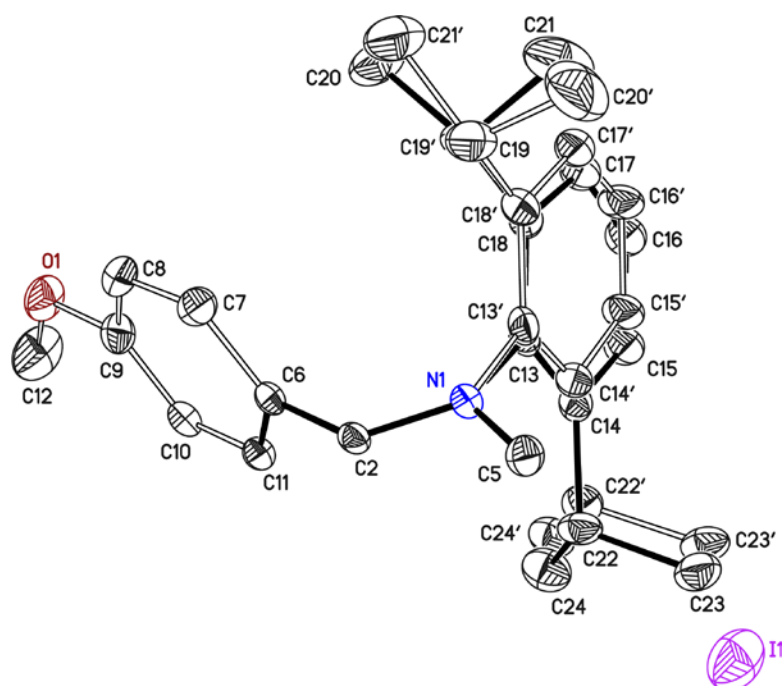


Figure 5.13: Asymmetric unit of compound **14**. The anisotropic displacement parameters are shown at the 50% probability level. Hydrogen atoms are omitted for clarity.

Published in: "Palladium-Catalyzed Direct C2-Arylation of an N-Heterocyclic Carbene: An Atom-Economic Route to Mesoionic Carbene Ligands." R. S. Ghadwal, S. O. Reichmann, R. Herbst-Irmer, *Chem. Eur. J.* **2015**, *21*, 4247-4251.

CCDC number	1024657	Z	2
Structure code	SR_134	Crystal dimensions [mm]	0.12 × 0.11 × 0.09
Empirical formula	C ₃₄ H ₄₃ IN ₂ O	$\rho_{\text{calcd.}}$ [g/cm ³]	1.325
Formula weight [g/mol]	622.60	μ [mm ⁻¹]	1.054
Sample temperature [K]	100(2)	<i>F</i> (000)	644
Wavelength [Å]	0.71073	Θ range [°]	2.180 to 26.367
Crystal system	Monoclinic	Reflections collected	45199
Space group	<i>P2₁/m</i>	Unique reflections	3313
Unit cell dimensions [Å]		<i>R</i> _{int}	0.0327
a =	9.760(2)	Completeness to $\theta_{\text{full}} = 25.242^\circ$	99.8%
b =	17.115(3)	restraints/parameters	805 / 315
c =	10.091(2)	Goof	1.079
$\alpha =$	90°	<i>R</i> 1 (<i>I</i> > 2 σ (<i>I</i>))	0.0280
$\beta =$	112.24(2)°	<i>wR</i> 2 (all data)	0.0656
$\gamma =$	90°	max. diff. peak/hole [e ⁻ ·Å ⁻³]	0.683 and -0.726
Volume [Å ³]	1560.2(6)		

5.5.14.1,3-bis(2,6-diisopropylphenyl)-2-(4-(methoxycarbonyl)phenyl)-imidazolium iodide (IPrPh-4-CO₂Me)I (15)

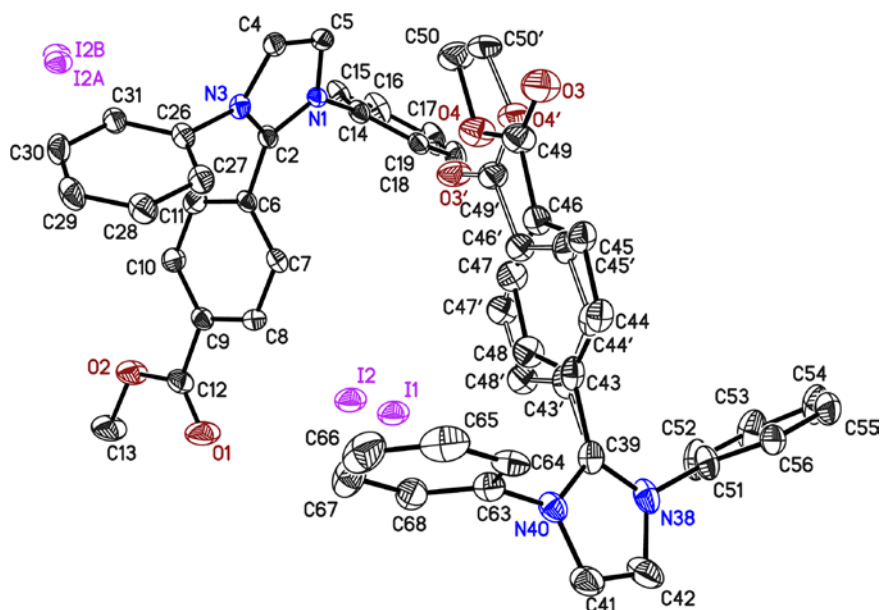


Figure 5.14: Asymmetric unit of compound **15**. The anisotropic displacement parameters are shown at the 50% probability level. Hydrogen atoms are omitted for clarity.

Published in: "Palladium-Catalyzed Direct C2-Arylation of an N-Heterocyclic Carbene: An Atom-Economic Route to Mesoionic Carbene Ligands." R. S. Ghadwal, S. O. Reichmann, R. Herbst-Irmer, *Chem. Eur. J.* **2015**, *21*, 4247-4251.

CCDC number	1019232	Z	4
Structure code	SR_138	Crystal dimensions [mm]	0.189 × 0.138 × 0.098
Empirical formula	C ₃₅ H ₄₃ N ₂ O ₂	$\rho_{\text{calcd.}}$ [g/cm ³]	1.335
Formula weight [g/mol]	650.61	μ [mm ⁻¹]	1.021
Sample temperature [K]	100(2)	<i>F</i> (000)	1344
Wavelength [Å]	0.71073	Θ range [°]	1.073 to 26.515
Crystal system	Monoclinic	Reflections collected	56139
Space group	<i>P</i> 2 ₁	Unique reflections	13331
Unit cell dimensions [Å]		<i>R</i> _{int}	0.0657
a =	10.071(2)	Completeness to $\theta_{\text{full}} = 25.242^\circ$	100%
b =	16.944(2)	restraints/parameters	512 / 838
c =	18.991(3)	GooF	1.041
$\alpha =$	90°	<i>R</i> 1 (<i>I</i> > 2 σ (<i>I</i>))	0.0418
$\beta =$	92.63(2)°	<i>wR</i> 2 (all data)	0.0943
$\gamma =$	90°	max. diff. peak/hole [e ⁻ Å ⁻³]	0.825 and -0.797
Volume [Å ³]	3237.3(9)	Absolute structure parameter ^[189]	0.125(10)
Extinction coefficient	–		

5.5.15.1,3-bis(2,6-diisopropylphenyl)-2-(*p*-tolyl)-imidazolium bromide (IPrPh-4-Me)Br (**21**)

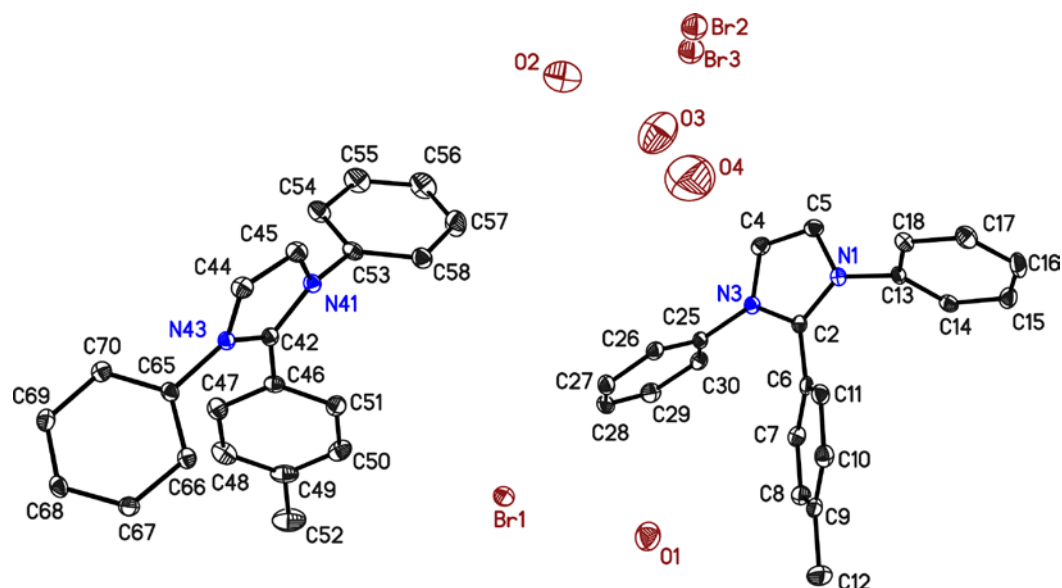


Figure 5.15: Asymmetric unit of compound **21**. The anisotropic displacement parameters are shown at the 50% probability level. Hydrogen atoms and isopropyl groups are omitted for clarity.

Structure code	SR_170a	Z	2
Empirical formula	C ₆₈ H ₉₁ Br ₂ N ₄ O ₄	Crystal dimensions [mm]	0.354 × 0.203 × 0.116
Formula weight [g/mol]	1187.25	$\rho_{\text{calcd.}}$ [g/cm ³]	1.243
Sample temperature [K]	100(2)	μ [mm ⁻¹]	1.327
Wavelength [Å]	0.71073	<i>F</i> (000)	1256
Crystal system	Triclinic	Θ range [°]	1.233 to 26.338
Space group	<i>P</i> -1	Reflections collected	74925
Unit cell dimensions [Å]		Unique reflections	12887
a =	12.723(2)	<i>R</i> _{int}	0.0282
b =	15.216(2)	Completeness to $\theta_{\text{full}} = 25.242^\circ$	99.9%
c =	18.315(3)	restraints/parameters	0 / 743
$\alpha =$	110.39(3)°	Goof	1.054
$\beta =$	102.30(2)°	<i>R</i> 1(<i>I</i> > 2 σ (<i>I</i>))	0.0384
$\gamma =$	96.93(2)°	<i>wR</i> 2 (all data)	0.1044
Volume [Å ³]	3172.8(10)	max. diff. peak/hole [e ⁻ Å ⁻³]	1.0002 and -0.871

In the present sample water molecules are incorporated in the crystal. Three water molecules could be refined. Nonetheless residual electron density represents more water molecules with occupation factors lower than one. A further refinement does not lead to a satisfying result. It has to be mentioned that the adequate description of the solvent molecules in the crystal structure could not be reached, however the refinement of the desired compound **21** seems utterly acceptable.

5.5.16.1,3-bis(2,6-diisopropylphenyl)-2-(4-methoxyphenyl)- imidazolium bromide (IPrPh-4-OMe)Br (22)

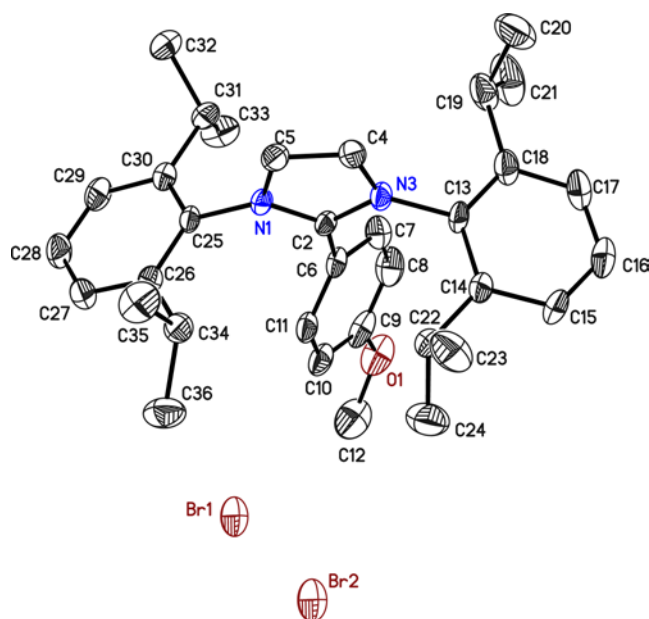


Figure 5.16: Asymmetric unit of compound **22**. The anisotropic displacement parameters are shown at the 50% probability level. Hydrogen atoms are omitted for clarity.

Structure code	SR_191	Z	4
Empirical formula	C ₃₄ H ₄₃ BrN ₂ O	Crystal dimensions [mm]	0.16 × 0.15 × 0.11
Formula weight [g/mol]	575.61	$\rho_{\text{calcd.}}$ [g/cm ³]	1.175
Sample temperature [K]	100(2)	μ [mm ⁻¹]	1.290
Wavelength [Å]	0.71073	<i>F</i> (000)	1216
Crystal system	Monoclinic	Θ range [°]	1.599 to 26.028
Space group	<i>P</i> 2 ₁ / <i>n</i>	Reflections collected	61312
Unit cell dimensions [Å]		Unique reflections	6411
	<i>a</i> = 9.813(2)	<i>R</i> _{int}	0.0340
	<i>b</i> = 16.405(2)	Completeness to $\theta_{\text{full}} = 26.028^\circ$	99.9%
	<i>c</i> = 20.399(3)	restraints/parameters	0 / 356
	α = 90°	GooF	1.226
	β = 97.91(2)°	<i>R</i> 1(<i>I</i> > 2 σ (<i>I</i>))	0.0738
	γ = 90°	<i>wR</i> 2 (all data)	0.2071
Volume [Å ³]	3252.6(9)	max. diff. peak/hole [e ⁻ ·Å ⁻³]	2.509 and -0.765

In the present sample water molecules are incorporated in the crystal. Residual electron density represents disordered water molecules. A further refinement of the water molecules does not lead to a satisfying results. It has to be mentioned that the adequate description of the solvent molecules in the crystal structure is not meaningful, however the refinement of the desired compound **22** seems utterly acceptable.

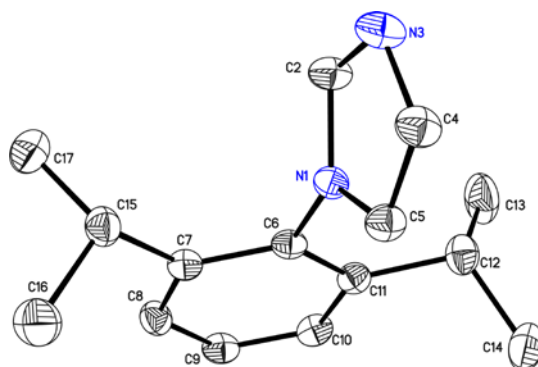
5.5.17.1-(2,6-diisopropylphenyl)-1*H*-imidazole

Figure 5.17: Asymmetric unit of 1-(2,6-diisopropylphenyl)-1*H*-imidazole. The anisotropic displacement parameters are shown at the 50% probability level. Hydrogen atoms are omitted for clarity.

Structure code	SR_SM	Z	4
Empirical formula	C ₁₅ H ₂₀ N ₂	Crystal dimensions [mm]	0.16 × 0.15 × 0.11
Formula weight [g/mol]	228.33	$\rho_{\text{calcd.}}$ [g/cm ³]	1.120
Sample temperature [K]	100(2)	μ [mm ⁻¹]	0.066
Wavelength [Å]	0.71073	<i>F</i> (000)	496
Crystal system	Monoclinic	Θ range [°]	1.871 to 25.350
Space group	<i>P</i> 2 ₁ / <i>c</i>	Reflections collected	22867
Unit cell dimensions [Å]		Unique reflections	2480
	<i>a</i> = 5.662(2)	<i>R</i> _{int}	0.0388
	<i>b</i> = 16.551(3)	Completeness to θ_{full} =	100%
	<i>c</i> = 14.447(2)	restraints/parameters	0 / 185
	α = 90°	Goof	1.043
	β = 99.79(2)°	<i>R</i> 1(<i>I</i> > 2 σ (<i>I</i>))	0.0397
	γ = 90°	<i>wR</i> 2 (all data)	0.0942
Volume [Å ³]	1353.7(6)	max. diff. peak/hole [e ⁻ ·Å ⁻³]	0.180 and -0.207

5.5.18.[1,3-bis(2,6-diisopropylphenyl)-2-phenyl-imidazol-4-ylidene] copper(I) iodide (IPrPh)CuI (26)

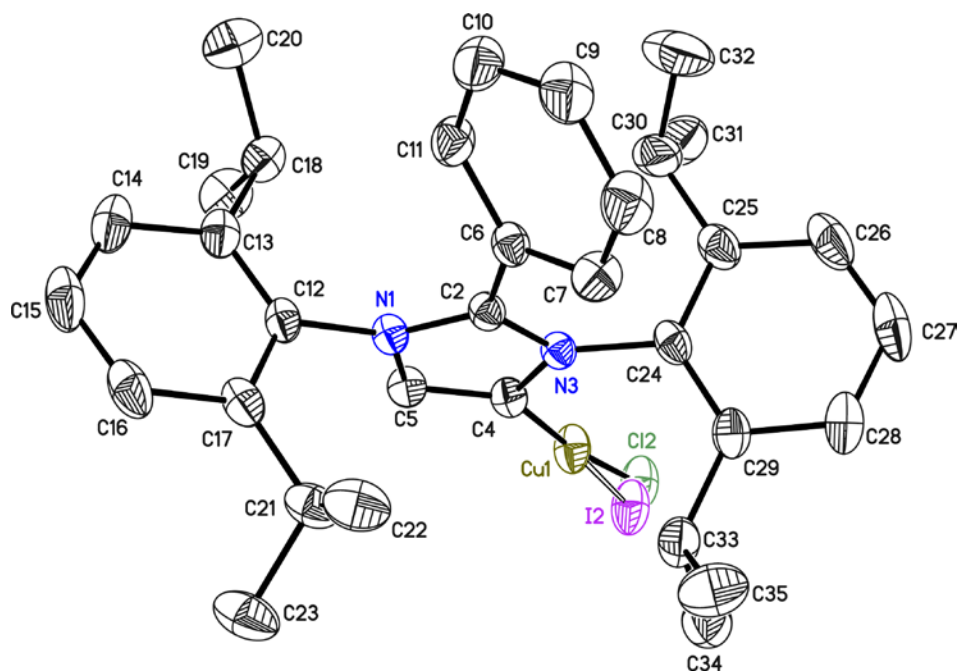
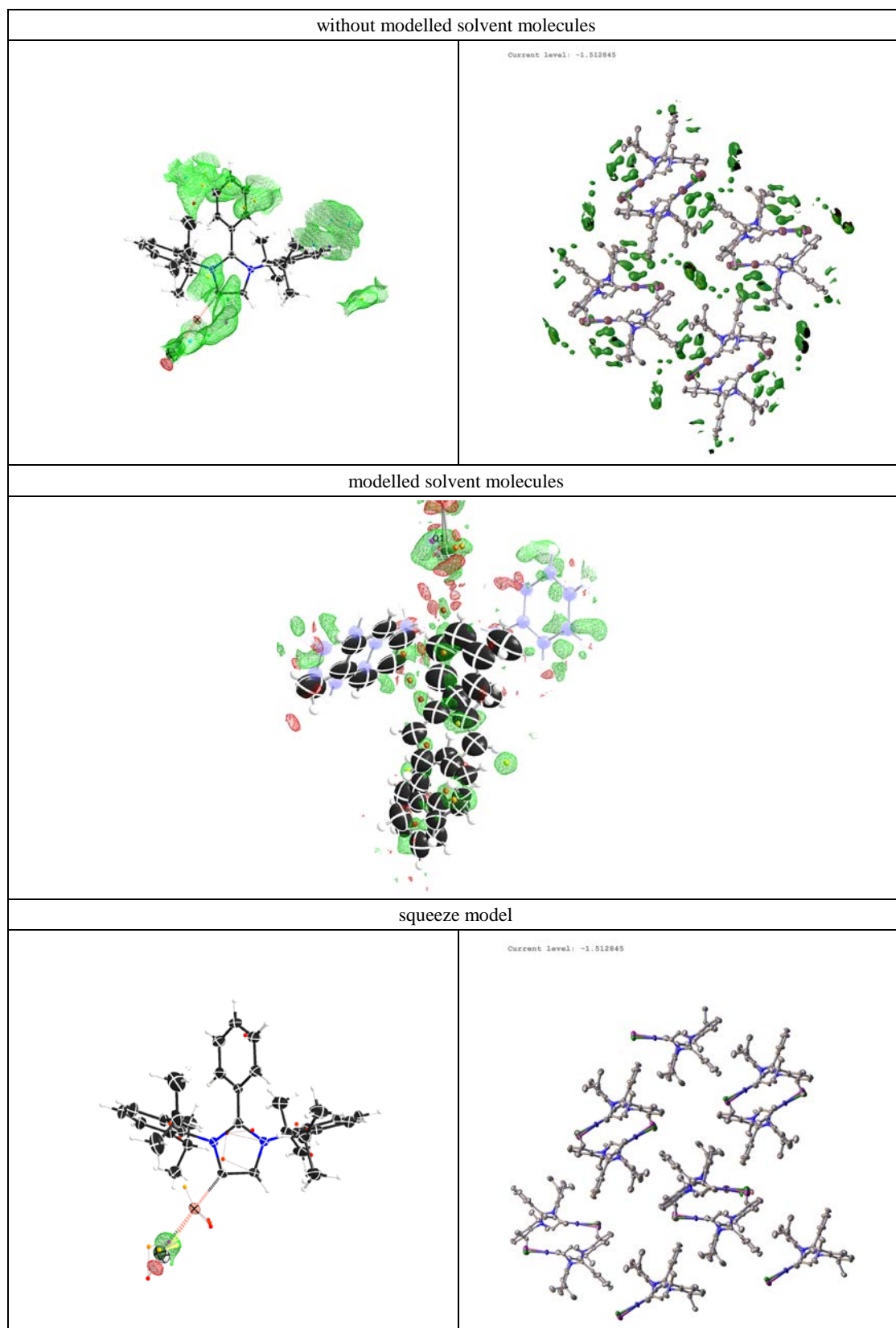


Figure 5.18: Asymmetric unit of compound **26**. The anisotropic displacement parameters are shown at the 50% probability level. Hydrogen atoms are omitted for clarity.

Published in: "Palladium-Catalyzed Direct C2-Arylation of an N-Heterocyclic Carbene: An Atom-Economic Route to Mesoionic Carbene Ligands." R. S. Ghadwal, S. O. Reichmann, R. Herbst-Irmer, *Chem. Eur. J.* **2015**, *21*, 4247-4251.

CCDC number	1019233	Z	4
Structure code	SR_098	Crystal dimensions [mm]	0.239 × 0.173 × 0.146
Empirical formula	C ₃₃ H ₄₀ Cl _{0.39} Cu I _{0.61} N ₂	$\rho_{\text{calcd.}}$ [g/cm ³]	0.959
Formula weight [g/mol]	619.14	μ [mm ⁻¹]	0.987
Sample temperature [K]	100(2)	<i>F</i> (000)	1279
Wavelength [Å]	0.71073	Θ range [°]	1.564 to 28.298
Crystal system	Monoclinic	Reflections collected	134343
Space group	<i>P2₁/c</i>	Unique reflections	10640
Unit cell dimensions [Å]		<i>R</i> _{int}	0.0479
a =	12.423(2)	Completeness to $\theta_{\text{full}} = 25.242$	100%
b =	20.420(3)	restraints/parameters	0 / 346
c =	17.498(2)	GooF	1.086
$\alpha =$	90°	<i>R</i> 1(<i>I</i> > 2 σ (<i>I</i>))	0.0526
$\beta =$	105.05(2)°	<i>wR</i> 2 (all data)	0.1421
$\gamma =$	90°	max. diff. peak/hole [e ⁻ ·Å ⁻³]	2.543 and -1.385
Volume [Å ³]	4286.6(11)		

Diffuse residual electron density was observed in the crystal voids. The pictures show the residual electron density in the solvent channels. Heavily disordered lattice solvent (toluene) could be modelled in the voids (see figure below). However, the refined model with solvent molecules was not satisfying. Therefore the SQUEEZE routine of PLATON program package was used, which allows for the mathematical compensation of the electron distribution of disordered solvent contained in the voids to the calculated diffraction intensities.^[188]



	without solvent	with solvent	squeeze
R1*	0.1274	0.0771	0.0631
wR2*	0.3395	0.1774	0.1421

*indices for all data

**5.5.19. [(1,3-bis(2,6-diisopropylphenyl)-2-phenyl-imidazol-4-ylidene)-
(1,3-bis(2,6-diisopropylphenyl)-imidazol-2-ylidene)] copper(I)
iodide [(IPrPh)CuIPr]I (27)**

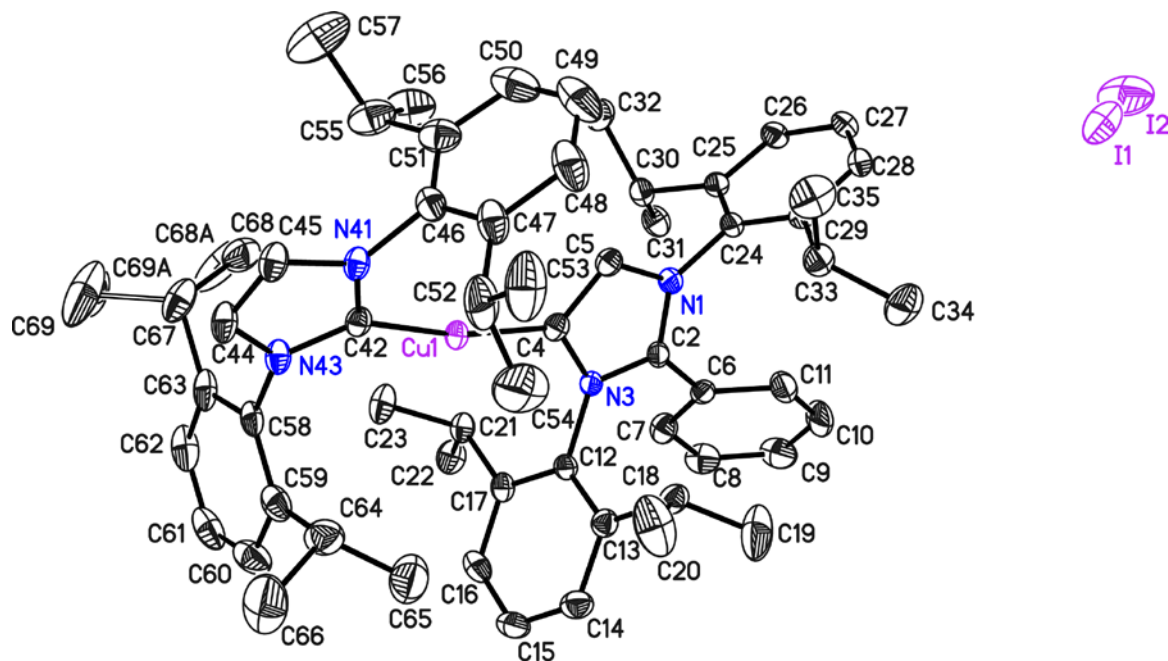


Figure 5.19: Asymmetric unit of compound 27. The anisotropic displacement parameters are shown at the 50% probability level. Hydrogen atoms are omitted for clarity.

Structure code	SR_211	Z	4
Empirical formula	C ₆₀ H ₇₆ CuIN ₄	Crystal dimensions [mm]	0.14 × 0.11 × 0.08
Formula weight [g/mol]	1043.68	$\rho_{\text{calcd.}}$ [g/cm ³]	1.225
Sample temperature [K]	100(2)	μ [mm ⁻¹]	0.970
Wavelength [Å]	0.71073	<i>F</i> (000)	2184
Crystal system	Monoclinic	Θ range [°]	1.444 to 25.681
Space group	<i>P</i> 2 ₁ / <i>c</i>	Reflections collected	72914
Unit cell dimensions [Å]		Unique reflections	10760
a =	14.199(2)	<i>R</i> _{int}	0.0564
b =	20.651(3)	Completeness to $\theta_{\text{full}} = 25.242$	100%
c =	19.460(2)	restraints/parameters	56 / 642
$\alpha =$	90°	GooF	1.020
$\beta =$	97.46(2)°	<i>R</i> 1 (<i>I</i> > 2 σ (<i>I</i>))	0.0296
$\gamma =$	90°	<i>wR</i> 2 (all data)	0.0680
Volume [Å ³]	5657.8(13)	max. diff. peak/hole [e ⁻ Å ⁻³]	0.467 and -0.305

**5.5.20.[(1,3-bis(2,6-diisopropylphenyl)-2-phenyl-imidazol-4-ylidene)-
(1,3-bis(2,6-diisopropylphenyl)-imidazol-2-ylidene)] copper(I)
tetrafluoroborate [(IPrPh)Cu(IPr)]BF₄ (27a)**

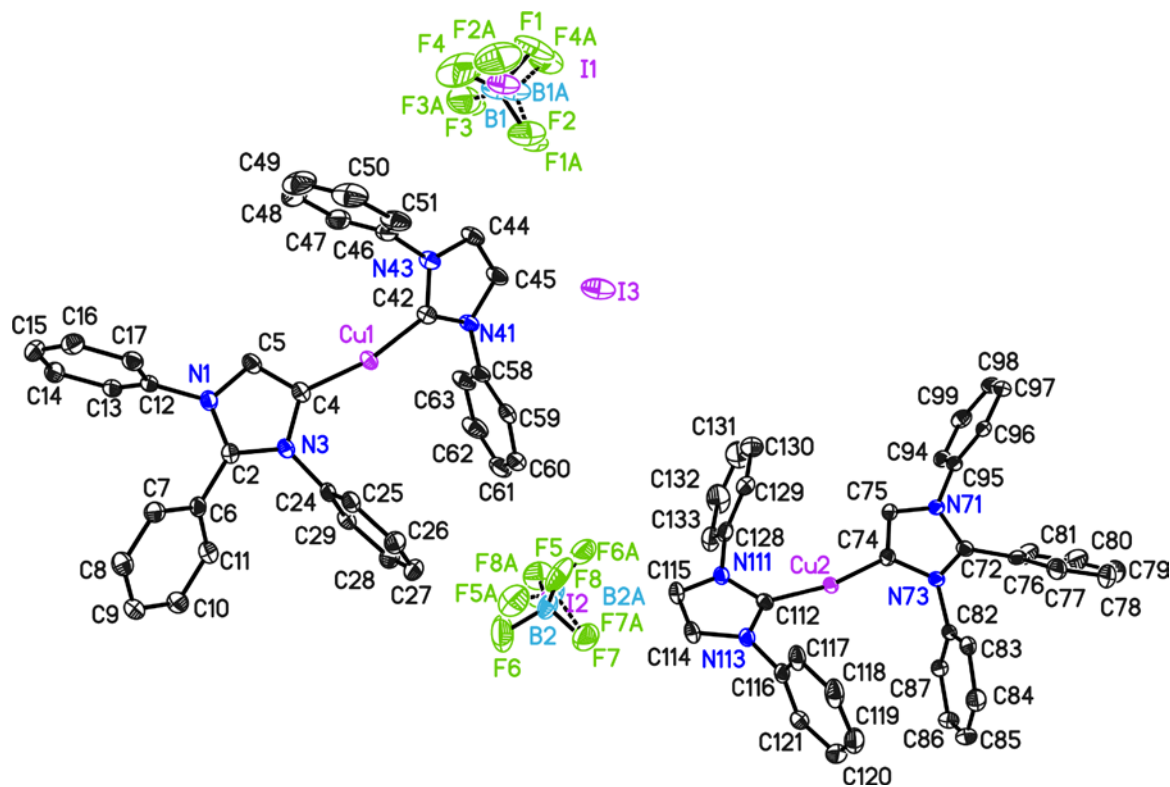


Figure 5.20: Asymmetric unit of compound **27a**. The anisotropic displacement parameters are shown at the 50% probability level. Hydrogen atoms are omitted for clarity.

Structure code	SR_250	Z	4
Empirical formula	C ₁₂₀ H ₁₅₂ B _{1.70} Cu ₂ F _{6.80} I _{0.30} N ₈	Crystal dimensions [mm]	0.289 × 0.205 × 0.138
Formula weight [g/mol]	2019.22	ρ_{calc} [g/cm ³]	1.182
Sample temperature [K]	100(2)	μ [mm ⁻¹]	0.517
Wavelength [Å]	0.71073	<i>F</i> (000)	4286
Crystal system	Monoclinic	Θ range [°]	1.207 to 25.366
Space group	<i>P</i> 2 ₁ / <i>n</i>	Reflections collected	253770
Unit cell dimensions [Å]		Unique reflections	20798
	<i>a</i> = 19.402(2)	<i>R</i> _{int}	0.0602
	<i>b</i> = 20.807(2)	Completeness to $\theta_{\text{full}} = 25.242^\circ$	100%
	<i>c</i> = 28.343(3)	restraints/parameters	833 / 1430
	α = 90°	GooF	1.062
	β = 97.25(2)°	<i>R</i> 1(<i>I</i> > 2 σ (<i>I</i>))	0.0444
	γ = 90°	<i>wR</i> 2 (all data)	0.1110
Volume [Å ³]	11351(2)	max. diff. peak/hole [e ⁻ Å ⁻³]	0.887 and -0.674

5.5.21. Bis[1,3-bis(2,6-diisopropylphenyl)-2-phenyl-imidazol-4-ylidene] copper(I) iodide [(IPrPh)₂Cu]I (28)

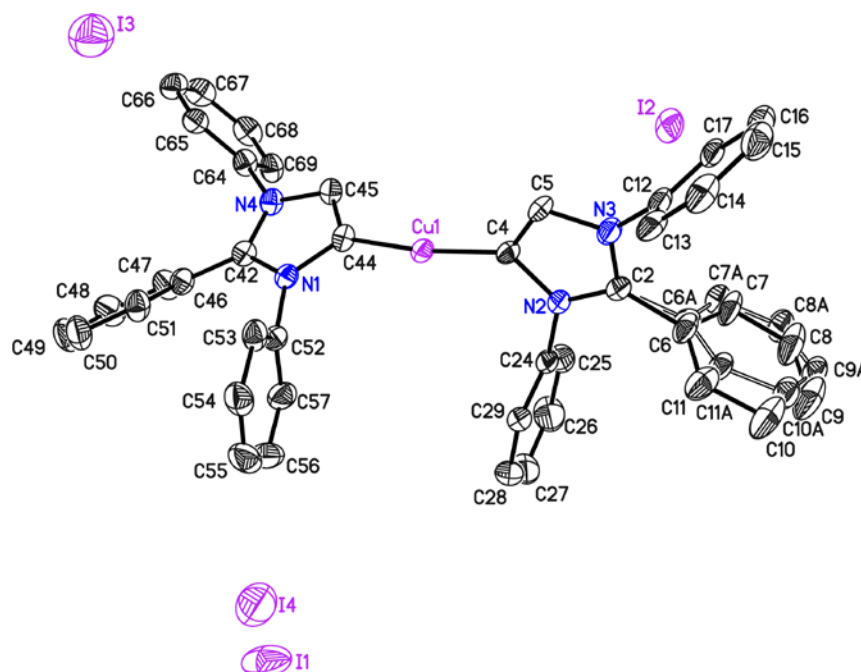


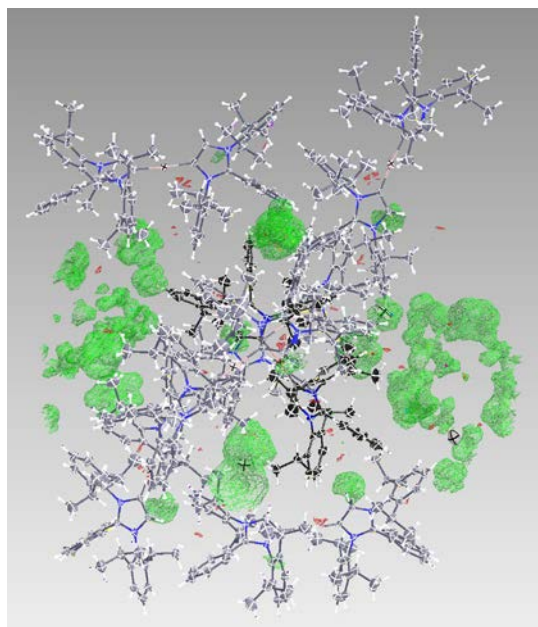
Figure 5.21: Asymmetric unit of compound **28**. The anisotropic displacement parameters are shown at the 50% probability level. Hydrogen atoms and isopropyl groups are omitted for clarity.

Structure code	SR_241	Z	12
Empirical formula	C ₆₆ H ₈₀ CuIN ₄	Crystal dimensions [mm]	0.18 × 0.19 × 0.090
Formula weight [g/mol]	1119.78	$\rho_{\text{calcd.}}$ [g/cm ³]	1.005
Sample temperature [K]	100(2)	μ [mm ⁻¹]	0.746
Wavelength [Å]	0.71073	<i>F</i> (000)	7032
Crystal system	Hexagonal	Θ range [°]	0.953 to 25.349
Space group	<i>P</i> 6 ₃ 22	Reflections collected	338168
Unit cell dimensions [Å]		Unique reflections	15214
	<i>a</i> = 24.661(2)	<i>R</i> _{int}	0.0509
	<i>b</i> = 24.661(2)	Completeness to $\theta_{\text{full}} = 25.242^\circ$	100%
	<i>c</i> = 42.161(3)	restraints/parameters	352 / 737
	$\alpha = 90^\circ$	GooF	1.126
	$\beta = 99^\circ$	<i>R</i> 1 (<i>I</i> > 2 σ (<i>I</i>))	0.0331
	$\gamma = 120^\circ$	<i>wR</i> 2 (all data)	0.0956
Volume [Å ³]	22206(4)	max. diff. peak/hole [e ⁻ ·Å ⁻³]	1.095 and -0.403

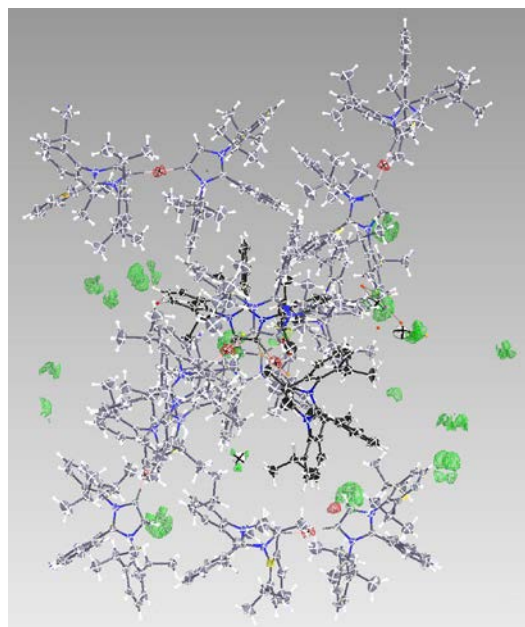
Diffuse concentrated residual electron density was observed in the crystal voids. The pictures show the residual electron density in the solvent channels. Heavily disorder lattice solvent (THF) could hardly be modelled into these voids. However, the refined model with solvent molecules was not satisfying. Therefore, the SQUEEZE routine of PLATON program package was used, which allows for the mathematical compensation of the electron distribution of disordered solvent contained in the voids to the calculated diffraction intensities.^[188a]

	without solvent	with solvent	squeeze
R1*	0.3399	0.0497	0.0378
wR2*	0.6779	0.1398	0.0956

*indices for all data



without modelled solvent molecules



Squeezed model

5.5.22. Bis[1,3-bis(2,6-diisopropylphenyl)-2-phenyl-imidazol-4-ylidene] silver (I) tetrafluoroborate [(IPrPh)₂Ag]BF₄ (29)

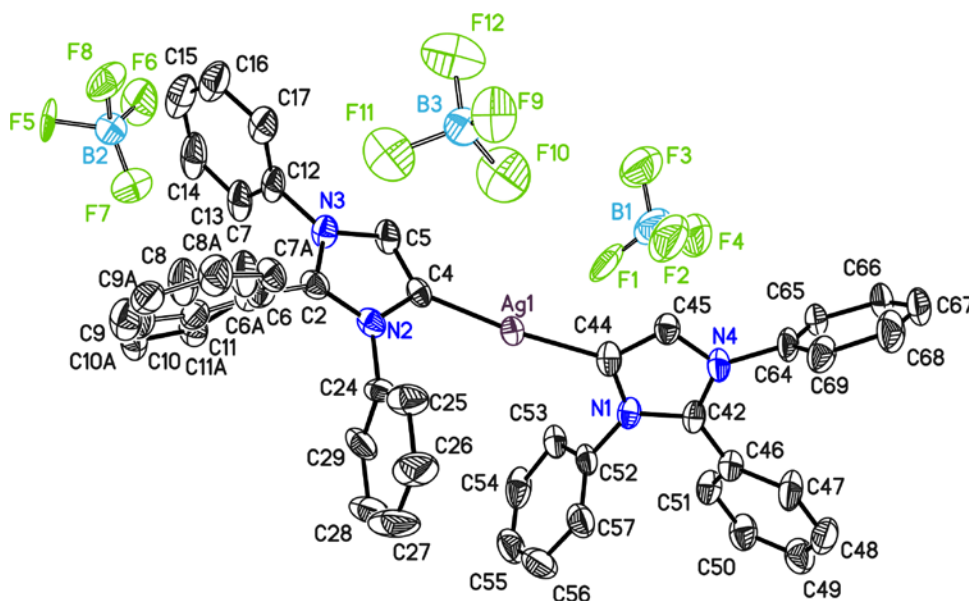


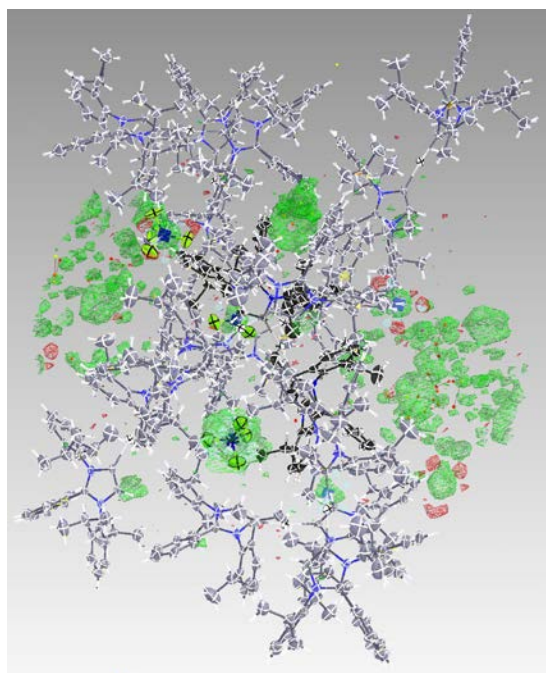
Figure 5.22: Asymmetric unit of compound **29**. The anisotropic displacement parameters are shown at the 50% probability level. Hydrogen atoms and isopropyl groups are omitted for clarity.

Structure code		Z	12
Empirical formula	C ₆₆ H ₈₀ AgB _{1.17} F ₄ N ₄	Crystal dimensions [mm]	0.243 × 0.229 × 0.098
Formula weight [g/mol]	1125.79	$\rho_{\text{calcd.}}$ [g/cm ³]	0.987
Sample temperature [K]	100(2)	μ [mm ⁻¹]	0.309
Wavelength [Å]	0.71073	<i>F</i> (000)	7114
Crystal system	Monoclinic	Θ range [°]	0.973 to 25.349
Space group	<i>P</i> 6 ₃ 22	Reflections collected	407983
Unit cell dimensions [Å]		Unique reflections	13908
a =	25.038(2)	<i>R</i> _{int}	0.0539
b =	25.038(2)	Completeness to $\theta_{\text{full}} = 25.242^\circ$	100%
c =	41.865(3)	restraints/parameters	649 / 834
$\alpha =$	90°	GooF	1.067
$\beta =$	90°	<i>R</i> 1 (<i>I</i> > 2 σ (<i>I</i>))	0.0515
$\gamma =$	120°	<i>wR</i> 2 (all data)	0.1630
Volume [Å ³]	22729(2)	max. diff. peak/hole [e ⁻ ·Å ⁻³]	2.463 and -0.395

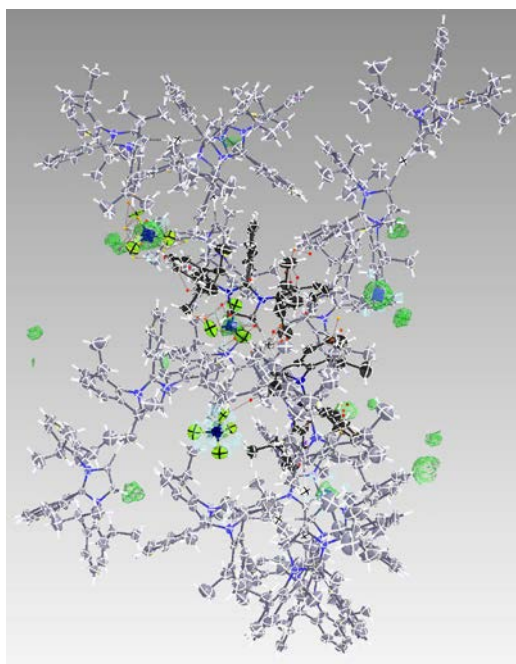
Diffuse concentrated residual electron density was observed in the crystal voids. The pictures show the residual electron density in the solvent channels. Heavily disorder tetrafluoroborate anions and lattice solvent (DCM) could hardly be modelled into these voids. Disordered tetrafluoroborate and lattice solvent (DCM) are placed on the same position. However, the refined model with solvent molecules was not satisfying. Therefore, the SQUEEZE routine of PLATON program package was used, which allows for the mathematical compensation of the electron distribution of disordered solvent contained in the voids to the calculated diffraction intensities.^[188a]

	modelled	squeeze
R1*	0.0905	0.0567
wR2*	0.2662	0.1622

*indices for all data



without modelled solvent molecules



Squeeze model

5.5.23. Bis(1,3-Bis(2,6-diisopropylphenyl)imidazole-2-ylidene) palladium iodide

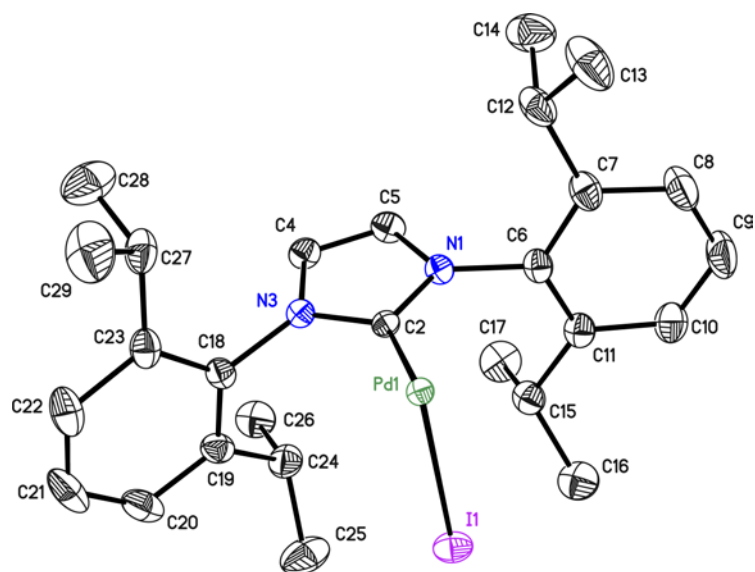


Figure 5.23: Asymmetric unit of $(\text{IPr}_2\text{Pd})\text{I}_2$. The anisotropic displacement parameters are shown at the 50% probability level. Hydrogen atoms are omitted for clarity.

Structure code	SR_160	Z	2
Empirical formula	$\text{C}_{54}\text{H}_{72}\text{I}_2\text{N}_4\text{Pd}$	Crystal dimensions [mm]	$0.12 \times 0.15 \times 0.19$
Formula weight [g/mol]	1137.35	$\rho_{\text{calcd.}}$ [g/cm^3]	1.459
Sample temperature [K]	100(2)	μ [mm^{-1}]	1.589
Wavelength [\AA]	0.71073	$F(000)$	1152
Crystal system	Monoclinic	Θ range [$^\circ$]	1.797 to 26.391
Space group	$P 2_1/n$	Reflections collected	41508
Unit cell dimensions [\AA]		Unique reflections	5301
	a = 13.195(2)	R_{int}	0.0363
	b = 14.072(2)	Completeness to $\theta_{\text{full}} = 25.242^\circ$	100%
	c = 14.768(3)	restraints/parameters	0 / 285
	$\alpha = 90^\circ$	Goof	1.053
	$\beta = 109.27(2)^\circ$	$R1(I > 2\sigma(I))$	0.0214
	$\gamma = 90^\circ$	$wR2$ (all data)	0.0552
Volume [\AA^3]	2588.5(8)	max. diff. peak/hole [$\text{e} \cdot \text{\AA}^{-3}$]	0.718 and -0.631

5.5.24.2-(1-benzyl-1-1,2,3-triazol-4-yl)propan-2-ol

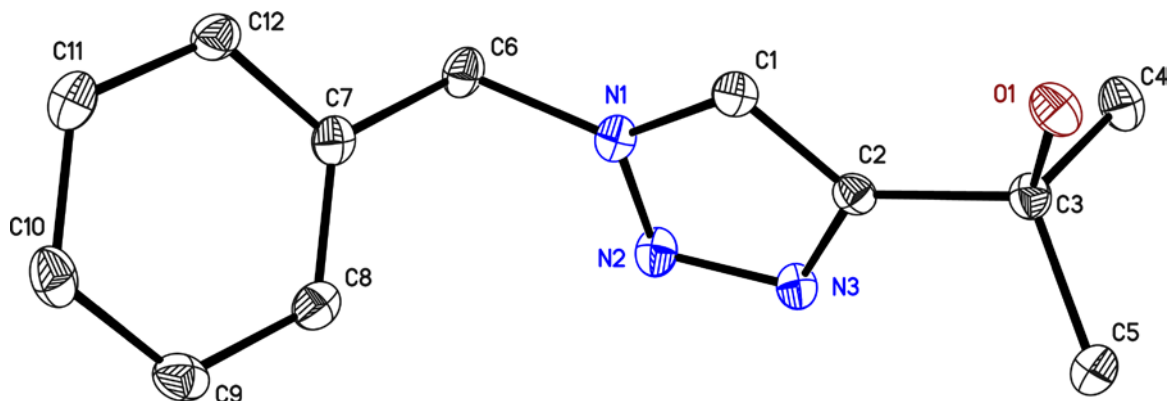


Figure 5.24: Asymmetric unit of 2-(1-benzyl-1-1,2,3-triazol-4-yl)propan-2-ol. The anisotropic displacement parameters are shown at the 50% probability level. Hydrogen atoms are omitted for clarity.

Structure code	SR_281	Z	4
Empirical formula	C ₁₂ H ₁₅ N ₃ O	Crystal dimensions [mm]	0.127 × 0.134 × 0.368
Formula weight [g/mol]	217.27	$\rho_{\text{calcd.}}$ [g/cm ³]	1.283
Sample temperature [K]	100(2)	μ [mm ⁻¹]	0.085
Wavelength [Å]	0.71073	<i>F</i> (000)	464
Crystal system	Monoclinic	Θ range [°]	1.774 to 26.353
Space group	<i>P</i> 2 ₁ / <i>c</i>	Reflections collected	33085
Unit cell dimensions [Å]		Unique reflections	2300
a =	11.515(3)	<i>R</i> _{int}	0.0241
b =	10.493(2)	Completeness to $\theta_{\text{full}} = 25.242^\circ$	100 %
c =	9.342(2)	restraints/parameters	0 /149
$\alpha =$	90°	GooF	1.089
$\beta =$	94.62(2)°	<i>R</i> 1(<i>I</i> > 2 σ (<i>I</i>))	0.0353
$\gamma =$	90°	<i>wR</i> 2 (all data)	0.0852
Volume [Å ³]	1125.1(5)	max. diff. peak/hole [e ⁻ Å ⁻³]	0.280 and -0.207b

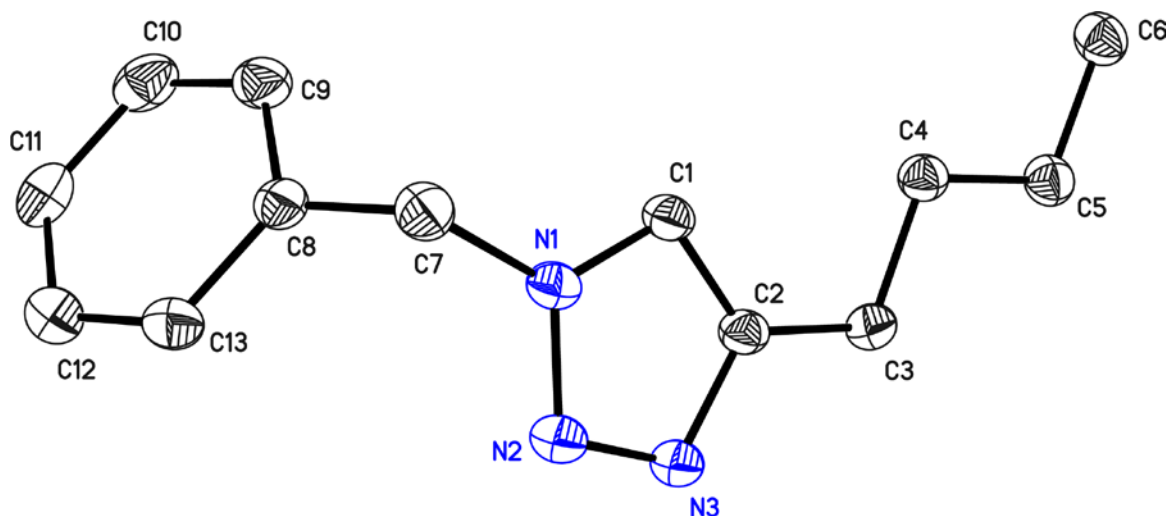
5.5.25.1-benzyl-4-butyl-1*H*-1,2,3-triazole

Figure 5.25: Asymmetric unit of compound 1-benzyl-4-butyl-1*H*-1,2,3-triazole. The anisotropic displacement parameters are shown at the 50% probability level. Hydrogen atoms are omitted for clarity.

Structure code	SR_279_Triazol	Z	4
Empirical formula	C ₁₃ H ₁₇ N ₃	Crystal dimensions [mm]	0.11 × 0.15 × 0.16
Formula weight [g/mol]	215.29	$\rho_{\text{calcd.}}$ [g/cm ³]	1.207
Sample temperature [K]	100(2)	μ [mm ⁻¹]	0.074
Wavelength [Å]	0.71073	<i>F</i> (000)	464
Crystal system	Monoclinic	Θ range [°]	1.647 to 26.560
Space group	<i>P</i> 2 ₁ / <i>c</i>	Reflections collected	30375
Unit cell dimensions [Å]		Unique reflections	2462
a =	13.06(2)	<i>R</i> _{int}	0.0387
b =	5.473(2)	Completeness to $\theta_{\text{full}}=25.242^\circ$	100%
c =	17.510(3)	restraints/parameters	0 / 146
α =	90°	GooF	1.065
β =	108.84(2)°	<i>R</i> 1(<i>I</i> > 2 σ (<i>I</i>))	0.0364
γ =	90°	<i>wR</i> 2 (all data)	0.0980
Volume [Å ³]	1184.6(6)	max. diff. peak/hole [e ⁻ Å ⁻³]	0.186 and -0.235

5.5.26.2-(1-benzyl-1H-1,2,3-triazol-4-yl)ethanol

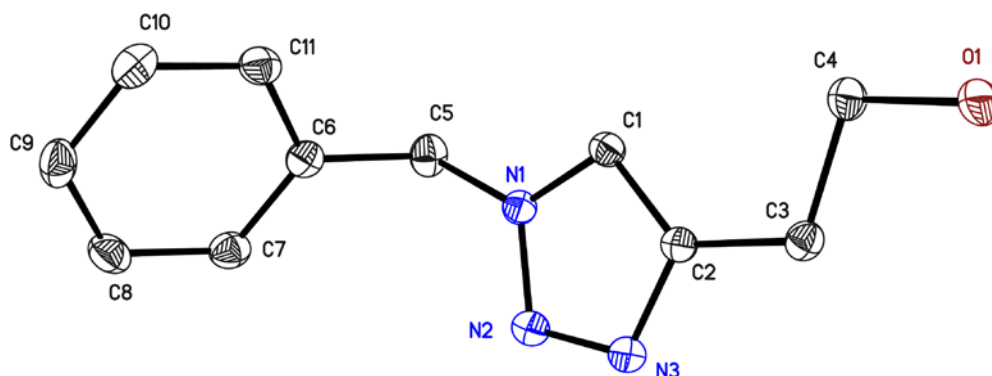


Figure 5.26: Asymmetric unit of 2-(1-benzyl-1H-1,2,3-triazol-4-yl)ethanol. The anisotropic displacement parameters are shown at the 50% probability level. Not freely refined hydrogen atoms are omitted for clarity.

Structure code	SR_269a	Z	4
Empirical formula	C ₁₁ H ₁₃ N ₃ O	Crystal dimensions [mm]	0.10 × 0.12 × 0.15
Formula weight [g/mol]	203.24	$\rho_{\text{calcd.}}$ [g/cm ³]	1.377
Sample temperature [K]	100(2)	μ [mm ⁻¹]	0.088
Wavelength [Å]	0.71073	<i>F</i> (000)	432
Crystal system	Monoclinic	Θ range [°]	1.837 to 25.347
Space group	<i>P</i> 2 ₁ / <i>c</i>	Reflections collected	16590
Unit cell dimensions [Å]		Unique reflections	1886
a =	22.580(3)	<i>R</i> _{int}	0.0265
b =	5.375(2)	Completeness to $\theta_{\text{full}} = 25.242^\circ$	99.9%
c =	8.599(2)	restraints/parameters	0 / 138
$\alpha =$	90°	GooF	1.089
$\beta =$	100.86(2)°	<i>R</i> 1 (<i>I</i> > 2 σ (<i>I</i>))	0.0342
$\gamma =$	90°	<i>wR</i> 2 (all data)	0.842
Volume [Å ³]	1024.9(5)	max. diff. peak/hole [e·Å ⁻³]	0.227 and -0.212

6. Crystal Structure Determination in Collaborations

6.1. Structures determined for Svenja Düfert

6.1.1. 7-methoxy-1-methyl-10a,11-dihydro-5H-benzo[e]furo[3',4':6,7]naphtho[1,8-bc]oxepin-13(10H)-one

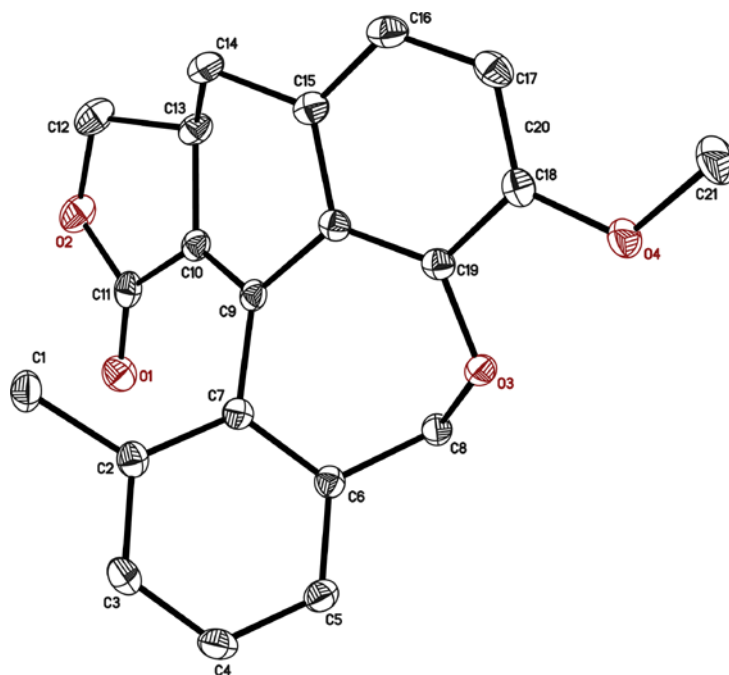


Figure 6.1: Asymmetric unit of 7-methoxy-1-methyl-10a,11-dihydro-5H-benzo[e]furo[3',4':6,7]naphtho[1,8-bc]oxepin-13(10H)-one. Anisotropic displacement parameters are depicted at the 50% probability level. Hydrogen atoms are omitted for clarity.

Structure code	SCSC511	Z	4
Empirical formula	C ₂₁ H ₁₈ O ₄	Crystal dimensions [mm]	0.626 × 0.329 × 0.136
Formula weight [g/mol]	334.35	$\rho_{\text{calcd.}}$ [g/cm ³]	1.395
Sample temperature [K]	100(2)	μ [mm ⁻¹]	0.096
Wavelength [Å]	0.71073	<i>F</i> (000)	704
Crystal system	Monoclinic	Θ range [°]	1.811 to 26.759
Space group	<i>P</i> 2 ₁ / <i>c</i>	Reflections collected	42667
Unit cell dimensions [Å]		Unique reflections	3394
a =	11.783(2)	R _{int}	0.0272
b =	12.227(3)	Completeness to θ_{max}	99.8%
c =	11.583(2)	restraints/parameters	0 / 228
α =	90°	Goof	1.060
β =	107.39(2)°	<i>R</i> 1(<i>I</i> > 2 σ (<i>I</i>))	0.0354
γ =	90°	<i>w</i> R2 (all data)	0.0939
Volume [Å ³]	1592.5(6)	max. diff. peak/hole [e ⁻ Å ⁻³]	0.315 and -0.223

6.2. Structures determined for Jonas Ammermann

6.2.1. 1-(5-Methyl-3-(9*H*-xanthen-9-yl)-1*H*-indole-1-yl)ethan-1-one

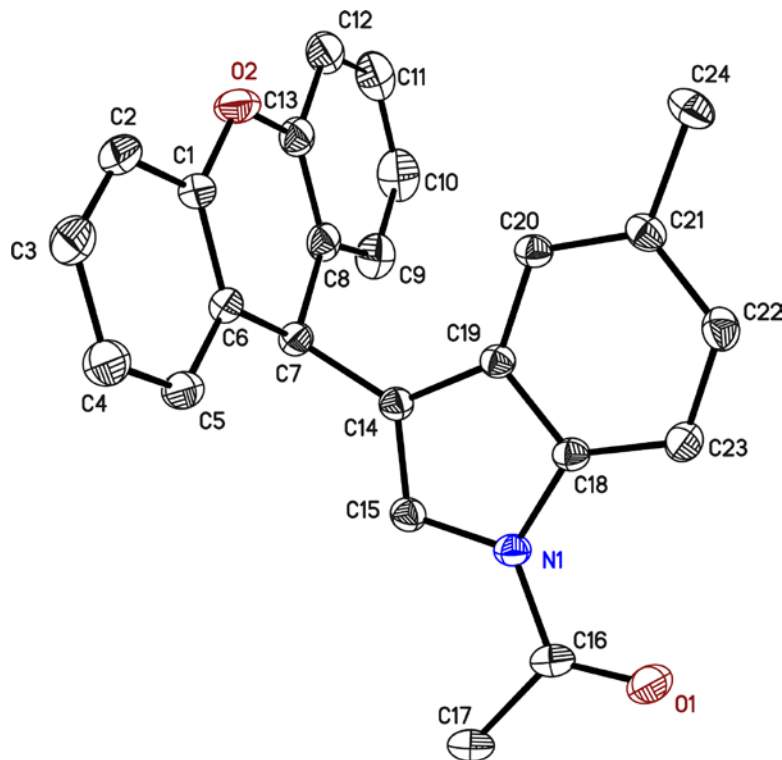


Figure 6.2: Asymmetric unit of 1-(5-Methyl-3-(9*H*-xanthen-9-yl)-1*H*-indole-1-yl)ethan-1-one. Anisotropic displacement parameters are depicted at the 50% probability level. Hydrogen atoms are omitted for clarity.

Published in “A Facile Synthesis of 3-Substituted Benzofurans And Indoles Through A palladium-catalyzed Domino Carbopalladation/CH-activation/Isomerization Process.” L.F. Tietze, T. Hungerland, J. Ammermann, C. Eichhorst, S.O. Reichmann, D. Stalke, *Ind. Chem. Soc.* **2013**, *90*, 1537-1555.

CCDC number	948415		
Structure code	CS_LK_SOR_JA	Z	4
Empirical formula	C ₂₄ H ₁₉ NO ₂	Crystal dimensions [mm]	0.348 × 0.096 × 0.054
Formula weight [g/mol]	353.40	$\rho_{\text{calcd.}}$ [g/cm ³]	1.303
Sample temperature [K]	100(2)	μ [mm ⁻¹]	0.083
Wavelength [Å]	0.71073	<i>F</i> (000)	744
Crystal system	Monoclinic	Θ range [°]	1.551 to 29.595
Space group	<i>P</i> 2 ₁ / <i>n</i>	Reflections collected	41195
Unit cell dimensions [Å]		Unique reflections	5024
	a = 6.393(2)	<i>R</i> _{int}	0.0242
	b = 26.264(2)	Completeness to $\theta_{\text{full}} = 25.242^\circ$	99.8%
	c = 10.740(2)	restraints/parameters	0 / 246
	$\alpha = 90^\circ$	GooF	1.037
	$\beta = 92.95(2)^\circ$	<i>R</i> 1(<i>I</i> > 2 σ (<i>I</i>))	0.0414
	$\gamma = 90^\circ$	<i>wR</i> 2 (all data)	0.1144
Volume [Å ³]	1801.0(7)	max. diff. peak/hole [e ⁻ Å ⁻³]	0.390 and -0.192

6.3. Structures determined for Bernd Waldecker

6.3.1. 4,9-Bis(9*H*-xanthene-9-ylidene)-1,3,4,6,8,9-hexahydropyrano[3,4-*g*]-isochromene

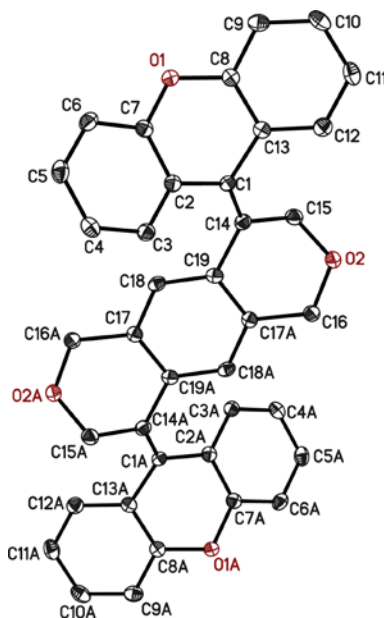


Figure 6.3: Asymmetric unit of 4,9-Bis(9*H*-xanthene-9-ylidene)-1,3,4,6,8,9-hexahydropyrano[3,4-*g*]-isochromene. Anisotropic displacement parameters are depicted at the 50% probability level. Hydrogen atoms are omitted for clarity.

Published in “Four- and Sixfold Tandem-Domino Reactions Leading to Dimeric Tetrasubstituted Alkenes Suitable as Molecular Switches.” L. F. Tietze, B. Waldecker, D. Ganapathy, C. Eichhorst, T. Lenzer, K. Oum, S. O. Reichmann, D. Stalke, *Angew. Chem. Int. Ed.* **2015**, *54*, 10317-10321; *Angew. Chem.* **2015**, *127*, 10457-10461.

CCDC number	1049106		
Structure code	SR_BW1	Z	1
Empirical formula	C ₃₈ H ₂₆ O ₄	Crystal dimensions [mm]	0.201 × 0.120 × 0.093
Formula weight [g/mol]	546.59	$\rho_{\text{calcd.}}$ [g/cm ³]	1.430
Sample temperature [K]	100(2)	μ [mm ⁻¹]	0.092
Wavelength [Å]	0.71073	<i>F</i> (000)	286
Crystal system	Triclinic	Θ range [°]	2.005 to 26.454
Space group	<i>P</i> 1	Reflections collected	26056
Unit cell dimensions [Å]		Unique reflections	2615
	<i>a</i> = 6.745(2)	<i>R</i> _{int}	0.0513
	<i>b</i> = 9.358(2)	Completeness to $\theta_{\text{full}} = 25.242^\circ$	100%
	<i>c</i> = 10.196(3)	restraints/parameters	0 / 191
	α = 88.07(3)°	GooF	1.038
	β = 85.26(2)°	<i>R</i> 1(<i>I</i> > 2 σ (<i>I</i>))	0.0339
	γ = 81.86(2)°	<i>wR</i> 2 (all data)	0.0820
Volume [Å ³]	634.7(3)	max. diff. peak/hole [e ⁻ Å ⁻³]	0.244 and -0.208
Extinction coefficient	–	Absolute structure parameter	–

6.3.2. 4,6-Bis(9*H*-xanthene-9-ylidene)-4,6,7,9-tetrahydro-1*H*,3*H*-pyrano[3,4-*g*]-isochromene

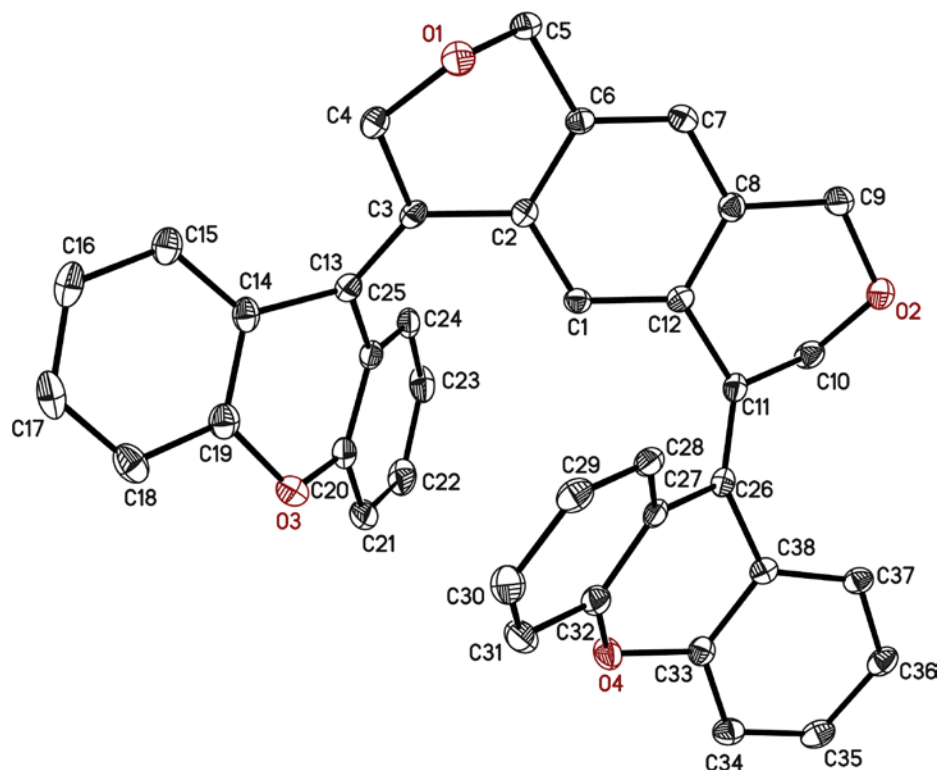


Figure 6.4: Asymmetric unit of 4,6-Bis(9*H*-xanthene-9-ylidene)-4,6,7,9-tetrahydro-1*H*,3*H*-pyrano[3,4-*g*]-isochromene. Anisotropic displacement parameters are depicted at the 50% probability level. Hydrogen atoms are omitted for clarity.

Published in “Four- and Sixfold Tandem-Domino Reactions Leading to Dimeric Tetrasubstituted Alkenes Suitable as Molecular Switches.” L. F. Tietze, B. Waldecker, D. Ganapathy, C. Eichhorst, T. Lenzer, K. Oum, S. O. Reichmann, D. Stalke, *Angew. Chem. Int. Ed.* **2015**, *54*, 10317-10321; *Angew. Chem.* **2015**, *127*, 10457-10461.

CCDC number	1049107	Z	2
Structure code	SR_BW_2	Crystal dimensions [mm]	0.302 × 0.09 × 0.073
Empirical formula	C ₃₈ H ₂₆ O ₄	$\rho_{\text{calcd.}}$ [g/cm ³]	1.385
Formula weight [g/mol]	546.59	μ [mm ⁻¹]	0.089
Sample temperature [K]	100(2)	<i>F</i> (000)	572
Wavelength [Å]	0.71073	Θ range [°]	2.056 to 27.488
Crystal system	Monoclinic	Reflections collected	29508
Space group	<i>P</i> 2 ₁	Unique reflections	5920
Unit cell dimensions [Å]		<i>R</i> _{int}	0.0231
a =	8.104 (2)	Completeness to $\theta_{\text{full}} = 25.242^\circ$	100%
b =	16.329 (3)	restraints/parameters	1 / 379
c =	10.548 (2)	GooF	0.978
$\alpha =$	90°	<i>R</i> 1(<i>I</i> > 2 σ (<i>I</i>))	0.0298
$\beta =$	110.10(2)°	<i>wR</i> 2 (all data)	0.0761
$\gamma =$	90°	max. diff. peak/hole [e·Å ⁻³]	0.244 and -0.1796
Volume [Å ³]	1310.8 (5)	Absolute structure parameter	–
Extinction coefficient	–		

6.4. Structures determined for Simon Biller

6.4.1. (+)-(R)-Linorexpin

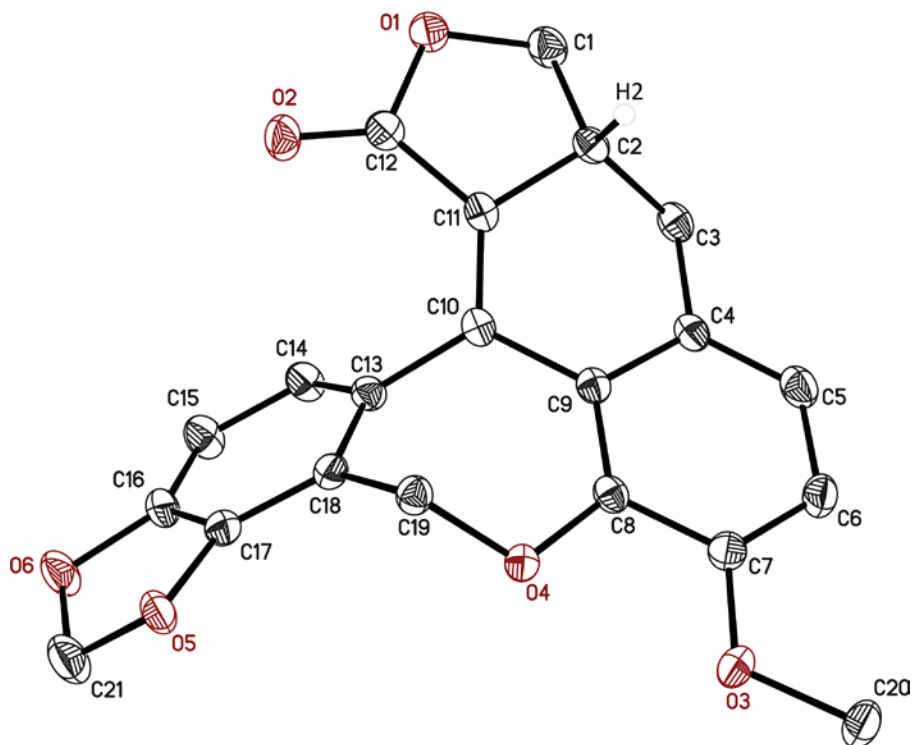


Figure 6.5: Asymmetric unit of (+)-(R)-Linorexpin. Anisotropic displacement parameters are depicted at the 50% probability level. Hydrogen atoms apart from H2 are omitted for clarity.

Structure code	SR_SB_030815	Z	2
Empirical formula	C ₂₁ H ₁₆ O ₆	Crystal dimensions [mm]	0.200 × 0.150 × 0.080
Formula weight [g/mol]	364.34	$\rho_{\text{calcd.}}$ [g/cm ³]	1.443
Sample temperature [K]	100(2)	μ [mm ⁻¹]	0.888
Wavelength [Å]	1.54178	<i>F</i> (000)	380
Crystal system	Monoclinic	Θ range [°]	2.813 to 74.522
Space group	<i>P</i> 2 ₁	Reflections collected	18983
Unit cell dimensions [Å]		Unique reflections	3351
a =	4.800(2)	<i>R</i> _{int}	0.0273
b =	11.119(2)	Completeness to $\theta_{\text{full}} = 67.679^\circ$	99.8%
c =	15.738(3)	restraints/parameters	1 / 246
$\alpha =$	90°	GooF	1.062
$\beta =$	93.47(2)°	<i>R</i> 1(<i>I</i> > 2 σ (<i>I</i>))	0.0259
$\gamma =$	90°	<i>wR</i> 2 (all data)	0.0633
Volume [Å ³]	838.4(4)	max. diff. peak/hole [e ⁻ Å ⁻³]	0.170 and -0.146
Extinction coefficient	0.0074(9)	Absolute structure parameter	0.04(4)

6.4.2. 2-((2-(4-bromo-3-methylphenyl)-2-oxoethyl)thio)-6-oxo-4-(thiophen-2-yl)-1,6-dihydropyrimidine-5-carbonitrile

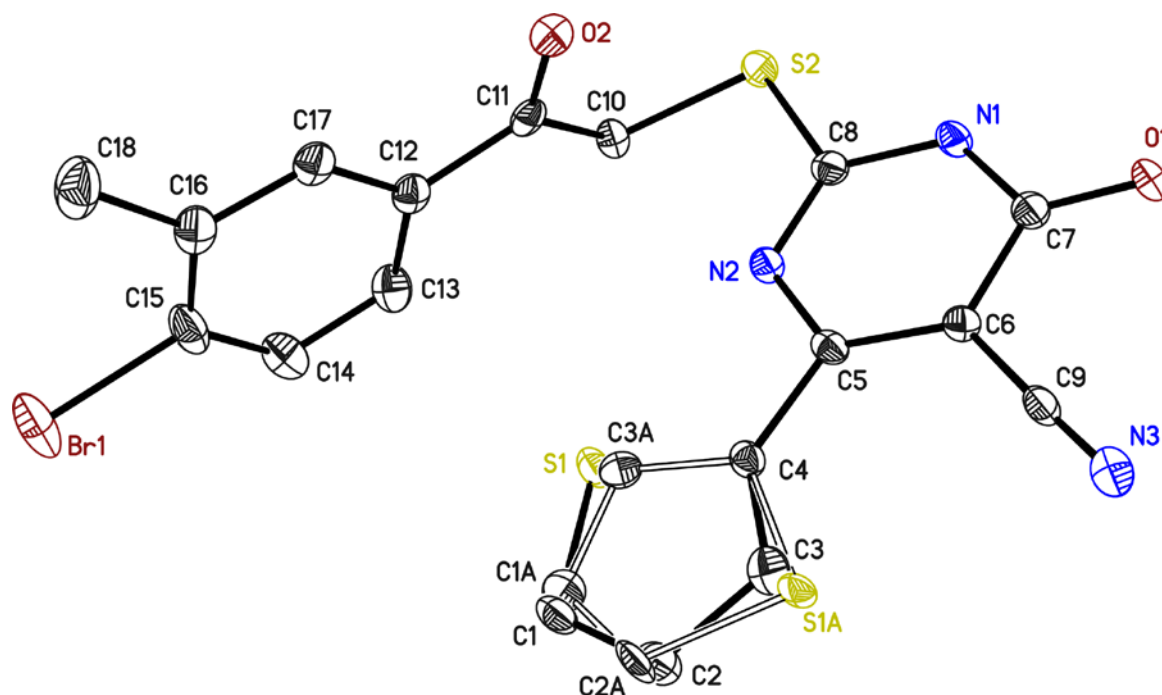


Figure 6.6: Asymmetric unit of 2-((2-(4-bromo-3-methylphenyl)-2-oxoethyl)thio)-6-oxo-4-(thiophen-2-yl)-1,6-dihydropyrimidine-5-carbonitrile. Anisotropic displacement parameters are depicted at the 50% probability level. Hydrogen atoms are omitted for clarity.

Structure code	SR_SB_X	Z	4
Empirical formula	C ₁₈ H ₁₂ N ₃ BrO ₂ S ₂	Crystal dimensions [mm]	0.240 × 0.210 × 0.160
Formula weight [g/mol]	446.3	$\rho_{\text{calcd.}}$ [g/cm ³]	1.671
Sample temperature [K]	100(2)	μ [mm ⁻¹]	2.571
Wavelength [Å]	0.71073	<i>F</i> (000)	896
Crystal system	Monoclinic	Θ range [°]	1.495 to 26.033
Space group	<i>P</i> 2 ₁ / <i>n</i>	Reflections collected	14869
Unit cell dimensions [Å]		Unique reflections	3488
	a = 14.386(2)	<i>R</i> _{int}	0.0266
	b = 4.959(2)	Completeness to $\theta_{\text{full}} = 25.242^\circ$	99.8%
	c = 25.571(3)	restraints/parameters	70 / 273
	$\alpha = 90^\circ$	Goof	1.024
	$\beta = 103.47(2)^\circ$	<i>R</i> 1(<i>I</i> > 2 σ (<i>I</i>))	0.0353
	$\gamma = 90^\circ$	<i>wR</i> 2 (all data)	0.0866
Volume [Å ³]	1774.1(8)	max. diff. peak/hole [e ⁻ Å ⁻³]	1.045 and -0.879

6.5. Structure determined for Yan Li

6.5.1. SOR_LY_023

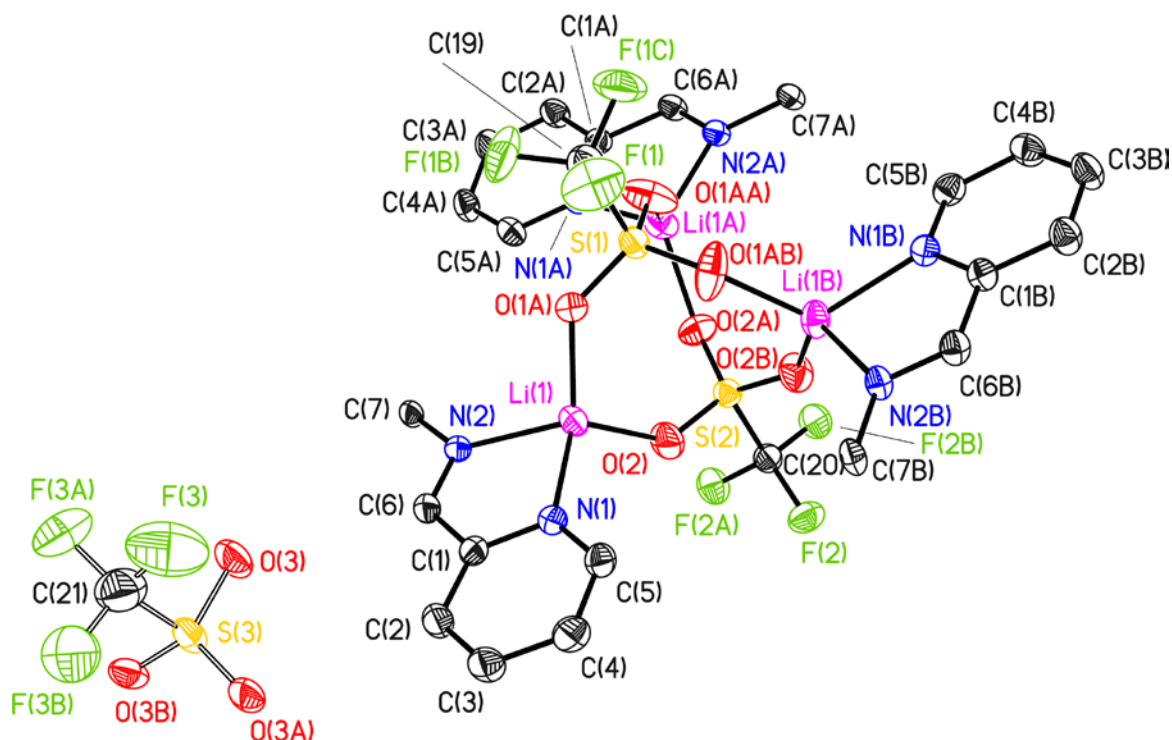


Figure 6.7: Asymmetric unit of SOR_LY_023. Anisotropic displacement parameters are depicted at the 50% probability level. Hydrogen atoms are omitted for clarity.

Structure code	SOR_LY_023	Z	6
Empirical formula	C ₅₇ H ₆₆ N ₆ F ₉ Li ₃ O ₉ S ₃	Crystal dimensions [mm]	0.10 × 0.06 × 0.01
Formula weight [g/mol]	1267.15	$\rho_{\text{calcd.}}$ [g/cm ³]	1.312
Sample temperature [K]	100(2)	μ [mm ⁻¹]	0.198
Wavelength [Å]	0.71073	<i>F</i> (000)	3960
Crystal system	Monoclinic	Θ range [°]	1.742 to 26.728
Space group	<i>R</i> 3 <i>c</i>	Reflections collected	20858
Unit cell dimensions [Å]		Unique reflections	4537
a =	16.138(2)	<i>R</i> _{int}	0.0326
b =	16.138(2)	Completeness to $\theta_{\text{full}} = 25.242^\circ$	99.7%
c =	42.653(3)	restraints/parameters	130 / 327
$\alpha =$	90°	GooF	1.062
$\beta =$	90°	<i>R</i> 1(<i>I</i> > 2 σ (<i>I</i>))	0.0323
$\gamma =$	120°	<i>wR</i> 2 (all data)	0.0792
Volume [Å ³]	9620(2)	max. diff. peak/hole [e·Å ⁻³]	0.285 and -0.265

6.6. Structures determined for Alexander Paesch

6.6.1. 2-Phenyl-4-diphenylphospan-1,3-bis(2,6-diisopropylphenyl)-imidazolium-Kupfer(I)iodid ($[(\text{Ph}_2\text{P-IPrPh})\text{-Cu(I)-I}]$)

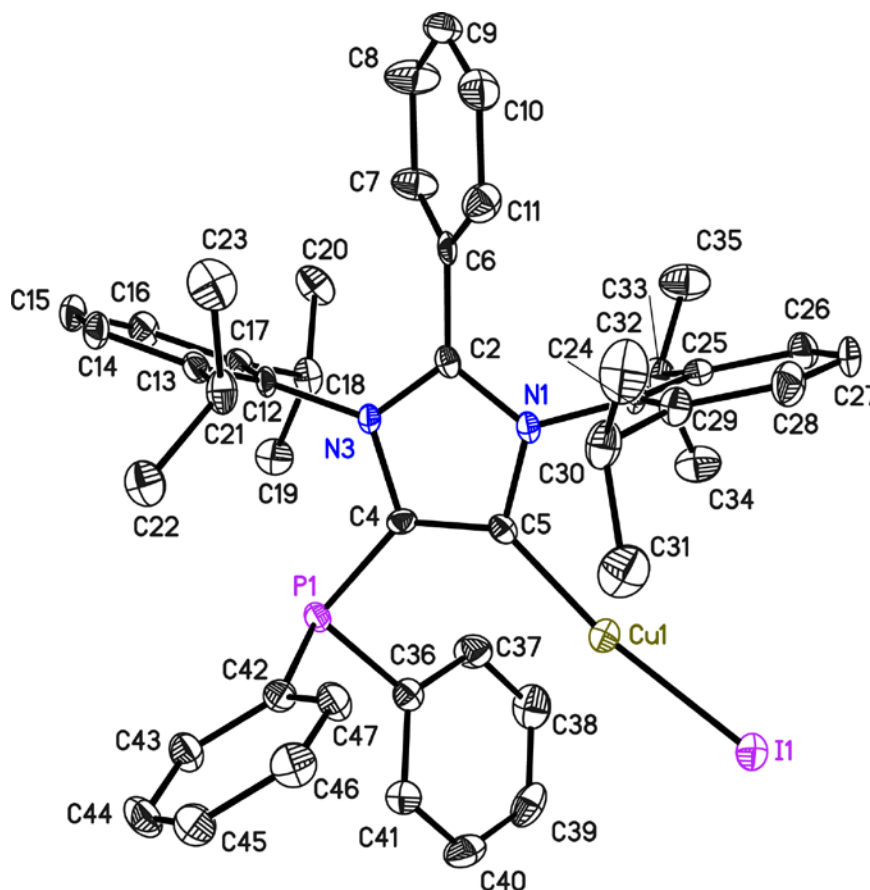


Figure 6.8: Asymmetric unit of 2-phenyl-4-diphenylphosphine-1,3-bis(2,6-diisopropylphenyl)-imidazolium-copper(I)iodide ($[(\text{Ph}_2\text{P-IPrPh})\text{-Cu(I)-I}]$). Anisotropic displacement parameters are depicted at the 50% probability level. Hydrogen atoms are omitted for clarity.

Structure code	SR_AP_18	Z	4
Empirical formula	$\text{C}_{44}\text{H}_{49}\text{CuIN}_2\text{P}$	Crystal dimensions [mm]	$0.18 \times 0.13 \times 0.07$
Formula weight [g/mol]	839.27	$\rho_{\text{calcd.}}$ [g/cm ³]	1.380
Sample temperature [K]	100(2)	μ [mm ⁻¹]	1.377
Wavelength [Å]	0.71073	$F(000)$	1720
Crystal system	Monoclinic	Θ range [°]	1.455 to 25.349
Space group	$P2_1/n$	Reflections collected	106743
Unit cell dimensions [Å]		Unique reflections	7414
	a = 10.226(2)	R_{int}	0.0900
	b = 18.652(2)	Completeness to $\theta_{\text{full}} = 25.242^\circ$	100%
	c = 21.549(3)	restraints/parameters	0 / 459
	$\alpha = 90^\circ$	GooF	1.035
	$\beta = 100.53(2)^\circ$	$R1(I > 2\sigma(I))$	0.0342
	$\gamma = 90^\circ$	wR2 (all data)	0.0808
Volume [Å ³]	4040.9(9)	max. diff. peak/hole [e ⁻ Å ⁻³]	1.616 and -0.873

6.6.2. Bis[2-phenyl-1,3-bis(2,6-diisopropylphenyl)-imidazolium]-palladium(II)dichloride ([IPrPh)₂-Pd(II)-Cl₂]

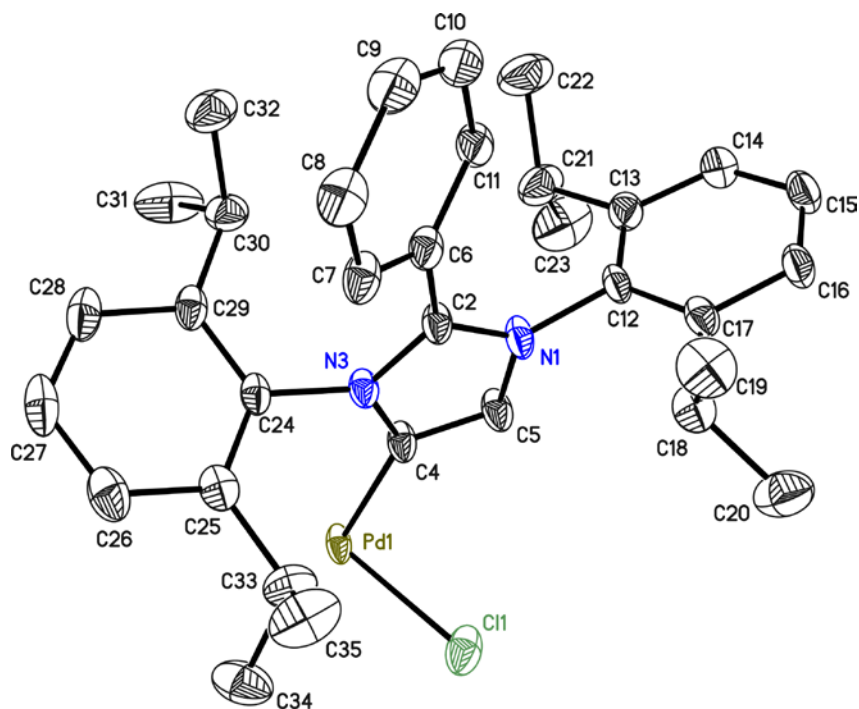


Figure 6.9: Asymmetric unit of bis[2-phenyl-1,3-bis(2,6-diisopropylphenyl)-imidazolium]-palladium(II)dichloride ([IPrPh)₂-Pd(II)-Cl₂]). Anisotropic displacement parameters are depicted at the 50% probability level. Hydrogen atoms are omitted for clarity.

Structure code	SR_AP_19	Z	2
Empirical formula	C ₉₄ H ₁₁₂ N ₄ Cl ₂ Pd	Crystal dimensions [mm]	0.297 × 0.156 × 0.095
Formula weight [g/mol]	1475.17	$\rho_{\text{calcd.}}$ [g/cm ³]	1.186
Sample temperature [K]	100(2)	μ [mm ⁻¹]	0.336
Wavelength [Å]	0.71073	<i>F</i> (000)	1568
Crystal system	Monoclinic	Θ range [°]	1.457 to 26.392
Space group	<i>P</i> 2 ₁ / <i>n</i>	Reflections collected	116397
Unit cell dimensions [Å]		Unique reflections	8448
	a = 16.581(2)	<i>R</i> _{int}	0.0731
	b = 12.031(6)	Completeness to $\theta_{\text{full}} = 25.242^\circ$	100%
	c = 20.983(3)	restraints/parameters	828 / 597
	$\alpha = 90^\circ$	GooF	1.029
	$\beta = 99.25(2)^\circ$	<i>R</i> 1(<i>I</i> > 2 σ (<i>I</i>))	0.0437
	$\gamma = 90^\circ$	<i>wR</i> 2 (all data)	0.1201
Volume [Å ³]	4131.4(11)	max. diff. peak/hole [e ⁻ Å ⁻³]	1.538 and -0.639

7. References

- [1] J. B. Dumas, E. Peligot, *Ann. chim. Phys.* **1835**, 58, 5-74.
- [2] A. J. Arduengo III, R. Krafczyk, *Chem. unserer Zeit* **1998**, 32, 6-14.
- [3] J. U. Nef, *Justus Liebigs Ann. Chem.* **1897**, 298, 202-374.
- [4] a) A. Geuther, *Justus Liebigs Ann. Chem.* **1862**, 123, 121-122; b) W. von E. Doering, A. K. Hoffmann, *J. Am. Chem. Soc.* **1954**, 76, 6162-6165.
- [5] a) E. Buchner, T. Curtius, *Ber. Dtsch. Chem. Ges.* **1885**, 8, 2377-2379; b) H. Staudinger, O. Kupfer, *Ber. Dtsch. Chem. Ges.* **1912**, 45, 501-509.
- [6] L. Tschugajeff, M. Skanawy-Grigorjewa, A. Posnjak, *Z. Anorg. Allg. Chem.* **1925**, 148, 37-42.
- [7] F. E. Hahn, M. C. Jahnke, *Angew. Chem. Int. Ed.* **2008**, 47, 3122-3172; *Angew. Chem.* **2008**, 120, 3166-3216.
- [8] R. Breslow, *J. Am. Chem. Soc.* **1958**, 80, 3719-3726.
- [9] H. W. Wanzlick, E. Schikora, *Angew. Chem.* **1960**, 72, 494.
- [10] H. W. Wanzlick, *Angew. Chem.* **1962**, 74, 129-134; *Angew. Chem. Int. Ed.* **1962**, 1, 75-80.
- [11] E. O. Fischer, A. Maasböl, *Angew. Chem.* **1964**, 76, 645; *Angew. Chem. Int. Ed.* **1964**, 3, 580-581.
- [12] K. Öfele, *J. Organomet. Chem.* **1968**, 12, 42-43.
- [13] R. R. Schrock, *J. Am. Chem. Soc.* **1974**, 96, 6796-6797.
- [14] A. Igau, A. Baceiredo, G. Trinquier, G. Bertrand, *Angew. Chem. Int. Ed. Engl.* **1989**, 28, 621-622; *Angew. Chem.* **1989**, 101, 617-618.
- [15] A. J. Arduengo III, in *US Patent*, E.I. Du Pont de Nemours and Company, **1992**.
- [16] A. J. Arduengo III, R. L. Harlow, M. Kline, *J. Am. Chem. Soc.* **1991**, 113, 361-363.
- [17] G. Parkin, R. H. Crabtree, D. M. P. Mingos, *Comprehensive Organometallic Chemistry III, Vol. 1*, Elsevier, New York, **2007**.
- [18] W. A. Herrmann, L. J. Gooßen, M. Spiegler, *J. Organomet. Chem.* **1997**, 547, 357-366.
- [19] N. Kuhn, T. Kratz, *Synthesis* **1993**, 1993, 561-562.
- [20] W. A. Herrmann, C. Köcher, L. J. Gooßen, G. R. J. Artus, *Chem. Eur. J.* **1996**, 2, 1627-1636.
- [21] I. Fleming, *Frontier orbitals and organic chemical reactions*, Wiley, New York, **1976**.
- [22] a) M. Soleilhavoup, A. Baceiredo, O. Treutler, R. Ahlrichs, M. Nieger, G. Bertrand, *J. Am. Chem. Soc.* **1992**, 114, 10959-10961; b) A. Igau, H. Grutzmacher, A. Baceiredo, G. Bertrand, *J. Am. Chem. Soc.* **1988**, 110, 6463-6466.
- [23] a) H. Tomioka, *Acc. Chem. Res.* **1997**, 30, 315-321; b) W. Kirmse, *Angew. Chem. Int. Ed.* **2003**, 42, 2117-2119; *Angew. Chem.* **2003**, 115, 2165-2167.
- [24] a) H. E. Zimmerman, D. H. Paskovich, *J. Am. Chem. Soc.* **1964**, 86, 2149-2160; b) W. Sander, G. Bucher, S. Wierlacher, *Chem. Rev.* **1993**, 93, 1583-1621.
- [25] a) A. J. Arduengo, H. V. R. Dias, R. L. Harlow, M. Kline, *J. Am. Chem. Soc.* **1992**, 114, 5530-5534; b) A. J. Arduengo, H. V. R. Dias, D. A. Dixon, R. L. Harlow, W. T. Klooster, T. F. Koetzle, *J. Am. Chem. Soc.* **1994**, 116, 6812-6822; c) C. Boehme, G. Frenking, *J. Am. Chem. Soc.* **1996**, 118, 2039-2046; d) C. Heinemann, T. Müller, Y. Apeloig, H. Schwarz, *J. Am. Chem. Soc.* **1996**, 118, 2023-2038; e) D. Nemcsok, K. Wichmann, G. Frenking, *Organometallics* **2004**, 23, 3640-3646.
- [26] D. Bourissou, O. Guerret, F. P. Gabbaï, G. Bertrand, *Chem. Rev.* **2000**, 100, 39-92.
- [27] L. Pauling, *J. Chem. Soc., Chem. Commun.* **1980**, 688-689.
- [28] F. E. Hahn, *Angew. Chem. Int. Ed.* **2006**, 45, 1348-1352; *Angew. Chem.* **2006**, 118, 1374-1378.
- [29] a) P. Bazinet, G. P. A. Yap, D. S. Richeson, *J. Am. Chem. Soc.* **2003**, 125, 13314-13315; b) E. Despagnet-Ayoub, R. H. Grubbs, *J. Am. Chem. Soc.* **2004**, 126, 10198-10199; c) C. C. Scarborough, M. J. W. Grady, I. A. Guzei, B. A. Gandhi, E. E. Bunel, S. S. Stahl, *Angew. Chem.* **2005**, 117, 5403-5406; *Angew. Chem. Int. Ed.* **2005**, 44, 5269-5272.
- [30] a) R. W. Alder, P. R. Allen, M. Murray, A. G. Orpen, *Angew. Chem. Int. Ed. Engl.* **1996**, 35, 1121-1123; *Angew. Chem.* **1996**, 108, 1211-1213; b) A. J. Arduengo, J. R. Goerlich, W. J. Marshall, *Liebigs Ann.* **1997**, 1997, 365-374; c) R. W. Alder, C. P. Butts, A. G. Orpen, *J. Am. Chem. Soc.* **1998**, 120, 11526-11527; d) C. Buron, H. Gornitzka, V. Romanenko, G. Bertrand, *Science* **2000**, 288, 834-836; e) S. Sole, H. Gornitzka, W. W. Schoeller, D. Bourissou, G. Bertrand, *Science* **2001**, 292, 1901-1903; f) V. Lavallo, J. Mafhouz, Y. Canac, B. Donnadiu, W. W. Schoeller, G. Bertrand, *J. Am. Chem. Soc.* **2004**, 126, 8670-8671; g) V. Lavallo, Y. Canac, C. Präsang, B. Donnadiu, G. Bertrand, *Angew. Chem.* **2005**, 117, 5851-5855; *Angew. Chem. Int. Ed.* **2005**, 44, 5705-5709.
- [31] R. A. Kelly III, H. Clavier, S. Giudice, N. M. Scott, E. D. Stevens, J. Bordner, I. Samardjiev, C. D. Hoff, L. Cavallo, S. P. Nolan, *Organometallics* **2008**, 27, 202-210.
- [32] A. Poater, B. Cosenza, A. Correa, S. Giudice, F. Ragone, V. Scarano, L. Cavallo, *Eur. J. Inorg. Chem.* **2009**, 1759-1766.

- [33] a) A. G. Orpen, N. G. Connelly, *J. Chem. Soc., Chem. Commun.* **1985**, 1310-1311; b) L. Cavallo, A. Correa, C. Costabile, H. Jacobsen, *J. Organomet. Chem.* **2005**, *690*, 5407-5413; c) E. A. B. Kantchev, C. J. O'Brien, M. G. Organ, *Angew. Chem. Int. Ed.* **2007**, *46*, 2768-2813.
- [34] a) A. C. Hillier, W. J. Sommer, B. S. Yong, J. L. Petersen, L. Cavallo, S. P. Nolan, *Organometallics* **2003**, *22*, 4322-4326; b) R. Dorta, E. D. Stevens, C. D. Hoff, S. P. Nolan, *J. Am. Chem. Soc.* **2003**, *125*, 10490-10491.
- [35] a) I. I. A. J. Arduengo, M. Tamm, J. C. Calabrese, F. Davidson, W. J. Marshall, *Chem. Lett.* **1999**, *28*, 1021-1022; b) R. Fränkel, C. Birg, U. Kernbach, T. Habereeder, H. Nöth, W. P. Fehlhammer, *Angew. Chem. Int. Ed.* **2001**, *40*, 1907-1910; *Angew. Chem.* **2001**, *113*, 1961-1964; c) I. S. Edworthy, A. J. Blake, C. Wilson, P. L. Arnold, *Organometallics* **2007**, *26*, 3684-3689; d) A. Stasch, S. P. Sarish, H. W. Roesky, K. Meindl, F. Dall'Antonia, T. Schulz, D. Stalke, *Chemistry – An Asian Journal* **2009**, *4*, 1451-1457; e) Y. Wang, Y. Xie, M. Y. Abraham, P. Wei, H. F. Schaefer, P. v. R. Schleyer, G. H. Robinson, *J. Am. Chem. Soc.* **2010**, *132*, 14370-14372; f) M. S. Hill, G. Kociok-Köhn, D. J. MacDougall, *Inorg. Chem.* **2011**, *50*, 5234-5241; g) A. Jana, R. Azhakar, G. Tavčar, H. W. Roesky, I. Objartel, D. Stalke, *Eur. J. Inorg. Chem.* **2011**, 3686-3689.
- [36] a) W. A. Herrmann, O. Runte, G. Artus, *J. Organomet. Chem.* **1995**, *501*, C1-C4; b) J. Gottfriedsen, S. Blaurock, *Organometallics* **2006**, *25*, 3784-3786.
- [37] a) J. A. Arduengo III, F. Davidson, R. Krafczyk, J. W. Marshall, R. Schmutzler, *Monat. Chem.* **2000**, *131*, 251-265; b) D. P. Curran, A. Solovyev, M. Makhlof Brahmī, L. Fensterbank, M. Malacria, E. Lacôte, *Angew. Chem. Int. Ed.* **2011**, *50*, 10294-10317; c) Y.-L. Rao, L. D. Chen, N. J. Mosey, S. Wang, *J. Am. Chem. Soc.* **2012**, *134*, 11026-11034.
- [38] a) D. A. Dixon, A. J. Arduengo, *The Journal of Physical Chemistry* **1991**, *95*, 4180-4182; b) C. A. Dyker, V. Lavallo, B. Donnadiu, G. Bertrand, *Angew. Chem. Int. Ed.* **2008**, *47*, 3206-3209; *Angew. Chem.* **2008**, *120*, 3250-3253; c) B. Bantu, G. Manohar Pawar, K. Wurst, U. Decker, A. M. Schmidt, M. R. Buchmeiser, *Eur. J. Inorg. Chem.* **2009**, *2009*, 1970-1976; d) H. Li, C. Risko, J. H. Seo, C. Campbell, G. Wu, J.-L. Brédas, G. C. Bazan, *J. Am. Chem. Soc.* **2011**, *133*, 12410-12413.
- [39] a) T. K. Panda, C. G. Hrib, P. G. Jones, J. Jenter, P. W. Roesky, M. Tamm, *Eur. J. Inorg. Chem.* **2008**, *2008*, 4270-4279; b) A. G. Trambitas, T. K. Panda, J. Jenter, P. W. Roesky, C. Daniliuc, C. G. Hrib, P. G. Jones, M. Tamm, *Inorg. Chem.* **2010**, *49*, 2435-2446.
- [40] N. Kuhn, H. Bohnen, J. Fahl, D. Bläser, R. Boese, *Chem. Ber.* **1996**, *129*, 1579-1586.
- [41] a) A. J. Arduengo, F. Davidson, R. Krafczyk, W. J. Marshall, M. Tamm, *Organometallics* **1998**, *17*, 3375-3382; b) A. R. Kennedy, R. E. Mulvey, S. D. Robertson, *Dalton Trans.* **2010**, *39*, 9091-9099.
- [42] a) A. J. Arduengo, H. V. R. Dias, J. C. Calabrese, F. Davidson, *J. Am. Chem. Soc.* **1992**, *114*, 9724-9725; b) X.-W. Li, J. Su, G. H. Robinson, *Chem. Commun.* **1996**, 2683-2684; c) M. D. Francis, D. E. Hibbs, M. B. Hursthouse, C. Jones, N. A. Smithies, *J. Chem. Soc., Dalton Trans.* **1998**, 3249-3254; d) S. J. Bonyhady, D. Collis, G. Frenking, N. Holzmann, C. Jones, A. Stasch, *Nat. Chem.* **2010**, *2*, 865-869; e) C. Fliedel, G. Schnee, T. Avilés, S. Dagorne, *Coord. Chem. Rev.* **2014**, *275*, 63-86.
- [43] a) N. Kuhn, T. Kratz, D. Bläser, R. Boese, *Chem. Ber.* **1995**, *128*, 245-250; b) Y. Wang, Y. Xie, P. Wei, R. B. King, H. F. Schaefer, P. von R. Schleyer, G. H. Robinson, *Science* **2008**, *321*, 1069-1071; c) R. S. Ghadwal, S. S. Sen, H. W. Roesky, G. Tavcar, S. Merkel, D. Stalke, *Organometallics* **2009**, *28*, 6374-6377; d) R. S. Ghadwal, H. W. Roesky, S. Merkel, J. Henn, D. Stalke, *Angew. Chem. Int. Ed.* **2009**, *48*, 5683-5686; *Angew. Chem.* **2009**, *121*, 5793-5796; e) R. S. Ghadwal, H. W. Roesky, C. Schulzke, M. Granitzka, *Organometallics* **2010**, *29*, 6329-6333; f) R. S. Ghadwal, S. S. Sen, H. W. Roesky, M. Granitzka, D. Kratzert, S. Merkel, D. Stalke, *Angew. Chem. Int. Ed.* **2010**, *49*, 3952-3955; *Angew. Chem.* **2010**, *122*, 4044-4047; g) R. S. Ghadwal, H. W. Roesky, S. Merkel, D. Stalke, *Chem. Eur. J.* **2010**, *16*, 85-88; h) R. S. Ghadwal, H. W. Roesky, M. Granitzka, D. Stalke, *J. Am. Chem. Soc.* **2010**, *132*, 10018-10020; i) R. S. Ghadwal, R. Azhakar, H. W. Roesky, K. Pröpper, B. Dittrich, C. Goedecke, G. Frenking, *Chem. Commun.* **2012**, *48*, 8186-8188; j) R. S. Ghadwal, R. Azhakar, H. W. Roesky, *Acc. Chem. Res.* **2013**, *46*, 444-456; k) K. C. Mondal, H. W. Roesky, M. C. Schwarzer, G. Frenking, B. Niepötter, H. Wolf, R. Herbst-Irmer, D. Stalke, *Angew. Chem. Int. Ed.* **2013**, *52*, 2963-2967; *Angew. Chem.* **2013**, *125*, 3036-3040; l) H. W. Roesky, *J. Organomet. Chem.* **2013**, *730*, 57-62; m) Y. Wang, Y. Xie, P. Wei, H. F. Schaefer, G. H. Robinson, *Dalton Trans.* **2016**.
- [44] a) A. J. Arduengo, R. Krafczyk, W. J. Marshall, R. Schmutzler, *J. Am. Chem. Soc.* **1997**, *119*, 3381-3382; b) A. J. Arduengo, J. C. Calabrese, A. H. Cowley, H. V. R. Dias, J. R. Goerlich, W. J. Marshall, B. Riegel, *Inorg. Chem.* **1997**, *36*, 2151-2158; c) N. Burford, C. A. Dyker, A. D. Phillips, H. A. Spinney, A. Decken, R. McDonald, P. J. Ragona, A. L. Rheingold, *Inorg. Chem.* **2004**, *43*, 7502-7507; d) B. D. Ellis, C. A. Dyker, A. Decken, C. L. B. Macdonald, *Chem. Commun.* **2005**, 1965-1967; e) Y. Wang, Y. Xie, P. Wei, R. B. King, I. I. H. F. Schaefer, P. v. R. Schleyer, G. H.

- Robinson, *J. Am. Chem. Soc.* **2008**, *130*, 14970-14971; f) S. M. I. Al-Rafia, M. J. Ferguson, E. Rivard, *Inorg. Chem.* **2011**, *50*, 10543-10545; g) T. Böttcher, O. Shyshkov, M. Bremer, B. S. Bassil, G.-V. Röschenthaler, *Organometallics* **2012**, *31*, 1278-1280.
- [45] D. Holschumacher, C. G. Daniliuc, P. G. Jones, M. Tamm, *Z. Naturforsch.* **2011**, *66b*, 371-377.
- [46] a) A. J. Arduengo, F. Davidson, H. V. R. Dias, J. R. Goerlich, D. Khasnis, W. J. Marshall, T. K. Prakasha, *J. Am. Chem. Soc.* **1997**, *119*, 12742-12749; b) M. L. Cole, C. Jones, P. C. Junk, *New J. Chem.* **2002**, *26*, 1296-1303; c) N. Kuhn, A. Abu-Rayyan, M. Göhner, M. Steimann, *Z. Anorg. Allg. Chem.* **2002**, *628*, 1721-1723.
- [47] a) R. W. Alder, M. E. Blake, C. Bortolotti, S. Bufali, C. P. Butts, E. Linehan, J. M. Oliva, A. Guy Orpen, M. J. Quayle, *Chem. Commun.* **1999**, 241-242; b) P. L. Arnold, M. Rodden, C. Wilson, *Chem. Commun.* **2005**, 1743-1745.
- [48] A. G. M. Barrett, M. R. Crimmin, M. S. Hill, G. Kociok-Köhn, D. J. MacDougall, M. F. Mahon, P. A. Procopiou, *Organometallics* **2008**, *27*, 3939-3946.
- [49] a) B. Quillian, P. Wei, C. S. Wannere, P. v. R. Schleyer, G. H. Robinson, *J. Am. Chem. Soc.* **2009**, *131*, 3168-3169; b) G. E. Ball, M. L. Cole, A. I. McKay, *Dalton Trans.* **2012**, *41*, 946-952; c) M. N. Hopkinson, C. Richter, M. Schedler, F. Glorius, *Nature* **2014**, *510*, 485-496; d) M. Chen, Y. Wang, R. J. Gilliard, Jr, P. Wei, N. A. Schwartz, G. H. Robinson, *Dalton Trans.* **2014**, *43*, 14211-14214.
- [50] a) A. J. Arduengo, H. V. R. Dias, J. C. Calabrese, F. Davidson, *Inorg. Chem.* **1993**, *32*, 1541-1542; b) B. Gehrhus, P. B. Hitchcock, M. F. Lappert, *J. Chem. Soc., Dalton Trans.* **2000**, 3094-3099; c) P. A. Rupar, M. C. Jennings, K. M. Baines, *Organometallics* **2008**, *27*, 5043-5051; d) A. Sidiropoulos, C. Jones, A. Stasch, S. Klein, G. Frenking, *Angew. Chem. Int. Ed.* **2009**, *48*, 9701-9704; *Angew. Chem.* **2009**, *121*, 9881-9884; e) N. Katir, D. Matioszek, S. Ladeira, J. Escudié, A. Castel, *Angew. Chem. Int. Ed.* **2011**, *50*, 5352-5355; *Angew. Chem.* **2011**, *123*, 5464-5467; f) G. Prabusankar, A. Sathyanarayana, P. Suresh, C. Naga Babu, K. Srinivas, B. P. R. Metla, *Coord. Chem. Rev.* **2014**, *269*, 96-133.
- [51] M. Y. Abraham, Y. Wang, Y. Xie, P. Wei, H. F. Schaefer, P. v. R. Schleyer, G. H. Robinson, *Chem. Eur. J.* **2010**, *16*, 432-435.
- [52] a) J. L. Dutton, R. Tabeshi, M. C. Jennings, A. J. Lough, P. J. Ragona, *Inorg. Chem.* **2007**, *46*, 8594-8602; b) J. L. Dutton, T. L. Battista, M. J. Sgro, P. J. Ragona, *Chem. Commun.* **2010**, *46*, 1041-1043.
- [53] N. Kuhn, A. Abu-Rayyan, K. Eichele, S. Schwarz, M. Steimann, *Inorg. Chim. Acta* **2004**, *357*, 1799-1804.
- [54] C. D. Abernethy, M. L. Cole, C. Jones, *Organometallics* **2000**, *19*, 4852-4857.
- [55] I. I. I. A. J. Arduengo, R. Krafczyk, R. Schmutzler, W. Mahler, W. J. Marshall, *Z. Anorg. Allg. Chem.* **1999**, *625*, 1813-1817.
- [56] a) N. Kuhn, A. Abu-Rayyan, C. Piludu, M. Steimann, *Heteroat. Chem* **2005**, *16*, 316-319; b) J. Beckmann, P. Finke, S. Heitz, M. Hesse, *Eur. J. Inorg. Chem.* **2008**, *2008*, 1921-1925.
- [57] N. Kuhn, T. Kratz, G. Henkel, *J. Chem. Soc., Chem. Commun.* **1993**, 1778-1779.
- [58] H. Nakai, Y. Tang, P. Gantzel, K. Meyer, *Chem. Commun.* **2003**, 24-25.
- [59] C. Jones, A. Sidiropoulos, N. Holzmann, G. Frenking, A. Stasch, *Chem. Commun.* **2012**, *48*, 9855-9857.
- [60] A. Aprile, R. Corbo, K. Vin Tan, D. J. D. Wilson, J. L. Dutton, *Dalton Trans.* **2014**, *43*, 764-768.
- [61] a) P. L. Arnold, I. A. Marr, S. Zlatogorsky, R. Bellabarba, R. P. Tooze, *Dalton Trans.* **2014**, *43*, 34-37; b) S. Long, B. Wang, H. Xie, C. Yao, C. Wu, D. Cui, *New J. Chem.* **2015**, *39*, 7682-7687.
- [62] a) S. P. Downing, S. C. Guadaño, D. Pugh, A. A. Danopoulos, R. M. Bellabarba, M. Hanton, D. Smith, R. P. Tooze, *Organometallics* **2007**, *26*, 3762-3770; b) C. Lorber, L. Vendier, *Dalton Trans.* **2009**, 6972-6984; c) J. Li, C. Schulzke, S. Merkel, Herbert W. Roesky, Prinson P. Samuel, A. Döring, D. Stalke, *Z. Anorg. Allg. Chem.* **2010**, *636*, 511-514; d) D. Zhang, G. Zi, *Chem. Soc. Rev.* **2015**, *44*, 1898-1921.
- [63] Z. Wang, L. Jiang, D. K. B. Mohamed, J. Zhao, T. S. A. Hor, *Coord. Chem. Rev.* **2015**, *293-294*, 292-326.
- [64] a) M. F. Lappert, P. L. Pye, *J. Chem. Soc., Dalton Trans.* **1977**, 2172-2180; b) T. Yagyu, K. Yano, T. Kimata, K. Jitsukawa, *Organometallics* **2009**, *28*, 2342-2344; c) S. J. Hock, L.-A. Schaper, W. A. Herrmann, F. E. Kuhn, *Chem. Soc. Rev.* **2013**, *42*, 5073-5089.
- [65] P. P. Samuel, K. C. Mondal, N. Amin Sk, H. W. Roesky, E. Carl, R. Neufeld, D. Stalke, S. Demeshko, F. Meyer, L. Ungur, L. F. Chibotaru, J. Christian, V. Ramachandran, J. van Tol, N. S. Dalal, *J. Am. Chem. Soc.* **2014**, *136*, 11964-11971.
- [66] a) J.-R. Wang, L. Liu, Y.-F. Wang, Y. Zhang, W. Deng, Q.-X. Guo, *Tetrahedron Lett.* **2005**, *46*, 4647-4651; b) S. A. Llewellyn, M. L. H. Green, A. R. Cowley, *Dalton Trans.* **2006**, 4164-4168; c) A. Shaabani, E. Farhangi, A. Rahmati, *Applied Catalysis A: General* **2008**, *338*, 14-19; d) D. O.

- Silva, J. D. Scholten, M. A. Gelesky, S. R. Teixeira, A. C. B. Dos Santos, E. F. Souza-Aguiar, J. Dupont, *ChemSusChem* **2008**, *1*, 291-294.
- [67] D. S. McGuinness, K. J. Cavell, B. W. Skelton, A. H. White, *Organometallics* **1999**, *18*, 1596-1605.
- [68] a) F. Lazreg, C. S. J. Cazin, in *N-Heterocyclic Carbenes*, Wiley-VCH Verlag GmbH & Co. KGaA, **2014**, pp. 199-242; b) S. Diez-Gonzalez, E. C. Escudero-Adan, J. Benet-Buchholz, E. D. Stevens, A. M. Z. Slawin, S. P. Nolan, *Dalton Trans.* **2010**, *39*, 7595-7606; c) R. S. Ghadwal, S. O. Reichmann, R. Herbst-Irmer, *Chem. Eur. J.* **2015**, *21*, 4247-4251; d) F. Lazreg, F. Nahra, C. S. J. Cazin, *Coord. Chem. Rev.* **2015**, *293-294*, 48-79.
- [69] S. Budagumpi, S. Endud, *Organometallics* **2013**, *32*, 1537-1562.
- [70] a) X. Gu, X. Zhu, Y. Wei, S. Wang, S. Zhou, G. Zhang, X. Mu, *Organometallics* **2014**, *33*, 2372-2379; b) X. Gu, L. Zhang, X. Zhu, S. Wang, S. Zhou, Y. Wei, G. Zhang, X. Mu, Z. Huang, D. Hong, F. Zhang, *Organometallics* **2015**, *34*, 4553-4559.
- [71] M. Bortoluzzi, E. Ferretti, F. Marchetti, G. Pampaloni, S. Zacchini, *Chem. Commun.* **2014**, *50*, 4472-4474.
- [72] V. V. Krishna Mohan Kandepi, J. M. S. Cardoso, B. Royo, *Catal. Lett.* **2010**, *136*, 222-227.
- [73] H. Braband, U. Abram, *Organometallics* **2005**, *24*, 3362-3364.
- [74] W.-M. Xue, M. C.-W. Chan, Z.-M. Su, K.-K. Cheung, S.-T. Liu, C.-M. Che, *Organometallics* **1998**, *17*, 1622-1630.
- [75] a) W. A. Herrmann, L. J. Goossen, C. Köcher, G. R. J. Artus, *Angew. Chem. Int. Ed. Engl.* **1996**, *35*, 2805-2807; *Angew. Chem.* **1996**, *108*, 2980-2982; b) A. Kascatan-Nebioglu, M. J. Panzner, J. C. Garrison, C. A. Tessier, W. J. Youngs, *Organometallics* **2004**, *23*, 1928-1931; c) C. A. Quezada, J. C. Garrison, M. J. Panzner, C. A. Tessier, W. J. Youngs, *Organometallics* **2004**, *23*, 4846-4848; d) J. Lemke, N. Metzler-Nolte, *Eur. J. Inorg. Chem.* **2008**, *2008*, 3359-3366; e) D. M. Khramov, E. L. Rosen, J. A. V. Er, P. D. Vu, V. M. Lynch, C. W. Bielawski, *Tetrahedron* **2008**, *64*, 6853-6862; f) X.-Y. Yu, H. Sun, B. O. Patrick, B. R. James, *Eur. J. Inorg. Chem.* **2009**, *2009*, 1752-1758.
- [76] Y. Fujii, J. Terao, N. Kambe, *Chem. Commun.* **2009**, 1115-1117.
- [77] a) H. Yao, Y. Zhang, H. Sun, Q. Shen, *Eur. J. Inorg. Chem.* **2009**, *2009*, 1920-1925; b) M. Zhang, X. Ni, Z. Shen, *Organometallics* **2014**, *33*, 6861-6867.
- [78] T. R. Helgert, T. K. Hollis, A. G. Oliver, H. U. Valle, Y. Wu, C. E. Webster, *Organometallics* **2014**, *33*, 952-958.
- [79] a) P. B. Hitchcock, M. F. Lappert, P. L. Pye, *J. Chem. Soc., Dalton Trans.* **1978**, 826-836; b) M. F. Lappert, P. L. Pye, *J. Chem. Soc., Dalton Trans.* **1978**, 837-844; c) W. A. Herrmann, M. Elison, J. Fischer, C. Köcher, G. R. J. Artus, *Chem. Eur. J.* **1996**, *2*, 772-780; d) R. Castarlenas, M. A. Esteruelas, E. Oñate, *Organometallics* **2005**, *24*, 4343-4346.
- [80] a) M. T. Powell, D.-R. Hou, M. C. Perry, X. Cui, K. Burgess, *J. Am. Chem. Soc.* **2001**, *123*, 8878-8879; b) H. M. Lee, T. Jiang, E. D. Stevens, S. P. Nolan, *Organometallics* **2001**, *20*, 1255-1258; c) L. D. Vazquez-Serrano, B. T. Owens, J. M. Buriak, *Chem. Commun.* **2002**, 2518-2519; d) F. E. Hahn, C. Holtgrewe, T. Pape, M. Martin, E. Sola, L. A. Oro, *Organometallics* **2005**, *24*, 2203-2209; e) L. D. Vazquez-Serrano, B. T. Owens, J. M. Buriak, *Inorg. Chim. Acta* **2006**, *359*, 2786-2797; f) C.-Y. Wang, C.-F. Fu, Y.-H. Liu, S.-M. Peng, S.-T. Liu, *Inorg. Chem.* **2007**, *46*, 5779-5786; g) D. Gnanamgari, A. Moores, E. Rajaseelan, R. H. Crabtree, *Organometallics* **2007**, *26*, 1226-1230; h) R. Corberán, M. Sanaú, E. Peris, *Organometallics* **2007**, *26*, 3492-3498; i) A. C. Marr, C. L. Pollock, G. C. Saunders, *Organometallics* **2007**, *26*, 3283-3285; j) A. M. Voutchkova, D. Gnanamgari, C. E. Jakobsche, C. Butler, S. J. Miller, J. Parr, R. H. Crabtree, *J. Organomet. Chem.* **2008**, *693*, 1815-1821; k) G. Song, X. Wang, Y. Li, X. Li, *Organometallics* **2008**, *27*, 1187-1192.
- [81] a) I. E. Markó, S. Stérin, O. Buisine, G. Mignani, P. Branlard, B. Tinant, J.-P. Declercq, *Science* **2002**, *298*, 204-206; b) I. G. Jung, J. Seo, S. I. Lee, S. Y. Choi, Y. K. Chung, *Organometallics* **2006**, *25*, 4240-4242; c) V. Lillo, J. Mata, J. Ramírez, E. Peris, E. Fernandez, *Organometallics* **2006**, *25*, 5829-5831.
- [82] a) K. M. Lee, C. K. Lee, I. J. B. Lin, *Angew. Chem. Int. Ed. Engl.* **1997**, *36*, 1850-1852; b) M. V. Baker, P. J. Barnard, S. J. Berners-Price, S. K. Brayshaw, J. L. Hickey, B. W. Skelton, A. H. White, *Dalton Trans.* **2006**, 3708-3715; c) B. Trillo, F. López, S. Montserrat, G. Ujaque, L. Castedo, A. Lledós, J. L. Mascareñas, *Chem. Eur. J.* **2009**, *15*, 3336-3339; d) S. Orbisaglia, B. Jacques, P. Braunstein, D. Hueber, P. Pale, A. Blanc, P. de Frémont, *Organometallics* **2013**; e) M. Baron, S. Bellemin-Laponnaz, C. Tubaro, B. Heinrich, M. Basato, G. Accorsi, *J. Organomet. Chem.* **2016**, *801*, 60-67.
- [83] P. L. Arnold, S. T. Liddle, *Chem. Commun.* **2005**, 5638-5640.
- [84] B. Wang, D. Cui, K. Lv, *Macromolecules* **2008**, *41*, 1983-1988.
- [85] Z. R. Turner, R. Bellabarba, R. P. Tooze, P. L. Arnold, *J. Am. Chem. Soc.* **2010**, *132*, 4050-4051.
- [86] G. C. Vougioukalakis, R. H. Grubbs, *Chem. Rev.* **2010**, *110*, 1746-1787.

- [87] J. Louie, R. H. Grubbs, *Chem. Commun.* **2000**, 1479-1480.
- [88] A. Zanardi, E. Peris, J. A. Mata, *New J. Chem.* **2008**, 32, 120-126.
- [89] Z. Liu, T. Zhang, M. Shi, *Organometallics* **2008**, 27, 2668-2671.
- [90] H. Ren, P. Yao, S. Xu, H. Song, B. Wang, *J. Organomet. Chem.* **2007**, 692, 2092-2098.
- [91] T. Ohishi, M. Nishiura, Z. Hou, *Angew. Chem. Int. Ed.* **2008**, 47, 5792-5795; *Angew. Chem.* **2008**, 120, 5876-5879.
- [92] M. Arisawa, Y. Terada, K. Takahashi, M. Nakagawa, A. Nishida, *J. Org. Chem.* **2006**, 71, 4255-4261.
- [93] E. M. Phillips, J. M. Roberts, K. A. Scheidt, *Org. Lett.* **2010**, 12, 2830-2833.
- [94] V. Cesar, S. Bellemin-Laponnaz, L. H. Gade, *Chem. Soc. Rev.* **2004**, 33, 619-636.
- [95] a) A. C. Filippou, O. Chernov, G. Schnakenburg, *Angew. Chem.* **2009**, 121, 5797-5800; b) H. Braunschweig, R. D. Dewhurst, K. Hammond, J. Mies, K. Radacki, A. Vargas, *Science* **2012**, 336, 1420-1422; c) A. Higelin, S. Keller, C. Göhringer, C. Jones, I. Krossing, *Angew. Chem.* **2013**, 125, 5041-5044; *Angew. Chem. Int. Ed.* **2013**, 52, 4941-4944.
- [96] a) *N-Heterocyclic Carbenes in Synthesis*, ed. S. P. Nolan, Wiley-VCH, Weinheim, Germany, **2006**; b) *N-Heterocyclic Carbenes in Transition Metal Catalysis*, ed. F. Glorius, Springer, Berlin, **2007**; c) *N-Heterocyclic Carbenes in Transition Metal Catalysis and Organocatalysis*, ed. C. S. J. Cazin, Springer, Heidelberg, Germany, **2011**.
- [97] D. Wang, C. Richter, A. Rühling, P. Drücker, D. Siegmund, N. Metzler-Nolte, F. Glorius, H.-J. Galla, *Chem. Eur. J.* **2015**, 21, 15123-15126.
- [98] R. E. Andrew, L. Gonzalez-Sebastian, A. B. Chaplin, *Dalton Trans.* **2016**, 45, 1299-1305.
- [99] A. V. Zhukhovitskiy, M. J. MacLeod, J. A. Johnson, *Chem. Rev.* **2015**, 115, 11503-11532.
- [100] a) H. D. Velazquez, F. Verpoort, *Chem. Soc. Rev.* **2012**, 41, 7032-7060; b) L.-A. Schaper, S. J. Hock, W. A. Herrmann, F. E. Kühn, *Angew. Chem. Int. Ed.* **2013**, 52, 270-289; c) E. Levin, E. Ivry, C. E. Diesendruck, N. G. Lemcoff, *Chem. Rev.* **2015**, 115, 4607-4692.
- [101] a) D. Enders, T. Balensiefer, *Acc. Chem. Res.* **2004**, 37, 534-541; b) F. Boeda, S. P. Nolan, *Annu. Rep. Prog. Chem. Sect. B: Org. Chem.* **2008**, 104, 184-210; c) S. Díez-González, N. Marion, S. P. Nolan, *Chem. Rev.* **2009**, 109, 3612-3676; d) G. C. Fortman, S. P. Nolan, *Chem. Soc. Rev.* **2011**, 40, 5151-5169; e) X. Bantreil, S. P. Nolan, *Nature Protocols* **2011**, 6, 69-77; f) A. Grossmann, D. Enders, *Angew. Chem. Int. Ed.* **2012**, 51, 314-325.
- [102] P. J. Barnard, M. V. Baker, S. J. Berners-Price, B. W. Skelton, A. H. White, *Dalton Trans.* **2004**, 1038-1047.
- [103] a) T. Sajoto, P. I. Djurovich, A. Tamayo, M. Yousufuddin, R. Bau, M. E. Thompson, R. J. Holmes, S. R. Forrest, *Inorg. Chem.* **2005**, 44, 7992-8003; b) R. Visbal, M. C. Gimeno, *Chem. Soc. Rev.* **2014**, 43, 3551-3574.
- [104] a) A. Kascatan-Nebioglu, M. J. Panzner, C. A. Tessier, C. L. Cannon, W. J. Youngs, *Coord. Chem. Rev.* **2007**, 251, 884-895; b) L. Mercks, M. Albrecht, *Chem. Soc. Rev.* **2010**, 39, 1903-1912; c) W. Liu, R. Gust, *Chem. Soc. Rev.* **2013**, 42, 755-773; d) S. A. Patil, S. A. Patil, R. Patil, R. S. Keri, S. Budagumpi, G. R. Balakrishna, M. Tacke, *Future Medicinal Chemistry* **2015**, 7, 1305-1333; e) C. Hemmert, H. Gornitzka, *Dalton Trans.* **2016**, 45, 440-447.
- [105] S. Naumann, A. P. Dove, *Polymer Chemistry* **2015**, 6, 3185-3200.
- [106] T. H. T. Hsu, J. J. Naidu, B.-J. Yang, M.-Y. Jang, I. J. B. Lin, *Inorg. Chem.* **2012**, 51, 98-108.
- [107] G. P. Moss, P. A. S. Smith, D. Taverni, *Pure Appl. Chem.* **1995**, 67, 1307-1375.
- [108] G. Ung, G. Bertrand, *Chem. Eur. J.* **2011**, 17, 8269-8272.
- [109] O. Schuster, L. Yang, H. G. Raubenheimer, M. Albrecht, *Chem. Rev.* **2009**, 109, 3445-3478.
- [110] S. Grundemann, A. Kovacevic, M. Albrecht, J. W. Faller Robert, H. Crabtree, *Chem. Commun.* **2001**, 2274-2275.
- [111] E. Aldeco-Perez, A. J. Rosenthal, B. Donnadiou, P. Parameswaran, G. Frenking, G. Bertrand, *Science* **2009**, 326, 556-559.
- [112] A. M. Magill, K. J. Cavell, B. F. Yates, *J. Am. Chem. Soc.* **2004**, 126, 8717-8724.
- [113] T. K. Sen, S. C. Sau, A. Mukherjee, A. Modak, S. K. Mandal, D. Koley, *Chem. Commun.* **2011**, 47, 11972-11974.
- [114] a) S. C. Sau, S. R. Roy, T. K. Sen, D. Mullangi, S. K. Mandal, *Adv. Synth. Catal.* **2013**, 355, 2982-2991; b) S. R. Roy, S. C. Sau, S. K. Mandal, *J. Org. Chem.* **2014**, 79, 9150-9160; c) Y. D. Bidal, M. Lesieur, M. Melaimi, F. Nahra, D. B. Cordes, K. S. Athukorala Arachchige, A. M. Z. Slawin, G. Bertrand, C. S. J. Cazin, *Adv. Synth. Catal.* **2015**, 357, 3155-3161.
- [115] a) T. Karthikeyan, S. Sankararaman, *Tetrahedron Lett.* **2009**, 50, 5834-5837; b) X. Xu, B. Xu, Y. Li, S. H. Hong, *Organometallics* **2010**, 29, 6343-6349; c) S. C. Sau, S. Santra, T. K. Sen, S. K. Mandal, D. Koley, *Chem. Commun.* **2012**, 48, 555-557; d) S. Modak, M. K. Gangwar, M. Nageswar Rao, M. Madasu, A. C. Kalita, V. Dorcet, M. A. Shejale, R. J. Butcher, P. Ghosh, *Dalton Trans.*

- 2015**, *44*, 17617-17628; e) P. K. Hota, G. Vijaykumar, A. Pariyar, S. C. Sau, T. K. Sen, S. K. Mandal, *Adv. Synth. Catal.* **2015**, *357*, 3162-3170.
- [116] R. Manzano, T. Wurm, F. Rominger, A. S. K. Hashmi, *Chem. Eur. J.* **2014**, *20*, 6844-6848.
- [117] a) X. Gong, H. Zhang, X. Li, *Tetrahedron Lett.* **2011**, *52*, 5596-5600; b) M. Heckenroth, V. Khlebnikov, A. Neels, P. Schurtenberger, M. Albrecht, *ChemCatChem* **2011**, *3*, 167-173; c) J. Witt, A. Pöthig, F. E. Kühn, W. Baratta, *Organometallics* **2013**, *32*, 4042-4045.
- [118] R. Manzano, F. Rominger, A. S. K. Hashmi, *Organometallics* **2013**, *32*, 2199-2203.
- [119] D. Mendoza-Espinosa, B. Donnadiou, G. Bertrand, *J. Am. Chem. Soc.* **2010**, *132*, 7264-7265.
- [120] M. Baya, B. Eguillor, M. A. Esteruelas, M. Oliván, E. Oñate, *Organometallics* **2007**, *26*, 6556-6563.
- [121] W. A. Herrmann, C.-P. Reisinger, M. Spiegler, *J. Organomet. Chem.* **1998**, *557*, 93-96.
- [122] C. A. Tolman, *Chem. Rev.* **1977**, *77*, 313-348.
- [123] W. Strohmeier, F.-J. Müller, *Chem. Ber.* **1967**, *100*, 2812-2821.
- [124] D. J. Nelson, S. P. Nolan, *Chem. Soc. Rev.* **2013**, *42*, 6723-6753.
- [125] A. R. Chianese, X. Li, M. C. Janzen, J. W. Faller, R. H. Crabtree, *Organometallics* **2003**, *22*, 1663-1667.
- [126] S. Wolf, H. Plenio, *J. Organomet. Chem.* **2009**, *694*, 1487-1492.
- [127] J. Huang, H.-J. Schanz, E. D. Stevens, S. P. Nolan, *Organometallics* **1999**, *18*, 2370-2375.
- [128] M. V. Baker, P. J. Barnard, S. K. Brayshaw, J. L. Hickey, B. W. Skelton, A. H. White, *Dalton Trans.* **2005**, 37-43.
- [129] H. V. Huynh, Y. Han, R. Jothibasur, J. A. Yang, *Organometallics* **2009**, *28*, 5395-5404.
- [130] T. L. Amyes, S. T. Diver, J. P. Richard, F. M. Rivas, K. Toth, *J. Am. Chem. Soc.* **2004**, *126*, 4366-4374.
- [131] R. W. Alder, P. R. Allen, S. J. Williams, *J. Chem. Soc., Chem. Commun.* **1995**, 1267-1268.
- [132] W. S. Matthews, J. E. Bares, J. E. Bartmess, F. G. Bordwell, F. J. Cornforth, G. E. Drucker, Z. Margolin, R. J. McCallum, G. J. McCollum, N. R. Vanier, *J. Am. Chem. Soc.* **1975**, *97*, 7006-7014.
- [133] a) W. L. Jorgensen, J. M. Briggs, J. Gao, *J. Am. Chem. Soc.* **1987**, *109*, 6857-6858; b) Y. Guissani, B. Guillot, S. Bratos, *The Journal of Chemical Physics* **1988**, *88*, 5850-5856; c) W. L. Jorgensen, J. M. Briggs, *J. Am. Chem. Soc.* **1989**, *111*, 4190-4197; d) C. Lim, D. Bashford, M. Karplus, *The Journal of Physical Chemistry* **1991**, *95*, 5610-5620.
- [134] a) B. M. Day, T. Pugh, D. Hendriks, C. F. Guerra, D. J. Evans, F. M. Bickelhaupt, R. A. Layfield, *J. Am. Chem. Soc.* **2013**, *135*, 13338-13341; b) B. M. Day, K. Pal, T. Pugh, J. Tuck, R. A. Layfield, *Inorg. Chem.* **2014**, *53*, 10578-10584.
- [135] A. J. Arduengo III, R. Krafczyk, R. Schmutzler, H. A. Craig, J. R. Goerlich, W. J. Marshall, M. Unverzagt, *Tetrahedron* **1999**, *55*, 14523-14534.
- [136] Sigma Aldrich Co. LLC, 1,3-Bis(2,6-diisopropylphenyl)-1,3-dihydro-2H-imidazol-2-ylidene, Retrieved May 06, 2016, from www.sigmaaldrich.com/catalog/product/aldrich/696196?lang=de®ion=DE.
- [137] a) E. Jafarpour, E. D. Stevens, S. P. Nolan, *J. Organomet. Chem.* **2000**, *606*, 49-54; b) L. Hintermann, *Beilstein J. Org. Chem.* **2007**, *3*, No. 22.
- [138] a) J. I. Bates, P. Kennepohl, D. P. Gates, *Angew. Chem. Int. Ed.* **2009**, *48*, 9844-9847; *Angew. Chem.* **2009**, *121*, 10028-10031; b) O. Kühn, *Functionalised N-Heterocyclic Carbene Complexes*, John Wiley & Sons, Ltd, **2010**; c) D. Mendoza-Espinosa, B. Donnadiou, G. Bertrand, *Chemistry – An Asian Journal* **2011**, *6*, 1099-1103; d) A. Solov'yev, E. Lacôte, D. P. Curran, *Org. Lett.* **2011**, *13*, 6042-6045; e) Y. Wang, M. Y. Abraham, R. J. Gilliard, P. Wei, J. C. Smith, G. H. Robinson, *Organometallics* **2012**, *31*, 791-793; f) S. Kronig, E. Theuergarten, C. G. Daniliuc, P. G. Jones, M. Tamm, *Angew. Chem.* **2012**, *124*, 3294-3298; g) Y. Wang, Y. Xie, M. Y. Abraham, R. J. Gilliard, P. Wei, C. F. Campana, H. F. Schaefer, P. v. R. Schleyer, G. H. Robinson, *Angew. Chem.* **2012**, *124*, 10320-10323; *Angew. Chem. Int. Ed.* **2012**, *51*, 10173-10176; h) P. K. Majhi, S. Sauerbrey, G. Schnakenburg, A. J. Arduengo, R. Streubel, *Inorg. Chem.* **2012**, *51*, 10408-10416; i) J. Ruiz, A. F. Mesa, *Chem. Eur. J.* **2012**, *18*, 4485-4488; j) P. K. Majhi, G. Schnakenburg, Z. Kelemen, L. Nyulaszi, D. P. Gates, R. Streubel, *Angew. Chem.* **2013**, *125*, 10264-10267; *Angew. Chem. Int. Ed.* **2013**, *52*, 10080-10083.
- [139] R. S. Ghadwal, S. O. Reichmann, E. Carl, R. Herbst-Irmer, *Dalton Trans.* **2014**, *43*, 13704-13710.
- [140] a) H. Kaur, F. K. Zinn, E. D. Stevens, S. P. Nolan, *Organometallics* **2004**, *23*, 1157-1160; b) A. Szadkowska, A. Makal, K. Woźniak, R. Kadyrov, K. Grela, *Organometallics* **2009**, *28*, 2693-2700; c) J. Chun, I. G. Jung, H. J. Kim, M. Park, M. S. Lah, S. U. Son, *Inorg. Chem.* **2009**, *48*, 6353-6355.
- [141] M. Bielawski, M. Zhu, B. Olofsson, *Adv. Synth. Catal.* **2007**, *349*, 2610-2618.
- [142] a) F. M. Beringer, W. J. Daniel, S. A. Galton, G. Rubin, *J. Org. Chem.* **1966**, *31*, 4315-4318; b) P. Gao, P. S. Portoghesi, *J. Org. Chem.* **1995**, *60*, 2276-2278; c) J. H. Ryan, P. J. Stang, *Tetrahedron*

- Lett.* **1997**, *38*, 5061-5064; d) V. K. Aggarwal, B. Olofsson, *Angew. Chem. Int. Ed.* **2005**, *44*, 5516-5519; *Angew. Chem.* **2005**, *117*, 5652-5655.
- [143] a) N. W. Alcock, R. M. Countryman, *J. Chem. Soc., Dalton Trans.* **1977**, 217-219; b) H.-J. Frohn, M. E. Hirschberg, R. Boese, D. Bläser, U. Flörke, *Z. Anorg. Allg. Chem.* **2008**, *634*, 2539-2550.
- [144] W. J. Marshall, V. V. Grushin, *Organometallics* **2003**, *22*, 1591-1593.
- [145] a) Sigma Aldrich Co. LLC, Silver hexafluorophosphate, Retrieved May 08, 2016, from www.sigmaaldrich.com/catalog/product/aldrich/227722?lang=de®ion=DE; b) Sigma Aldrich Co. LLC, Potassium hexafluorophosphate, Retrieved May 08, 2016, from www.sigmaaldrich.com/catalog/product/aldrich/200913?lang=de®ion=DE; c) Sigma Aldrich Co. LLC, Silver tetrafluoroborate, Retrieved May 08, 2016, from www.sigmaaldrich.com/catalog/product/aldrich/208361?lang=de®ion=DE; d) Sigma Aldrich Co. LLC, Sodium tetrafluoroborate, Retrieved May 08, 2016, from www.sigmaaldrich.com/catalog/product/aldrich/202215?lang=de®ion=DE; e) Sigma Aldrich Co. LLC, Silver trifluoromethanesulfonate, Retrieved May 08, 2016, from www.sigmaaldrich.com/catalog/product/aldrich/483346?lang=de®ion=DE; f) Sigma Aldrich Co. LLC, Sodium trifluoromethanesulfonate, Retrieved May 08, 2016, from www.sigmaaldrich.com/catalog/product/aldrich/367907?lang=de®ion=DE; g) Sigma Aldrich Co. LLC, Potassium trifluoromethanesulfonate, Retrieved May 08, 2016, from www.sigmaaldrich.com/catalog/product/aldrich/422843?lang=de®ion=DE.
- [146] a) R. Neufeld, D. Stalke, *Chemical Science* **2015**, *6*, 3354-3364; b) D. Stalke, S. Bachmann, R. Neufeld, M. Dzieski, *Chem. Eur. J.* **2016**, n/a-n/a.
- [147] P. Müller, R. Herbst-Irmer, A. L. Spek, T. R. Schneider, M. R. Sawaya, *Crystal Structure Refinement - A Crystallographer's Guide to SHELXL Vol. 8*, Oxford University Press, Oxford (England), **2006**.
- [148] T. Dröge, F. Glorius, *Angew. Chem.* **2010**, *122*, 7094-7107; *Angew. Chem. Int. Ed.* **2010**, *49*, 6940-6952.
- [149] a) C. Amatore, A. Bucaille, A. Fuxa, A. Jutand, G. Meyer, A. Ndedi Ntepe, *Chem. Eur. J.* **2001**, *7*, 2134-2142; b) E. Alvaro, J. F. Hartwig, *J. Am. Chem. Soc.* **2009**, *131*, 7858-7868; c) B. A. Harding, P. R. Melvin, W. Dougherty, S. Kassel, F. E. Goodson, *Organometallics* **2013**, *32*, 3570-3573.
- [150] a) S. Shekhar, P. Ryberg, J. F. Hartwig, J. S. Mathew, D. G. Blackmond, E. R. Strieter, S. L. Buchwald, *J. Am. Chem. Soc.* **2006**, *128*, 3584-3591; b) K. Vikse, T. Naka, J. S. McIndoe, M. Besora, F. Maseras, *ChemCatChem* **2013**, *5*, 3604-3609.
- [151] D. S. McGuinness, N. Saendig, B. F. Yates, K. J. Cavell, *J. Am. Chem. Soc.* **2001**, *123*, 4029-4040.
- [152] N. M. Camasso, M. S. Sanford, *Science* **2015**, *347*, 1218-1220.
- [153] C. Allègre, G. Manhès, É. Lewin, *Earth. Planet. Sci. Lett.* **2001**, *185*, 49-69.
- [154] a) Sigma Aldrich Co. LLC, Tris(dibenzylideneacetone)dipalladium(0), Retrieved May 08, 2016, from www.sigmaaldrich.com/catalog/product/aldrich/328774?lang=de®ion=DE; b) Sigma Aldrich Co. LLC, Nickel(II)bromide, Retrieved May 08, 2016, from www.sigmaaldrich.com/catalog/product/aldrich/217891?lang=de®ion=DE.
- [155] a) S. Z. Tasker, E. A. Standley, T. F. Jamison, *Nature* **2014**, *509*, 299-309; b) E. A. Standley, S. Z. Tasker, K. L. Jensen, T. F. Jamison, *Acc. Chem. Res.* **2015**, *48*, 1503-1514.
- [156] a) B. Saito, G. C. Fu, *J. Am. Chem. Soc.* **2007**, *129*, 9602-9603; b) D.-G. Yu, X. Wang, R.-Y. Zhu, S. Luo, X.-B. Zhang, B.-Q. Wang, L. Wang, Z.-J. Shi, *J. Am. Chem. Soc.* **2012**, *134*, 14638-14641; c) C.-Y. Huang, A. G. Doyle, *J. Am. Chem. Soc.* **2012**, *134*, 9541-9544; d) S. D. Ramgren, L. Hie, Y. Ye, N. K. Garg, *Org. Lett.* **2013**, *15*, 3950-3953.
- [157] T. Zell, P. Fischer, D. Schmidt, U. Radius, *Organometallics* **2012**, *31*, 5065-5073.
- [158] D. G. Gusev, *Organometallics* **2009**, *28*, 6458-6461.
- [159] M. D. Hanwell, D. E. Curtis, D. C. Lonie, T. Vandermeersch, E. Zurek, G. R. Hutchison, R. Sayle, E. J. Milner-White, *Journal of Cheminformatics* **2012**, *4*, 1-17.
- [160] a) W. A. Herrmann, *Angew. Chem.* **2002**, *114*, 1342-1363; *Angew. Chem. Int. Ed.* **2002**, *41*, 1290-1309; b) C. Samojłowicz, M. Bieniek, K. Grela, *Chem. Rev.* **2009**, *109*, 3708-3742.
- [161] a) S. Díez-González, N. M. Scott, S. P. Nolan, *Organometallics* **2006**, *25*, 2355-2358; b) S. Díez-González, E. D. Stevens, N. M. Scott, J. L. Petersen, S. P. Nolan, *Chem. Eur. J.* **2008**, *14*, 158-168; c) T. Le Gall, S. Baltatu, S. K. Collins, *Synthesis* **2011**, *2011*, 3687-3691.
- [162] a) D. S. Laitar, E. Y. Tsui, J. P. Sadighi, *Organometallics* **2006**, *25*, 2405-2408; b) Y. Lee, A. H. Hoveyda, *J. Am. Chem. Soc.* **2009**, *131*, 3160-3161.
- [163] K. B. Selim, H. Nakanishi, Y. Matsumoto, Y. Yamamoto, K.-i. Yamada, K. Tomioka, *J. Org. Chem.* **2011**, *76*, 1398-1408.
- [164] a) S. Díez-González, A. Correa, L. Cavallo, S. P. Nolan, *Chem. Eur. J.* **2006**, *12*, 7558-7564; b) S. Díez-González, E. D. Stevens, S. P. Nolan, *Chem. Commun.* **2008**, 4747-4749; c) P. Li, L. Wang, Y.

- Zhang, *Tetrahedron* **2008**, *64*, 10825-10830; d) M.-L. Teyssot, A. Chevry, M. Traïkia, M. El-Ghozzi, D. Avignat, A. Gautier, *Chem. Eur. J.* **2009**, *15*, 6322-6326; e) J.-M. Collinson, J. D. E. T. Wilton-Ely, S. Díez-González, *Chem. Commun.* **2013**, *49*, 11358-11360.
- [165] a) V. V. Rostovtsev, L. G. Green, V. V. Fokin, K. B. Sharpless, *Angew. Chem.* **2002**, *114*, 2708-2711; b) C. Nolte, P. Mayer, B. F. Straub, *Angew. Chem. Int. Ed.* **2007**, *46*, 2101-2103; c) S. Díez-González, S. P. Nolan, *Angew. Chem. Int. Ed.* **2008**, *47*, 8881-8884.
- [166] P. Stollberg, D. Stalke, *in preparation* **2016**.
- [167] a) W. Schlenk, A. Thal, *Ber. Dtsch. Chem. Ges.* **1913**, *46*, 2840-2854; b) W. Schlenk, J. Holtz, *Berichte der Deutschen Chemischen Gesellschaft* **1917**, *50*, 262-274; c) W. Schlenk, in *Die Methoden der Organischen Chemie*, 2. Aufl. ed. (Ed.: J. Houben), G. Thieme, Leipzig, **1924**, p. 720; d) T. T. Tidwell, *Angew. Chem. Int. Ed.* **2001**, *40*, 331-337.
- [168] G. R. Fulmer, A. J. M. Miller, N. H. Sherden, H. E. Gottlieb, A. Nudelman, B. M. Stoltz, J. E. Bercaw, K. I. Goldberg, *Organometallics* **2010**, *29*, 2176-2179.
- [169] T. J. Teuteberg, Göttingen, **2016**.
- [170] a) V. P. W. Böhm, C. W. K. Gstöttmayr, T. Weskamp, W. A. Herrmann, *J. Organomet. Chem.* **2000**, *595*, 186-190; b) S. Fantasia, S. P. Nolan, *Chem. Eur. J.* **2008**, *14*, 6987-6993; c) J.-H. Lee, H.-T. Jeon, Y.-J. Kim, K.-E. Lee, Y. Ok Jang, S. W. Lee, *Eur. J. Inorg. Chem.* **2011**, 1750-1761; d) X. Cai, S. Majumdar, G. C. Fortman, C. S. J. Cazin, A. M. Z. Slawin, C. Lhermitte, R. Prabhakar, M. E. Germain, T. Palluccio, S. P. Nolan, E. V. Rybak-Akimova, M. Temprado, B. Captain, C. D. Hoff, *J. Am. Chem. Soc.* **2011**, *133*, 1290-1293.
- [171] I. Jllia, F. Meganem, J. Herscovici, C. Girard, *Molecules* **2009**, *14*, 528.
- [172] R. B. Nasir Baig, R. S. Varma, *Green Chemistry* **2012**, *14*, 625-632.
- [173] D. Wang, N. Li, M. Zhao, W. Shi, C. Ma, B. Chen, *Green Chemistry* **2010**, *12*, 2120-2123.
- [174] M. Obata, A. Kitamura, A. Mori, C. Kameyama, J. A. Czaplewska, R. Tanaka, I. Kinoshita, T. Kusumoto, H. Hashimoto, M. Harada, Y. Mikata, T. Funabiki, S. Yano, *Dalton Trans.* **2008**, 3292-3300.
- [175] a) T. Kottke, D. Stalke, *J. Appl. Crystallogr.* **1993**, *26*, 615-619; b) T. Kottke, D. Stalke, *Angew. Chem. Int. Ed.* **1993**, *32*, 580-582.
- [176] T. Schulz, K. Meindl, D. Leusser, D. Stern, J. Graf, C. Michaelsen, M. Ruf, G. M. Sheldrick, D. Stalke, *J. Appl. Crystallogr.* **2009**, *42*, 885-891.
- [177] COSMO, Bruker-AXS, Madison (WI), USA, **2011**.
- [178] a) in *SAINT*, v7.68A, Bruker AXS, Madison (WI), USA, **2009**; b) in *Bruker AXS Inst. Inc.*, Madison (WI), USA, **2012**.
- [179] G. M. Sheldrick, SADABS 2016/2, Göttingen, **2016**.
- [180] G. M. Sheldrick, TWINABS-2012/1, Göttingen, **2012**.
- [181] G. M. Sheldrick, XPREP Version 2015/1 for Windows, Madison, **2015**.
- [182] G. M. Sheldrick, *Acta Crystallogr. Sect. A* **1990**, *46*, 467-473.
- [183] G. M. Sheldrick, *Acta Crystallogr. Sect. A* **2008**, *64*, 112-122.
- [184] C. B. Hübschle, G. M. Sheldrick, B. Dittrich, *J. Appl. Crystallogr.* **2011**, *44*, 1281-1284.
- [185] G. M. Sheldrick, XP in SHELXTL v2008/2 ed., Madison (WI), USA, **2008**.
- [186] A. Solovyeu, Q. Chu, S. J. Geib, L. Fensterbank, M. Malacria, E. Lacôte, D. P. Curran, *J. Am. Chem. Soc.* **2010**, *132*, 15072-15080.
- [187] a) M. Walker, E. Pohl, R. Herbst-Irmer, M. Gerlitz, J. Rohr, G. M. Sheldrick, *Acta Crystallogr., Sect. B* **1999**, *55*, 607-616; b) R. Marsh, *Acta Crystallogr., Sect. B* **1986**, *42*, 193-198; c) R. Marsh, *Acta Crystallogr., Sect. B* **1981**, *37*, 1985-1988; d) V. Schomaker, R. E. Marsh, *Acta Crystallogr., Sect. B* **1979**, *35*, 1933-1934.
- [188] a) P. van der Sluis, A. L. Spek, *Acta Crystallogr. Sect. A* **1990**, *46*, 194-201; b) A. Spek, *J. Appl. Cryst.* **2003**, *36*, 7-13.
- [189] a) H. Flack, *Acta Crystallogr. Sect. A* **1983**, *39*, 876-881; b) H. D. Flack, G. Bernardinelli, *J. Appl. Crystallogr.* **2000**, *33*, 1143-1148.

Appendix

My academic teachers were among others:

L. Ackermann, G. Beuermann, P. Botschwina, M. Buback, U. Diederichsen, C. Ducho, G. Eckold, H. Frauendorf, R. Ghadwal, W. Hack, R. Machinek, J. Magull, S. Mayr, F. Meyer, G.M. Sheldrick, L.F. Tietze, S. Schmatz, J. Schröder, D. Stalke, C. Steinem, M. Suhm, P. Vana, D.B. Werz

Curriculum Vitae

Name: Sven Ole Reichmann
Date of birth: 19.10.1984 in Vorwerk
Nationality: German
E-mail: sreichm@gwdg.de

Scientific career

- 04/2013 – 13.10.2016 PhD studies “Unconventional carbene-donor ligands for the development of new catalysts” in the research group of Prof. Dr. Dietmar Stalke under the supervision of PD Dr. Rajandra S. Ghadwal within the Georg-August University School of Science (Gauss) doctoral program at the Georg-August-University Göttingen
- 02/2011 – 02/2013 Studies of Chemistry at the Georg–August University Göttingen. Master of Science in 02/2013
- 05/2012 – 11/2012 Work on the synthetic chemical graduation master thesis “Funktionalisierung von *N*-Heterocyclischen Carbenen zur Entwicklung neuer Ligandsysteme für Hauptgruppenelemente” in the research group of Prof. Dr. D. Stalke at the Georg-August-University Göttingen (Grade: 1.0)
- 09/2011 – 02/2012 Project work in the workgroup of Dr. Michael Hall at the Newcastle University, Newcastle upon Tyne (United Kingdom)
- 10/2006 – 02/2011 Studies of Chemistry at the Georg-August-University Göttingen. Bachelor of Science in 02/2011
- 6/2005 Abitur at Ratsgymnasium Rotenburg
- 1997 – 2005 Ratsgymnasium Rotenburg

Awards

- 10.12.2010 Students' choice for the award „Preis für die beste, nichtselbstständige Lehre am Institut für Anorganische Chemie“

Skills

Languages: German (mother tongue)
English (fluent),
Spanish (basics)

Computer applications: Scientific data progressing (ChemDraw, Bruker APEXII, SHELXTL Paket, ShelXle, Mercury, PLATON, XD2006)
Basic knowledge in MS Word, Excel, Adobe Photoshop, PovRay

Conferences and Presentations

Talks

09.-10.10.2014 *Center for Materials Crystallography, Annual meeting, Aarhus*

Posters

05.06.2013 *Göttinger Chemie-Forum, Göttingen*
26-29.06.2013 *Center for Materials Crystallography, Annual meeting, Aarhus*
24-26.09.2014 *17th Wöhler Tagung, Saarbrücken*
16-17.10.2014 *Niedersächsisches Katalyse-Symposium (NiKaS), Göttingen*
25-28.03.2015 *17th JCF-Spring Symposium, Münster*
30.08-02.09.2015 *WIFO 2015 Dresden*

Publications

1. R. S. Ghadwal, S. O. Reichmann, F. Engelhardt, D. M. Andrada, G. Frenking, *Chem. Commun.*, **2013**, 49, 9440-9442.
2. L.F. Tietze, T. Hungerland, J. Ammermann, C. Eichhorst, S.O. Reichmann, D. Stalke, *Ind. Chem. Soc.* **2013**, 90, 1537-1555.
3. R. S. Ghadwal, S. O. Reichmann, E. Carl, R. Herbst-Irmer, *Dalton Trans.* **2014**, 43, 13704-13710.
4. R. S. Ghadwal, S. O. Reichmann, R. Herbst-Irmer, *Chem. Eur. J.* **2015**, 21, 4247-4251.
5. L.F. Tietze, B. Waldecker, D. Ganapathy, C. Eichhorst, T. Lenzer, K. Oum, S.O. Reichmann, D. Stalke, *Angew. Chem.* **2015**, 127, 10457-10641; *Angew. Chem. Int. Ed.* **2015**, 55, 10317-10321.

Göttingen, 31. October 2016

Sven Reichmann

Göttingen, 31.10.2016

Eidesstattliche Erklärung

Hiermit erkläre ich, Sven Ole Reichmann (geb. 19.10.1984 in Vorwerk), dass die hier vorliegende Dissertation mit dem Titel „Unconventional Carbene-Donor Ligands for the Development of New Catalysts“ von mir selbstständig und ohne unerlaubte Hilfe angefertigt wurde. Dabei wurden ausschließlich die angegebenen Quellen und Hilfsmittel benutzt. Alle sinngemäß oder wörtlich übernommenen Ausführungen sind als solche gekennzeichnet.

Sven Ole Reichmann